Model-based optimization of electrical system in the early development stage of hybrid drivetrains

Quentin Werner

École Doctorale IAEM Lorraine
Mention Systèmes Électroniques, Génie Électrique

Model-based optimization of electrical system in the early development stage of hybrid drivetrains

THÈSE

Présentée et soutenue publiquement le 9 mai 2017

Pour l'obtention du

Doctorat de l'Université de Lorraine

Spécialité : Génie Électrique

par

Quentin WERNER

Composition du jury :

Rapporteurs :

Prof. Xuefang LIN-SHI	INSA de Lyon
Dr. Abdesslem DJERDIR	Université de Technologie Belfort-Montbéliard

Examinateurs :

Prof. Betty LEMAIRE-SEMAIL	Université Lille 1, L2EP
Dr. Alexandre DE BERNARDINIS	ENS Cachan, IFSTTAR
Dr. Steffen HENZLER	Daimler AG (Encadrant entreprise)
Dr. Randy DOOLITTLE	Daimler AG (Encadrant entreprise)
Prof. Noureddine TAKORABET	Université de Lorraine, (Directeur de thèse)
Prof. Serge PIERFEDERICI	Université de Lorraine, (Co-Directeur de thèse)

Invité :

Prof. Napat WATJANATEPIN	Rajamangala University, Thailand

Thèse préparée au Groupe de Recherche en Électrotechnique et Électronique de Nancy
Site de l'ENSEM - EA N° 4366
En partenariat Avec DAIMLER AG (Stuttgart, Allemagne)

Abstract

This work analyses the challenges faced by the electric components for traction purpose in hybrid drivetrains. It investigates the components and their interactions as an independent entity in order to refine the scope of investigation and to find the best combinations of components instead of the best components combinations.

Hybrid vehicle is currently a topic of high interest because it stands for a suitable short-term solution towards zero emission vehicle. Despite its advantages, it is a challenging topic because the components need to be integrated in a conventional drivetrain architecture. Therefore, the focus of this work is set on the determination of the right methods to investigate only the electric components for traction purpose. The aim and the contributions of this work lies thereby in the resolution of the following statement:

Determine the sufficient level of details in modeling electric components at the system level and develop models and tools to perform dynamic simulations of these components and their interactions in a global system analysis to identify ideal designs of various drivetrain electric components during the design process.

To address these challenges, this work is divided in four main parts within six chapters. First the current status of the hybrid vehicle, the electric components and the associated optimization methods and simulation are presented (first chapter). Then for each component, the right modeling approach is defined in order to investigate the electrical, mechanical and thermal behavior of the components as well as methods to evaluate their integration in the drivetrain (second to fourth chapter). After this, a suitable method is defined to evaluate the global system and to investigate the interactions between the components based on the review of relevant previous works (chapter five). Finally the last chapter presents the optimization approach considered in this work and the results by analyzing different system and cases (chapter six).

Thanks to the analysis of the current status, previous works and the development of the simulations tools, this work investigates the relationships between the voltage, the current and the power in different cases. The results enable, under the considered assumptions of the work, to determine the influence of these parameters on the components and of the industrial environment on the optimization results. Considering the current legislative frame, all the results converge toward the same observation referred to the reference systems: a reduction of the voltage and an increase of the current leads to an improvement of the integration and the performance of the system. These observations are linked with the considered architecture, driving cycle and development environment but the developed methods and approaches have set the basis to extend the knowledge for the optimization of the electric system for traction purpose. Beside the main optimization, special cases are investigated to show the influence of additional parameters (increase of the power, 48V-system, machine technology, boost-converter…).

In order to conclude, this work have set the basis for further investigations about the electric components for traction purpose in more electrified vehicle. Due to the constantly changing environment, the new technologies and the various legislative frame, this topic remains of high interest and the following challenges still need to be deeper investigated:

- Application of the methods for other drivetrain architecture (series hybrid, power-split hybrid, fuel-cell vehicle, full electric vehicle)
- Investigation of new technologies such as silicon-carbide for the power electronics, lithium–sulfur battery or switch reluctance machine
- Investigation of other driving cycle, legislative frame
- Integration of additional power electronics structure
- Further validation of the modeling approaches with additional components

Résumé

Introduction :

Ce travail de thèse traite un sujet d'actualité majeur : la réduction des émissions et de la consommation dans l'industrie automobile. Il analyse les challenges auxquels est confronté le développement des systèmes de propulsion. Dans le cadre de la réduction des émissions plusieurs solutions sont possibles et elles s'étendent de l'optimisation des véhicules conventionnels jusqu'au développement de véhicules électriques ou à pile à combustible en passant par les véhicules hybrides. Le travail présenté ici se concentre sur le développement des systèmes de propulsion hybrides électriques et plus particulièrement leurs composants électriques. L'accent est mis sur l'optimisation coordonnée de ces composants en les considérants comme une seule et unique entité. L'analyse des composants électriques pour le système de propulsion et de leurs interactions est un sujet de recherche important afin de les dimensionner et de les d'intégrer de manière optimale dans la chaine de traction plutôt que de combiner des composants optimisés de manière indépendante. Les véhicules hybrides et leurs systèmes de propulsion sont un domaine de recherche qui suscite un grand intérêt parce qu'il s'agit d'une solution efficace à court terme afin de préparer la transition énergétique vers les véhicules à zéro émission. Même si cette solution présente de nombreux avantages, elle reste un sujet de recherche complexe car les composants électriques doivent être intégrés au sein d'un système de propulsion conventionnel. Le but de ce travail est axé sur la détermination de méthodes appropriées pour étudier les composants électriques d'un point de vue scientifique tout en considérant les contraintes du milieu industriel et ainsi de répondre à la problématique suivante :

Déterminer le niveau suffisant de détails pour modéliser les systèmes électrique pour les systèmes de traction pour véhicules hybrides *afin d'identifier le dimensionnement idéal des composants pour différents systèmes pendant la phase de développement*

La réponse à cette problématique, détaillée dans ce rapport, est divisée en quatre parties majeures : état de l'art, modélisations des composants, modélisation des systèmes et optimisation des systèmes de propulsion hybrides qui s'étendent sur six chapitres.

Chapitre 1:

Le premier chapitre présente les points suivants : l'état de l'art des véhicules hybrides électrique ainsi que leurs composants et leurs architectures, les spécificités et les challenges de l'industrie automobile, les différentes solutions pour l'analyse, la modélisation et l'optimisation des systèmes hybrides de propulsion afin de déterminer à la fin du chapitre les limites et les objectifs concret de ce travail de recherche. L'état de l'art des véhicules hybrides commence par l'introduction de la définition d'un système hybride de propulsion : « un système avec au moins deux convertisseurs d'énergie et deux systèmes de stockage d'énergie dont le but premier est la propulsion du véhicule ». Basé sur cette définition, le cadre de ce travail de recherche est réduit à l'étude des systèmes hybrides de propulsion électrique où la conversion de l'énergie est assurée d'une part par le moteur à combustion et d'autre part par une machine électrique et où le stockage de l'énergie est assuré par un réservoir de carburant et un système de stockage électrique avec ou sans possibilité de recharge externe. Suite à ça, les différentes architectures pour le système de propulsion sont présentées : série, parallèle et « power-split » ainsi que leurs fonctionnalités de manière succincte.

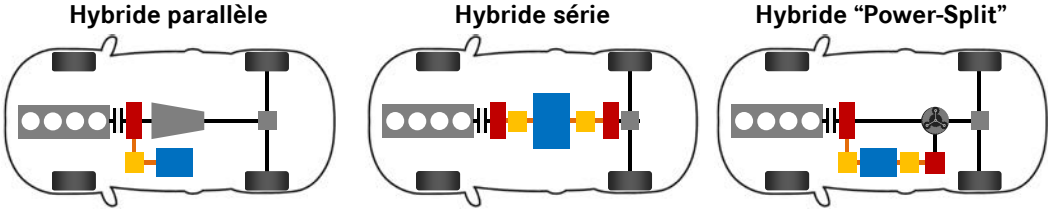

Figure: Architecture de véhicules hybrides

Une analyse plus détaillée est réalisée pour les composants électriques du système de propulsion qui sont au cœur

de ce travail de recherche. Cette analyse commence par les machines électriques qui réalisent la conversion électromécanique au sein du système électrique. Son rôle ainsi que les spécificités dans le cadre de l'industrie automobile sont présentés avant de discuter de manière plus approfondie des différentes technologies utilisées actuellement. Même si les véhicules électrique ou à pile à combustible ne sont pas étudiés dans le cadre de ce travail, l'analyse de leur composants et de leur système de propulsion permet d'avoir un bon aperçu des différentes technologies et de leur pertinence pour une application automobile. Une attention particulière est aussi accordée à l'intégration de la machine au sein du système de propulsion qui influence grandement sa topologie ainsi que la pertinence des différentes technologies.

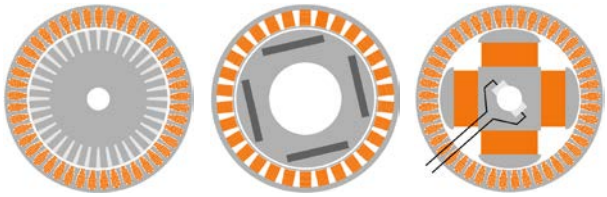

Figure: Technologie de machines électriques utilisées dans les véhicules hybrides ou électriques

Ensuite, les différentes solutions pour les systèmes de stockage électrique sont discutés et l'analyse des solutions actuelles permet à nouveau de limiter l'étendu du domaine d'investigation en considérant uniquement la solution la plus répandue à l'heure actuelle : les batteries. Leurs spécificités, les différentes technologies ainsi que leur intégration au sein des véhicules hybrides sont discutées afin de comprendre les enjeux de leur développement dans l'industrie automobile. Finalement l'analyse des composants électriques se termine par le cas de l'électronique de puissance. Celle-ci est généralement composée de un ou deux sous-composants : l'onduleur et un convertisseur DC/DC. Si l'onduleur est un composant obligatoire du système de propulsion dû aux technologies choisies pour le système de stockage et la conversion électromécanique, le convertisseur DC/DC (généralement de type Boost) est considéré de manière plus superficielle puisqu'il n'est présent que dans certains systèmes de propulsion. Concernant les technologies et les topologies pour l'électronique de puissance, leur nombre est plutôt restreint et est limité aux cas suivants : les Mosfet et les IGBT pour les semi-conducteurs et une architecture conventionnelle triphasée pour l'onduleur. D'autres technologies (carbure de silicium) et technologies (onduleur multiniveaux ou onduleur à source impédance en Z) sont en cours d'études mais ne sont pas considérées dans ce travail. La partie sur l'analyse des systèmes de propulsion hybride se termine par la présentation des spécificités de l'industrie automobile concernant l'évaluation et le développement des systèmes de propulsion ainsi que les différents challenges (concepts de véhicule et niveau de tension) qui influencent directement le développement des méthodes et de la démarche d'optimisation réalisée au cours de cette thèse.

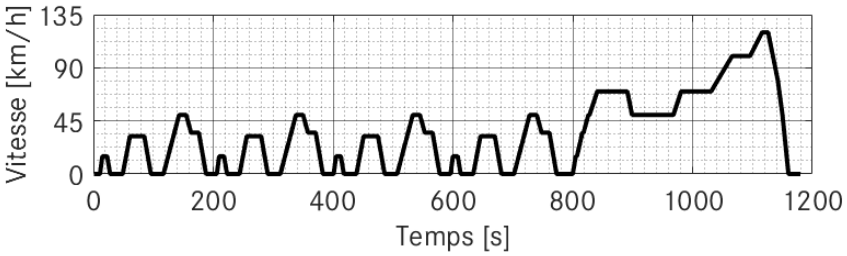

Figure: Exemple de cycle de fonctionnement dans l'industrie automobile (NEDC)

La seconde partie de ce premier chapitre est axée sur les différentes solutions pour la modélisation des systèmes électrique pour les véhicules hybrides. Elle montre d'abord le potentiel des outils de simulation au cours du développement des véhicules et de leur utilisation. Suite à ça, les différents niveaux d'investigations et les paramètres associés pour l'évaluation du système électrique sont présentés avant d'analyser les travaux précédents dans le domaine du point de vue de l'approche considérée (niveau d'investigation) et de la méthode d'évaluation (paramètres considérés). Les travaux précédents sont classés par niveau d'investigation et analysés afin de déterminer dans la partie suivante les objectifs et les limites de ce travail de recherche. Finalement, cette partie se

conclue par l'analyse des approches pour la modélisation et en particulier l'analyse de la causalité et du sens de simulation. La causalité est définie comme le lien qui réunit la cause à l'effet. Dans le cadre de ce travail de recherche, elle peut être considérée comme directe : la cause est déterminée en fonction de l'effet ou indirecte : l'effet est déterminé en fonction de la cause. Les différents sens de simulation (backward, forward et bidirectionnel) sont analysés et leurs avantages et inconvénients sont présentés en considérant leur causalité ainsi que leur limite concernant l'évaluation et le dimensionnement des composants. La dernière partie de ce chapitre est axée sur la détermination des objectifs et des limites de cette thèse en considérant l'état de l'art analysé dans les parties précédentes. Elle commence par les objectifs qui sont fixés par l'intermédiaire des paramètres suivants : le niveau d'évaluation, le niveau de modélisation, les composants considérés et les paramètres considérés. Il est ainsi décidé que les composants vont être considéré en tant qu'entité unique : le système eDrive, avec une modélisation de type système (seuls les entrées et les sorties de chaque composant sont considérées) et en considérant les composants suivants : machine électrique, électronique de puissance et batterie, et les paramètres suivants : le niveau de tension, l'architecture électrique ainsi que les stratégies de module. Ayant fixé ces différents aspects, les objectifs du travail de thèse sont de déterminer le potentiel des véhicules hybrides et de leur développement en considérant les composants électriques sous la forme d'un système afin de déterminer la combinaison optimale de composants au lieu de combiner des composants optimisés. Afin de limiter l'étendu du travail de recherche, des hypothèses sont faites concernant les interfaces du système.

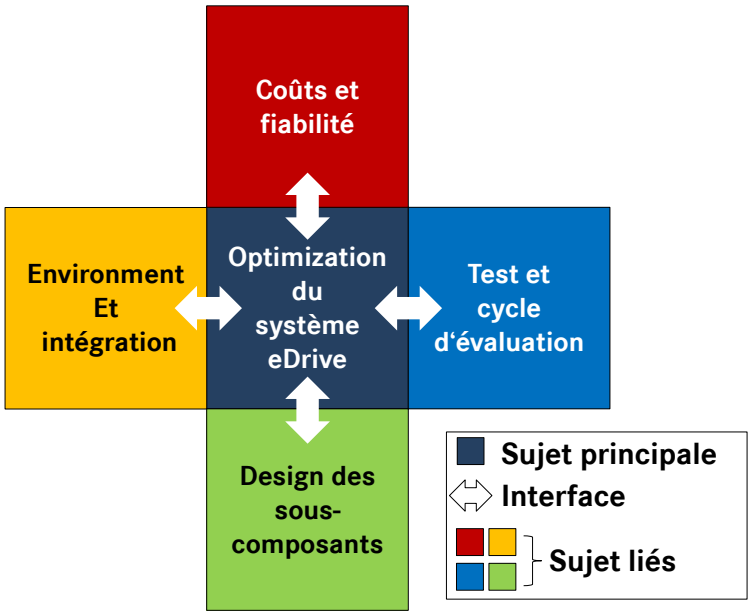

Figure: Limites du sujet

Le nombre de technologies considérées est limité : seules les machines synchrones à aimants permanents et les machines asynchrones avec un rotor en cage d'écureuil sont considérés, seules les technologies IGBT et Mosfet sont considérées tandis que seul les batteries de type lithium-ion sont considérées. Finalement les méthodes et modélisations requises (électrique, thermique et intégrabilité) sont déterminées et les approches sont fixés grâce aux conditions suivantes : le système sera modélisé de manière bidirectionnelle en considérant une causalité directe. Les modélisations seront développées en ayant pour but de trouver le bon compromis entre la précision et la complexité du modèle. En d'autres termes, le but est de modéliser seulement ce qui est nécessaire afin de répondre aux enjeux de la thèse afin de ne pas complexifier les modèles et ainsi d'augmenter inutilement le temps de simulation.

Chapitre 2 :

Le second chapitre est organisé autour de la modélisation des machines électriques. Il présente d'abord les différentes structures, les différentes technologies ainsi que leur principe de fonctionnement afin de fixer les objectifs pour la détermination et le développement de méthodes appropriées. La première méthode analysée est

Résumé

la modélisation du comportement électromécanique de la machine qui a pour objectif de déterminer les différents paramètres pour l'évaluation du système (couple, puissance) ainsi que pour les différentes interfaces entre les composants (interface électrique avec l'onduleur) et les modélisations (interface avec le modèle thermique) en fonction du couple demandé, de la vitesse de rotation, de la tension aux bornes de l'onduleur ainsi que les températures dans le stator et le rotor. Pour ce faire, les différentes solutions issus de l'état de l'art dans le domaine sont présentées, expliquées et analysées. Ces méthodes comprennent les approches suivantes : méthode par élément finis, réseau de perméances, circuits équivalents, méthodes analytiques, solutions basées sur des cartographies de la machine ou simple relation énergétique entre la puissance mécanique et électrique.

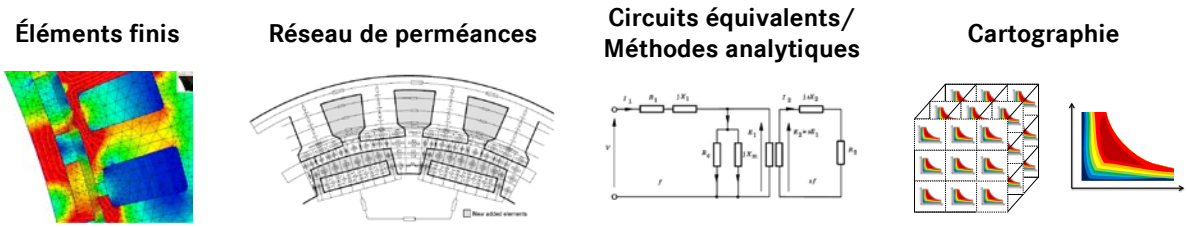

Figure: Méthodes pour la modélisation des machines électriques

Elles sont ensuite comparées en considérant de manière qualitative leur exactitude, leur influence sur le temps de simulation et leur pertinence pour les challenges considérés dans ce travail. Deux solutions ressortent de cette analyse et sont comparées en détail afin de déterminer la solution appropriée. La solution à base de cartographies de machine dépendantes de toutes les entrées de la modélisation est retenue parce qu'elle présente le meilleur compromis entre exactitude et temps de simulation ainsi qu'une indépendance technologique vis-à-vis de la machine. La solution retenue est ensuite comparée avec des mesures réalisées sur un banc d'essai pour chaque technologie considérée et pour différentes valeurs de la tension. Pour valider l'approche considérée, les paramètres suivants sont analysés : la courbe limite de la machine afin de valider la méthode de dimensionnement, les pertes pour valider l'aspect énergétique du problème et le courant qui est un facteur majeur pour les interactions machine/onduleur. Malgré certaines hypothèses faites aux cours des mesures et du développement de la modélisation, on peut voir grâce à cette comparaison que la solution choisie est appropriée. De plus à la fin de cette partie, la valeur-ajoutée de la modélisation est montrée en analysant l'influence du niveau de tension sur les performances de la machine dans le cadre de deux études. La même approche est utilisée au sein de la deuxième partie qui traite de la modélisation thermique. Dans ce cas, le nombre de solutions répondant aux objectifs de ce travail de thèse est limité et ainsi la modélisation s'oriente rapidement vers une solution unique basée sur une approche nodale.

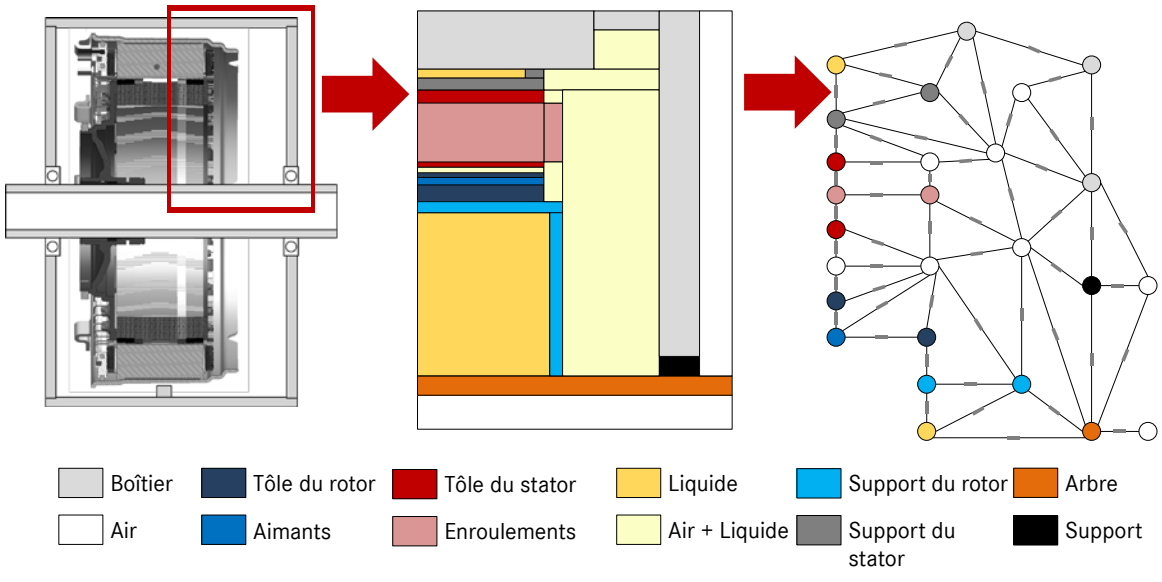

Figure: Structure de la machine et modélisation grâce à une solution nodale

Résumé

Les différentes hypothèses utilisées dans le reste de la thèse sont définies afin de trouver un compromis entre complexité de simulation et temps d'exécution. Ainsi seul deux températures sont considérées : une pour le stator qui correspond à la valeur moyenne de tous les nœuds appartenant aux enroulements du stator et une pour le rotor avec une différenciation entre les machines à aimants permanents et les machines asynchrones. Dans le premier cas, seule la température moyenne dans les aimants est considérée et dans le second cas, seule la température moyenne dans la cage du rotor est considérée. Comme pour le modèle électromécanique, la méthode choisie est validée en utilisant des mesures sur banc d'essai. Les essais statiques et dynamiques montrent tous les deux une bonne corrélation et précision des modèles qui répondent au cahier des charges fixé par la thèse. La valeur ajoutée de la modélisation thermique est ajoutée en montrant l'influence de la variation de température sur les pertes dans le système et le courant requis au niveau de la machine. Même si sur le cycle considéré, cette influence peut être négligée, le développement d'un système hybride est composée de plusieurs critères parmi lesquels l'évaluation de la puissance en continue qui requiert un modèle thermique. Le second chapitre est clos par l'analyse de solution pour l'évaluation de l'intégrabilité ou non de la machine électrique. Les méthodes employées couramment sont la conception assistée par ordinateur qui est trop complexe et trop détaillé pour l'approche choisie pour ce travail de thèse et les méthodes à base de densité de puissance qui ne permettent pas d'évaluer les dimensions exactes de la machine. Dans le cadre de cette thèse l'évaluation est ainsi réduite au volume de la machine seule qui est comparée au volume disponible. Contrairement à la plupart des travaux précédents, le volume de la machine n'est pas limité au seul volume des matériaux actifs : tôles statorique et rotorique mais à l'intégralité des matériaux : enroulements, tôles et excitation du rotor (aimants ou cage d'écureuil). Ainsi la comparaison des technologies se fait en considérant un environnement plus global comme montrée par l'évaluation de la valeur ajoutée. En effet, celle-ci montre les différences de performance entre deux machines où la longueur sans les enroulements et deux machines où la longueur totale de la machine sont considérées. Ce chapitre a ainsi montré pour chacune des modélisations étudiées la démarche à avoir afin de déterminer une solution qui répond au cahier des charges de ce travail de thèse aussi bien en terme de complexité que de précision tout en considérant les différents paramètres permettant de répondre aux enjeux du développement des véhicules hybrides.

Chapitre 3 :

Le troisième chapitre est basé sur la même structure que le second afin de présenter le cas de la modélisation de l'électronique de puissance. Tout au long du chapitre, les deux convertisseurs énoncés dans le premier chapitre sont considérés : l'onduleur multiphasé et le convertisseur Boost. Ce chapitre comme le précédent commence par détailler les structures et le principe de fonctionnement de chacun des deux convertisseurs. Les convertisseurs sont considérés avec des méthodes de contrôle standard et seule la détermination de la modélisation appropriée est analysée tandis qu'aucune étude au niveau de la régulation ou de l'optimisation du contrôle est effectuée. Comme pour la machine, la première approche étudiée est la modélisation énergétique des convertisseurs. Différentes méthodes allant de la modélisation des différentes jonctions dans les semi-conducteurs aux modélisations grâce à des cartographies des convertisseurs en passant par des circuits équivalents et des méthodes analytiques sont étudiées.

Circuit équivalent **Modèle analytique** **Cartographie**

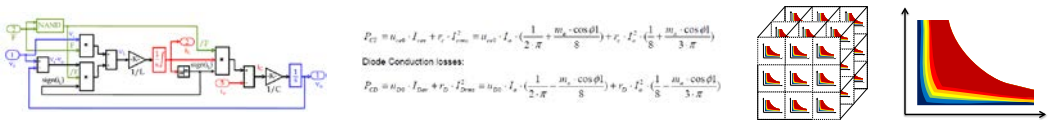

Figure: Méthodes pour la modélisation des convertisseurs

Il en ressort très rapidement que la méthode basée sur une solution analytique représente le meilleur compromis entre précision et simplicité de la méthode. En plus de la méthode choisie, une analyse poussée de la dépendance en courant en en température des composants est réalisée. De plus, les pertes dans les composants passifs sont aussi intégrés (connexion, interconnexion et condensateurs) afin de modéliser l'aspect énergétique de l'ensemble du convertisseur. Par ailleurs et pour chacun des convertisseurs, la méthode des pertes au niveau des semi-

conducteurs est développée pour chacune des technologies considérées : Mosfet et IGBT. Suite à ça, le modèle est validé à l'aide de mesures sur banc d'essai ou des valeurs externes pour différentes valeurs de la tension et pour chaque technologie. Dans le cas de l'onduleur, les valeurs mesurées sur banc d'essai permettent de valider le comportement des pertes et de montrer l'influence des composants passifs pour les différentes valeurs de la tension et les deux différentes technologies. Le cas du convertisseur Boost est plus compliqué étant donné que ce convertisseur est présent seulement dans les modèles de la marque Toyota. La validation a donc été réalisée à l'aide de mesures effectuées par un institut américain ce qui impose de faire de nombreuses suppositions vis-à-vis des mesures. Cependant les résultats valident la dépendance en courant du modèle développé dans ce travail de thèse et montrent de bons résultats. Suite à la validation, une courte comparaison est faire pour montrer que vis à vis-à-vis du cahier des charges de ce travail de recherche, une méthode basée sur des circuits équivalents n'apportait pas de valeur ajoutée. Comme dans le chapitre précédent, la partie se termine par une étude de la modélisation afin de montrer sa valeur ajoutée. Ici la dépendance en tension et en courant de l'onduleur est montrée pour une valeur constante du facteur de puissance et du facteur de modulation afin d'avoir un premier aperçu des facteurs d'influence sur le comportement énergétique de l'onduleur. La seconde modélisation traitée dans ce chapitre concerne le comportement thermique des convertisseurs et plus particulièrement la température de jonction (i.e. la température au niveau des semi-conducteurs). Pour ce faire une analyse des différentes solutions est réalisée. Comme pour la machine électrique, deux solutions majeures sont identifiées : la modélisation par éléments finis ou la solution nodale. La solution nodale est dans le cas de l'électronique de puissance, elle aussi, la solution la plus adaptée. Cependant contrairement à la machine électrique et de par sa structure stratifiée (superposition de différents matériaux entre la partie active et le système de refroidissement), le cas de l'onduleur peut être réduit à une combinaison d'éléments résistifs et capacitifs grâce à une analogie thermique/électrique en supposant l'interaction entre les différents semi-conducteurs au sein d'un même module négligeable.

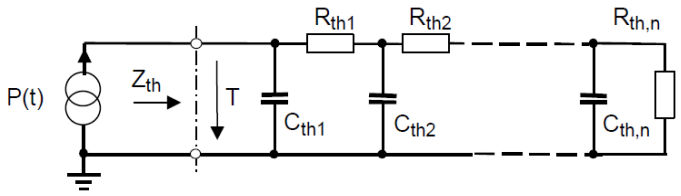

Figure: Modèle thermique équivalent d'un module IGBT

Comme pour la modélisation énergétique, la modélisation est validée en comparant les résultats simulés à des mesures effectuées sur un prototype. Une première hypothèse vis-à-vis des résultats doit être considérée étant donné que la mesure de la température au sein du convertisseur ne se fait pas directement sur le semi-conducteur mais sur une couche inférieure. Malgré cela, les résultats restent probants et peuvent être validés en considérant les variations sur plusieurs couches au sein du circuit électrique équivalent. Les contributions pour l'analyse du système sont montrées en calculant le courant maximum disponible en fonction de la durée d'utilisation. Les valeurs calculées grâce à cette analyse seront utilisées plus tard pour la modélisation des limites du système. La dernière partie de ce chapitre traite de l'estimation des dimensions et du poids des convertisseurs. Comme pour les autres approches, une analyse des solutions est effectuée mais dû aux challenges imposés par l'environnement industriel, aucune solution ne semble convenir. Pour ce travail de thèse, une nouvelle méthode est développée. Le but est de déterminer d'un point de vue global, l'influence direct des paramètres considérés (courant et tension) et des interactions avec les autres composants (batterie et machine électrique) sur le dimensionnement des différents sous-composants des convertisseurs. Pour chacun d'entre eux des approximations sont réalisés et grâce à un algorithme de construction les dimensions et le poids des convertisseurs peuvent être évalués. La valeur ajoutée de cette méthode repose sur le fait que les dimensions et non le volume sont calculées afin de vraiment vérifier l'intégrabilité ou non des convertisseurs.

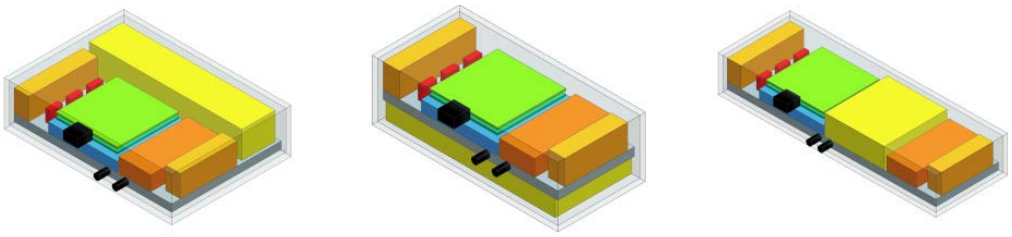

Figure: Architecture utilisée pour la détermination des dimensions de l'onduleur

Dans le cas de l'onduleur, le degré de liberté est fixé au niveau du condensateur qui est utilisé afin de « remplir » la place disponible, rôle joué par l'inductance d'entrée au niveau du convertisseur Boost. Comme pour les autres modélisations, cette partie du chapitre se termine par un aperçu des contributions de la modélisation pour l'analyse des systèmes hybrides. Il peut être observé que la tension et le courant sont deux des facteurs dominants dans la détermination du volume du convertisseur. Le courant pas son influence sur le dimensionnement des connecteurs et interconnections et la tension par son influence sur le condensateur et sur les distances de sécurités électriques. Ce chapitre a ainsi montré comment pour chaque modélisation, une solution appropriée peut être trouvée afin de répondre au cahier des charges de cette thèse. Grâce à la flexibilité de l'environnement Matlab/Simulink, les différentes simulations peuvent être implémentées dans le même environnement afin de simplifier l'optimisation globale.

Chapitre 4 :

Le quatrième chapitre, comme les deux précédents, présente l'analyse et l'implémentation d'un composant électrique : la batterie. Le chapitre commence par une présentation de la structure de la batterie (organisation des cellules) et sur les composants annexes qui sont compris dans le système batterie (connecteurs, système de refroidissement, Cell Management System....) ainsi que le principe de fonctionnement de la batterie et les pertes au sein de celle-ci. Ceci permet de définir les différentes entrées et sorties nécessaires pour la modélisation électrique, thermique et l'évaluation de l'intégration. La première partie est dédiée à la modélisation électrique de la batterie et contrairement aux autres composants, la plupart des méthodes sont basées sur la même approche circuit avec une variation du niveau de détails. Les modèles les plus poussés considèrent les paramètres physiques de la batterie comme la porosité ou le vieillissement des cellules. Des modèles plus simples développés grâce à une spectroscopie par impédance permettent de modéliser le comportement dynamique de la batterie. Finalement des modèles résistifs permettent d'évaluer les chutes de tensions au niveau de la batterie.

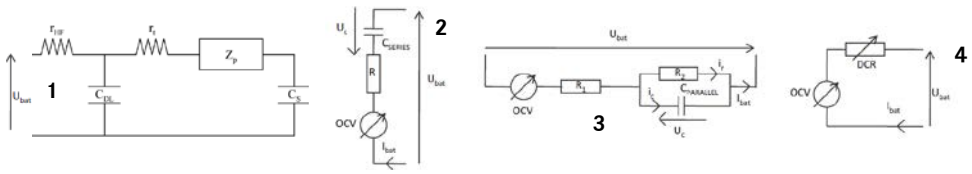

Figure: Circuits équivalents pour la modélisation électrique de la batterie

Même si la dernière simulation est la moins détaillée, elle répond à tous les points du cahier des charges de ce travail de thèse : elle permet d'évaluer l'influence de la tension et du courant pour un grand nombre de composants en considérant le rôle du niveau de charge, de la température et du signe du courant. Les modèles à base de circuit RC ont le désavantage de requérir une spectroscopie par impédance qui est un processus couteux et long, ce qui ne correspond pas à l'étape de développement considérée. L'implémentation est réalisée grâce à Matlab et les différentes validations au niveau des cellules ainsi que les comparaisons avec les méthodes à base de circuit RC montrent que la solution choisie est le meilleur compromis entre exactitude et complexité permettant de considérer l'influence des différents challenges du développement des véhicules hybrides. A la fin de la partie, l'importance de la chute de tension et plus particulièrement de sa dépendance en fonction du temps et de l'état de charge est analysée afin de montrer que considérant les cycles d'évaluation de l'industrie automobile, la solution choisie est la plus appropriée. Concernant la modélisation thermique, l'analyse et l'implémentation ne sont pas discutées en détail

parce que les mêmes solutions que pour l'électronique de puissance sont disponibles et ainsi seuls les paramètres de la modélisation changent. Comme pour les autres simulations, la solution choisie est validée avec des données de mesure. La dernière partie du chapitre est consacrée à l'évaluation de l'intégration des batteries. Même si la solution finale est très proche de la méthode utilisée pour l'électronique de puissance, le cheminement est différent. En effet, dans le cas de la batterie, les valeurs de densité d'énergie du système global et des cellules sont connues. Ainsi, une première approche est développée basée sur ces valeurs. La première ébauche utilise le même rapport de proportionnalité entre le système global et les cellules pour chaque dimension (longueur, largeur et hauteur). Cette solution montre rapidement ces limites même si elle permet dans de nombreux cas de données un aperçu de l'intégrabilité. La seconde ébauche est réalisée avec des facteurs différents pour chaque dimension. Le problème de cette méthode réside dans l'évaluation de ces facteurs. Les valeurs maximales et minimales requièrent de connaitre les sous composants du système et la solution perd ainsi son avantage vis-à-vis d'une méthode similaire à celle de l'électronique de puissance. Ainsi comme pour l'onduleur et le convertisseur Boost, des méthodes sont déterminées pour chaque sous-composant et un algorithme de construction est développé afin de déterminer les dimensions et le poids de la batterie. Deux différentes structures sont considérées, une pour les applications « hautes » puissances (P>30kW) et une pour les applications « basses » puissances (P<30kW).

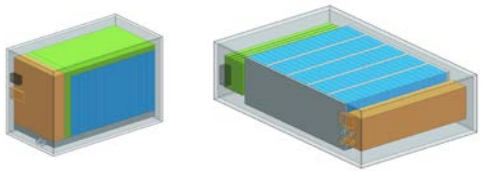

Figure: Architecture utilisée pour la détermination des dimensions des batteries

Chacune des méthodes est validée grâce à des exemples de systèmes faisant partie de l'état de l'art. Finalement les contributions pour le développement des systèmes hybrides sont montrées en analysant la configuration de la batterie (nombre de cellules en série et en parallèle) qui représente directement l'influence du courant de la tension sur le système pour un nombre de cellules constant. Comme on le voit, une augmentation du courant global présente une réduction du volume en doublant le nombre de cellules en parallèle mais le nombre de cellules augmentant, les avantages au niveau du volume se réduisent jusqu'à excéder le volume du système de base. Ce chapitre conclu ainsi la seconde partie de la thèse, où l'influence des challenges et de l'environnement sur le développement des méthodes de modélisation des composants est montrée. Comme pour les composants précédents, des solutions adaptées sont trouvées pour la batterie afin de répondre au cahier des charges de cette thèse en trouvant un compromis entre exactitude et complexité qui permet de couvrir l'ensemble du domaine de recherche.

Chapitre 5 :

Le cinquième chapitre est axé autour de la modélisation du système global. Il commence par présenter de manière générale la définition d'un système et des différentes contraintes pour la modélisation. Les différentes représentations et la dépendance dans le temps sont discutées. Finalement la modélisation du système (optimisation coordonnée des composants grâce à certaines approximations) est montrée et les objectifs de cette thèse sont présentés en détail. Ces objectifs résument l'approche globale : évaluation de l'intégrabilité et des performances en fonction des profils de vitesse et de couple ainsi que du volume disponible. Cette approche globale est la combinaison de deux sous-approches : l'évaluation des performances du système en fonction des profils de vitesse et de couple grâce à la modélisation électrothermique des composants et l'évaluation des dimensions et du poids en fonction du volume disponible et des paramètres des composants. Afin d'atteindre ces objectifs la première partie discute des aspects suivants : la combinaison des différentes modélisations, la modélisation des limites du système et finalement le cas particulier du convertisseur Boost. La combinaison des différentes modélisations représente le premier challenge de ce chapitre. En effet, même si les modèles de composants ont été développés afin d'être intégré au sein d'une modélisation système, l'interface entre la batterie et l'électronique de puissance est dépendante d'une interface avec le reste du véhicule : la charge appliqué par le système 12V sur le système haute tension. Ainsi le courant appliqué au niveau de la batterie est dépendant de la puissance requise au niveau de l'onduleur ainsi que de la puissance requise par le système 12V. Pour ce faire, un « composant » supplémentaire

est intégré au sein du système : le PDU (Power Distribution Unit / Unité de Distribution de la Puissance). Ce composant qui représente une connexion en parallèle des composants est nécessaire afin de définir une seule et unique source de charge pour la batterie. Ainsi les modélisations restent les mêmes et ce composant aussi présent dans les véhicules permet de modéliser avec plus d'exactitude le comportement du système ainsi que l'organisation du câblage dans le véhicule en définissant la longueur des câbles entre les composants. Le second challenge concerne les interfaces avec l'évaluation du système. En utilisant les différents paramètres calculés grâce aux deux sous-approches, trois indicateurs sont définis pour l'évaluation du système. Le premier est le TPI (Torque Profile Indicateur / Indicateur de Profile de Couple) et permet d'évaluer quel pourcentage du profil de couple peut être réalisé par le système. Pour ce faire, le rapport entre le couple actuel et le couple de référence est intégré au cours de la simulation et finalement divisé par le temps de simulation. Si le profil peut être entièrement réalisé, le TPI est égal à 1 sinon il prend une valeur entre 0 et 1. Le second paramètre est le SOCI (State Of Charge Indicator / Indicateur d'État de Charge) qui permet d'évaluer les pertes et l'énergie consommée par le système. Il correspond à la valeur de l'état de charge à la fin de la simulation. Il permet de comparer à intégration et performance équivalente, le système avec la plus grande autonomie électrique/hybride et ainsi le système qui apporte le plus de réduction des émissions et de la consommation. Le troisième paramètre est le SII (System Integration Indicator / Indicateur d'Intégration du Système). Ce paramètre est composée de trois sous-paramètres : les CIIs (Composant Integration Indicator / Indicateur d'Intégration du Composant). Pour chaque composant un facteur est calculé, il représente le produit du rapport entre les valeurs de référence (valeurs maximales disponibles) et les valeurs calculées (longueur, largeur, hauteur et poids) grâce aux méthodes développées dans cette thèse. De plus, une contrainte est appliqué sur ce paramètre : si une des valeurs calculées est plus grande que la valeur maximale autorisée pour ce critère, le CII est égal à zéro afin d'éviter que les paramètres se compensent et assure que le composant est vraiment intégrable au sein du véhicule. L'intégration est ainsi évaluée grâce au produit des CIIs de chaque composant et grâce à la contrainte aucun système avec deux composants ayant une forte densité de puissance et un composant ayant une faible densité de puissance ne pourra être évalué comme système potentiel.

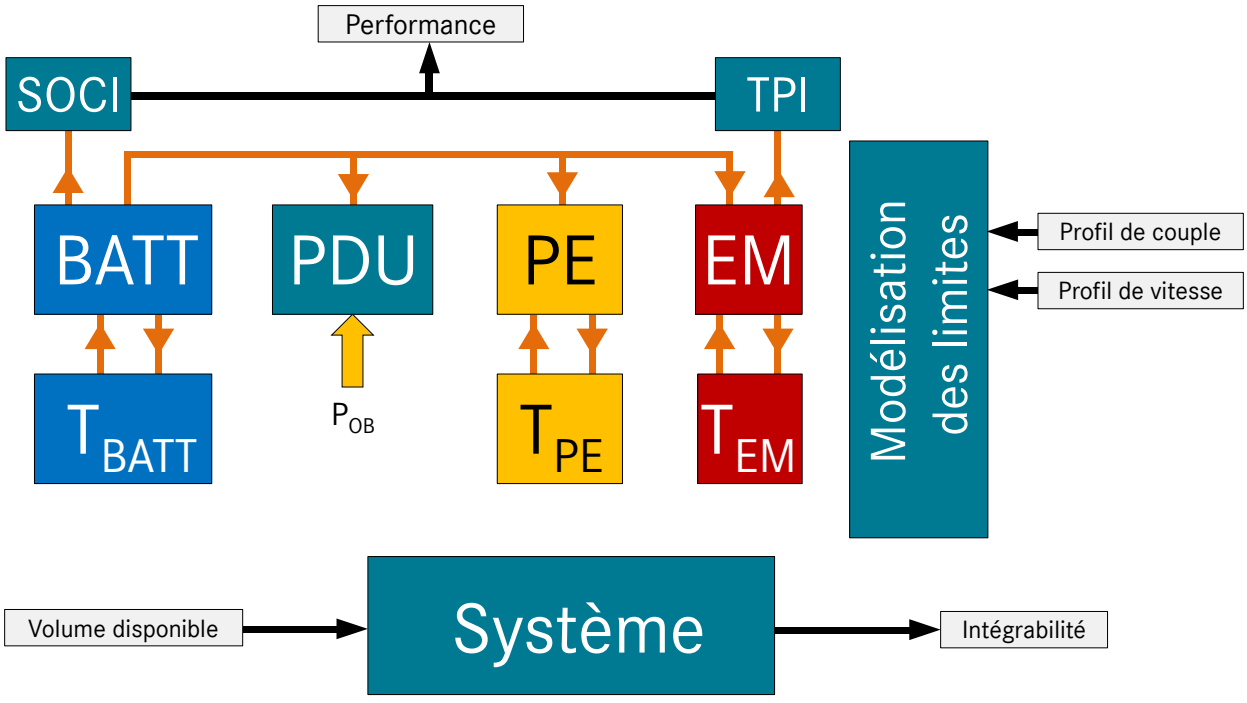

Figure: Implémentation du modèle global du système électrique

Le deuxième challenge de la combinaison des composants relève de la détermination des limites. Elles sont, dans le cadre de cette thèse, au niveau de l'entrée du système et sont traduites par une saturation au niveau du profil de couple. Ces limites considèrent les aspects énergétiques, thermiques et électriques du système. Les limites énergétiques traduisent les limites du système en fonction de l'état de charge. Ainsi quand l'état de charge est égal à zéro, aucune charge ne doit être appliquée au niveau de la batterie. De plus les pertes de la machine et de

l'onduleur quand aucune charge mécanique n'est appliquée ne sont pas égales à zéro. Ceci implique que dans le cas d'un état de charge égal à zéro, le système doit fonctionner en générateur afin d'éviter d'appliquer une charge sur la batterie. Quand l'état de charge est à sa valeur maximale, le système est seulement autorisé á fonctionner en régime moteur afin de ne pas dépasser la capacité maximale de la batterie. Les limites thermiques du système sont la combinaison des limites de chaque composant. Pour chaque composant une pré-analyse est réalisée afin de déterminer la puissance en continu de chacun d'entre eux, cette valeur est définie comme la puissance permettant un refroidissement du composant et ainsi permet au système après un certain temps de fonctionner en régime maximum à nouveau. Les limites en terme de puissance au niveau de chaque composant sont ensuite traduites en terme de couple en utilisant les pertes au sein du système afin d'en faire des valeurs de saturation applicables directement sur le profil de couple. Les limites électriques du système sont traduites par des limites de courant en fonction de la tension au niveau de l'onduleur et de la batterie. Ces limites sont fixées afin d'éviter de dépasser les valeurs minimales et maximales de la tension au sein du système. Pour ce faire, les limites en courant sont converties en limite de puissance dépendantes de la tension, elles-mêmes converties en limite de couple comme précédemment pour les limites thermiques. Toutes ces limites sont implémentées dans la simulation en entrée dans un bloc qui contrôle l'énergie qui peut être appliquée au système et non les flux d'énergie au sein de celui-ci. La suite de ce chapitre présente la validation de cette modélisation globale développée grâce à la combinaison de solutions appropriées pour la modélisation des composants. Deux validations sont réalisées : une première sur banc d'essai où seul le comportement de l'ensemble machine/onduleur est analysé et une seconde où le même système est mesuré dans un prototype avec la batterie permettant ainsi de valider le comportement global du système. Pour la première validation, les paramètres suivants sont considérés : le couple, la vitesse et la puissance DC. Cela permet de valider le comportement mécanique (couple et vitesse) ainsi que les pertes au sein du système (puissance DC). La comparaison entre les résultats de la simulation et les mesures montrent une haute corrélation et de faibles écarts. Le comportement de la batterie a été remplacé par une courbe de tension pour le simulateur de tension sur le banc d'essai. Malgré les hypothèses au niveau de la simulation, cette première validation montre que les solutions choisies sont adaptées pour une modélisation globale du système électrique dans les véhicules hybrides. La seconde validation considère les paramètres suivants : le couple, la tension, la puissance DC et l'état de charge ainsi que les températures afin de valider les aspects électriques, thermiques et énergétiques. Dans un premier temps la comparaison du couple, de la tension, de la puissance DC et de l'état de charge montre une haute corrélation et de faibles écarts même si ceux-ci tendent à augmenter en fin de simulation.

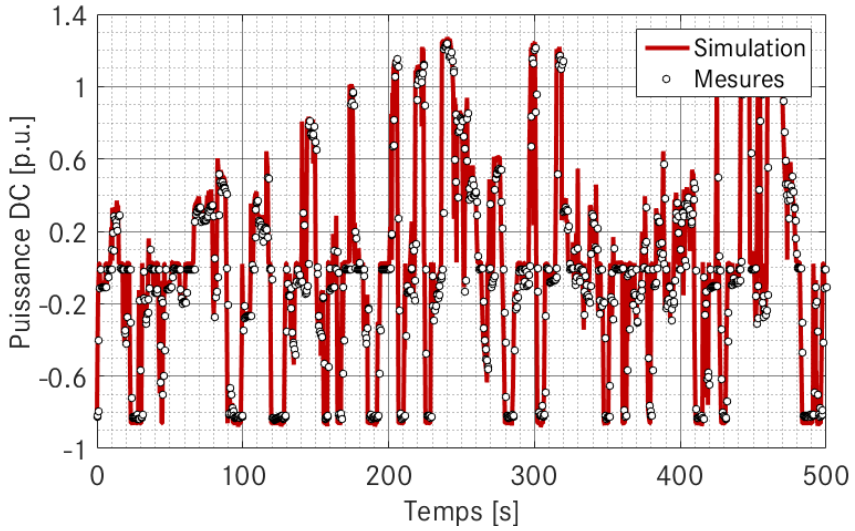

Figure: Validation du modèle global, comparaison de la puissance DC

La comparaison du comportement thermique entre la simulation et les mesures présentent de plus gros écarts aussi bien au niveau du comportement que des écarts principalement pour la machine électrique et l'onduleur. Dans le cas de la machine, ces écarts sont dus à une approximation au niveau de la modélisation thermique : le flux est supposé constant dans la simulation alors que du à l'intégration du système de refroidissement, le flux réel au sein de la machine dépend de la vitesse de rotation. Pour l'onduleur, les déviations sont dues à des différences au niveau

du pas de simulation et du pas de mesure. En effet les pics au niveau de la simulation sont présents uniquement entre deux points de mesure, ce qui implique qu'ils ne sont pas forcément faux mais que la dynamique de la modélisation est supérieure au temps de mesure de la température au sein du véhicule. Ainsi les deux validations malgré certaines approximations montrent que les solutions choisis au niveau du système et des composants sont appropriées pour modéliser le comportement global du système. Grâce à ces validations et aux adaptations faites au niveau de la machine, la fin du chapitre peut montrer les contributions de cette modélisation pour l'évaluation des systèmes hybrides. Ces contributions sont montrées en analysant d'abord les limites mécaniques du système, puis les propriétés du système (efficacité, tension et courant) et finalement le comportement énergétique en comparant les méthodes indépendantes et dépendantes du temps. Que ce soit en analysant les limites du système, les variations de tension, du courant ou de l'efficacité, les mêmes conclusions peuvent être faites. La contribution majeure de ce travail de thèse au niveau de la modélisation et de l'analyse du système est la modélisation des variations de tension et son implémentation au sein de la méthode de dimensionnement au lieu d'attendre la phase d'évaluation pour en tenir compte. Cette contribution se voit en comparant la méthode développée pour ce travail de thèse avec différentes approches où la tension est supposée constante. Que ce soit avec ou sans pré-analyse du système aucune méthode ne permet de décrire et de dimensionner correctement le système. Certaines méthodes présentent de faibles écarts avec la méthode globale mais seulement pour un domaine défini.

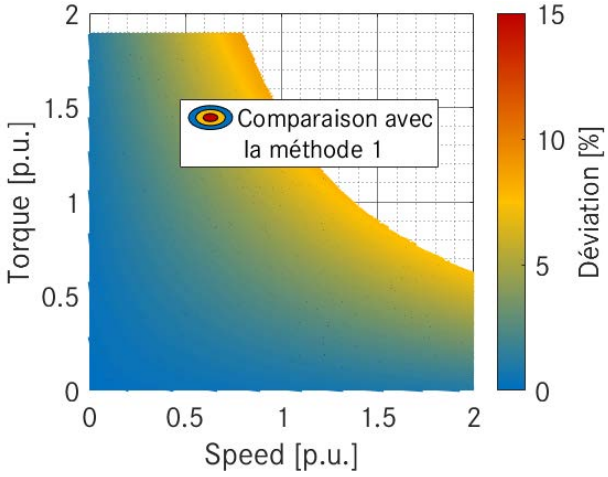

Figure: Comparaison de la méthode développée avec le calcul en circuit ouvert (méthode 1)

L'analyse, de la dépendance en temps de la modélisation, montre l'importance d'un second paramètre qui est lui aussi considéré normalement seulement durant la phase d'évaluation et pas durant la phase de dimensionnement : l'influence des variations de l'état de charge. Même si certaines approximations peuvent être réalisées pour analyser le système de manière statique, ses variations jouent un rôle majeur et leur considération durant la phase de dimensionnement est non négligeable. La dernière partie de ce chapitre compare les résultats de l'analyse indépendante des composants avec les résultats du système global au niveau de l'efficacité et de l'intégration. Cette analyse des différentes approches montrent une fois de plus que même si l'un des composants joue un rôle majeur dans le dimensionnement du système, une analyse conjointe du système comme la méthode développée dans ce travail de thèse est nécessaire. En effet même si la plupart des challenges peuvent être analysés au niveau des composants (influence de la tension), les résultats concernant le système global et le compromis à réaliser concernant les différents composants peuvent être relativement éloignés des résultats de cette analyse individuelle des composants. Ces analyses permettent cependant de réduire le champ d'étude et de dimensionner ainsi de manière plus efficace le système. Ce chapitre a ainsi montré comment les différentes modélisations peuvent être combinées afin de développer une approche globale. Pour cela, certaines adaptations sont nécessaires et la mise en place des limites du système permettent de modéliser correctement les aspects électriques, thermiques et énergétiques. Cette modélisation a aussi été validée grâce à des mesures sur banc d'essai et sur un prototype qui montre la justesse des méthodes choisies. Finalement les contributions de la méthode globale sont montrées pour différents aspects et paramètres du système qui montrent l'importance d'une analyse du système.

Chapitre 6 :

Le dernier chapitre est organisé autour de la thématique de l'optimisation du système. Il présente dans un premier temps les bases des méthodes d'optimisation et d'évaluation, ensuite la détermination et l'implémentation de la solution choisie, puis l'application aux systèmes électriques dans les véhicules hybrides et finalement les résultats pour différents systèmes et applications. La première partie est théorique et présente les définitions de bases concernant les contraintes et les critères, ces définitions sont utilisés afin de déterminer au sein du cahier des charges quels paramètres sont évalués et quels paramètres servent de contrainte pour la démarche d'optimisation. Suite à ça, les différentes méthodes d'évaluation sont présentées pour des approches multicritère comme celle de ce travail de thèse : la méthode de la somme pondérée, l'optimum au sens de Pareto ainsi que d'autres méthodes moins conventionnelles. Finalement la partie se termine avec la présentation des différents types d'algorithme d'optimisation. La seconde partie détermine grâce aux observations et définitions la méthode appropriée pour le cas considéré dans ce travail de thèse : l'environnement automobile. L'influence majeure de cet environnement et le challenge majeur de ce sujet de recherche est la détermination de la meilleure combinaison de composant au lieu de la combinaison des meilleurs composants. Il est supposé dans ce travail de thèse, qu'une solution basée sur la méthode de la somme pondérée ou l'optimum au sens de Pareto n'est pas appropriée. Ainsi une solution booléenne basée sur les paramètres définis dans le chapitre précédent est choisie. Les performances du système sont ainsi optimisées en considérant le produit du TPI et du SOCI mettant sur pied d'égalité les performances du système et l'aspect énergétique du problème. La valeur ajoutée de cette méthode est montrée sur un ensemble de composants en comparant cette approche avec la somme pondérée. Le reste de cette partie est ensuite axée sur la détermination de l'algorithme d'optimisation adéquat pour le problème choisi. Pour cette détermination, deux facteurs importants sont à considérer : aucun nouveau sous-composant ne peut être généré et la plupart des sous-composants ne sont disponibles que sous une forme discrète (pas de variation continu des niveaux de tensions mais définition pour une plage de valeurs). Ces facteurs jouent un rôle important dans la détermination de l'algorithme et la solution choisie s'oriente vers une solution basée sur un algorithme d'exploration. Ces algorithmes permettent de couvrir de manière efficace un grand nombre de solutions dans le champ de recherche. Parmi ceux.ci l'algorithme DIRECT (DIvided RECTangles) est retenu de par sa simplicité d'implémentation.

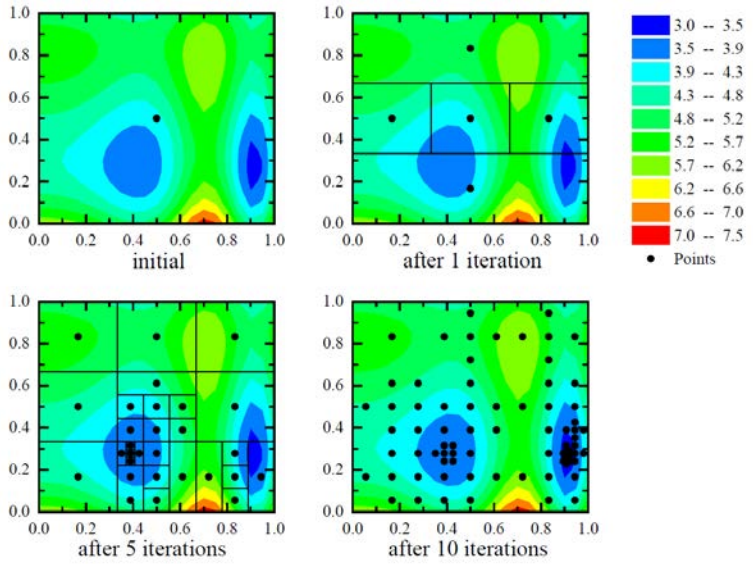

Figure: Exemple d'utilisation de l'algorithme pour un problème de minimisation [47]

En effet, pour considérer un problème discret sans utiliser d'arrondis, un critère est ajouté sur l'algorithme afin de considérer seulement des solutions discrètes. Cette valeur ajoutée est montrée sur un exemple en comparant la solution discrète avec la solution basée sur les arrondis. Considérant des arrondis, le système est généralement surdimensionné et la valeur ajoutée vis-à-vis des méthodes précédentes (optimisation coordonnés des composants) est moindre. Finalement l'implémentation est présentée. La partie suivant se concentre sur les conditions aux limites du problème et plus particulièrement les aspects suivants : niveau de tension, l'architecture du système, la topologie

de l'électronique de puissance, les technologies de machines et les stratégies de module, ainsi que la détermination du système considéré et du processus d'optimisation. Le rôle de chaque aspect est présenté et certaines limites concernant les variations de ceux-ci sont introduites (par exemple : seules les machines synchrones à aimants permanents et asynchrone à cage d'écureuil sont considérées). Ensuite le système étudié dans ce chapitre est présenté : un système de type parallèle où la machine électrique est intégrée entre la boite de vitesse et le moteur thermique après l'embrayage. Cette architecture est une solution courante au sein de l'entreprise où la thèse a été effectuée mais aussi sur le marché des véhicules hybrides de par sa simplicité d'implémentation. Elle permet de couvrir de nombreux niveaux de puissances (trois sont considérés dans ce travail) et différents niveaux de tension.

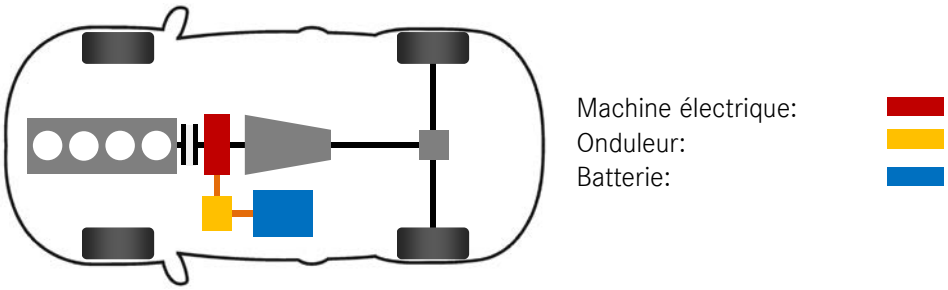

Figure: Architecture considérée pour l'optimisation et l'analyse du système eDrive

Suite à ça, l'approche pour l'optimisation est elle aussi définie. Elle est divisée en deux parties, une première partie où des filtres sont implémentés afin de réduire le nombre de solutions à considérer et une seconde où la méthode définie dans la partie précédente est utilisée. De plus pour certains paramètres des hypothèses sont faites afin de déterminer les limites du système. La dernière partie de ce chapitre présente les résultats d'optimisation en commençant par l'apport des filtres puis en montrant les résultats de l'optimisation globale du système pour différentes valeurs de la puissance électrique avant de discuter des cas particuliers. Les filtres tout d'abord sont tout d'abord redondants vis-à-vis de la puissance : si la puissance maximale de la batterie est inférieure à la puissance mécanique requise au niveau de la machine, le système est exclu. Une seconde série de filtres considèrent l'intégration : en effet le calcul des dimensions et des masses des composants étant très peu couteux en temps de simulation, toutes les combinaisons possibles sont calculées afin de filtrer les solutions non intégrables. Finalement des filtres concernant les spécificités de l'industrie automobile (tension maximale ou stratégie de module par exemple) sont introduits afin de limiter avant l'évaluation le champ de recherche. Suite à ça, les résultats globaux de l'optimisation pour trois niveaux de puissance sont analysés et l'ensemble des résultats convergent dans la même direction : considérant les méthodes actuelles comme référence, une réduction de la tension est positive pour la réduction des pertes mais aussi pour une réduction du volume. Cette conclusion globale est en partie liée aux pertes au sein de l'onduleur mais aussi au cycle de fonctionnement considéré. En effet, le cycle actuel de certification ne présente aucun enjeu majeur pour les niveaux de puissance considérés dans ce travail et offre une flexibilité au niveau du dimensionnement des composants. Ainsi pour ces gammes de puissance, la machine ne fonctionne jamais à la limite maximale de tension et de par ce fait le courant AC ne joue aucun rôle au niveau des variations de pertes. Seule la tension DC qui influence les pertes dans l'onduleur peut être variée et sa réduction entraine une réduction globale des pertes dans l'onduleur. L'augmentation du courant AC est seulement la conséquence des critères de puissance qui malgré la réduction de la tension doivent être remplis. Ainsi il peut être conclu, que considérant le cycle actuel de certification, une réduction de la tension et une augmentation du courant représentent un avantage énergétique pour les systèmes hybrides avec l'architecture considérée. Le chapitre traite aussi à la fin différents cas spécifiques qui montre la flexibilité de l'environnement de simulation développé dans ce travail de thèse mais aussi les différents enjeux du développement des systèmes hybrides : technologie 48V, systèmes à haute puissance (P>150kW), les systèmes avec convertisseur Boost, les différentes technologies de machines ainsi que les stratégies de module.

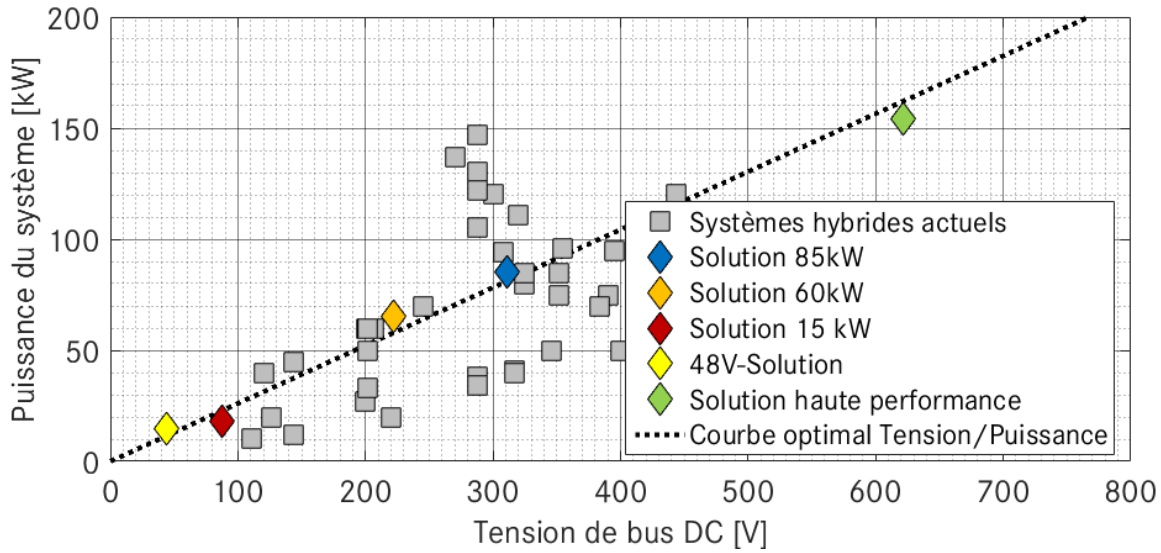

Figure: Relation entre la tension et la puissance pour l'architecture considérée

Globalement ce chapitre a montré le potentiel d'une optimisation globale des systèmes électriques en choisissant la bonne approche et en considérant de manière efficace les contraintes imposées par l'environnement automobile et les critères de celui-ci. Ces résultats montrent ainsi pour l'architecture considérée une dépendance linéaire entre la tension et la puissance du système qui requiert d'être encore testée pour d'autres architectures.

Conclusion :

Grâce à l'analyse du développement actuel et des travaux précédents sur le sujet ainsi qu'au développement d'outils de simulation, cette thèse étudie et analyse les relations entre le niveau de tension et de courant, et les performances du système dans différents cas. Les résultats permettent de déterminer l'influence de ces paramètres sur les composants ainsi que l'impact de l'environnement industriel sur les résultats. En tenant compte du cadre législatif actuel, les résultats convergent globalement tous dans la même direction: une réduction du niveau de tension, respectivement une augmentation du courant, entraine une amélioration du système global par rapport aux méthodes de dimensionnement actuelles. Ces observations sont liées à l'architecture, au cycle d'évaluation et à l'environnement considéré mais les méthodes et l'approche développées ont posé les bases pour étendre les connaissances dans le domaine de l'optimisation des véhicules hybrides. En plus de l'optimisation générale, des cas particuliers sont analysés afin de montrer la modularité des méthodes et l'influence de paramètres supplémentaires (système 48V ou convertisseur Boost). Afin de conclure, cette thèse a mis en place les bases pour l'étude des composants électriques pour les véhicules hybrides. De part un environnement fluctuant et les nombreuses technologies possibles, ce sujet suscite encore un grand intérêt et les points suivants peuvent être encore étudiés de manière plus détaillée: application des méthodes pour d'autres systèmes de propulsion (autre architectures hybrides, véhicule à pile à combustible ou tout électrique), étude de nouvelles technologies comme le carbure de silicium pour l'électronique de puissance, la machine à reluctance variable ou le sulfure de lithium pour les batteries, analyse d'autre cycle d'évaluation ainsi que leur cadre législatif, mise en place de structures additionnelles pour l'électronique de puissance ainsi que des validations supplémentaires avec d'autres composants. La méthode développée pourrait aussi être étendue à l'ensemble du système électrique dans le véhicule afin de considérer d'autres enjeux tel que l'optimisation de la tension en considérant conjointement les performances du système et le temps de recharges par exemple.

Acknowledgment

This thesis would not have been possible without the help and the support of so many people in so many ways. It is also the product of several years of works which I survived thanks to a large amount of coffee, chocolate and other sweets. All the people I encountered during these years have changed me and have directly or indirectly influenced the results of this work. I would like to thank all the people, who have made this thesis possible.

Among them, I want to thank professors Noureddine Takorabet and Serge Pierfederici for their support, their advice and their pertinent remarks during these three years. I also want to thank the professors Xuefang Lin-Shi, Abdesslem Djerdir, Betty Lemaire-Semail and the Dr. Alexandre de Bernardinis who accepted to be my rapporteurs and examiners for this thesis. Finally I want to thank Prof. Bernard Davat, head of the GREEN, who accepts to supervise this work in the laboratory.

Then I want to thank particularly Dr. Steffen Henzler, who offers me the possibility to join his team, for his support during these years, purposeful remarks and suggestions during the thesis. I also what to thank Dr. Randy Doolittle for his advices, his remarks and his support during this thesis but also for the good working atmosphere in our room during these years. Finally I want to thank particularly Dr. Corrado Nizzola, head of the department, for his advices and his support.

Beside them, I want to thank all the employees of the Daimler AG which contributes in any way to this work and particularly the colleagues of the department: Florian, Mark, Tobias, Randy, Harald, Matthias, Jaime, Robert, Markus, Heiner, Michael, Robert, Sicong, Nis, Wolfgang, Nadine, Holger, Johannes, Manuel, Andreas, Simon, Andreas, Dennis, Denis, Felix, Daniel, Norbert, Aleksandar, Philipp, Simon, Maria, Madeleine and particularly Manuela. I also want to thank all the students who were in the department and particularly the following ones: Christina, Matthias, Robin, Matthias, Antonio, Markus, Daniel, Axel, Wilco and Daniel.

Moreover I want to thank all the employees of the University which contributes scientifically or administratively to this work and especially the other PhD students from the GREEN laboratory: Ivano, Jérémy, Geoffrey, Davide, Adrien and Najla as well as the other colleagues from the laboratory: Farid, Babak, Julien, Jean-Philippe, Thierry, Fadi, Latifa and Denis for the good atmosphere during each of my visits.

Furthermore I want to thank my family and my relatives for their support during these three years and particularly my mother for her support during all these years, for always standing behind me in all situations. I would also like to thank those who have already left us, even though they are no longer there, they have helped me becoming the person I am right now.

Finally I want to thank all the people I may have forgotten and Maya for the last proofreading...

Thanks to all

“Theory is when you know everything but nothing works. Practice is when everything works but no one knows why. Here theory and practice are combined: Nothing works and no one knows why”

Anonym

Contents

Index of figures

Index of figures

Index of tables

Nomenclature

Abbreviations:

AC:	Alternating current
AWD:	All Wheel Drive
BAT:	Battery
BEV:	Battery Electrical Vehicle
BMU:	Battery Management Unit
CAD:	Computer Aided Design
CMU:	Cells Management Unit
DC:	Direct current
DCM:	Direct Current Machine
DIRECT:	DIvided RECTangles
ECE:	Economic Commission for Europe
EM:	Electric Machine
ESS:	Energy Storage System
FE:	Finite Element
FEA:	Finite Element Analysis
FCEV:	Fuel-Cell Electrical Vehicle
GA:	Genetic Algorithm
GSA:	Global System Approach
HEV:	Hybrid Electrical Vehicle
HP:	High Power
ICE:	Internal Combustion Engine
IGBT:	Isolated Gate Bipolar Transistor
IM:	Induction Machine
LFP:	Lithium iron phosphate
LCO:	Lithium cobalt oxide
LMO:	Lithium manganese oxide
LP:	Low Power
Mosfet:	Metal–oxide–semiconductor field-effect transistor
NCA:	Lithium nickel cobalt aluminum oxide
NEDC:	New European Driving Cycle
NMC:	Lithium nickel manganese cobalt
OBC:	On-Board Charger
OCV:	Open Circuit Voltage
PA:	Product Approach
PAB:	Product Approach combined with Boolean approach
PDU:	Power Distribution Unit
PE:	Power Electronics
PHEV:	Plug-In Hybrid Electrical Vehicle
PMSM:	Permanent Magnet Synchronous Machine

PSO:	Particle Swarm Optimization
RWD:	Rear Wheel Drive
SESM:	Separately Excited Synchronous Machine
SHEV:	Sports Hybrid Electrical Vehicle
SOC:	State Of Charge
SRM:	Switched-Reluctance Machine
VDA:	German Association of the Automotive Industry (Verband der Automobilindustrie)
VEGA:	Vector Evaluated Genetic Algorithm
WLTC:	Worldwide harmonized Light vehicles Test Cycle
WSM:	Weighted Sum Method

Symbols:

A:	Cross section area
$\hat{B}$:	Magnetic flux density
$Battery_{l/w/h}$:	Battery length/width/height
$\hat{B}_{gen}$:	Magnetic flux density in generator mode
$\hat{B}_{mot}$:	Magnetic flux density in motor mode
C_0:	Capacitance of the capacitor C0
$C1$:	Capacitance of the first RC-circuit
$C2$:	Capacitance of the second RC-circuit
Cap_{equi}:	Equivalent capacity
C_{eddy}:	Eddy-current losses coefficient
$Cells_{l/w/h}$:	Cells length/width/height
C_{hyst}:	Hysteresis losses coefficient
CII:	Component Integrability Indicator
$\cos\varphi$:	Power factor
C_{thi}:	Thermal capacitance of the sub-part i
C_x:	Capacity of the component/sub-component x
D:	Duty ratio
$D_{generator}$:	Duty ration during generator operation
D_{max}:	Worst-case/maximal duty ratio
D_{motor}:	Duty ration during motor operation
E_{off}:	Off-switching energy
E_{on}:	On-switching energy
E_{rec}:	Diode recovery energy
ESR_{C0}:	Equivalent Series Resistance of the capacitor C0
E_x:	Energy of the component/sub-component x
f:	Frequency
f_i:	Simulated values
f_{output}:	Inverter output frequency
f_{switch}:	Switching frequency
i:	Index

I_0:	Equivalent current for loss calculation
I_{AC}:	AC-Current
I_{ACrms}:	rms Value of the AC-current
I_{Batt}:	Battery current
I_C:	Iron losses equivalent current
I_{cell}:	Cell current
I_{Crms}:	rms Value of the capacitor current
i_d:	d-axis current
I_{DC}:	DC-current
i_{dq}:	d-axis and q-axis current
I_{max}:	Maximal current
I_{nom}:	Nominal current
i_q:	q-axis current
I_r':	Rotor current
I_s:	Stator-/Phase-current
I_{sL}:	Stator leakage current
I_{switch}:	Switching current
$I_{switch_{off}}$:	Off-Switching current
$I_{switch_{on}}$:	On-Switching current
$I_{switch_{rec}}$:	Diode recovery current
I_μ:	Magnetization current
k:	Material parameter
k_i:	Material parameter
K_T:	Temperature coefficient
L_d:	d-axis inductance
L_m:	Coupling inductance
L_q:	q-axis inductance
$L_{\sigma s}$:	Stator leakage inductance
$L_{\sigma r}'$:	Rotor leakage inductance
M:	Number of series paths in battery
m_f:	Frequency modulation ratio
m_i:	Modulation index/Modulation factor
n:	Rotational speed
N:	Number of parallel paths in battery
n_{phase}:	Number of phases
$NpMs$:	Battery configuration with M series paths and N parallel paths
N_w:	Number of winding
OCV_{max}:	Maximal open circuit voltage
p:	Pole pair number
P_{AC}:	AC-Power
P_{Batt}:	Battery power
$P_{busbar\ AC}$:	Losses in the AC-busbar

$P_{busbar\ DC}$:	Losses in the DC-busbar
$P_{busbar\ input}$:	Losses in the input busbar of the DC/DC-converter
P_{C0}:	Losses in the capacitor C0
P_{CD}:	Diode conduction losses
P_{chem}:	Chemical power of the battery
P_{copper}:	Copper losses/ohmic losses/Joule losses
P_{CT}:	Transistor conduction losses
P_{Ctotal}:	Total conduction losses of the converter
P_{DC}:	DC-Power
P_{EM}:	Electrical Machine Power
p_f:	Pulse number per half cycle
$\overline{P\ *_{FE}}$:	Iron losses for alternating current
P_{Fe}:	Iron losses for direct current
P_{iron}:	Iron losses in electric machine
$P_{loss/cell}$:	Cell losses
P_{mech}:	Mechanical power
P_{OB}:	Chassis power
P_{switch}:	Switching losses
P_x:	Power or loss power of the component/sub-component x
R:	Electrical resistance
$R1$:	Resistance of the first RC-circuit
$R2$:	Resistance of the second RC-circuit
$R_{busbar\ AC}$:	Resistance of the AC-busbar
$R_{busbar\ DC}$:	Resistance of the DC-busbar
$R_{busbar\ input}$:	Resistance of the input busbar
$R_{busbar-module}$:	Module busbar resistance
$R_{busbar-system}$:	Busbar resistance of the battery system
r_c:	Collector emitter on-state resistance
R_C:	Iron losses equivalent resistance
r_D:	Diode resistance
R_{DSon}:	Drain source on-state resistance
R_{max}:	Maximal resistance
R_r':	Rotor resistance
R_s:	Stator phase resistance
R_{thi}:	Thermal resistance of the sub-part i
s:	Slip
S_{AC}:	AC apparent power
SII:	System Integrability Indicator
SOC_{equi}:	Equivalent state of charge
$SOCI$:	State of charge indicator
S_x:	Apparent power of the component/sub-component x
T:	Temperature

t_0:	Required time
T_{EM}:	Electric Machine Torque
t_i:	Initial time
T_{IM}:	Induction Machine Torque
$T_{IM-rotor_{mean}}$:	Mean IM rotor temperature
T_{nom}:	Nominal temperature
TPI:	Torque profile indicator
T_{PMSM}:	Permanent Magnet Synchronous Machine Torque
$T_{PM-rotor_{mean}}$:	Mean PMSM rotor temperature
$T_{stator_{mean}}$:	Mean stator temperature
T_{switch}:	Switching period
U_0:	Required voltage
U_{Batt}:	Battery voltage
U_C:	Iron losses equivalent voltage
U_{ce0}:	IGBT on-state zero-current collector-emitter voltage
U_{cell}:	Cell voltage
U_d:	d-axis voltage
U_{Design}:	Design voltage
U_{D0}:	Diode zero-current voltage
U_{DC}:	DC-Voltage
U_{max}:	Maximal voltage
U_{module}:	Module voltage
U_{nom}:	Nominal voltage
U_q:	q-axis voltage
U_q:	Induced voltage
U_s:	Stator-/Phase-voltage
U_{system}:	Battery system voltage
U_{WoC}:	Worst-case voltage
U_x:	Voltage of the component/sub-component x
$V_{Battery}$:	Battery volume
V_{busbar}:	Busbar volume
$V_{busbar/ref}$:	Reference busbar volume
V_{cells}:	Cells volume
V_{core}:	Core volume
$V_{heatsink}$:	Heatsink volume
$W_{heatsink}$:	Heatsink weight
y_i:	Measured values
$\bar{y}$:	Mean value of the measured values y_i
α:	Steinmetz parameter
β:	Steinmetz parameter
ΔU:	Voltage ripple
ΔI:	Current ripple

η_x:	Efficiency of the component/sub-component x
Ψ_{PM}:	Permanent Magnet Flux Linkage
ω_{el}:	Electrical rotational speed
ω:	Rotational speed
π:	PI-Number
$\rho_{heatsink}$:	Heatsink density

Introduction

This work analyzes the challenges faced by electric components in hybrid vehicles. The system in interest is called the electric drive system or eDrive system. This system considers the behavior and the interactions between the following components: the electric machine, the power electronics and the energy storage system. The analysis of these components as an entity for hybrid electrical vehicle development is a topic of high interest because it allows shifting the challenges to a restrained scope and to refine the analysis but also to identify optimized system instead of combining optimized components.

This introduction begins with a brief discussion of the motivation and the current situation of hybrid electrical vehicle, which is used to show the relevancy of a global approach for the investigation of electric components. Following this, the contribution and the guiding statement of this work are discussed before introducing the structure of the work.

Motivation

Automobile symbolizes freedom in our modern society for more than a century. However, this object of fascination and its industry are currently confronted with new social, environmental and economic challenges which have resulted in a deep transformation of the sector [1]. Facing this situation, most governments and international institutions have set up norms and standards for the quantification the automotive impact [2] and thus defined goals for the development of sustainable vehicles (Appendix 1).

The solutions are various and multiple because the sector needs to develop sustainable concepts which fulfill ecological requirements without hindering the customers' expectation toward automobile. These solutions extend from the optimization of internal combustion engine vehicle up to vehicle electrification [3]. However with more than 80 million vehicles produced every year [4] and cultural disparities around the world, no solutions have taken a clear leadership and each improvement path still need to be investigated considering the influence of the different sources of emission in a vehicle as shown on Figure 1.

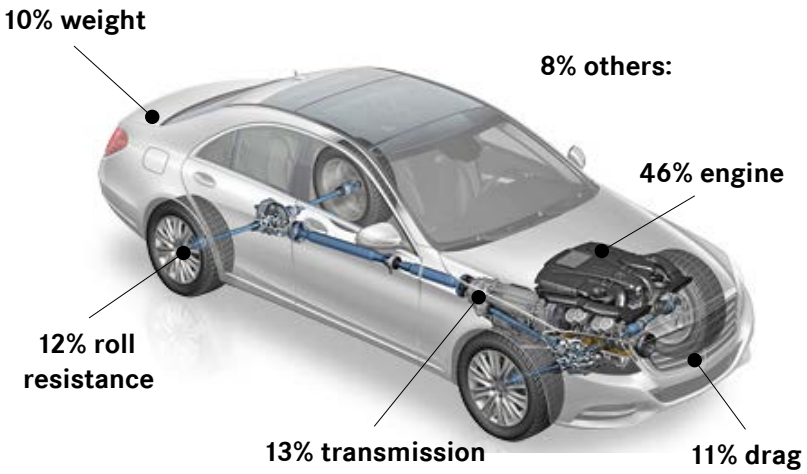

Figure 1: Sources of CO_2-emissions in a mid-class segment vehicle adapted from [3]

Among the solutions for more electrified vehicle, the hybrid electrical vehicles have taken a light edge but remain currently marginal in the global automotive market [5]. The interest for this technology arises as it stands for a suitable short-term solution to reduce greenhouse gas emissions, cut down the consumption as well as it meets customers' expectation. Hybrid electrical vehicle is a widely research topic and are presents in the automotive industry since its early days for the purpose of combining the good efficiency of electric drives with the high energy

density of fossil fuels. The investigations extend from components optimization (design, control or cooling) up to drivetrain and vehicle investigations (architecture or power/energy combination). However, through multiple technological improvements and due to their distinct intrinsic characteristics, component development has reached a critical point where one component optimization could worsen or hinder the performance of another one.

Contribution of the work

Among the many challenges faced by hybrid electrical vehicle, this work aims to investigate the electric drive system and the interactions within it. Contrary to previous works, they are considered as an entity for an optimization purpose. By choosing this approach, this work can contribute to the better understanding of the electric drive system and allows studying a wide parameter range. This parameter range is depicted by the investigation of voltage and current levels, power electronics topologies and module strategies for example. The aim and the contributions of this work lie thereby in the resolution of the following statement:

Determine the sufficient level of details in modeling electric components at the system level and develop models and tools to perform dynamic simulations of these components and their interactions in a global system analysis to identify ideal designs of various drivetrain electric components during the design process.

To achieve this aim and bring further answers concerning the potential of hybrid electrical vehicles, this work studies in details the following aspects: suitable modeling approach, global system analysis and electric drive system optimization. For this purpose, a complete analysis of the spectrum of modeling methods needs to be performed. It includes a review of previous works and investigation on electric components modelings, hybrid vehicle optimization as well as the investigation of alternative solutions from the global literature. Using a suitable approach, the electric drive system needs to be investigated from a more global point of view. Considering it as a standalone entity, the challenges faced by hybrid electrical vehicles can be better addressed by determining the best combinations of components instead of the best component combination. The final aspect considered in this work lies in the definition and the identification of what can be considered as an optimum solutions. It is particularly important because this work show improvement toward integration, efficiency and power density without considering new technologies or new concepts. It shows, thanks to well defined interfaces with the rest of the vehicle, suitable modeling approach and a global system approach, the potential of electric component with the currently available technologies.

Organization

This work is organized in four main parts throughout six chapters, the first part presents the current status of hybrid electrical vehicle, the electrical components for traction purpose and previous works on the topic in order to determine the aim and the scope of the work. Then the different component modeling approaches and their implementation are detailed based on the analysis of previous works and reference articles. After this, the third part presents the coupling of all the methods and modeling in order to present a global analysis of the electrical system for hybrid vehicle. Finally, the last part presents the optimization approach and the results of the different investigations considered in this work.

The first chapter introduces the necessary background for the understanding of hybrid electrical vehicles: drivetrains architectures, functionalities and components. For each components, the specificities of the automotive industry are discussed (integration, performance and technology). Then the challenges resulting from the industrial environment of this work are discussed and the relevant challenges are identified. After this, a wide review of previous works on the topic is done: the investigation and evaluation levels, the investigated components as well as the considered parameters and the modeling approaches are analyzed and discussed. Finally, based on the current status of development, the analysis of previous investigations on the topic and the challenges imposed by the automotive industry, the aim and the scope of this work is defined.

The second chapter discusses the topic of the electric machines, its modeling and method for the investigations in this work. Three main aspects are required for this work: the component behavior (electromechanical), the thermal behavior and the integration in the drivetrain. For each modeling or method, the different solutions are analyzed

based on previous works and the suitable solution is chosen. Based on automotive components, they are validating before presenting a first analysis of the challenges of this work considering only the case of the electric machine.

Based on the same structure as the second chapter, the third one presents the results for the modeling of power electronics. Considering the status presented in the first chapter, this work considers two type of converters: an inverter and a boost converter. Both of them are discussed and investigated within this chapter. As previously three main aspects are considered: the component behavior (electrical), the thermal behavior and the integration. For each modeling or method, a suitable solution is chosen and validated using results of automotive components measurements before analyzing how the challenges of this work influence the power electronics.

This fourth chapter closes the topics of components modeling by introducing the solutions for the battery. As for the electric machine and the power electronics, previous works are analyzed in order to define suitable solutions to model the electrochemical behavior (voltage and state of charge), the thermal behavior and to investigate the integration. The solution which are chosen under the constraints of a global system approach of the electric architecture are then validating with actual automotive components and the influence of the battery configurations (indirectly the current and the voltage) are discussed and analyzed to have a first overview of the challenges faced by the component.

The diverging results of the analyses presented in the previous chapter shows the relevancy of a global system approach, which is the topic of the fifth chapter. The focus is on the simulation of electrical system in hybrid electrical drivetrains. Some definitions are introduced before analyzing the current status in order to determine the suitable adaptation and new implementations to develop a global system approach. The contribution of the chosen bidirectional approach is shown on several examples after having validated the coupling of the different modeling based on test-bench and vehicle measurements of an actual system.

The chapter six closes this work by introducing the optimization approach. First the different evaluation approaches and optimization algorithm are discussed and analyzed considering the challenges considered in this work. For each of them a suitable solution is chosen for the considered optimization problem. Based on the results of the status presented in the first chapter, the results from the previous chapter about components modeling and system simulation, the contribution of this work is shown for several examples. These examples present a complete overview of the challenges faced by the components, show the influence of the automotive constraints and tends to determine the direction for future developments of both the components and the global system.

Chapter 1: Hybrid electrical vehicles in the automotive industry

This chapter discusses the current status of hybrid electrical vehicles in the automotive industry and introduces the technical background for the rest of the work. The chapter is divided in three main parts. The first one present the current status of hybrid electrical drivetrain, the electric components for traction purpose, the corresponding architecture as well as the specificities and the challenges in the automotive industry. The second one analyzes previous works on the topics of hybrid drivetrain optimization and modeling in order to determine in the last part, the scope and aim of this work.

1 Hybrid electrical drivetrains in the automotive industry

This section begins by introducing the required knowledge about the hybrid electrical vehicles, the drivetrains architectures, the functionalities and the components to discuss then the specificities and the challenges imposed by the automotive industry.

1.1 Hybrid electrical drivetrain

A defined in the ECE-R101 standard [6]; hybrid vehicles have: a drivetrain with at least two different energy converters and two different energy storage systems for the purpose of vehicle propulsion. According to this definition, the hybrid vehicle can be electrical as well as pneumatic or hydraulic [7]. Hybrid electrical vehicle consists in a conventional drivetrain combined with an electric machine (EM), a power electronics converter (PE) and an energy storage system (ESS). In battery electrical vehicle and fuel-cell vehicle, the only source of mechanical power is the electric machine and the energy comes from an electrical energy storage system or the fuel-cell stack via highly compressed hydrogen. The investigation in this work concerns itself primarily with Hybrid Electrical Vehicles (HEV) and their Plug-In variants (PHEV). Battery Electrical Vehicle (BEV) and Fuel-Cell Vehicles (FCEV) are only considered for a technological monitoring. An overview is shown on Figure 2.

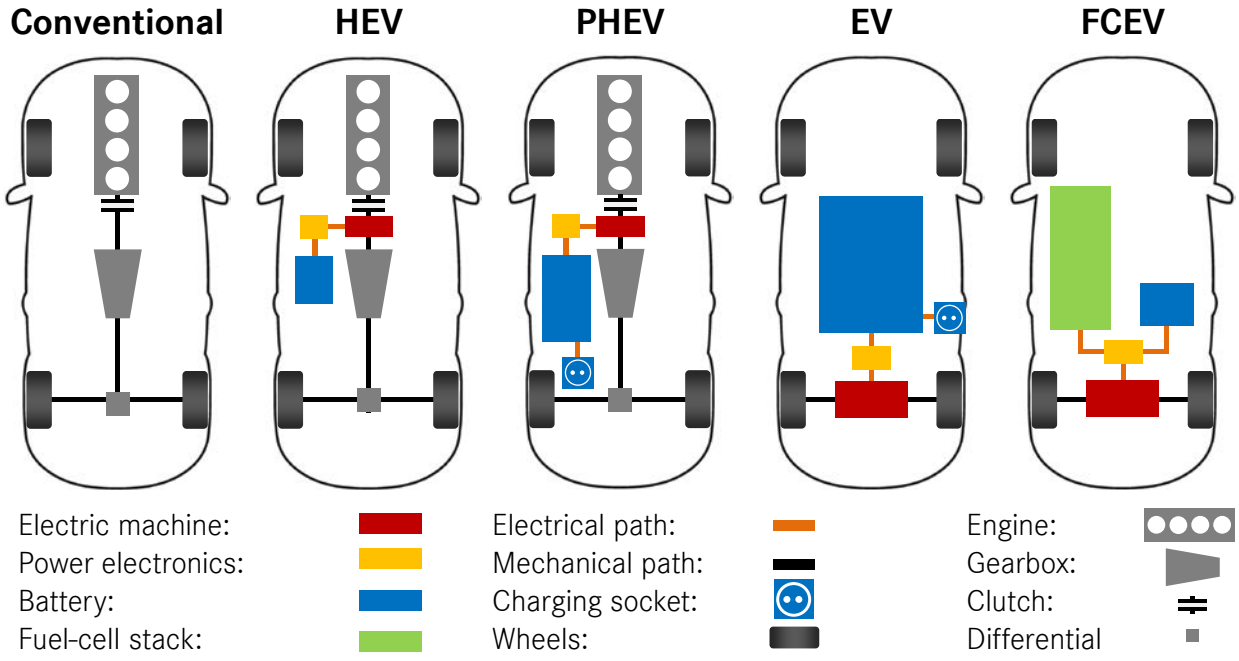

Figure 2: Drivetrain architecture in the automotive industry [8]

Despite some early concepts from beginning of the 20th century, hybrid electrical drivetrain is still an emerging technology. Recent development has been dominated by the Japanese manufacturers (Toyota since 1997 and Honda since 1999). Over the years, Toyota has established a leading position on the HEV-market but despite this situation, numerous and various technological improvements have been introduced by other manufacturers such as the first hybrid vehicle with Li-Ion battery (Mercedes-Benz S400 Hybrid, 2009), the first plug-in hybrid vehicle (Chevrolet Volt, 2010) and the first diesel hybrid vehicle (Peugeot Hybrid4 Architecture, 2011) [8].

1.1.1 Architectures

The combination of one or several electric machines (EM) with an internal combustion engine (ICE) allows the development of a wide range of concepts for passenger cars divided in three main categories: the series architecture, the parallel architecture and the power-split architecture as shown on the Figure 3.

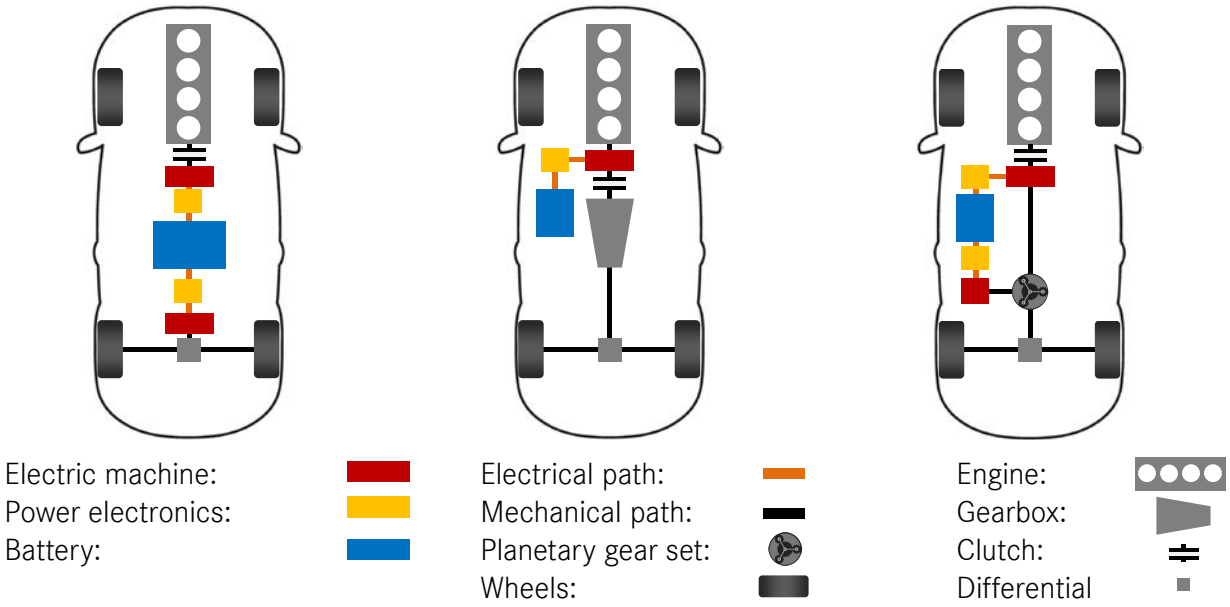

Figure 3: Series hybrid (left), parallel hybrid (middle) and power-split hybrid (right) adapted from [8]

The series architecture is the historical solution retained by Ferdinand Porsche in the first hybrid vehicle. This architecture aims to combine the density of fossil fuels energy with electrical drivetrain efficiency. For this purpose, the ICE is coupled with an electric generator which charges the energy storage system in order to further provide energy to the electric machine. There is no direct connection between the ICE and the wheels and therefore the ICE and its generator can be designed to work in their best-efficiency area but the global efficiency of the drivetrain is limited by the multiplication of the components efficiencies [9], [10]. Contrary to the series architecture, the parallel solution allows both the ICE and the electric machine to provide power to the wheel, as suggested by its name. The power of the energy converters is added in the drivetrain and it only requires one electric machine to work. The electric machine can be integrated in different positions: on input (P0) or output shaft of the ICE (P1), on the input shaft of the gearbox (P2), after the gearbox (P3) or on the not driven axle (P4). The parallel architecture is the most widespread solution when considering the number of concepts in which it is implemented [9], [10]. The parallel hybrid architecture, due to its numerous positions in the drivetrain offers a wide range of solutions as well as the opportunity to be combined. When adequately chosen; the combinations can result in drivetrains with additional functionalities and potential. For example, the P4 architecture offers all-wheel drive functionalities with without requiring an additional mechanical connection between the axles [8].Similar to the series architecture, the power-split architecture requires more than one electric machine. By combining two electric machines and a planetary gear set (see Figure 3), the power has the possibility to use several paths between the engine and the wheels. This architecture offers more chances to optimize the components operations because the drivetrain has more degrees of freedom to bring the power from the storage systems to the wheel. The position of electric machines depends on the power paths configuration and the drivetrain functionalities [9], [10] and [11].

1.1.2 Functionalities and power flows

Beside the architectures, the functionalities play a significant role because they allow optimizing the driving strategy compared to conventional drivetrain. They result from the bidirectionality of the electrical architecture and especially the possibility to regenerate energy. In this section, the different modes of the components and the different functionalities are lightly explained and more detailed information can be found in Appendix 2. One of the main assets of hybrid electrical vehicles lies in the bidirectionality of the components power flow. In motor mode the electrical power stored in the energy storage system is converted into mechanical power by the power electronics

and the electric machine whereas in generator mode the mechanical power is converted in electrical power and fed to the energy storage system as shown on Figure 4.

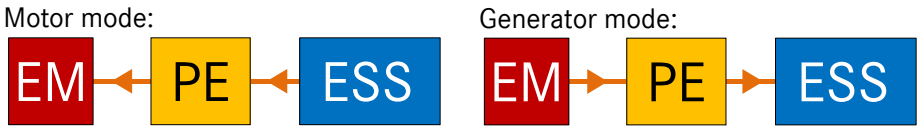

Figure 4: Motor mode (left) and generator mode (right) in electric drives adapted from [9]

Several functionalities can be implemented thanks to the addition of electric components. Among them, three categories can be identified: a first one where the aim is to support the combustion engine (boost, load point shifting and start/stop), a second one where the aim is to substitute it (electric drive) and a final one where the components bring additional possibilities (regenerative braking and sailing). No functionality is mandatory to consider a vehicle as hybrid or not but they play significant roles when defining the requirements or evaluating the system.

1.2 Electric components

This sub-section is focused on the electric components for hybrid drivetrains. It is divided in three main parts: the first one for the electric machine, the second one for the energy storage system and the last one for the power electronics. For each components, the specificities of the automotive industry, the technologies and the integration in hybrid drivetrains are discussed.

1.2.1 Electric machine

The electric machine is a multi-centennial technology but despite its high efficiency, it was hindered in automotive applications by the performance of electric energy storage systems. The emergence of new technologies with higher energy density at the end of the 20th century has enabled the electric machine to show its potential for vehicle propulsion purposes. In the automotive industry, the electric machine aims to substitute and enhance the combustion engine functionalities. For traction purpose, electric machines have to work in several quadrants (motor/generator mode and two rotational directions) and over a wide torque and speed range [10]. Therefore the machines in automotive applications are generally defined by their torque/speed characteristic. This characteristic is generally defined in two mains areas due to the intrinsic machine characteristics: in the constant torque area (blue area), the machine has not reached its full voltage capability and aims to maximize the torque under current limits while in the field-weakening area (red area) it aims to maximize the power by adjusting the flux-linkage in rotor as it can be seen on Figure 5.

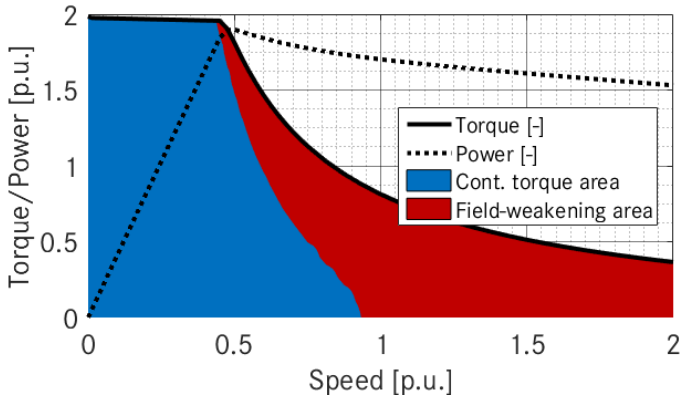

Figure 5: Electric machine limit curves in automotive applications

Among the numerous machine technologies, only some of them are currently used in hybrid and electrical vehicle. Despite some concepts at the end of the 20th century, the Direct Current Machines (DCM) are no longer used and among the alternating current machine, only three types are currently used in the automotive industry for the traction purpose: Induction Machine (IM), Permanent Magnet Synchronous Machine (PMSM) and Separately Excited Synchronous Machine (SESM). In hybrid vehicles, the electric components are integrated in a vehicle which already

includes the conventional drivetrain components. Hence the main requirements are the power density to reduce integration issues, the efficiency to exploit the full potential of the stored electrical energy as well as the reliability to ensure the vehicle safety and to avoid an increase of the required maintenance. Outside the current automotive industry applications, several laboratories and institutes are working on the switched reluctance machine (SRM) as [12], [13] and [14] as alternatives to the currently employed technologies.

	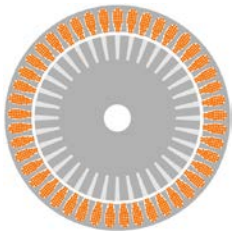	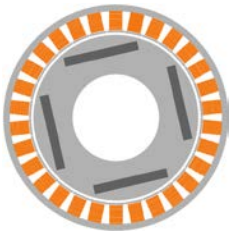	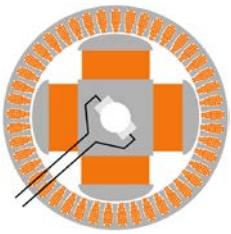
	IM	**PMSM**	**SESM**
Power density	0	+ +	+
Efficiency	0	+ +	+
Costs	+ +	-	++
Reliability	+ +	+	-
Maturity	+	+ +	0

Table 1: Comparison of electric machine for automotive applications adapted from [12]

The PMSM is the technology which suits the best these requirements but is the most cost-intensive. The IM stands for a cost-efficient alternative especially for electrical vehicle applications where the power density is not the main criterion (e.g. Tesla Roadster [15]). The SESM is an unusual solution and can be considered as a mean solution between the IM and the PMSM because it combines most of the advantages of both the technologies [16]. Concern for the reliability due to the required brushes for the rotor excitation is however an important drawback by the SESM. Beside the technological challenge, the electric machine position and its mechanical connection play a significant role during the design phase. The position and connection are generally linked with the functionalities and the architecture. Unlike the electric machines in the conventional industry where air-cooling is a widespread solution (1), the electric machines in hybrid vehicles often require liquid-cooling to enable the following integrations: on the ICE-shaft with a belt solution (2), direct on the ICE-shaft (3), integrated in the gearbox (4), parallel to the axle (5), coaxial integrated (6) or direct in the wheel (7). An overview is presented on the Figure 6.

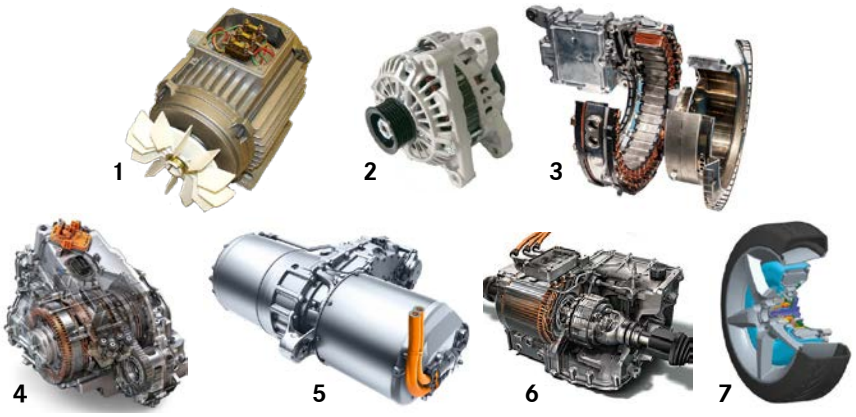

1: Conventional industry integration

2: Integration with a belt-connection

3: Integration on the engine shaft

4: Gearbox integrated solution

5: Axle-parallel integration

6: Coaxial integration

7: In-wheel solution

Figure 6: Integration possibilities of electric machine [17], [18], [19], [20] and [21]

1.2.2 Energy storage system

Electrical energy storage systems (ESS) hinder the development of hybrid and electrical vehicle since more than a century. Despite the development of new technologies which have highly enhanced the possibilities (from 1800kg for 50km range at the beginning of 20th century [9] down to 830kg for 500 km range in 2010 [22]), the weight and volume for the storage system remain more than nineteen times higher than in a conventional vehicle [22]. It is even more challenging for hybrid vehicle because it needs to find a place among the components of the conventional

vehicle. Here are discussed first the specific requirements from the automotive industry, then the different energy storage system and cells technologies and finally the different solutions for their integration in automotive drivetrain. Over the years, the storage capacity can be altered and thus the performance could be reduced. To prevent this phenomenon, a light over-dimensioning can be performed. Only a part of the energy storage system capacity is used in order to maintain constant performance. Hence the customers never experience an electrical range reduction or reduced functionalities even at the end of the vehicle lifecycle. The solutions for the storage of electrical energy are various but only the Nickel–metal hydride battery (NiMH) and lithium based batteries have found applications in the automotive industry. The first hybrid electrical vehicles were developed with NiMH battery until the launch of the Mercedes S400 hybrid [23]. The lithium based solutions tend to take a monopoly due to higher power and energy density but some manufacturers still have faith in this technology for the HEV without plug-in functionality [24]. Among the batteries there are different cells-technologies (especially for lithium-ion battery). The main differentiation is done with the cathode material which often defines the name of the cell-technology. This range of technologies enables to cover a wide area of applications as shown in [25], from power cells to energy cells. The different materials are not directly investigated in this work but the cathode and anode material impacts directly the voltage behavior due to a SOC-dependency, the energy and power density [9] as it can be seen on Figure 7 where the voltage versus Li/Li+ of different cathode technologies are presented (LFP: lithium iron phosphate, LCO: lithium cobalt oxide, LMO: lithium manganese oxide, NCA: lithium nickel cobalt aluminum oxide and NMC: lithium nickel manganese cobalt).

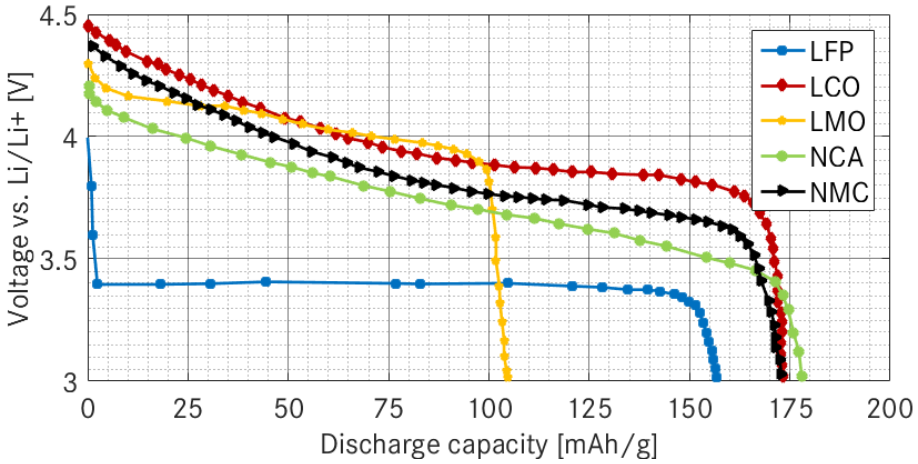

Figure 7: SOC and technology dependency of cell voltage in lithium-based battery [9]

The majority of the hybrid electrical vehicles are derived from existing one and the battery is often not the cornerstone of the development despite being challenging. Among the hybrid vehicles, the Chevrolet Volt (1) is one of the only concepts where the vehicle is built around the battery. The available volume is generally restrained and the battery is set in the remaining areas: the motor area (2), tank area (3) or in trunk area (4) as shown on Figure 8.

Figure 8: Integration of battery in hybrid vehicles [18], [23], [26] and [19]

1.2.3 Power electronics

Since the invention of the first silicon transistor in 1948 and through several technological improvements, silicon based solutions have found applications in almost all industrial sectors [27]. The major use of the semiconductors is the electrical energy conversion in all its forms. In the case of hybrid vehicle, the main conversion realized in the drivetrain electrical system is the conversion between Direct Current (DC) and Alternating Current (AC) and vice

versa due to the electric machine and energy storage system technologies. Each industry sector has its own requirements towards semiconductors depending on the application frequency, voltage and current area. Hybrid vehicles require a controllable switch for the voltage area defined in the ECE – R100 norm [28] and a frequency around several kHz [8]. The solutions which suit properly these specifications are the Mosfet and the Isolated Gate Bipolar Transistor (IGBT), which are generally integrated in power module [29] or in intelligent power module [24].The DC/AC-conversion between the energy storage system and the electric machine is only characterized by the two interfaces of the component. The conversion can actually be divided into sub-conversions such as a combination of DC/DC and DC/AC. In the current hybrid vehicle drivetrains, two main solutions are used: stand-alone inverter [23] or combination of inverter and boost converter [24]. In this work the term power electronics referred to the entire component.

→ Inverter (DC to AC conversion): in hybrid vehicles, the inverter realizes the conversion between a DC intermediate circuit or energy storage system and an alternating current electric machine. As the other drivetrain electric components, the inverter needs to works in both direction (AC/DC and DC/AC). In current vehicles, only the two-level B6C-topology is used. Despite the potential shown by other solutions (e.g. H-Bridge, Multilevel, Z-source inverter or current source inverter), this work only investigates this topology in combination or not with a boost-converter.

→ Boost converter (DC to DC conversion): within the drivetrain electric components, two main applications of boost converter can be identified. The first one between the energy storage system and the inverter to adapt and control the voltage [30] and the second one to stabilize the voltage between fuel-cell stack and the buffer battery due to the large state-of-charge (SOC) variations of the system [31]. The DC/DC-converter is not a mandatory component but is considered in this work as an additional degree of freedom for the evaluation

Three phase inverter (B6C-topology):	Bidirectional boost converter topology:	
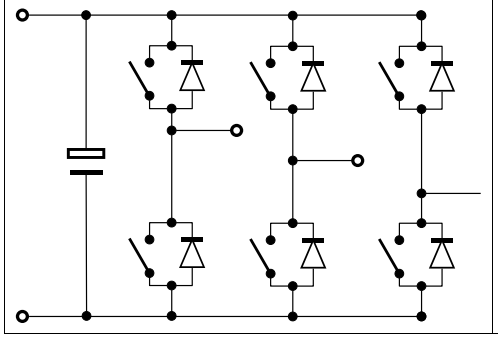	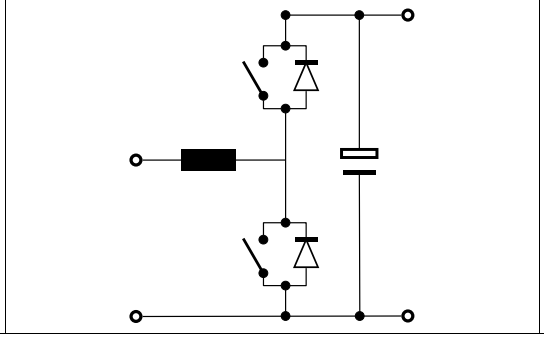	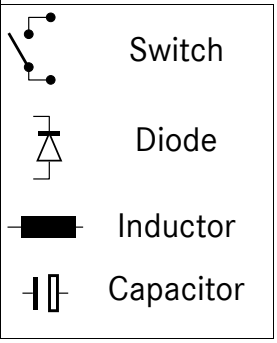

Table 2: Power electronics topology considered in this work [8]

The main requirements towards the power electronics are linked with their integration in the vehicle. Beside the different topologies and technologies, hybrid vehicles set new challenges toward the integration as discussed in [138]. These challenges extend from the temperature range to the power density through the vibration profile, the mechanical shock levels, the costs and the cooling system. Contrary to industry inverters, they are generally liquid-cooled and applications dependent to meet these requirements. Due to their compactness, the power electronics can be both integrated as a stand-alone component (1) or directly in the drivetrain (2) as it can be seen on Figure 9. If the first solution offers more modularity, the second does not require cables to supply the electric machine.

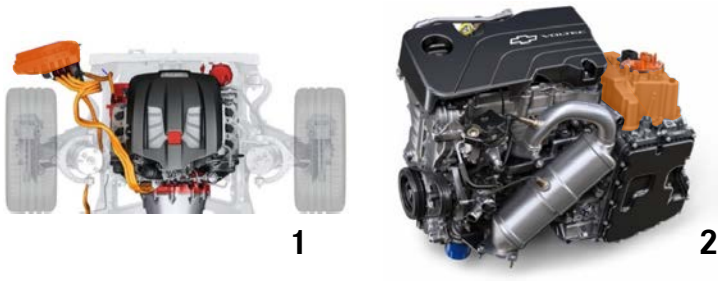

Figure 9: Different examples of power electronics integration [18] and [33]

1.3 Electrical architecture in hybrid vehicles

Depending on the drivetrain architecture and power electronics topology, the electrical architecture can strongly differ. This section discusses the electrical architectures which are categorized based on the number of electric machines (EM) and the power electronics topologies. There is currently no mass-market vehicle with several batteries or energy storage systems. The interface with the rest of the vehicle electrical architecture is depicted by the power distribution unit (PDU). The three main architecture (one EM without DC/DC-converter, several EMs without DC/DC-converter and EMs with DC/DC-converter) are presented on the Figure 10. When considering the number of concepts, the architecture with only one electric machine (1 on Figure 10) and no DC/DC-converter is the most used one in hybrid electrical drivetrains. It has the lowest complexity for the control, the implementation and is the less challenging one for the components integration. It offers however less degree of freedom because it has only two driving modes (motor and generator) but allows implementing all hybrid functionalities. The addition of one or several electric machines increases the complexity of the system (2 on Figure 10). If offers more degrees of freedom but complicates the energy management. Due to the scope of this work, it has no direct influence on the components investigation. The main challenge lies on the vehicle side, where the driving strategy needs to be adapted to optimally utilize the several energy converters. In some architectures with several electric machines, a boost-converter is introduced between the battery and the inverter (3 on Figure 10). This additional component enables to control the input voltage independently from the battery and thus it allows optimizing the driving points. As the addition of an electric machine, the boost-converter offers an additional degree of freedom but contrary to the previous architecture, the challenge in this case lies on the electric components side. Indeed, the voltage conversion has to be chosen by considering the state-of-charge, the boost-converter efficiency for the desired conversion, and the efficiency of the two electric drives (inverter and electric machine) in the system.

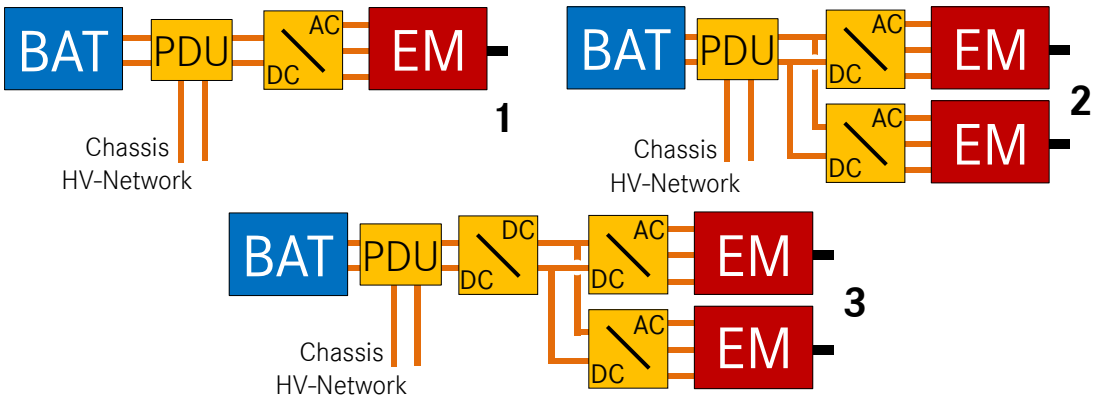

Figure 10: Electrical architectures in hybrid electrical drivetrains [23], [24] and [34]

1.4 Specificity of the automotive industry

The automotive industry is in continuous expansion [4]. With several millions manufactured vehicles every year, the industry has developed specific evaluation and process to adapt, structure and guide its development. This sub-section is divided in three parts: one about the vehicle evaluation, one about the development process and a final one about the development approaches for hybrid electrical vehicles.

1.4.1 Vehicle evaluation

Despite having different technologies and properties, the vehicles need to be compared on the same basis. Hence most of the countries or institutional organizations have developed legislative framework in the form of driving cycles and test protocols. It enables to compare in a fair way all the vehicles and to evaluate their consumption and their emission as depicted in [35] for Europe. The protocol defines how the evaluation has to be performed whereas the cycle depicts a typical trip for the vehicle in the related region of the world. The cycles are often constituted of sub-cycles that describe the vehicle speed for different types of route: city road, country road and highway for example. The hybrid vehicles are particularly affected by this evaluation because the associated method for each vehicle type is different [35]. These driving cycles (as the NEDC on Figure 11) their associated certification protocol are the legislative framework to evaluate the vehicles, their emissions and their consumption.

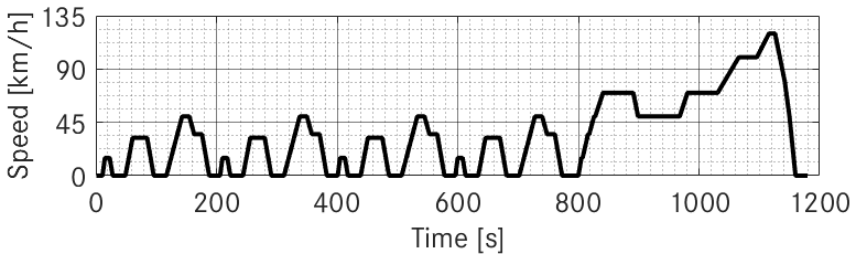

Figure 11: New European Driving Cycle (NEDC) [2]

1.4.2 Development process in the automotive industry

Due to the constant evolution of the market and the intent to always stay competitive, the automotive industry has to constantly adapt its development and most of the manufacturers have adopted a top-down approach depicted by a V-cycle as shown on Figure 12. It summarizes the different phases of the development from the requirements to the solution [36]. This process can be divided into two parts, the left one is the design phase and the right one is the industrialization phase.

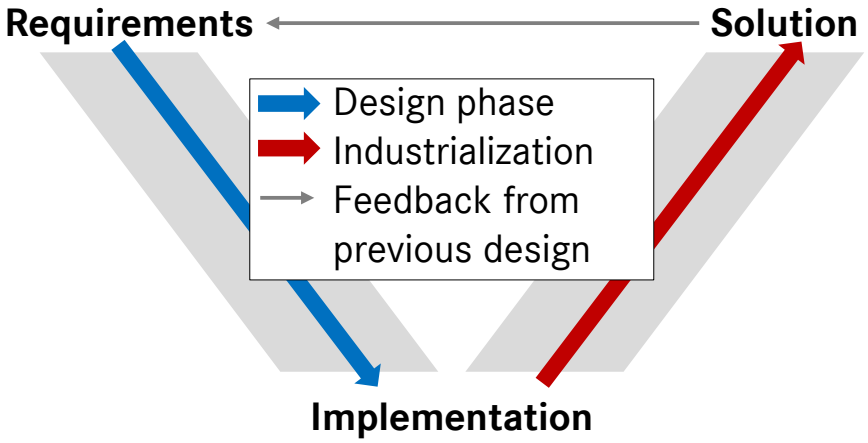

Figure 12: V-cycle approach as used in the automotive industry [36]

The design phase investigates the potential through a top-down approach. The top-level requirements are translated through several design iterations. First, the vehicle concept is defined based on customers' requirements and market analysis. This step is then followed by successive design steps which translate these requirements from superficial level down to the most detailed level (vehicle requirements down to sub-components requirements). The industrialization phase is composed of several validations and evaluations of the concept developed during the design phase. The final hardware for the commercialization is chosen based on the evaluations, the adapted tools and production methods are defined. Moreover the maturity of the components, the drivetrain and the vehicle implementation is enhanced thanks to refinement of the design.

1.4.3 Development approach of hybrid vehicle

From a statistical point of view, hybrid electrical vehicles have a dominant position over the other solutions: BEV and FCEV [5] but it still remains a niche market with a high multiplicity of solutions. Facing this situation, there are two main development approaches which directly affect the investigations done in this work: first the differentiation between purpose and derived hybrid drivetrain and secondly the use of module strategies. The purpose hybrid drivetrains are solutions where the drivetrain is not directly derived from conventional vehicles. The Toyota Prius for example is completely developed for the application, the combustion engine has a specific combustion cycle (Atkinson cycle) and the drivetrain architecture was developed to perfectly fit the requirements of a hybrid electrical vehicle. Contrary to purpose hybrid drivetrain, the derived ones use a conventional drivetrain structure in combination with the electric components. This approach is easier to set up because most of the basis development stages of the vehicle do not need to be changed as shown in [23]. The electric components for hybrid functionalities are integrated in the conventional drivetrain with the aim to have as few modifications as possible. These two

strategies are not fundamentally linked with the hybrid architecture. Even if all power-split systems are purpose hybrid drivetrains (specific engine, gearbox and electric components), there are parallel hybrid systems which are designed on purpose (Porsche 918 [37]) as well as derived from conventional drivetrain (Mercedes E300 [23]). Moreover, when analyzing the current market situation in Europe, it appears clearly that no solution has taken any leadership. Considering the market share, the purpose hybrid drivetrain has a leading position (almost exclusively due to the Toyota Group drivetrains), while considering the number of concepts, the derived drivetrain is the most chosen solution. They enable an easier implementation in vehicle (adaptation instead of new drivetrain development).

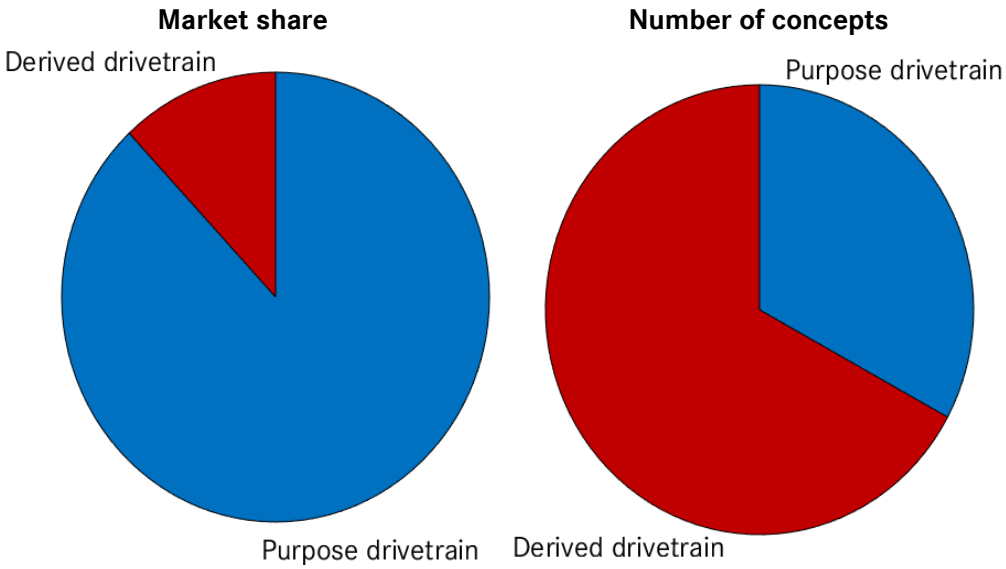

Figure 13: Market share and number of concepts for purpose and derived drivetrains in Europe [5]

Beside the drivetrain development approaches, module strategies are used to facilitate the acceptance of hybrid electrical vehicles. It can be used for different purpose and during each steps of the design: the same drivetrains can be used in different vehicles, the same component(s) can be used in several drivetrains, the same cells can be used to build different battery packs or the same IGBT and housing can be used to produce different power classes. To explain in details this strategy, the approach in [38] is detailed. Based on a module matrix, the whole range of electrified vehicle can be represented. The different vehicle concepts results from transitional evolution of the system. The transition from the HEV to the PHEV is done by adapting the battery which can also be adapted to develop an all-wheel drive variant where a second electric machine is added. The same machine is then used to develop a BEV by adapting the connection with the vehicle shaft. A remarkable point in this module strategy lies in the use of the same power electronics and therefore the same voltage level in all systems without any adaptations.

1.5 Challenges in automotive industry for hybrid electrical vehicle

New CO_2-emissions legislation do not set the same challenges and requirements for all automotive manufacturers (Appendix 1). Among them, the vehicle concept and class, the performance and particularly the weight play a major role. In this section, the several challenges faced by the hybrid electrical drivetrain as well as by the components are discussed with the focus being set in the first part on the vehicle concepts and in the second part on the voltage level.

1.5.1 Vehicle concepts

The specificities of the automotive industry have resulted in a complex market with numerous concepts. Facing this situation, no solution has taken a clear monopoly and the valued-added of each solution still needs to be proven. In this section, the aim is to discuss the different vehicle concepts and their influence on the components. The vehicle concepts are generally classified based on their power class in the following categories: micro-hybrid, mild-hybrid, full-hybrid and plug-in hybrid [8]. In order to compare the vehicle concept and not the vehicle class, the impact of the mass need to be considered and thus in the rest of this section, the concepts are discussed by considering the

ratio between power and mass or energy and mass. The vehicles are classified by type of vehicle: EV/HEV/PHEV/SHEV and then divided in three categories depending on their start of production (2013 symbolizes the start of the thesis) and their status of development (concept/prototype or commercialized vehicle).

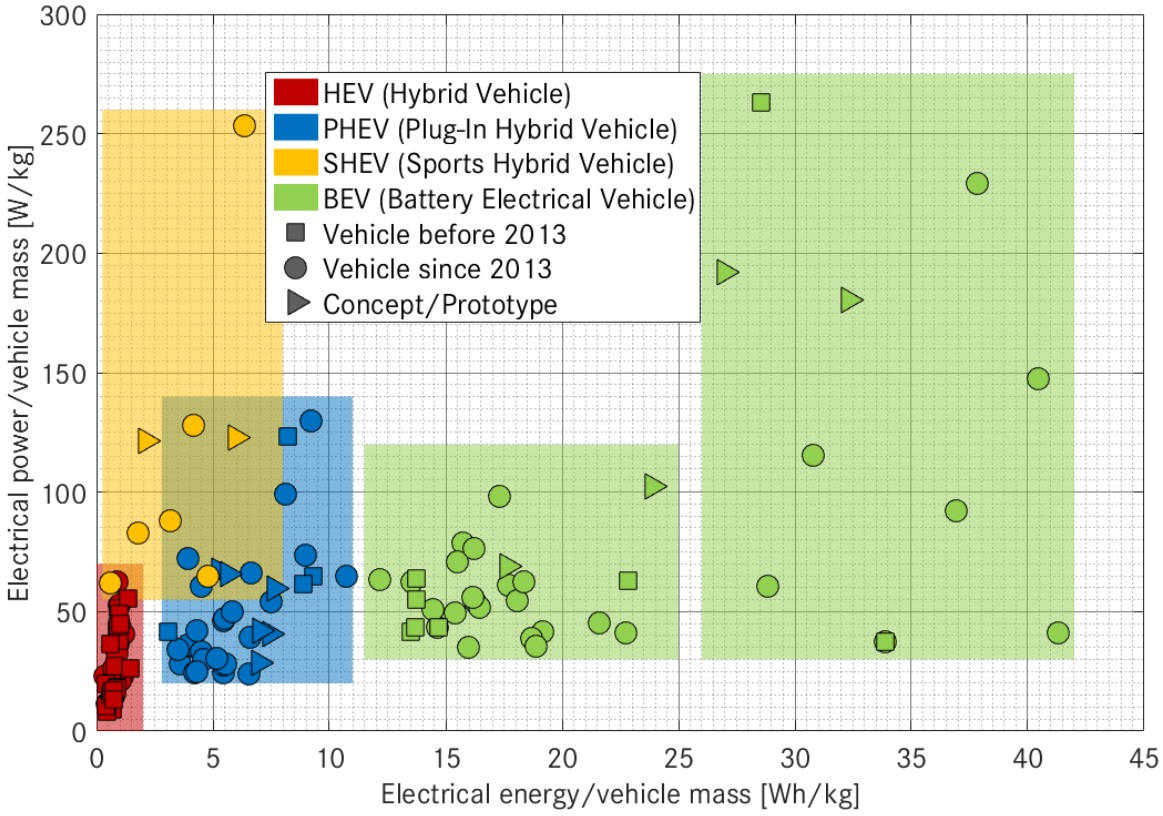

Figure 14: Embedded energy and power for different type of alternative drivetrains

By the end of the 20th century, the first hybrid electrical vehicles were only flagship vehicles to demonstrate the potential of the technology and to open the way toward an emission free mobility. Over the last decade, the hybrid technology has progressively been transferred to the whole range of vehicle and car segments. This massive electrification of vehicle sets new requirements for the development of alternative drivetrains and offers the possibility to develop module strategies. As it can be seen on the Figure 14, a significant trend toward the emergence of plug-in hybrid vehicle can be identified. These vehicles represent a further step toward full electrical vehicle and aim to combine advantages of both electric and conventional vehicle by reaching comparable electrical power to vehicle mass as electrical vehicles without reducing the combustion engine power. A second trend is the development of high performance hybrid electrical vehicles (SHEV). They set new requirements toward the electrical power and are often developed around the following statement: *how can I improve the performance of my vehicle without increasing its consumption and emissions?* [37]. This statement raises new challenges for electric components in hybrid vehicles which need to fulfill both ecological and high performance requirements. It is particularly challenging for the electric components to avoid a performance decrease due to repeated high loads.

1.5.2 Voltage level

This section discusses the topic of the voltage level. The voltage challenges are discussed first for high voltage (HV) system, then for low voltage (LV) systems and finally the HV-components which are not included in the drivetrain are considered. For a clear understanding, the voltage ranges as understood in the automotive industry are defined as follow: According to the ECE-R100 standards [28], high voltage components have a working voltage V_{DC} between 60V and 1500V or V_{AC} between $30V_{rms}$ and $1000V_{rms}$ and low voltage components have a working voltage below 60V or $30V_{rms}$. As for the architecture, no solution has taken a clear leadership over the others and only a light trend can be inferred between the power and the voltage level for (P)HEV applications. The situation is however even more challenging when considering the topic from a global point of view and over all applications. For the topologies with two boost-converter, two voltage levels need to be considered: the battery voltage level (200-250V) and the maximal

DC-link voltage level (200-650V). Concerning the other applications (principally BEV), the voltage level topic has led to a wide variety of solutions. There are high power electrical vehicles with a similar voltage level as in hybrid vehicles (Tesla Model S P85D [39] or Mercedes SLS e-cell [40]), high power electrical vehicle with a higher voltage solution (Porsche mission e [41]) and solutions with higher voltage potential without high power (AVL coup-e 800 [42]).

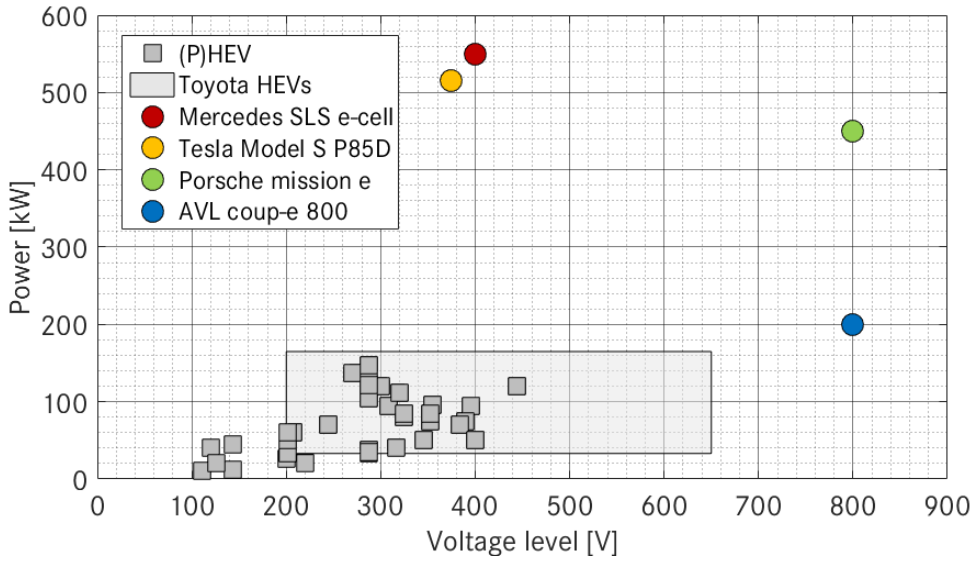

Figure 15: Voltage levels in the automotive industry

Beside the voltage level challenges within high voltage solutions: the applications below 60 V_{DC}, generally referred to as 48V-systems raise new challenges for low power solutions in the automotive industry and set different requirements for the drivetrains electric components (e.g. safety requirements). This new voltage level shows potential to achieve the basis functionality of hybrid vehicle without the requirements imposed by a higher working voltage [43]. Beside this, there are components which are not used for the traction purpose and are only considered as an electrical load. They must not stay completely unconsidered because they can play a significant role to address the voltage level challenge. These components, as shown on Figure 16, are directly connected on the DC-link and thus can be determinant to evaluate the suitability of a system. An electric drive system and its voltage level can only be chosen when the corresponding components to ensure other functions are available in this voltage range.

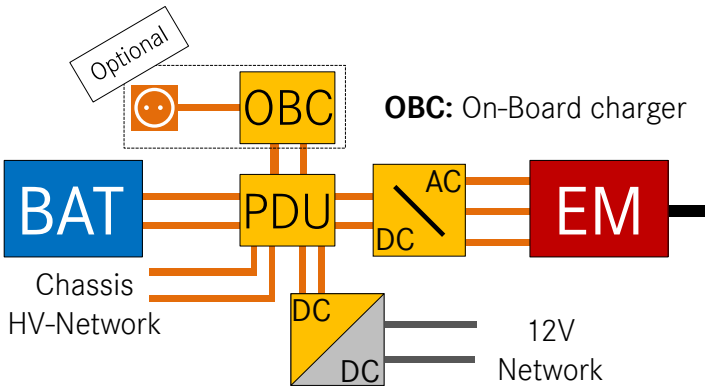

Figure 16: Global vehicle electric architecture adapted from [8]

2 Modeling electric drive system

To address the challenges and the specificities detailed in the previous section, a simulation based approach is chosen. To explain in details this choice, this section discusses the topic of modeling electric drive system with four main sections. Simulation is a well-known solution for the development and the design of system and/or components and the wide possibility offered by the currently available methods and solutions is one topic of interest in this work. The first section explains the role of simulations and their added-values and during the development

process. The second one discusses the different investigation levels of the development where the challenges could be addressed and how they influence the requirements. The third section performs a review of relevant previous work. Finally the fourth section analyze the modeling approaches in order to determine in the next section the most adapted solutions for modeling drivetrain electric components as a standalone entity by discussing the advantages and the drawbacks of the different evaluation level, modeling level, considered parameters and investigated components.

2.1 Simulation potential during vehicle development

Simulations are used during the vehicle development to perform virtual V-cycle during both the design and industrialization phase [36] and enable to support the process by giving technical feedback between the different development steps as shown on Figure 17. During the design phase, they are used to estimate and evaluate the vehicles, systems drivetrains or components under consideration whereas during the industrialization phase it enables to test other configurations for defined drivetrains, systems or components. To ensure the quality and the relevancy of the simulations, they need to be validated based on the results from previous V-cycles: hardware assembly, testing and measurements of the components as well as implementation in vehicle. In this work, the aim is to enhance the methods and simulation for the early development stage of electric components in hybrid drivetrains. The aim is to identify and analyze the potential systems which can fulfill the requirements. In the case of electric drive system investigations, it results in the identification of the suitable components combination and implementation in vehicle. For this purpose, the focus is set on the modeling approaches limited on the system level. It therefore needs to refine and translate the vehicle requirements for each component and then to coordinate their interactions to find the best solution from a global system point of view.

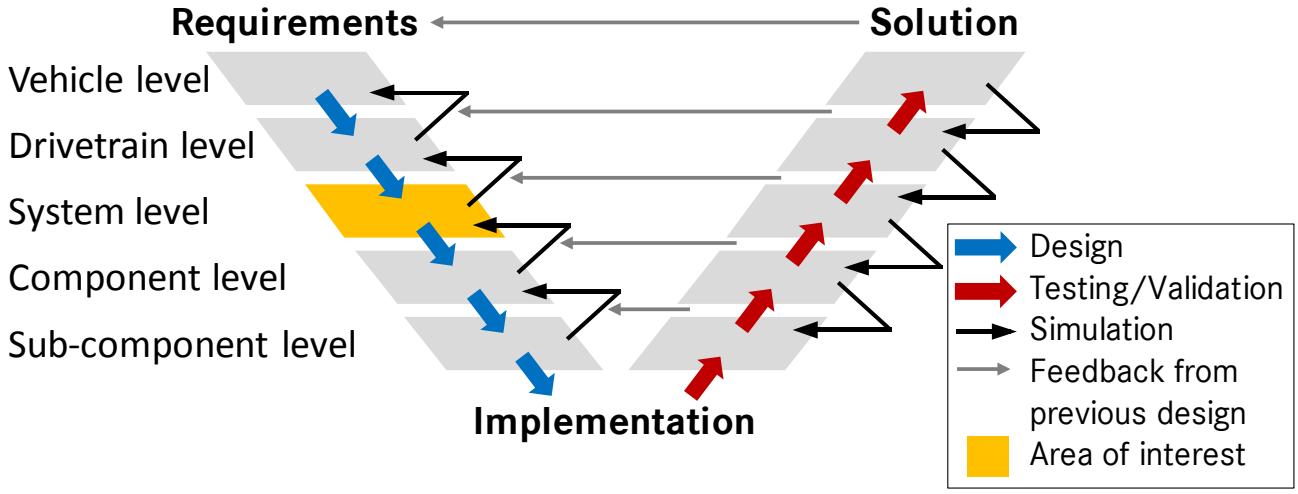

Figure 17: Simulation potential during the development process adapted from [36]

2.2 Investigation levels for hybrid system optimization

To address the challenges discussed in the first chapter, methods are required, which not only supervise the interactions between the components development but also coordinate them. Thus thanks to suitable modelings and interfaces; the design investigations could find the best component combinations instead of the best combination of components. Before determining the appropriate modeling approaches, the different investigation levels and their influence on the components modeling are explained and discussed.

2.2.1 Investigation levels

For the purpose of this work the components, their interactions and the global system have to be investigated. The first step is to determine the suitable level of investigation. In the case of electric drive system (electric machine, power electronics and battery), five levels can be identified: vehicle level, drivetrain level, system level, components level and sub-components level as it can be seen in Table 3.

Vehicle level	Drivetrain level	System level	Component level	Sub-component level
	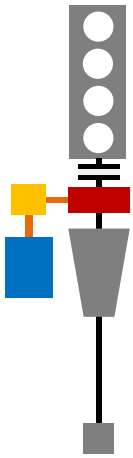	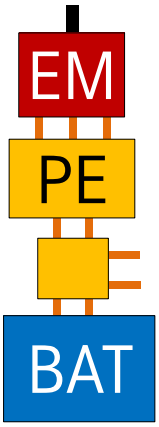		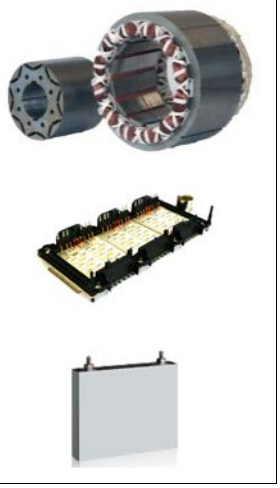

Table 3: Investigation level for the modeling of electric components in hybrid drivetrains

Vehicle level:
The vehicle level depicts concretely what the customers can experience: acceleration, vehicle dimensions, drivability, consumption and comfort for example. At this level, the electric components are only superficially investigated but the entire vehicle scope is considered.

Drivetrain level:
The differentiation between the vehicle and the drivetrain levels lies in the investigated parameters and components. Developing sustainable concepts at the drivetrain level means that only the components which propel the vehicle are evaluated. The drivetrain level, as defined in this work concentrates its investigations on the technological and economical aspects of the design as well as the implementation.

System level:
The system level referred in this work to the analysis of the electric components as an independent entity. It investigates only the electric components for the traction purpose in hybrid drivetrains by defining suitable interfaces with the rest of the vehicle.

Component and sub-component level:
The distinction between the component and sub-component level is defined in this work in the different investigated parameters and the interactions with their environment. In order to bring a better understanding about those differences, the limits between the levels are discussed through two relevant articles. Both articles aim to compare electric machine technologies for automotive applications. The first one [44] investigates the performance as well as the integration and environment issues while the second one [45] is focused on the purely electromagnetic comparison of the technologies. It is particularly observable for the volume investigation. The second article has fixed active materials dimensions (outer stator diameter, inner rotor diameter and axial core length) for the performance estimation contrary to the first one which compares the technologies by considering their influences not only on the performance but on the global volume as well (active materials, winding and rotor excitation). The components approach leads to machine designed for the real volume whereas the investigation of the sub-components depicts synthetically the technology performance from a strictly scientific and technical point of view.

2.2.2 Requirements and investigation level

The requirements and thus the components evaluation are strongly dependent on the investigation level. The translation and the interactions between the different levels play a major role in the resolution of the problem statement in this work. The vehicle level represents the final product, the drivetrain level translates the requirements, the system level specifies what needs to be evaluated, the component level what needs to be investigated and the sub-components level characterize what needs to be modelled.

Vehicle	Drivetrain	System	Component and sub-component		
			Electric machine	Power electronics	Battery
Power Acceleration Max. speed Comfort Drivability Consumption Emissions Electrical range Costs	Power Torque Gear ratio Weight Architecture Energy Efficiency Costs	Mech. power System torque Rot. speed Weight Integration Energy	Power factor Voltage Technology Dimensions Weight Losses Topology	Apparent power AC current Control-method Dimensions Weight Losses Topology Technology	DC power DC current Voltage Cells connection Dimensions Weight Losses Capacity State of charge

Table 4: Parameters at the different levels for hybrid drivetrain

Despite some similarities in their designation, the relationships between the different levels are only trivial between the vehicle, drivetrain and system level. The translations on deeper levels are more complex because they may be dependent on several components despite the system characteristics being often described by a single component one.

Mechanical power:

The system mechanical power (electric machine mechanical power) is specified using the vehicle power requirements and their translation at the drivetrain level based on the architecture and power distribution. They are then evaluated thanks to deeper level parameters as follows: the mechanical power provided by the electric machine (P_{EM}) is a function of the power factor ($\cos\varphi$), the machine efficiency (η_{EM}), the power electronics efficiency (η_{PE}) and the apparent power (S_{PE}) which can be driven by the power electronics. The apparent power depends on the AC current (I_{AC}) provided by the inverter, the number of phases (n_{phase}), the battery voltage (U_{DC}) at the inverter and the control method which define the available AC-voltage for the electric machine through the modulation factor (m_i). Finally the DC-power (P_{DC}) limits the power of the whole system. Even if the inverter can drive the apparent power, the mechanical power provides by the electric machine is always limited by the maximal DC-power (e.g. DC-current) which can be supplied by the battery.

$$P_{\mathrm{mech}} = \eta_{\mathrm{EM}} \cdot \eta_{\mathrm{PE}} \cdot S_{\mathrm{PE}} \cdot \cos\varphi \quad (1)$$

$$S_{\mathrm{PE}} = n_{phase} \cdot m_{\mathrm{i}} \cdot U_{\mathrm{DC}} \cdot I_{\mathrm{AC}} \quad (2)$$

$$P_{\mathrm{mech}} \leq \eta_{\mathrm{EM}} \cdot \eta_{\mathrm{PE}} \cdot P_{\mathrm{DC}} \quad (3)$$

Torque:

Similar to the mechanical power, the torque (electric machine torque) is specified using highest level requirements (drivability and acceleration) and is translated based on the architecture and the gear ratio. To be evaluated, it requires knowing the topology of the machines (e.g. stator configuration), the dimensions (e.g. bore volume) and the machine technology (e.g. PMSM) but also the maximal AC current that the power electronics can drive.

Rotational speed:

The rotational speed (the electric machine speed) is the outcome of the vehicle speed requirements and is characterized on the system level through the drivetrain architecture and gear ratio. It depends on the control-method, the machine technology and the voltage level.

Weight:

As shown on Figure 1, the weight influences directly the fuel consumption. The system weight (sum of components weight) is specified using emissions, electrical range and consumption requirements as well as from requested drivability.

Integration:
The integration depicts the possibility or not to integrate the components in the vehicle. Based on the vehicle comfort and utility requirements and the architecture, available volumes are defined for the components. These volumes are represented by maximal length, width and height which must not be exceeded. It is an important challenge for the electric components because the aim is not to achieve the best power or energy density but to fit into the requested volume. The evaluation at deeper level is then linked with the technology and the topology which directly influence the dimensions.

Energy:
The requested system energy (E_{Battery}) is based on the electrical range, consumption and emissions requirements. The available energy is evaluated with the battery voltage ($U_{Battery}$), the capacity ($C_{Battery}$) and the state of charge (SOC). The actual energy (E_{system}) supplied by the system is calculated with components efficiency.

$$E_{\mathrm{Battery}} = U_{Battery} \cdot C_{Battery} \quad (4)$$

$$E_{\mathrm{System}} = E_{Battery} \cdot \eta_{\mathrm{EM}} \cdot \eta_{\mathrm{PE}} \quad (5)$$

2.3 Previous works on hybrid drivetrain optimization

The statement of this work results from several iterations of hybrid electrical drivetrains development. To support this statement and to identify the suitable modeling approach and evaluation level, this section presents an overview of previous works on hybrid drivetrain optimization. It is divided in three sections: vehicle, drivetrain and system. At each level, relevant examples are chosen to show the possible approaches and the influence of the investigation level (The component and sub-component investigation are not considered because single component optimizations are irrelevant for the determination of a suitable global approach).

2.3.1 Vehicle level

When the focus of the optimization is set on the vehicle level, the investigations are generally concentrated on the vehicle consumption and emissions. The optimization is performed by variating the electrical power and energy and the evaluation is done by calculating the performance (consumption and/or emissions) and/or the effort (generally the costs). Within this type of investigation, some works as in [46] have a really deep level of investigation: the article investigates the best compromise between energy and power as in most of the optimizations at the vehicle level but the evaluation is done by estimating the lithium and copper costs. For this purpose, this paper requires using a sub-component level evaluation of the system in combination with a vehicle level modeling approach. Other works, as in [47], investigate the influence of the optimization algorithm. The focus is still set on the identification of the best vehicle configuration (engine and electric machine power, number of cell modules or gear ratio) but the results are strongly dependent on the chosen algorithm as it can be seen in Table 5. Using the same boundary conditions (objectives, evaluation and number of iterations), it shows the deviations between the different algorithms and how the hybrid vehicle is a challenging topic: despite having the same constraints, the final design is strongly varying.

Design variable	Initial value	Algorithm 1	Algorithm 2	Algorithm 3	Algorithm 4
Engine power [kW]	86	83.1	82.4	95.5	87.1
Electric machine power [kW]	65.9	20.2	21.9	24.2	14.8
Number of cell modules [-]	240	245	311	300	238
Gear ratio [-]	3.63	3.9	4.0	3.49	3.42

Table 5: Results of vehicle optimization for different algorithms [47]

Beside the approach, the implementation of the constraints plays a significant role for industrial applications. In hybrid vehicles, the main constraints are resulting from the integration. The work in [48] presents a good overview for the automotive applications. The Pareto front and the investigation area are both limited by the integration: due to the limited available volume for the battery, the maximal power and energy are limited. The article presents also a good overview of the influence of the driving cycle and the role of the legislative framework during design process.

2.3.2 Drivetrain level

At the drivetrain level, the focus is generally set on the architecture comparison, the functionalities analysis, the energy management or the module strategy but contrary to vehicle investigation, the concepts are generally fixed. The solution of the optimizations results then from the investigation of the best components implementation and not the best energy and power combination. The architecture comparisons are often hybrid investigations where both the vehicle and the drivetrain are considered as in [49] or only drivetrain investigation where more parameters are evaluated as in [50]. Both type of investigation are important during the design phase but the second one enables a better evaluation of the drawbacks and the advantages of each architecture. The investigations in [50] evaluate the overall efficiency as well as the engine efficiency and the regenerative braking one while the investigation in [49] only show the emissions reduction for the considered architectures depending on the effort (additional torque and/or power of the electric drive). However both of them show the potential for the emissions reduction thanks to the adaptation of the architectures without requiring any additional energy from the battery or additional power as it can be seen on Figure 18. Other types of investigation are focused on the functionalities as in [51], where different regenerative braking strategies are studied to evaluate their influence on driving performance and fuel economy. The reference is taken without hybrid system and the reduction is shown for each improvement of the implementation. It shows an improvement between 12.2% (hybrid system without regenerative braking) up to 34.3% of the consumption reduction (hybrid system and series braking with optimal energy recovery). As previously for the architectures, it shows the importance of the implementation, topic which is also investigated in [52], where the energy management is optimized. For this purpose the energetic macroscopic representation is introduced, which is chosen after reviewing the different energetic representation which could be applied for drivetrain investigation. Beside the influence of the implementation, this study is particularly interesting from a modeling point of view because it discusses the influence of the bidirectionality and the causality. First the bidirectionality plays a preponderant role for a drivetrain optimization because the aim is to develop an energy management solution which optimizes the energy for the entire drivetrain components and their interactions instead of the relevancy of the results because they are based on the components reactions to solicitations and not only supervises the energy management of each component. Secondly, the causality is an important parameter because it ensures solicitation for the desired reaction.

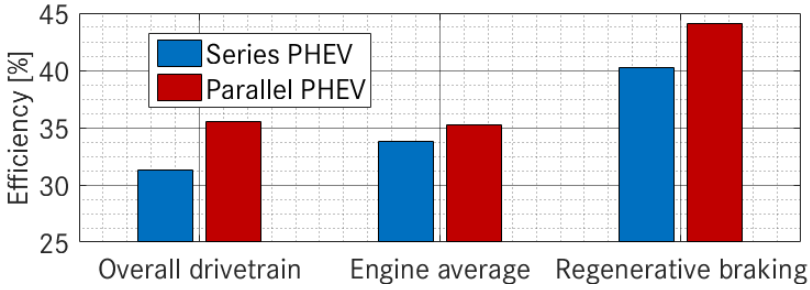

Figure 18: Drivetrain level optimization from [50]

2.3.3 System level

The system level in this work refers to the drivetrain electric components as an entity. Thanks to the defined interfaces and fixed requirements, it aims to identify the optimal combination of electric components for the application. However in the current literature, the difficulties of such investigations are often shifted on the component level by tightening the hypothesis ([53] , [54] and [55]), limited to costs and integration investigation [56] or can be constrained thanks to an additional component [57]. The shifting of the investigation on the component level limits the potential of the solution. For example in [53], the system investigation is reduced to a components investigation by fixing the DC-voltage and the AC-current, which depicts respectively the interactions with the battery and the power electronics. Based on these assumptions, the paper performs a components optimization for a brushless synchronous machine with wound-field excitation (WF-BSM) for hybrid electrical vehicles applications for a defined volume and a defined DC-Voltage (650V). The assumptions can also be done for the energy storage system as in [54], the machine and the inverter are fixed and the system optimization is focused on

the energy storage system for which different technologies are used. The investigations are performed for a 20 kW power cycle where the required energy and power are deduced from drivetrain investigation and the investigation consists in a volume, mass, efficiency and costs optimization. The case of the power electronics is a more sensible one because it has electrical interfaces with both the battery and the electric machine. It is especially challenging when evaluating the voltage level because current works are doing strong assumptions on the machine performance. In [55], the system optimization can be reduced to a power electronics investigation by only considering the voltage sensibility by the inverter on not on the entire system. The machine performance is supposed to be independent and the final decision concerning the voltage level is done based principally on the power electronics investigation (safety, losses and volume). The work in [56] is one of the few studies where the interactions between the components are considered and where the electric drive system is investigated as a standalone entity. Even if it brings a good overview of the costs development for hybrid components and the importance of developing hybrid vehicles, the interactions and the investigation are limited to a superficial level where only the power, the energy, the costs and the integration are considered. Other works such as [58], are investigating the electrical parameters, the integration, the module strategy and the costs. It requires however doing assumptions on each of the evaluation and generally combines inconsistent evaluation methods. For example, the power electronics integration is evaluated using scaling method on the chip area while the machine is considered by its entire volume. These types of investigations offer more flexibility and a wider parameter range with in return a lower accuracy of the results. Finally, there are works as in [57], which can be considered as a real system optimization because it evaluates the influence on both the power electronics and the electric machine. It however investigates only the electric drive system and the battery dependency can be neglected only thanks to the additional converter (DC/DC-converter between the battery and the inverter). The results bring however a first overview of the voltage dependency and a basis to further enhance the knowledge in the area of electric drive system optimization even if the battery is not considered.

2.4 Modeling approaches and environment

This fourth sub-section discusses the different modeling approaches independently from the considered system. The focus is thus set on the global system investigation and the considerations of the interactions in order to determine the best solution independently from the considered components.

2.4.1 Backward modeling approach

In the case of static investigation, two approaches can be used. In this part, the case of the backward modeling approach is discussed. The backward modeling consists in successive steps which allows analyzing based on the requirements, the design parameters for each component. In the case of the electric drive system, it results in successive evaluation of the electric machine, power electronics and battery depending on the technology limits to determine the design parameters. This solution is generally used for design purpose since it enables thanks to several hypotheses to design all the components independently one from another as in [54] or in [59]. In both articles, the components are designed successively: the electric machine translates the mechanical requirements into electrical ones and then the power electronics converts them for the energy storage system which can be finally designed. Adopting such an approach requires doing some assumptions about the components interactions. The backward approach as defined in [60] considers only the power flow between the components. For example the interface between the electric machine and the power electronics is defined by the AC-power and the interface between the power electronics and the battery by the DC-power. The representation for a hybrid electrical vehicle is shown on the following figure.

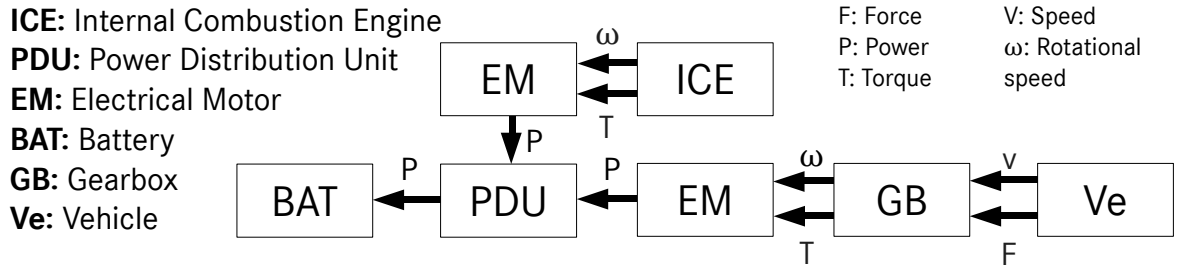

Figure 19: Representation of a hybrid electrical vehicle with the backward approach based on [60]

2.4.2 Forward modeling approach

Beside the backward approach, a system can also be investigated with a forward approach. This approach consists in several steps which allows evaluating based on the components parameters, the performance of the system. In the case of electric drive system, it results in successive evaluation of the battery, the power electronics and the electric machine to determine the system performance (torque and power). This solution is generally used for evaluation purpose where the components parameters are already known as in [61] and [62], where it is used to evaluate the fuel consumption of the vehicle configurations. The solution could also be used for design purpose in the case of a module strategy investigation since the aim is to identify if the same components can be used for different applications. As for the backward approach, it requires doing some assumptions on the components interactions and thus the approach considers only the power flow in the system. It is implemented within the two articles by using efficiency-based modeling approaches. It enables to deduce successively all the power flows in the system. In the case of the electric drive system the mechanical power can be deduced from the AC-power which is also deduced from the DC-power through the different components efficiency. The representation of a hybrid electrical vehicle with the forward approach is presented on the figure below.

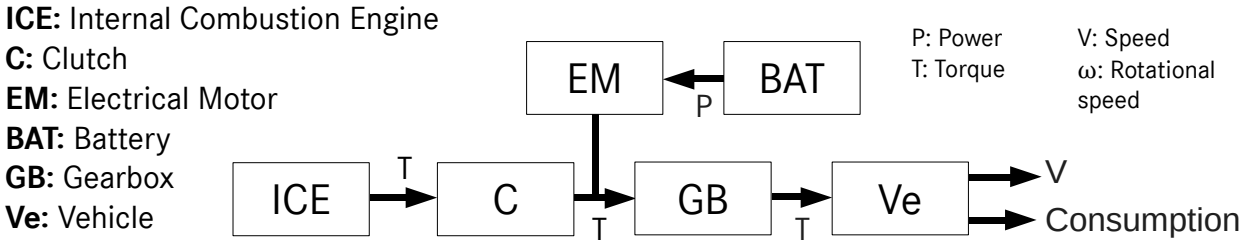

Figure 20: Representation of a hybrid electrical vehicle with the forward approach based on [61] and [62]

2.4.3 Bidirectional modeling approach

Beside the forward and the backward approach, the bidirectional approach considers the interactions between the components in both directions and the causality plays a preponderant role. Direct causality is required for design investigations to consider the influence of a design change on the system performance while the derived causality can be used to explain results observed during tests and measurements. The bidirectional approach is used in [52] and [63] for two different purposes. In the first one, the focus is set on the energy management of different drivetrain architectures. The energy management as the design requires having a good overview of the components and their interactions because it aims to define a suitable management for the entire system and not to combine good solutions for each component individually. The focus of the work in [63] is set on the comparison of two parallel hybrid drivetrains. The bidirectional modeling approach is therefore used to enhance the evaluation of the fuel consumption. The bidirectional approach requires therefore to go deeper in the modeling by considering not only the power flows in the system but by considering also their sub-parameters (for example the DC-power is considered through the DC-current and the DC-voltage). Figure 21 shows the representation used in [52] for the energy management. As it can be seen, a reference for the electric machine is required. It is represented by the requested torque while the actual torque is an output of the model.

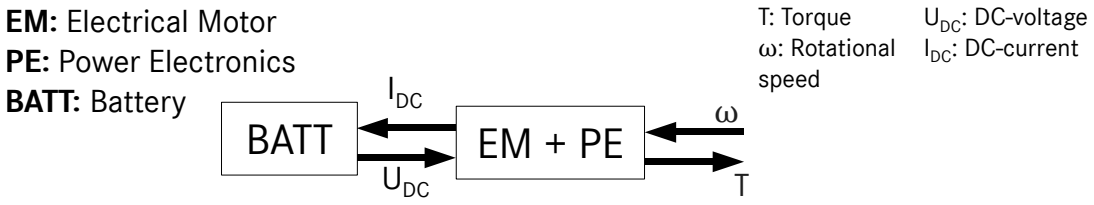

Figure 2 1: Representation of the electric drive system with bidirectional approaches based on [52]

3 Aim and scope of the work

In this last section, the aim and the scope of the work are defined. The limits, the boundary conditions and the hypotheses discussed in this section are deduced from the current state of development of hybrid vehicles, the challenges faced by the electric components and the analysis of previous works on the topic. The first sub-section introduces the aim of the work by discussing the investigation level, the considered parameters and the investigated components. The second sub-sections present the scope of the work to reach this aim. The third sub-section defines limits for the components and interfaces in order to deduce in the fourth sub-section the required modeling for the previously defined component and parameters but also to define the modeling approach.

3.1 Aim of the work

To define the aim of the work, the investigation levels and their influences on the modeling and optimization approach are analyzed. The aim of this work is set on the optimization of drivetrain electric components as an entity (electric drive system). The investigation is refined by defining in this section the evaluation level, the modeling level, the investigated components and finally the considered parameters. Table 6 shows an overview of the current status for the simulation and evaluation of hybrid electrical drivetrain and is used as guidelines for the rest of this part.

	Evaluation level	Modeling level	Considered parameters	Investigated components
[46]	Vehicle	Sub-component	Lithium costs Copper costs	Electric machine Battery
[47]	Vehicle	System	Power Energy	Electric machine Battery
[48]		Vehicle	Power Energy	Electric machine Battery
[49]	Drivetrain	Drivetrain	Torque Power	Electric machine Battery
[50]			Drivetrain architecture	
[51]			Functionality	
[52]			Energy management	
[38]		System	Module strategy	Electric machine Power electronics Energy storage
[58]		Component Sub-component System	Module Strategy Drivetrain architecture	Electric machine Power electronics Energy storage
Thesis	System		Voltage level Topology Module strategy	Electric machine Power electronics Battery
[53]	System	Components	Electric machine design	Electric machine
[54]			Energy storage design	Energy storage
[55]			Voltage level Topology	Power electronics
[57]			Voltage level Topology	Power electronics Electric machine
[56]		Vehicle/drivetrain	Power Energy Costs	Electric machine Power electronics Energy storage

Table 6: Previous work for the optimization of electric drive system

3.1.1 Evaluation level

The evaluation level is the first boundary conditions which need to be set. To further refine system optimizations, the evaluations in this work are done on the system level. As shown previously, it enables to consider the electric components individually ([53], [54] and [55]), combined [57] or as an entity [56]. Due to detailed or superficial investigation, the current investigations do not offer the possibility to address the challenges considered in this work or only for one or two components. Consequently one contribution of this work lies in the combination of the right modeling and evaluation level.

3.1.2 Modeling level

As already discussed, most of the previous works only consider system evaluation with superficial (vehicle/system) or detailed (components/sub-components) modeling level because choosing the system level for the evaluation and the modeling requires doing assumptions on both the high level requirements (vehicle/system) and low level parameters (components/sub-components). In previous works, the assumptions are only done on the requirements (system evaluation with components modeling) or on the modeling (system evaluation with drivetrain modeling). In this work, the system level is defined as follows: each modeling where the results are considering the challenges and the boundary conditions of system investigation are considered as system level modeling. For example, a method for the evaluation of component integration (estimation of the inverter dimensions) even if it considers sub-components (power modules or capacitors) can be considered as a system level method or modeling if the methods used for the sub-components considered only the system requirements (current and voltage) and does not deeply investigated the sub-components parameters (estimation of the chip surface in the power modules). The system level as already defined represents a compromise to investigate both the component parameters by considering their interactions as well as the boundary conditions from the automotive industry.

3.1.3 Investigated components

The investigated components and especially their interactions play a significant role for the valued-added of this work. Component constrained investigations based on entire system assumption ([53], [54] and [55]) have already been addressed most of the hybrid vehicle challenges considered in this work, but they only offer the possibility to identify optimized component solutions instead of the best components combination. Sometimes several components are considered [57] but the results are still constrained because it excludes the energy storage system. This work considers all the electrical components for the traction purpose which includes the battery, the power electronics and the electric machine.

3.1.4 Considered parameters

Beside the investigated components, the considered parameters need to be defined. The considered parameters are deduced from the challenges discussed in the first section. As shown in the previous section, they are generally considered at higher investigation level (module strategy) or lower level (voltage level and electrical architecture). To be correctly addressed, they are first separately discussed in the chapters about components modeling and secondly during global system analysis. They play a major role when choosing the modeling approaches because they defined what needs to be modelled and where assumptions can be made.

3.1.5 Aim and goals of this work

The aim of this work is to further investigate the potential of hybrid electrical vehicle regarding the voltage level, the electrical architecture and the module strategy. For this purpose, compromises need to be done as the considered parameters, the investigated components or the modeling and evaluation level. The goals addressed by this work could have been solved by combining previous work and modeling approach based on components investigation ([53], [54] and [55]). However in the case of an optimization, this solution would have led to high simulation effort (time and complexity). By introducing the right limits, interfaces, suitable modeling approaches can be found which can address the challenges of this work without leading to high simulation effort from the point of view of the electric drive system.

3.2 Scope of the work

To find a suitable compromise between the parameter range and the accuracy, boundary conditions need to be defined. The consistency of these boundary conditions ensures the relevancy of the results. They are presented on the Figure 22 and show the global scope of the investigation of hybrid electrical vehicles. In this work, the aim is to refine the design of the electric drive system by limiting this scope. This limitation requires excluding both vehicle and drivetrain topics as well as deep-components investigations. However due to their direct influence on the researched topic and thanks to the defined interfaces, these parameters can be considered but only indirectly.

Sub-component design:
Considering the aim of this work, detailed investigations of the sub-component design (electromagnetic design of electric machine, conception of semiconductors power module or battery cells) cannot be considered. The influence of this sub-component design can still be considered in the system evaluation by considering the influence of the design changes of the system parameter as for example variating the electric machine properties for different designs.

Environment and integration:
The environment and integration define external conditions for the investigation such as coolant flow and temperatures or available volume for the components. They are not a key point of the scope for this study but need to be considered through the behavior of the cooling system as well as thermal and integration limits of the systems which need to be evaluated.

Test and driving cycles:
As presented in this chapter, driving cycles and other tests represent the legislative framework for vehicle development and play a preponderant role. They are not directly investigated because only the electric components are considered but their protocol and the resulting driving cycles are used to define the evaluation of the electric drive system.

Costs and reliability:
Costs and reliability are parameters which affect the vehicle development since its beginning but cannot be considered directly in this work. Costs are a sensitive topic but cannot be investigated in this work due to the strategy used at higher or lower investigation levels. The topic of the reliability is included in this work in the sub-components design.

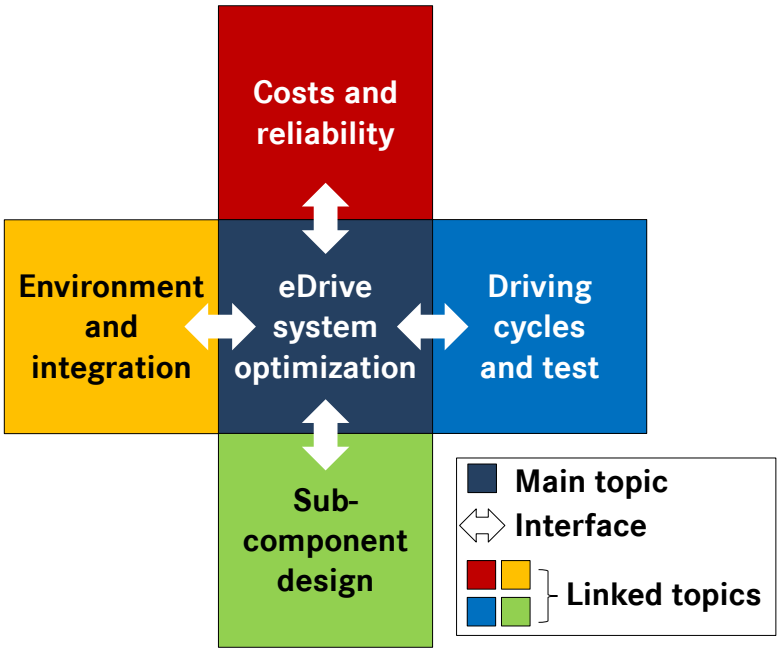

Figure 22: Scope of the work

3.3 Assumptions and interfaces

Since the scope and the aim of this work are set, this sub-section introduces the limits and the interfaces of the investigation in this work. First, limitations are set for the components in order to restrain the investigation range because the aim is to show the remaining potential of the current components by proposing an enhanced design approach and not by introducing new technologies. Then the aim is to define interfaces and limits for the modeling to ensure the relevancy of the results and finally to define the required modeling level to address the challenges of this work under the boundary conditions defined in the two previous sub-sections.

3.3.1 Components limitations/assumptions

To find a good compromise between the complexity and the parameter range, the work is limited to system evaluation and modeling of electric components. Beside the limits set for the investigations, additional restrictions are defined for the electric components and relevant technologies are chosen deduced from the current status of development presented in this chapter. Concerning the electric machine, this work considers only the following technologies: PMSM and IM. Regarding power electronics topologies and technologies, the modeling is limited to the three-phase voltage source inverter and the boost-converter as shown previously and the technologies are limited to IGBT and Mosfet. Finally this work considers only the following batteries technology: li-ion with no restrictions concerning the cell formats.

3.3.2 Interfaces and limits

Focused on the drivetrain electric components, this work aims to address the challenges that they are facing. For this purpose, the electrical, mechanical and thermal behavior of the components as well as their integration are investigated but limited to a system evaluation. This approach requires defining interfaces and limits in order to find a compromise between the investigated parameter and the complexity which may result. There are three main interfaces for the defined scope of this work: an electrical one with the HV-Network, a mechanical one at the electric machine shaft and a last one for the communication with the vehicle energy management.

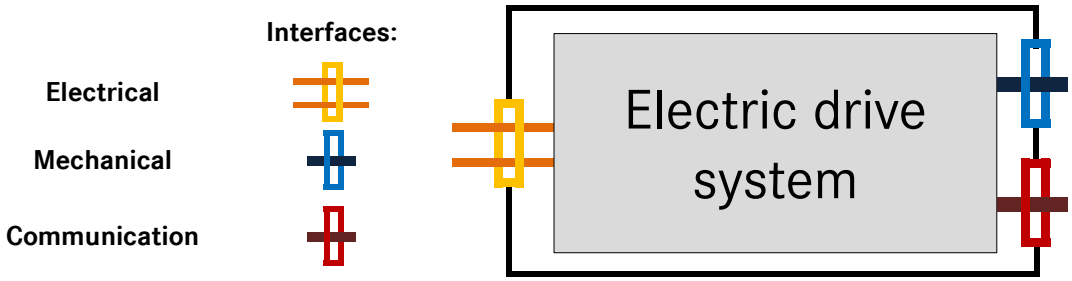

Figure 23: Limit and interfaces for electric drive system investigation

These limits and interfaces ensure the relevancy of the results by translating the global vehicle requirements as well as the deep sub-components performance at the considered level. These interfaces are consistently defined independently from the electrical architectures. They enable to restrict the investigating area and thus enhancing the analysis by focusing on the relevant components.

3.4 Modelings, methods and approach

Based on the scope and aim of this work as well as the previously defined limits, the required modelings and methods can be deduced. Then based on the analysis of the goal of this work and the previous works, the modeling approach is defined.

3.4.1 Required modeling and methods

This first part presents the different modeling and methods which are required to analyze electric drive systems and to determine optimized systems for the considered challenges in this work. The choice done for this study imposes thus developing three main types of modeling or methods which can be defined independently from the considered component: the component behavior, the integration investigation and the thermal behavior.

Component behavior:
The components behavior depicts how the requirements (drivetrain/vehicle level) can be achieved under different boundary conditions (parameters from component/sub-components level). Component modelings should allow evaluating the electric drive system requirements (power, torque, speed and energy) and addresses most of the challenges for the further developed of hybrid electrical drivetrains (voltage level, electrical architecture and module strategy). The resulting scheme is shown on Figure 24.

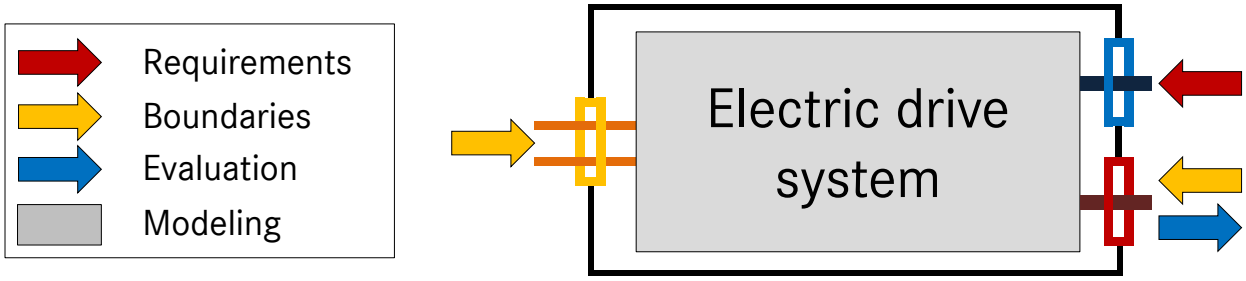

Figure 24: Scheme for behavior modeling of electric drive system

Thermal modeling:
The challenges imposed by the component environment require the components to be thermally investigated. Estimating the thermal behavior can enhance the evaluation of the component behaviors; allow calculating thermal limitations and thus having a better overview of the global system performance. Thermal component modeling investigated the heat source in the system (losses) to evaluate the components temperature by considering parameters from their environment (coolant flow and temperature).

Integration investigation:
The component integration is required to evaluate electric drive system requirements. The method should estimate the dimensions and the weight by aiming to identify the components which best fulfill the requirements (dimensions and weight). The main aim is to develop an approach which enables to investigate the integration instead of the power density and thus to identify the components which offers the highest performance for the defined volume and weight instead of the components with the best power or energy density.

3.4.2 Modeling approach

Before defining the suitable modeling approach for this work, the term causality need to be defined. It is an important topic for system investigations. Hence this section introduces first this term and then define the suitable modeling approach.

Causality:
The causality depicts the relationships between the causes and the effects. The causality can be direct: the effects are expressed depending on the causes or derived: the causes are explained based on the observed effects. Hence for the requirements of this work, the direct causality is chosen in order to analyze properly the challenges faces by the components. The main challenges lie then in the definition in the next chapter of the inter-connections between the components. The causality and its importance are discussed in details in [52].

Modeling approach:
The modeling approach is the second topic of interest in this part. As it is presented in the previous section, the backward approach is considered for design purpose, while the forward and bidirectional approaches are used for the energy management sizing or for performance evaluations. Generally, the current design methods for the eDrive System are combinations of the backward and the forward approaches and the investigations are generally reduced to successive components investigations with the backward approach for the design and to a vehicle investigation with the forward approach for the performance evaluation. The current approach is based on strong assumptions on the components, which are generally calculated in worst case to ensure the performance of the system. The method is summarized on Figure 25.

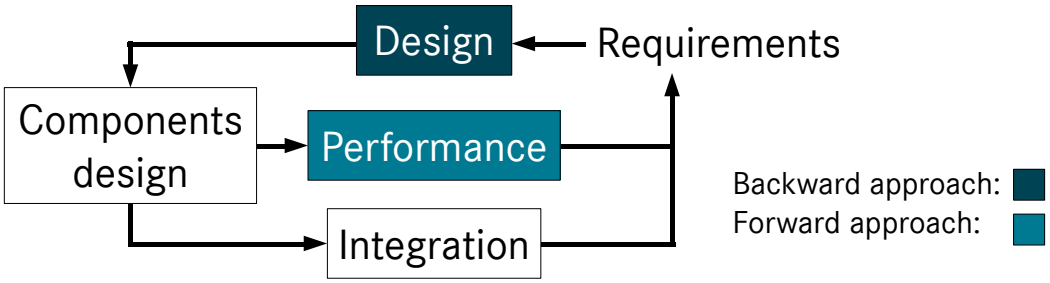

Figure 25: Current approach for the design of electric drive system for hybrid electrical drivetrains

The assumptions of this approach have some drawbacks concerning the accuracy of the results. The approximations are however done using worst-case calculation which could only result in an over-dimensioning of the system. Therefore this approach fulfills the requirements of the design purpose by ensuring the performance due to the over-dimensioning. Beside the component behaviors and performance, the integration (volume and weight) also needs to be evaluated. The evaluation is generally done in parallel of the sub-components design where the weight and volume requirements are considered for the design. The technology limits and therefore the evaluation of both the performance and the integration could lead in case of non-valid solutions to an adaptation of the requirements or the concepts. Using this approach and the feedback from the evaluation, the design could be refined. Due to the approximations of the approach, the solution generally results in the determination of the combinations of the best components and it requires several iterations of this process to identify the solutions. Considering this analysis, the bidirectional approach is chosen for this work. The aim is to determine simultaneously the performance and the design of the system in order to have a global system model. This model can then be used to address the challenges discussed in this work and to perform several analyses. An example of the application of this modeling approach for the electric drive system can be found in [52] and is shown on Figure 21. This figure is however only an overview and additional parameters need to be considered as inputs and outputs to accurately model the components. Therefore, the inputs and outputs are not defined in this chapter but the modeling approach and the causality are taken into consideration during the development and the implementation of each modeling and method for this work in the next chapters.

4 Chapter conclusion

Within this chapter, the current state of development and the investigation on the topic of hybrid electrical drivetrains is presented before introducing the aim and scope of the work. The first section discusses in details the different drivetrain architectures, the electrical components for the traction as well as the challenges and the specificities of the automotive industry. In order to define the suitable approach for this work, the second section performs an analysis of the current literature about modeling electric drive system. It presents on different investigation levels, the possible solutions to investigate the electrical components for the traction purpose. It shows the complexity of a global approach because compromises and approximations need to be done on both the superficial parameters (vehicle and drivetrain level) and the deep ones (component and sub-component level). Finally, the third section defined the approach which is followed in this work. When comparing it with the works previously analyzed, it shows the challenges of the chosen approach. It requires various and multi-domain knowledge for the modeling, the evaluation and the optimization of electric machine, power electronics and battery performance as an entity. These requirements are generally only partially fulfilled by the previous work due to the complexity of finding the right modeling approach to address the challenges. Considering the current status, the previous works and the challenges addressed by this work, the next chapters aims to find suitable modeling approaches to evaluate the electric drive system. They show how suitable hypothesis and approximations can be done to defined system level modeling approaches which address challenges which are generally addressed on the components or sub-components level (voltage level, power electronics topology, machine technology or electrical architecture) or on the drivetrain and vehicle level (module strategy).

Chapter 2: Modeling electric machine for hybrid electrical drivetrain

Having defined the scope, the investigation level, the considered components and parameters as well as the modeling approach, this chapter is focused on the determination of a suitable approach for the modeling of electric machines in hybrid electrical drivetrains. First, the machine structures, the working principle and the losses types are explained. Following this and for each considered modeling, a review of the different modeling approaches at the different investigation level is presented and their implementation, their validation and their contribution are detailed.

1 Electric machines structure, working principle and losses

This section discusses the structure, working principle and losses for the two technologies chosen previously: permanent magnet synchronous machine and induction machine. First the rotor and stator structures are presented and then the detailed structure for each technology as well as their working principle and losses are explained.

1.1 Electric machine structure

The structure of the electric machine is not only dependent on the technology but also on the winding and integration concept. The different combinations, based on current literature [44] and [31], are presented in the Table 8 based on their rotor and stator structure. Among the rotor structures, two main categories can be defined: the first one where the machine has a full rotor and the second one with an empty rotor which can be used for other components (e.g. the clutch in hybrid applications). Moreover, within the full rotor structures, two variants can be identified, one where active materials completely fill the rotor (variant 1) and the second one with cutting for the purpose of reducing the weight (variant 2).

		Full rotor		**Empty rotor**
		Variant 1	Variant 2	
Stator structure	Concentrated windings	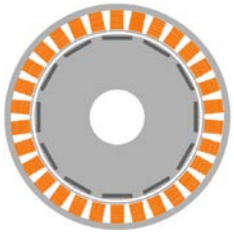	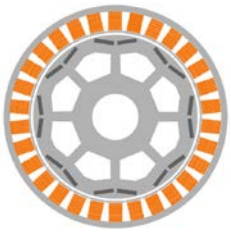	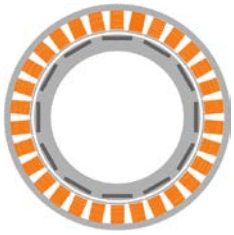
	Distributed windings	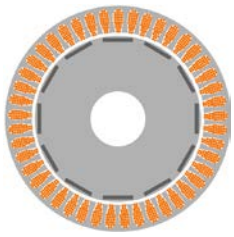	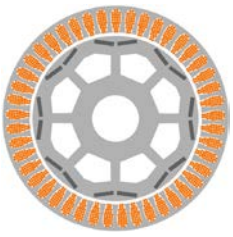	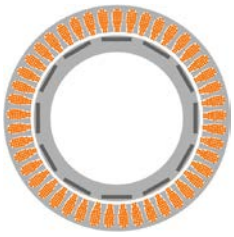

Table 7: Rotor and stator structure (PMSM as example)

Concerning the stator structure, the main influence lies in the winding technology as discussed and shown in [44] and [64]. The stator and rotor structure (design variations) are not directly investigated during the optimization approach but need to be considered due to their influence on the weight and volume estimation in this work. Beside consideration about the stator and rotor structure, the technology and its influence are described before introducing the working principles and the losses.

Induction machine:

The investigations in this work consider an induction machine with a squirrel-cage rotor. The machine is composed of a stator with a multiphase winding system and a laminated steel core and of a rotor with an aluminum bar cage and a laminated steel core as shown on Figure 26.

Permanent magnet synchronous machine:

Concerning the permanent magnet synchronous machine, this work considers the following structure: a stator with a multiphase winding system and a laminated steel core and a rotor with permanent magnet and a laminated steel core as shown on Figure 26.

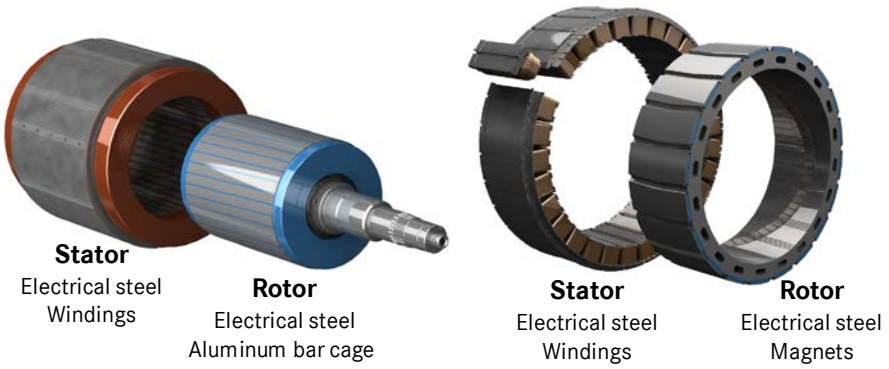

Figure 26: Induction machine (left) and Permanent magnet synchronous machine (right) structure

1.2 Working principle

Electric machines convert electrical power in mechanical power and vice-versa. In both machine technologies considered in this work, the stator is composed of a multi-phase system and they differ only by their rotor excitation. In this section, the IM and PMSM working principle are explained.

Induction machine:

When a voltage is applied on the stator, alternating current in each winding of the stator is appearing. It generates an alternating magnetic field which is closed via the rotor. The shift between the stator phases results in a rotating magnetic field. This field induces voltage in the rotor bar and due to the short-circuit ring at both rotor ends, a current flow is produced. As for the stator, this current generates a magnetic field and thus the rotor is pulled by the stator field which results in a rotational movement with a slight lag (slip) versus the stator field.

Permanent magnet synchronous machine:

Like the induction machine, the stator generates a rotating magnetic field due to the applied voltage. The field in the rotor is generated by the permanent magnets. This field rotates synchronously with the stator field to produce the rotational movement.

1.3 Losses

Based on the previously explained structures and working principles, this section presents the different losses categories in electric machine. They are shown in the following Sankey diagram, which represents the path between the AC-power (P_{AC}) and the machine power (P_{EM}). The main difference lies in the rotor losses, which are copper losses for IM and magnetic losses for PMSM. Besides the electrical and magnetic losses, the study in this work considers also the friction losses due to the machine rotational movement.

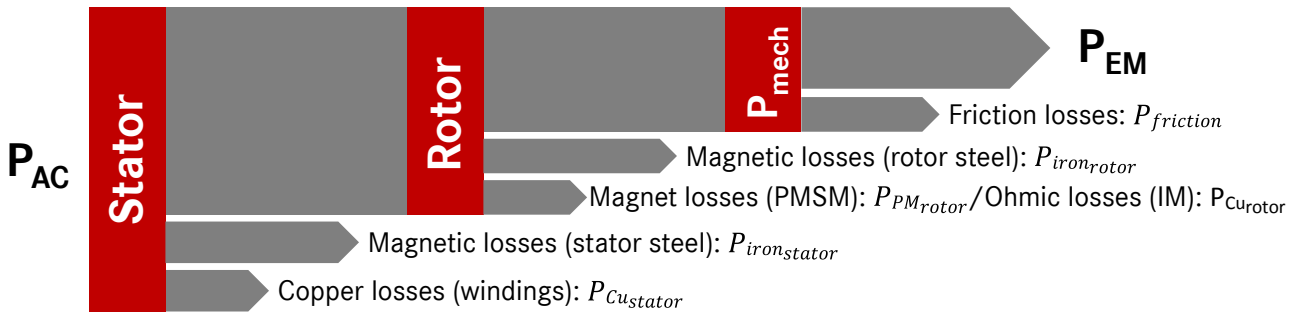

Figure 27: Sankey diagram for PMSM and IM as considered in this work, adapted from [8]

2 Component behavior modeling

Based on the structure, working principle and losses described in the previous section and by considering the challenges considered in this work, this section discusses the topic of component behavior modeling. It first presents relevant previous work on the topic. Based on the analysis of these works, two suitable solutions are developed and compared in order to determine the one which can address in a suitable way the challenges of this thesis. After this the chosen solution is validated based on automotive component measurements and finally the added values for system optimization is presented.

2.1 Modeling approach

From the considered parameters and the investigation level defined in the previous chapter, the modeling approach for the investigation of electric machine behavior can be deduced. It aims describing the translation of system mechanical requirements to electrical requirements. For this purpose, the approach described on Figure 28 is retained. This modeling approach enables to consider both the electrical (voltage), the thermal (temperature from both rotor and stator) as well as the mechanical behavior (torque and speed) of the electric machine as inputs. The outputs allow then depicting the achievable performance (actual torque) as wells as describing accurately the AC-interface with the power electronics (AC-current, voltage and power, power factor and efficiency) and with the thermal modeling (losses vector).

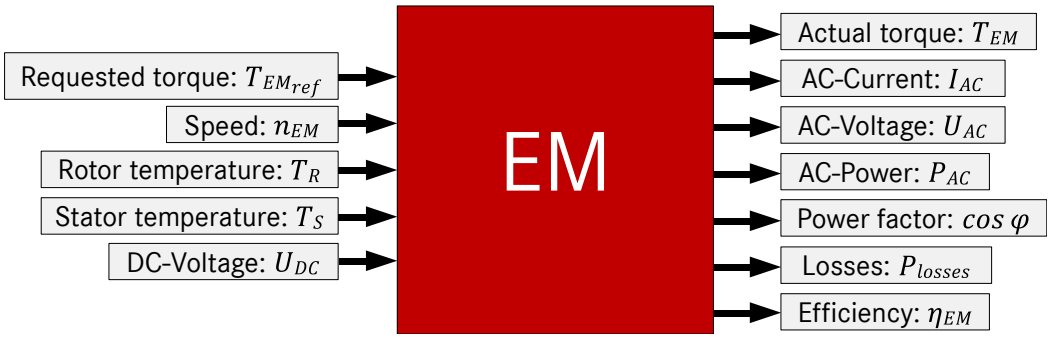

Figure 28: Component behavior modeling for the electric machine

2.2 Previous works and investigation level influence

In this section, previous works on the modeling of electric machine are analyzed. The works are organized based on the investigation level. For each level, examples are presented and their potential for the study in this work is discussed. The analysis begin with the sub-component level, then the component level, after this a system level example is discussed before introducing the more superficial levels.

2.2.1 Finite element analysis and permeance network

At detailed levels, the component behavior can be modelled using different method such as FE-Analysis (Finite Element, FEA) as in [20] or with permeance network as in [65]. At this level the parameter range is wide and enables to investigate numerous parameters: geometry, materials, and voltage, current or saturation phenomena. The FEA relies on the construction of a complex network in 2D- or 3D-environment such as Opera. It is composed of several domains which are subdivisions of the whole machine structure, in which the different magnetic and electrical characteristics are calculated. FEA is often used for electric machine design because it enables to analyze the performance with a high accuracy. In a similar manner, the permeance network aims to depict the magnetic and electrical behavior with a network. The permeance is a parameter which defines the capability of a path or a material to “conduct” magnetic flux. By resolving the permeance network, the performance of the machine can be estimated. It offers an alternative to FEA with a quite comparable accuracy. These solutions are generally used for component design purpose as in [20]. In this dissertation, the potential of direct drive electric motor is investigated. After determining the most suitable technology, it optimizes, based on a FEA, the geometry of the machine for defined voltage and current levels. The design is optimized for a voltage of 360VDC and a current of 230Arms. As other

works on the machine optimization (for example [53]), the focus at this level is set on the machine design optimization and it only considers the global system challenges by optimizing the performance and the losses to optimize the energy provided by the storage system. The permeance network offers similar possibilities and is investigated in details in [65], where the aim is to show its potential versus FEA. As explained in the article, the permeance network is a relevant alternative due to its higher speed and its comparable accuracy. These two characteristics are especially interesting for an optimization approach because it allows comparing lots of combination without requiring high simulation effort. These two approaches consider however a larger parameter range as the one required for this work: the scope is limited to a system optimization and no design of the sub-components is considered.

2.2.2 Circuit based approaches / mathematical model

Using these approaches, deep analyses of the design are not considered and the challenges lie in the modeling of the machine. Deduced from more detailed investigations, it aims to depict the machine performance in different operation conditions (voltage, current or temperature variations). Circuit based models can be both mathematically and graphically represented as in [8] and [66] and aim to accurately model the components behavior. In the case of the PMSM and the IM, transformations enable to reduce the investigation to less complex equivalent circuits. The mechanical behavior is then defined based on the electrical parameters which enables to couple the electrical and mechanical behavior of the machine. The machine characteristics can thus be estimated based on the mechanical requirements and the electrical limits. In [67], the theory about electric machine modeling is introduced and the different equivalent circuits for the different technologies are introduced. It presents a good overview of the different modeling approach and the assumptions which can be done for the modeling of both the electrical and thermal behavior of the machine. Based on a similar approach as the one presented in [8] or in [67], the circuit based model is used in [68] to evaluate the performance of a PMSM. The machine is represented using the Clark and Park transformation, which results in two equivalent electric circuits in a rotor-oriented reference frame. A particularly interesting point in this work is the discussion about the voltage and current limits. Using the rotor-oriented reference frame, the link between the machine currents and voltages, the maximal source voltage (U_{DCmax}) and the maximal inverter current (I_{ACmax}) are described (see equations (6) and (7)). These limitations have a high relevancy when considering the modeling approaches in Figure 28 and the challenges considered in this work. Based on this approach, the authors calculate efficiency maps, which they consider as a suitable solution to depict electric drive at the system level and use to evaluate the consumption and the performance of the drivetrain.

$$i_d^2 + i_q^2 \leq I_{ACmax}^2 \quad (6)$$

$$U_d^2 + U_q^2 \leq U_{DCmax}^2 \quad (7)$$

2.2.3 Data maps based approaches

As shown in [68], the data maps generated with circuit based model (or directly using FEA) can be used for the modeling purpose at different levels (system, drivetrain and vehicle). They generally differ by their considered parameters but independently from the investigation level, they all consider the electric machine as a black-box and do not aim to consider all the magnetic and electric parameters but only to evaluate the energetic and electro-mechanical behavior of the system as depicted in Figure 28. System level aims to consider as much parameters as possible (temperature, voltage and current influences) whereas the drivetrain and vehicle level consider superficially the machine (generally a single efficiency maps with power and torque limitations). The use for system level investigation is shown in [68], where the authors used the circuit based model as an intermediate tool to calculate maps which are then implemented in the simulation. In [68], the results are depicted only for the voltage level influence on the machine efficiency (see Figure 29) but it could be done for all the machine parameters and also for different boundary conditions (voltage, current and temperatures in both rotor and stator). It shows how data maps allow investigating electrical parameters and storing the relevant information without needing to use for each point the circuit based approach. When the focus is set on higher investigation level, the efficiency maps can be considered for a defined set of boundary conditions (relevant temperatures, design voltage and current) and the adaptation is done through torque and power scaling or limitations as in [69]. In this article, the torque is scaled to

investigate different power level between 10 and 100 kW and its influence on the electrical range, emissions and consumption. The data maps based solutions are also independent of the machine technology and offer the possibility to compare the machine technology as shown in [70].

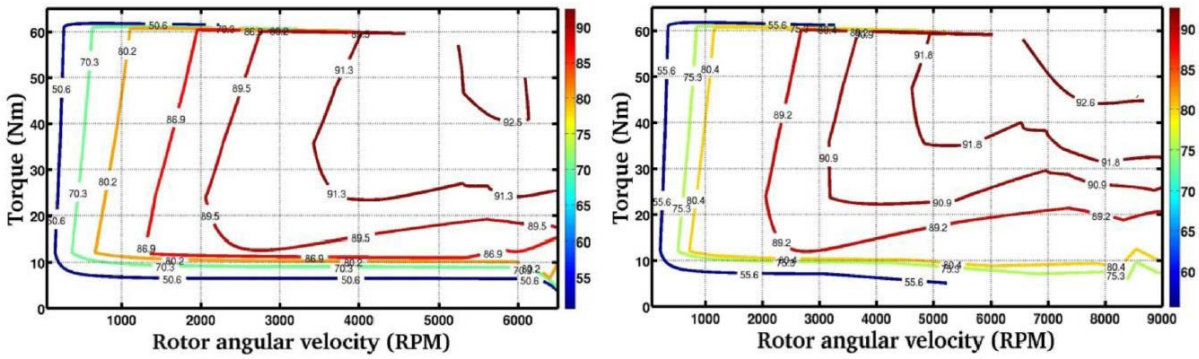

Figure 29: Efficiency maps for @260V and 340V [68]

2.2.4 Evaluation for electric drive system optimization

When determining the right method to fulfill the modeling approach defined in Figure 28, the following parameters need to be considered: the accuracy, the simulation effort and the parameter range. The accuracy is generally evaluated on a scale between 0 and 100% but it is here qualitatively evaluated before more detailed investigation in the next section. The simulation effort is more complicated to evaluate because it depends on more criterions: simulation time and complexity which are dependent on the simulation environment. Some methods can be easier to implement but require more simulation time and inversely. Finally the parameter range is more abstract and can be binary evaluated: the solution fulfills the requirements or not. The numbers of approaches which fulfill the problem statement are quite limited when considering the requirements in Figure 28. Among all the solutions, the circuit based method and the data maps based one stand for good compromises between accuracy and simulation effort. Both the method enable to investigate the electrical and thermal parameters needed to investigate the electrical and mechanical behavior of the electric machine.

	Representation	Accuracy	Simulation effort	Parameter range
Finite element analysis	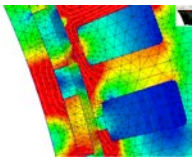	+ +	- -	✓
Permeance network	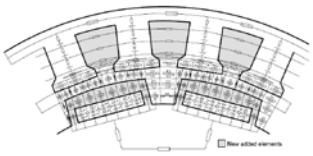	+	-	✓
Circuit based	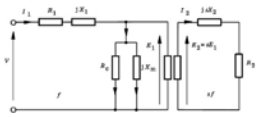	o	o	✓
Maps based	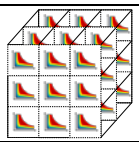	-	+	✓
Single maps	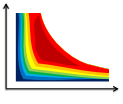	- -	+ +	X
Single efficiency		- -	++	X

Table 8: Comparison of approaches for the behavior modeling of electric machine

2.3 Modeling implementation

For the implementation of the modeling approach of electric machine, the process described on Figure 31 is used. The FEA allows identifying the machine parameters for the circuit based model as well as their dependency on the machine saturation or the temperatures. These parameters are stored using matrix which can be used within two approaches. In the first one, the machine parameters are directly implemented within the simulation using the circuit based model which calculate the machine characteristics for each driving points. The second one uses the circuit based model to generate data maps of the machine performance under different boundary conditions (voltage and temperatures), which are then implemented in the simulation. Both methods can fulfill the requirements but the circuit based solution calculates intrinsic properties which are not required and therefore the two methods is compared in details at the end of this sub-section to determine the most suitable one. The data maps can also come directly from the FEA, which reduce the approximations between the design and the global model.

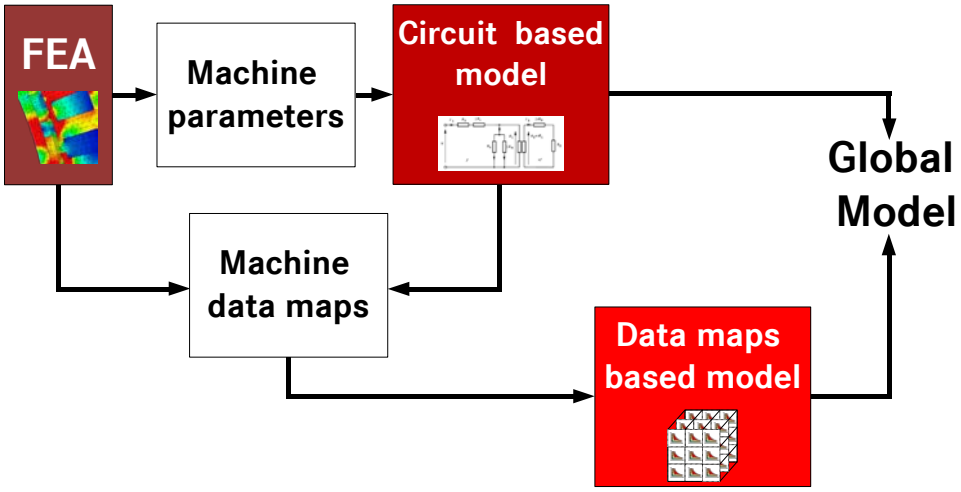

Figure 30: Process for the modeling of electric machine for electric drive system

2.3.1 Circuit based model

In this sub-section, the model is explained in three parts: first the model for the PMSM is detailed, then the model for the IM and finally the identification of the parameters.

Permanent magnet synchronous machine model:

To model a PMSM, equivalent circuits in a rotor-oriented frame is generated using the Clarke and Park transformations similar to the one used in [8] and [68]. Then three main equations are deduced (see (8), (9) and (10)), these equations represent the mechanical and electrical behavior of the machine. As shown later, the parameters are dependent on i_{dq} and the temperatures (rotor and stator) and extracted from the results of the FEA.

$$T_{PMSM} = \frac{3}{2} \cdot p \cdot \left(\Psi_{PM}(i_{dq}, T) + \left(L_d(i_{dq}, T) - L_q(i_{dq}, T)\right) \cdot i_d\right) \cdot i_q \quad (8)$$

$$U_d = R_s(T) \cdot i_d - \omega_{el} \cdot L_q(i_{dq}, T) \cdot i_q \quad (9)$$

$$U_q = R_s(T) \cdot i_q + \omega_{el} \cdot \left(L_d(i_{dq}, T) \cdot i_d + \Psi_{PM}(i_{dq}, T)\right) \quad (10)$$

where T_{PMSM} is the machine torque, p the number of poles, $\Psi_{PM}$the magnet flux linkage, idq the current in the dq-reference frame in which L_d, L_q are the inductances, U_d and U_q are the voltage while R_s is the stator resistance and ω_{el} the electrical rotational speed. These equations can be combined with loss models to create the energetic model of the machine. The losses are calculated with a global loss model (11) based on the Bertotti approach for the magnetic losses (P_{iron}) and a general loss model (12) for the coper losses (P_{copper}) using material specific coefficient (C_{hyst} and C_{eddy}) as well as the machine frequency. The Bertotti approach is chosen because it is the method used for the calculation of the losses during the post-processing of the electric machine design.

$$P_{iron} = C_{hyst}(i_{dq}, T) \cdot f + C_{eddy}(i_{dq}, T) \cdot f^2 \quad (11)$$

$$P_{copper} = n_{phase} \cdot R_s(T) \cdot {I_{AC}}^2 \quad (12)$$

Finally after the electrical and mechanical behavior, the friction losses are interpolated with the results of mechanical analysis of the machine structure. The results are stored as a matrix, where the first column contains the values of the rotational speed and the second column the values of the friction losses. The losses are then linearly interpolated between the values stored in the matrix as shown in Figure 31.

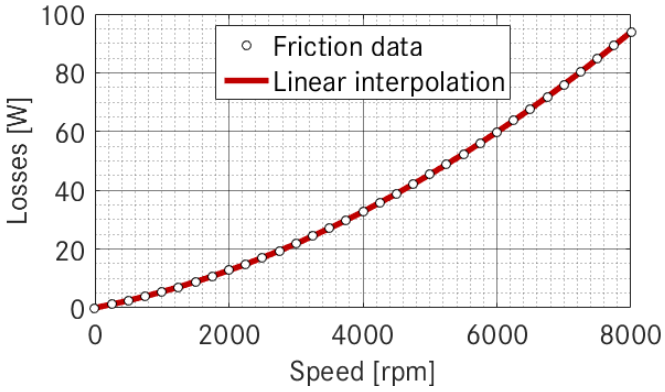

Figure 31: Interpolation approach for the friction losses

Induction machine:

As for the PMSM, an equivalent circuit can be used to model the IM. In this case, the model uses a single phase equivalent circuit as shown on Figure 32. From this circuit three equations can be deduced to model the electrical and mechanical behavior of the machine. For this technology, the dependency is related to the short-circuit current i_{SC} and the magnetization current i_μ. As for the PMSM, these equations can be coupled with loss model of the iron losses, the copper losses and the friction losses to develop the energetic model of the machine (with a dependency on i_μ for the iron loss parameters). Therefore, the equations enable to calculate the torque T_{IM}, the voltage $\underline{U_s}$ and the losses in the machine based on the equivalent rotor resistance R_r', the slip s, the rotational speed n, the stator resistance, the different currents in the machine, the electrical rotational speed ω and the inductances in the machine [67] .

$$T_{IM} = \frac{3 \cdot {I_r'}^2 \cdot R_r'(T)\,(1-s)}{2\pi \cdot n \cdot s} \quad (13)$$

$$\underline{U_s} = R_s(T) \cdot \underline{I_s} + j\omega \cdot L_{\sigma s}(i_{SC}, T) \cdot \underline{I_{sL}} + j\omega \cdot L_m(i_\mu, T) \cdot \underline{I_\mu} \quad (14)$$

$$0 = \frac{R_r'(T)}{s} \cdot \underline{I_r'} + j\omega \cdot L_{\sigma r}'(i_{SC}, T) \cdot \underline{I_r'} + j\omega \cdot L_m(i_\mu, T) \cdot \underline{I_\mu} \quad (15)$$

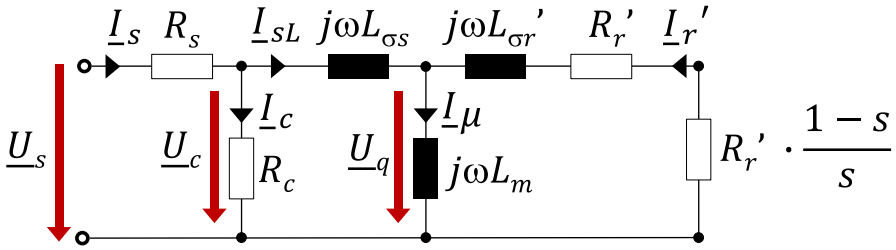

Figure 32: Single phase equivalent circuit of the induction machine [67]

Identification of the parameters:

Two main identifications are required to evaluate the characteristics of the machine using the circuit-based model. The first identification is related to the temperature dependency and the second one is the identification with the

FEA-results. Two types of temperature dependencies are considered: the dependency of magnetic parameters (inductances and loss parameters) and the dependency of metallic conductor materials (stator and rotor resistance). The first one is considered within the FEA-results which provide several series of data for different temperature of the magnetic materials (generally four values based on the data provided by material suppliers) while the second one is considered with a linear dependency on the temperatures as depicted by the equation (16) where K_T is the temperature coefficient and where T_{nom} and $R(T_{nom})$ are respectively the nominal temperature and nominal resistance. The identification of the parameters from FEA-results is done using matrix. These matrix are generated using an internal proprietary tool suite and are calculated using finite elements. For each temperature, a dataset of parameters is generated where each parameter is stored as a matrix dependent on i_{dq} for the PMSM and i_{SC} and i_{μ} for the IM. The variations of the inductance of the d-axis can be seen on Figure 33 for variation of i_{dq} in a PMSM.

$$R = R(T_{nom}) + \left(1 + K_T(T - T_{nom})\right) \quad (16)$$

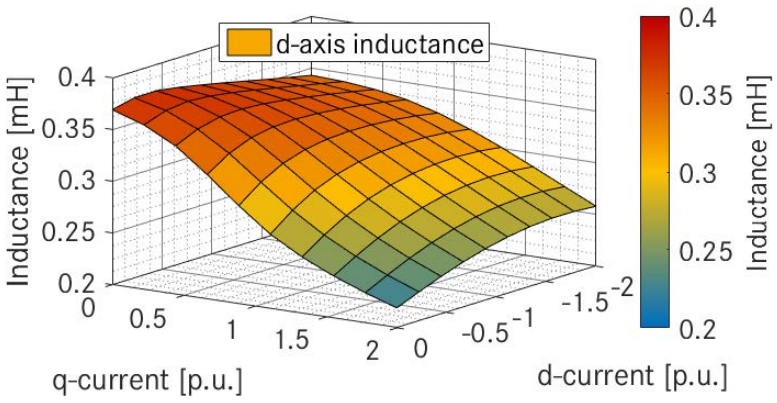

Figure 33: d-axis inductance dependency on i_{dq}

2.3.2 Circuit based modeling approach

As discussed previously, the circuit based approach and the data maps based approach show both a good compromise between accuracy and parameter range. In this sub-section, the approach to use directly the circuit based model for the modeling is presented for both machine technology. When using this approach, no direct connection can be done between the input- and the output-parameters and hence additional intrinsic parameters of the machine need to be calculated within several steps. First, the limits of the machine are calculated, then the parameters are actualized in the equations, next the electrical parameters are calculated to finally calculate the output parameters. The approach is summarized on Figure 34.

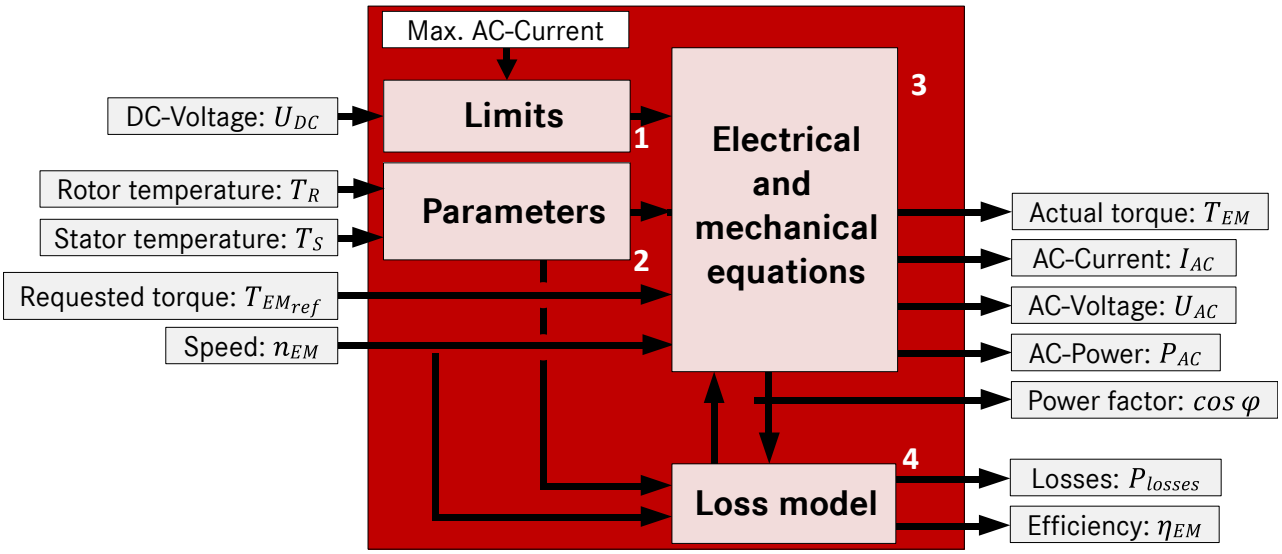

Figure 34: Circuit based modeling approach

Calculation of the limits (1):

Depending on the boundary conditions, the machine can only be driven in a defined part of the torque and range speed. These limitations are due to the maximal value of the phase-current (I_{AC}), the maximal value of the DC-voltage (U_{DC}) and the control method through the modulation (m_i), which is defined in this work as the ratio between the phase voltage and the DC-voltage. The AC-current is not a required input for the machine modeling because its limitation is also linked to the power electronics and thus the limitation is considered for its maximal value (used to calculate the magnetic fields during FEA). For the PMSM, the limitations are done for the values of i_{dq} and U_{dq} as depicted by the equations (17) and (18) and for the IM directly with the phase-current (I_S) and voltage (U_S) which are used during the modeling as shown in the equations (19) and (20) (the nomenclature is based on the equations and the representations from the figure and equations in the previous sub-section).

$$i_d{}^2 + i_q{}^2 \leq I_{AC}^2 \quad (17)$$

$$U_d{}^2 + U_q{}^2 \leq U_{DC}^2 \quad (18)$$

$$I_S \leq I_{AC} \quad (19)$$

$$U_S \leq m_i \cdot U_{DC} \quad (20)$$

Parameters identification (2):

The value of the currents and the voltage are limited by the previous steps, this step consists in the identification of the electrical and magnetic parameters of the machine from the FEA, which have as input the temperatures from both rotor and stator. In order to limit the complexity of the model and thus the simulation effort, the model considers one temperature for each machine sub-part (stator and rotor).

Machine performance calculation (3) and loss calculation (4):

The calculation of the machine performance is divided in two parts. First, the combination of the voltage and the current which fulfills the mechanical input are calculated considering the limits previously calculated. Using the loss model, the combination which maximizes the efficiency (and thus minimizes the losses) is chosen. Based on the calculated electrical parameters and the calculated losses, the machine outputs can be estimated (torque, power factor, AC-voltage, AC-current, AC-power, losses and efficiency).

2.3.3 Data maps based modeling approach

Data maps represent a practical way to store the data deduced from FE-analysis using circuit based model. As shown previously, they can also be used for modeling purposes. As defined in Figure 28, the following parameters need to be considered: torque, speed, temperatures (T_{rotor}, T_{stator}) and voltage (U_{DC}).

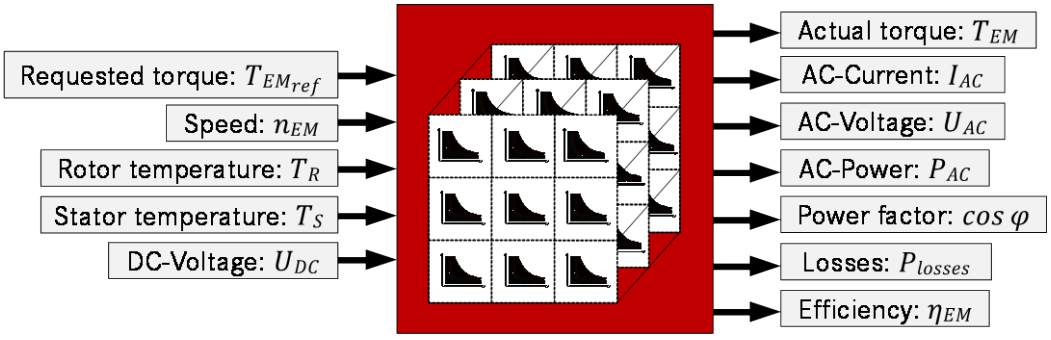

Figure 35: Modeling approach for electric machine with data maps based method

It results in a 5-dimensional approach for each output parameters. Each parameter is thus stored in a 5D-matrix with the following representation. For the purpose of this work, several maps need to be calculated to cover the whole application and investigation range. The required number of maps is discussed in the next sub-section where the modeling approaches are compared. Accuracy: contrary to the circuit based approach, this solution considers

really the machine has a black-box and does not investigate in details the intrinsic parameters. The resulting five-dimensional matrix can be then integrated in the global model using look-up tables based on linear interpolation as depicted on Figure 35.

2.3.4 Chosen method for electric drive system optimization

The two methods have shown potential to fulfill the requested interfaces for a system approach and offer the possibility to cover the whole investigation range. The circuit based approach is adaptive because it can calculate accurately each driving point but requires a model for each machine technology while the data maps based approach is modular thanks to its technology-independent approach but requires concession toward the accuracy. System optimization requires a solution which covers the parameter range and its variation with a good compromise between simulation effort and accuracy. These two parameters are evaluated in this sub-section for the two approaches discussed previously and finally the suitable is defined.

Accuracy:

The main advantages of the circuit based approach are directly linked with its simulation effort issue. It calculates directly based on the FEA-results the machine performance at each simulation step, whereas the data maps based approach interpolates linearly between the points and between the maps calculated at the beginning to cover the parameter range. Since the data maps based solutions seems to be the most suitable solution concerning the approach and the simulation effort, this sub-section studies the requirements to achieve a comparable accuracy as the circuit based approach. The lack of accuracy in the data maps-based approach is principally due to the speed, torque and voltage variations. The temperature dependency does not influence the accuracy because the values are already linearly interpolated between the different temperatures and thus the data-maps approach does not add any approximation.

→ Speed and torque: the machine performance needs to be accurately considered in the low speed range and the low torque range due to machine intrinsic properties. Hence the number of calculated points is high in low speed and torque range, medium in medium speed and torque range and low in high speed and torque range. For this purpose, the following grid is chosen. For the speed range 60 points are considered: 20 between 0 and 1/6 of the maximal speed, 20 between 1/6 and 1/2 of the maximal speed and 20 up to the maximal speed. For the torque range 121 points are considered (60 for motor mode, 60 for generator mode and 1 for the 0 Nm) with the same distribution as for the speed.

→ Voltage: using the previous hypotheses, the voltage dependency is evaluated. For different voltage steps, the accuracy is calculated as presented for the machine limit curve in Table 9. The results of the circuit based approach are taken as reference for U_{DC}=362.5V and then the limit curves are interpolated using the data maps based model. The accuracy of the data maps based model is always higher than 97% for the considered voltage steps. The method used to calculate the accuracy is presented in (21).

$$Accuracy = 1 - \frac{|Value - Reference|}{Reference} \quad (21)$$

Voltage step [V]	5	10	25	50	100
Accuracy [%]	99.9	99.9	99.3	98.58	97.8

Table 9: Voltage dependency of the accuracy for the calculation of limit curves

Considering the results in the previous table, the value of 25V is retained for the voltage step to achieve a suitable accuracy. Considering that the current is always equal to the maximal current used during the design due to its relationships with both the machine and inverter design. These hypotheses results in the following number of maps to cover the entire solution area: 144 for an IM and 288 for a PM. Concerning the 48V-System, a 5V step is chosen to achieve a good accuracy, which results in calculating 48 maps for an IM and 96 maps for a PM.

Simulation effort:

The circuit based approach has two main challenges concerning the simulation effort. First, it requires a technology dependency: as shown previously the same circuit based model cannot be used for different technologies. When

investigating several technologies (IM and PMSM), it increases the simulation complexity because it requires two distinct model for the two machine technologies. Secondly, the circuit based approaches requires time-consuming solutions. The data maps based models have the advantage to store both the machine performance and limits while in circuit based approach, the machine limits need to be re-evaluated at each simulation step. The time gap between the two methods needs to be considered and is presented on Figure 36, where the advantage of the data maps based solution can be seen.

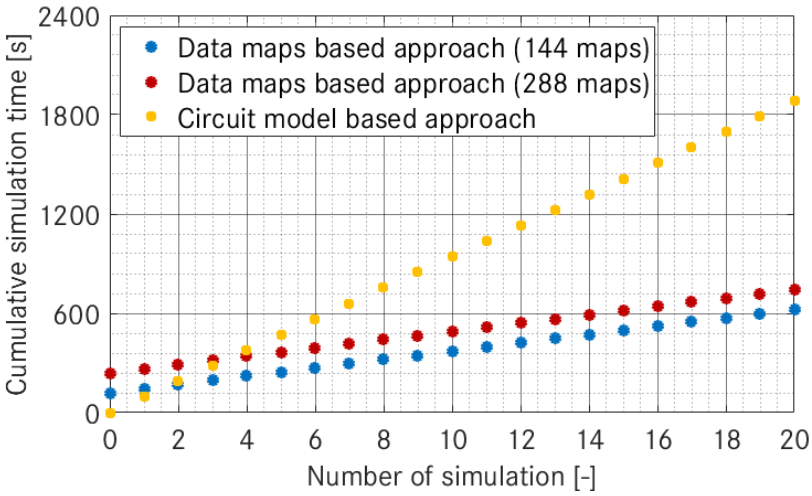

Figure 36: Combined simulation time for the two approaches considering the IM technology

Summary:

As it can be seen, the data maps based solution represents, when considering the requirements of this work, the best compromise between accuracy, simulation effort and parameter range. It offers also a high modularity because it can be used to model all the machine technologies based on a rotating field effect (some adaptations are required for technologies with active rotor excitation such as an additional map with the rotor excitation current for a separately excited synchronous machine). Based on the analysis in this sub-section, the following hypotheses are made for this work: two relevant temperatures are chosen for the metallic conductor materials and five for the permanent magnet.

2.4 Validation

After the determination of the suitable approach for a global system analysis and the implementation of the modeling, the chosen approach needs to be validated. For this purpose, a grid of operating points is measured with an automated test bench using the set-up depicted in Appendix 3. The measurements are done with a power analyzer and a thermal multiplexer to allow evaluating in the simulation the following parameters: the voltages, the currents, the temperatures, the speed, the torque, the losses and the powers. For each machine technology, the measured values are compared by evaluating the following parameters: the limit curves, the losses and the phase-current. These parameters are chosen because they validate from a system-point of view the mechanical, electrical and magnetic behavior of the machine. Limit curves validate the extrapolation of machine performance whereas the losses and phase-current are evaluated because they represent the interfaces with the thermal model and the power electronics. Then the following method is used to validate the simulation approach: for all the parameters, the correlation and the deviation between measurements and simulation as depicted respectively by the equation (22) and (23) is used, where y_i are the measured values, $\bar{y}$ is their mean value and f_i are the simulated values.

$$Correlation\ [\%] = \left(1 - \frac{\sum_i (y_i - f_i)^2}{\sum_i (y_i - \bar{y})^2}\right) \cdot 100\% \quad (22)$$

$$Deviation\ [\%] = \frac{|yi - fi\,|}{|fi|} \cdot 100\% \quad (23)$$

2.4.1 Permanent magnet synchronous machine

For the validation of the PMSM, two sets of measurements are done: One with 422 points to evaluate the accuracy of the losses and the phase current and one with 14 points are for the limit curves. To perform a reliable comparison between the simulation and the measurements, both the inputs (torque, speed, temperatures and DC-voltage) and the outputs of the modeling are measured to compare only the accuracy of the simulation.

Limit curves:

During the measurements of the limit curves, the temperatures are maintained within an acceptable range in order to have reliable results. Hence only the influence of the voltage and the current on the machine performance is investigated. The limit curves validation is an important step because it validates both the modeling approaches and the design of the components. The results presented on Figure 37 show a good correlation (99.59%) and a low deviation (under 3%) of the modeling approach and this despite the assumptions for the modeling implementation (data-maps based solution extrapolated from FE-analysis using analytic approach).

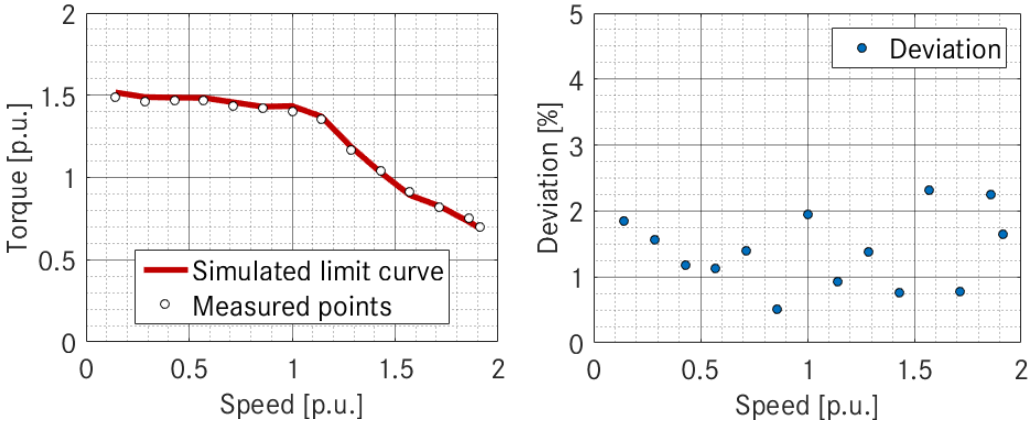

Figure 37: Limit curves comparison between simulation and measurements for a PMSM @370V

Losses and phase current:

The same test-bench and approach are used for the evaluation of the losses and all the inputs for the simulation are measured for each point in order to generate maps for the comparison between simulation and measurements. As it can be seen, both of them show a good correlation and a similar behavior over the torque and the speed range can be seen for both the losses and the phase current. Concerning the deviations, it can reach quite high values for the losses (up to 20%) for a speed between 0.5 and 1 while for the phase current the deviation is negligible except for a restrained area. Before analyzing with more details these results, the set-up of the test bench and the control of the machine need to be considered with more attention. Concerning the losses in the electric machine, they cannot be directly measured and are only estimated by measuring the mechanical power and the AC-power using the power analyzer. Based on these two values, the differences between the two interfaces can be estimated by subtracting the mechanical power from the AC-power (and inversely in generator mode). These losses however include all the losses between the two measurements devices and do not depict only the machine behavior but also other external effects such as the copper losses in cable or connectors. To estimate the losses in the cable and therefore to isolate the machine losses, the cable resistance is measured. Using this value, the losses in the cable can be abstracted and the losses in the machine can be approximated. Concerning the phase-current, there are several i_{dq} combinations which offer the possibility to achieve the requested torque for a given speed. During the simulation, the choice is made to choose the combination which minimizes the losses or the current. Due to the measurements device accuracy, controller quality of the power electronics or the accuracy of the measured machine parameters, these conditions are not always possible during the measurements and some deviations can appears. To evaluate the accuracy of the modeling, the previous figures show the iso-lines for the simulation and the measurements as well as the deviation between the two sets of data. The results are then evaluated separately for the two parameters considering the assumptions previously discussed. If the deviations for the phase current are acceptable considering these assumptions, the deviations for the losses cannot stay unconsidered. The losses of a PMSM are composed of the iron losses, which are directly dependent on the frequency (e.g. the speed), and the

current as well as the copper losses, which are dependent on the current. However no direct relationships can be found between the deviation and the loss dependencies. Since the same assumptions are made for all the machines and the fact that a deep component modeling is outside the scope of this work, the considered modeling approach is sufficient and suitable because it enables to compare the machines and the voltage level as shown later.

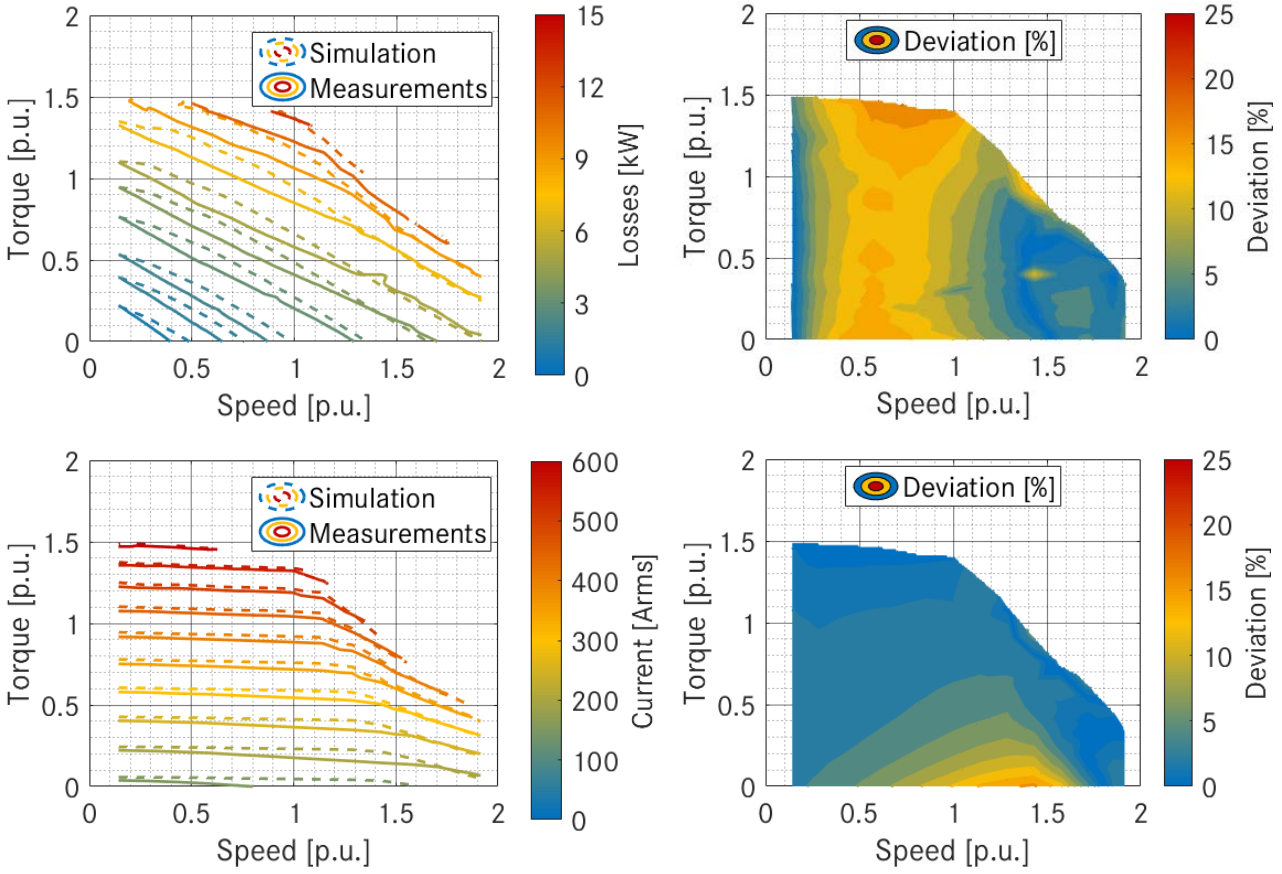

Figure 38: Losses and phase-current comparison between simulation and measurements for a PMSM @370V

2.4.2 Induction machine

The approach is also used for the induction machine with 686 measurement points for the losses and the phase-current and 24 points for the limit curves.

Limit curves:

Similar to the PMSM, the limit curves of the induction machine show good correlation (99.68%) but a little higher deviation (up to 6%). The comparison between the measurements and the simulation show still good results considering the approximation done for the modeling. The validation of the chosen solution for a second technology shows both its good compromise between simulation effort and accuracy as well as its modularity.

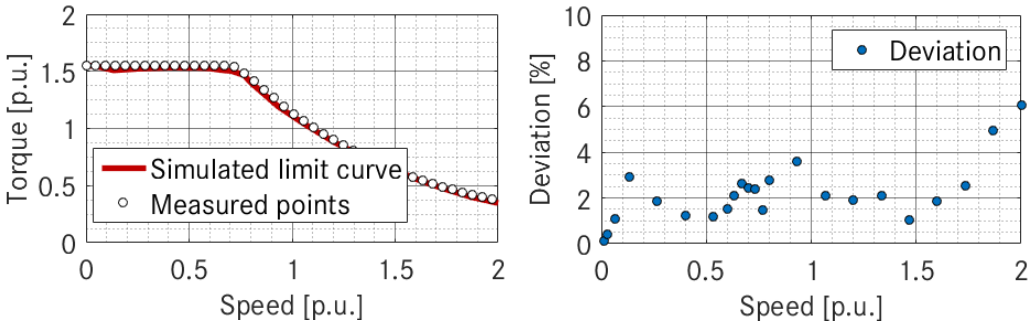

Figure 39: Limit curves comparison between simulation and measurements for an IM @350V

Losses and phase-current:

The losses and current behavior by the induction machine shows as good results as for the PMSM. It enables to depict the losses and the current in the machine over the speed and torque range with a high correlation (respectively 93.42% and 99.73%). Some deviations can be observed, particularly in low speed and low torque area but considering the approximation done during the modeling (maps-based solution), the measurement set-up (no direct measurement of the losses) and the different voltage and current combination which can fulfill a driving point, the results are showing sufficient accuracy and correlation to investigate the voltage and current level influence and to compare different machines.

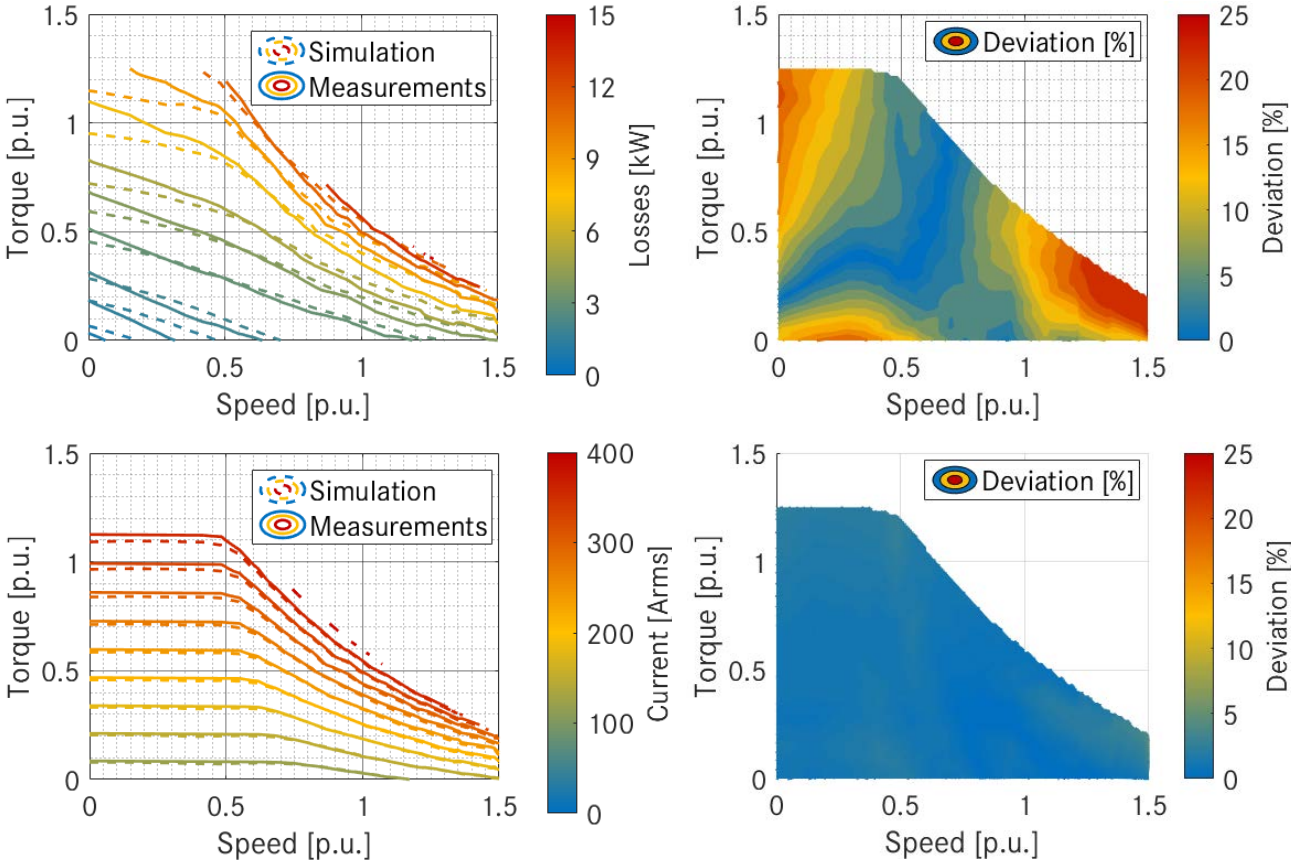

Figure 40: Losses and phase-current comparison between simulation and measurements for an IM @350V

2.4.3 Voltage dependency

Besides the validation of the modeling approach with relevant parameters (limit curves, losses and phase-current), an aim of this work is to show the remaining potential of electric components with the current technologies. For this purpose, it requires to have the possibility to vary the voltage level without decreasing the accuracy. For this purpose, the accuracy of the modeling is tested by variating the voltage level an analyzing the influence on the limit curves.

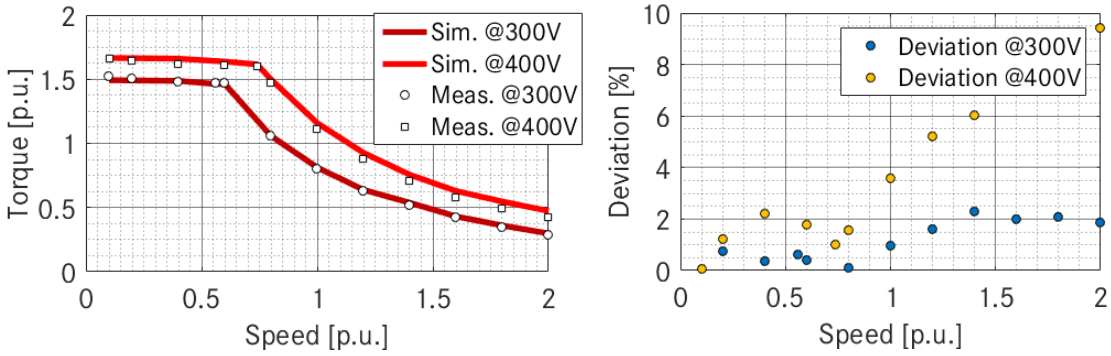

Figure 41: Voltage dependency evaluation for a PMSM @300V and 400V

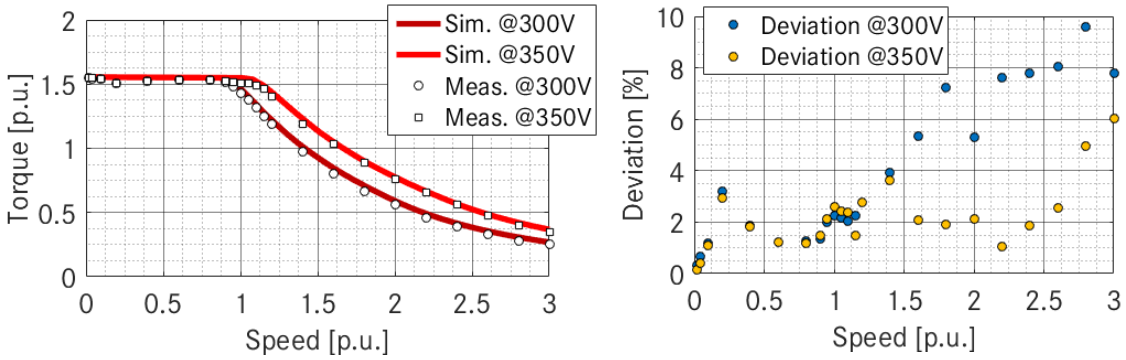

Figure 42: Voltage dependency evaluation for an IM @300V and 350V

Technology	DC-Voltage [V]	Correlation [%]
PMSM	300	99.97
	400	99.36
IM	300	99.97
	350	99.98

Table 10: Parameters for the validation of the voltage dependency

As previously for the validation of each technology, the comparison between simulation and measurements show a strong correlation and low deviation. The chosen modeling approach can accurately represent the voltage and current dependency of both machines technologies and therefore enables to evaluate them in variable boundary conditions during the design phase. Despite the approximation done for the modeling, the method achieves correlation higher than 99% and a deviation lower than 10%. Higher deviations can be observed in the high speed area which can be linked with friction effects from the test-bench which are not considered in the simulation. However the deviations remain under 10% and therefore the results are still fulfilling the aim of the work.

2.4.4 Summary

In this section several comparisons between measurements and simulation results are presented. Considering the approximations and hypotheses done during both the simulations and the measurements, the results as presented here are validating the chosen approach. More detailed investigations could be performed to identify the sources of the high deviations in some of the results. The aim of this work is however to identify the suitable solution for modeling the electric components from a global system point of view and to have the possibility to investigate voltage and current influence on the machine performance. Considering that the same approximations are done for all the machines and that the same simulation methods are used, the retained solution presents the best compromise between accuracy, parameter range and simulation effort.

2.5 Contribution for system evaluation

After having shown the implementation and the validation of the modeling approach. This sub-section show the contribution of the approach for system evaluation. For this purpose the influence of the voltage and the current is investigated. Two parameters are considered for the evaluation: the machine utilization and the efficiency at the maximal power. The term utilization refers in this work to the behavior between the provided apparent power and the maximal power of the machine (P_{mech}). The aim is therefore to show for which voltage and current level, the same machine provides the highest efficiency or the highest utilization. The utilization is calculated as in the equation (24). The apparent power is approximated using the DC-voltage (U_{DC}) and the AC-current (I_{AC}) because they are the system parameters which represent the battery and the power electronics influences. The results presented in the two sub-sections are calculated for a permanent magnet synchronous machine with a constant modulation factor for two investigations: one with a constant apparent power and one with a constant mechanical power.

$$Utilization = \frac{\max(P_{mech})}{U_{DC} \cdot I_{AC}} \quad (24)$$

2.5.1 Constant apparent power

For the investigation of a constant apparent power, the product of the DC-voltage and the AC-current is maintained constant. The apparent power is a relevant factor to evaluate the power electronics when considering only the electric machine because it applies a similar load on the inverter independently from the resulting mechanical power. The results on the following figure show the mechanical power, the machine utilization and the efficiency at the maximal mechanical power for a variation of the voltage between 250V and 850V.

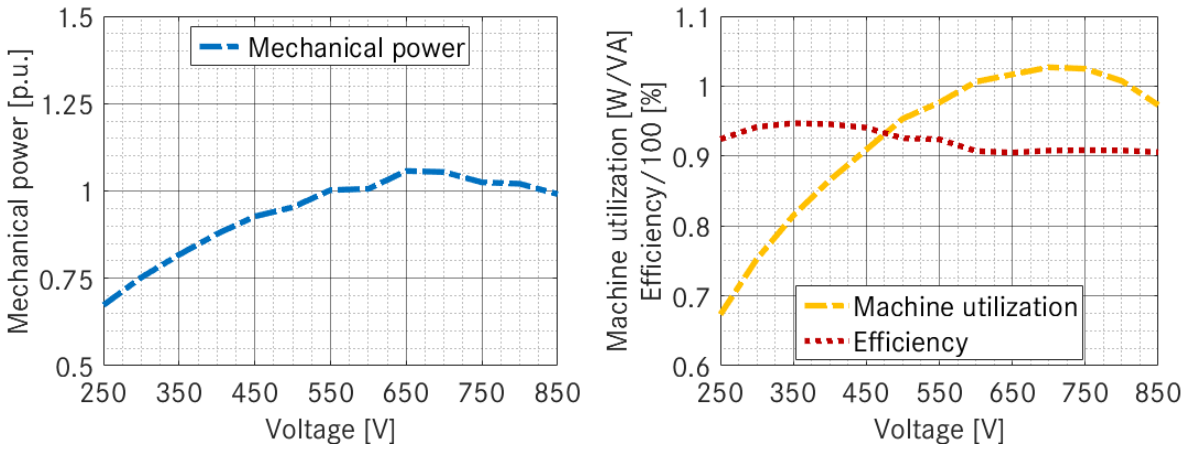

Figure 43: Influence of the voltage on the electric machine for a constant apparent power

In this investigation, where the product $U_{DC}.I_{AC}$ is maintained constant, the mechanical power and the machine utilization shows a similar behavior. There is an increasing behavior from 250V up to 650V followed by a decreasing behavior from this point. Considering the equations (17) and (18) and the fact that the current is reduced to achieve a constant apparent power, it can be assumed that the current is the limiting factor to use the entire potential of the machine. In the case of the efficiency at the maximal power, the peak value is achieved for approximately 300-350V, which corresponds to the area for which the machine is designed. The decrease of the efficiency is however not significant and this investigation tends to show that a voltage around 650V is the best solution to achieve the highest mechanical power per apparent power for the boundary conditions of this investigation.

2.5.2 Constant mechanical power

The electric drive system is evaluated by the mechanical power at the electric machine shaft and not the apparent power. Hence to perform a system investigation at the electric machine level, it is more relevant to consider a constant mechanical power and to evaluate the influence on the apparent power. Similar to above, the results are presented on Figure 44 for a voltage between 250V and 850V.

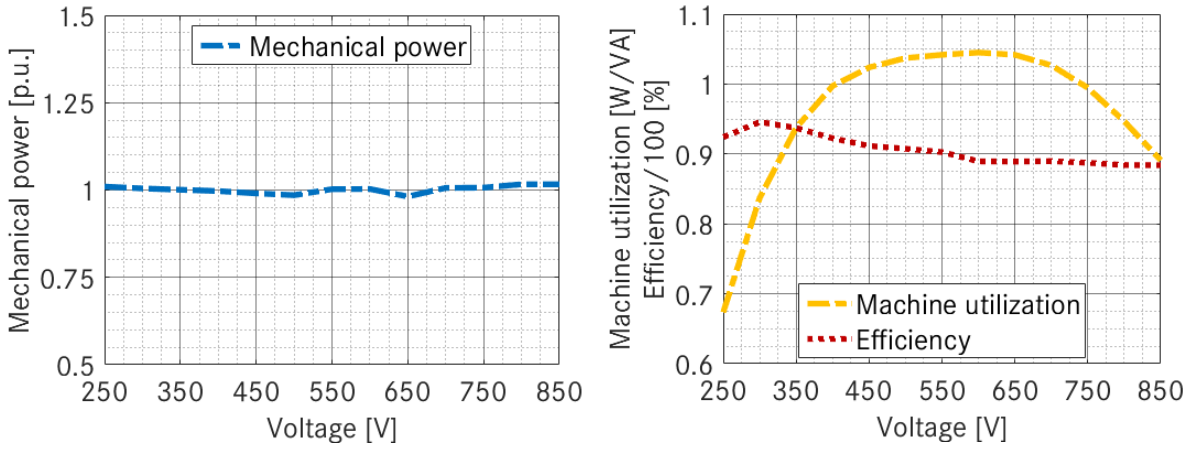

Figure 44: Influence of the voltage on the electric machine for a constant mechanical power

When considering a constant mechanical power, the area with the highest utilization is slightly shifted to lower voltage even if the best values stay around 600V and 650V. The decreasing behavior from these values is due to the same reason as previously: when increasing the voltage, the current is reduced and therefore it can be assumed that there is not enough current available to use the full potential of the machine. Concerning the efficiency, the max efficiency is also concentrated around 300V-350V, area for which the machine is designed. Both the investigations show the same trends, maximal utilization around 600V-650V and maximal efficiency around 300V-350V. However no conclusion can be done at this point because only the machine is considered but it gives a first overview of the machine voltage-dependency and it shows the contribution and the flexibility of the developed method.

3 Thermal modeling

Based on the machine structures, this section discusses the topic of thermal behavior modeling. For this purpose, the modeling approach is defined and previous works on the topic are presented. By analyzing these works, a suitable solution is chosen, implemented and validated based on automotive component measurements and finally the contribution for system evaluation is shown.

3.1 Modeling approach

The goal of the thermal modeling is to refine the component behavior modeling by estimating in real-time the temperatures in the components. In these cases, it aims to depict the temperature behavior based on the losses in the machine and the cooling properties (coolant temperature and flow). For this purpose, the approach described on Figure 45 is retained. The cooling properties are not investigated in this work and they are defined during the drivetrain design. They are considered as input parameters because the same machine can be used in several drivetrains and thus under several cooling conditions, which need to be considered but not investigated. As outputs, the temperatures in rotor and stator are considered.

Figure 45: Thermal modeling approach for the electric machine

3.2 Previous works and investigation level influence

When defining a modeling approach, the analysis of previous works plays an important role in order to identify the suitable solution to investigate. In this section, previous works on the topic are presented based on their investigation level. As before, the analysis begin with the sub-component level, then the component level, after this a system level example is discussed before introducing the more superficial levels.

3.2.1 Finite element analysis

As for the component behavior modeling, thermal behavior can be investigated using finite-element. The modeling approaches are similar to the previous one presented for the component behavior in the previous section. The finite element enables a high accuracy for the thermal investigation of components especially in 3D because the heat flow is generally anisotropic. They investigate convection, conduction as well as radiation effect. As shown in [71], it enables thanks to a well-defined network to determine the thermal behavior of the machine with a high accuracy and dynamic. The computation time is minimal (138 microsecond for 1 second in real time) but this evaluation considers only the thermal behavior and the interfaces with other models as required for this work are omitted. The model can be considered with only 2D by doing some approximations on the material parameters. The 2D-thermal model shows light deviations versus the 3D-solution but enables to reduce the complexity of the investigation as shown in [72]. As previously for the component behavior modeling, the finite element based approaches have a high accuracy with a trade-off concerning the simulation effort.

3.2.2 Nodal approach

Due to its structure, an electric machine requires a network to be modelled because the thermal path of the machine cannot be investigated with simple path between the loss sources and the cooling system. Hence the network can be only simplified by considering only one interface between two sub-parts by using a nodal approach (or lumped-parameter model [73]). The principle of this thermal approach relies on the fact that the temperature behavior can be estimated using equivalent circuit with resistance and capacitance. The good reliability of the lumped parameter model is already shown in [73], where several improvements are present to enhance its accuracy. The results in the following show the comparison between the conventional nodal model, the improved one and the same investigation using 2D-FEA (ANSYS software). The results (with or without improvement) show low deviations versus FEA.

Temperature of the PMSM @500 rpm	T1 Frame	T2 Yoke	T3 Teeth	T4 Coil side	T5 End-winding	T6 Layer	T7 Magnets
Conventional model	96.33	110.36	152	207.2	222.35	125.78	125.32
Improved nodal model	96.33	110.38	146.3	202.12	209.36	125.69	125.2
ANSYS 2D (Finite element)	97.26	110.7	145.6	202.5	-	124.6	124.0

Table 11: Results of the comparison between 2D FE-Analysis and nodal approach [73]

3.2.3 Higher level and evaluation for electric drive system optimization

Previous works are all based on a network for the thermal investigation of electric machines. The aim of this work is to find the best compromise between accuracy, parameter range and simulation effort. Both presented solutions fulfill the parameter range therefore the accuracy and the simulation effort plays the most preponderant role. No more superficial solution as the nodal model can be found due to the machine structure and therefore this solution is retained. Even if it is not really system approach because it calculates parameters which are not required, it is the most suitable solution for the optimization of the entire system. The model presented in the rest of this section is based on an internal modeling with adaptations to consider the relevant parameters for a global system optimization.

3.3 Modeling implementation

The implementation presented in this section is based on an internal proprietary software suite. The modeling is based on a nodal approach which is developed using the results of machine structure analysis and finite element investigations. The model is a transient model of the machine developed considering static and dynamic analysis. For the explanations of the implementation, the structure on Figure 46 is used as reference.

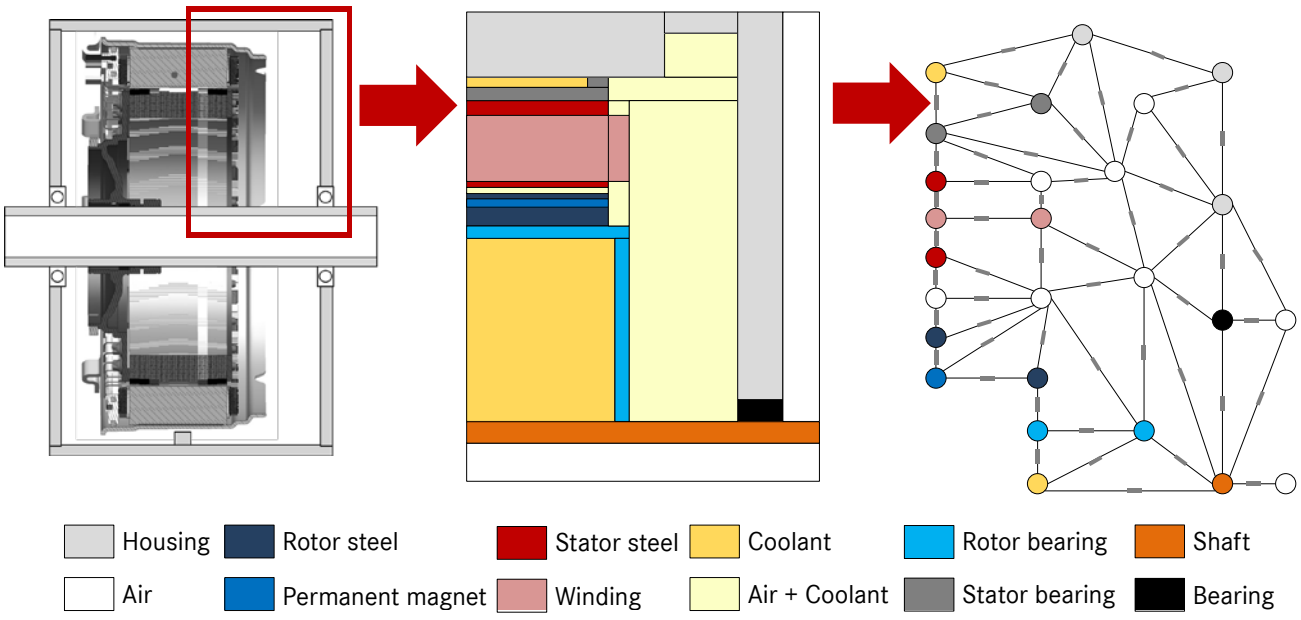

Figure 46: Machine structure and nodal network for the thermal modeling of a PMSM

As discussed before, the nodal model is a suitable solution for system investigation even if it considered not required parameters. The nodal model used for this work considers a 3D-network which is build based on the several layer of 2D-networks. The global network is generally composed of 50 up to several hundred nodes depending on the machine structure and its complexity. The network of one layer on Figure 46 is presented for a PMSM. The model is an overtaken from an already existing solution and the main adaptation lies in the definition of the suitable interfaces to couple the component behavior and the thermal model. The model is working using the following principle: the loss vector from the component behavior model is sent to the thermal model which calculates the temperature in each sub-part based on the losses and their location in the machine structure. Using the temperatures calculated with the model, the following approach is used to fulfill the requirements of this work. Only four values are considered: the maximal temperature in rotor and stator and the mean temperature in rotor and stator. If the first ones can be directly extracted from the model, the second ones require doing some assumptions. Only the temperatures in the winding, the magnet or the rotor cage are considered. Therefore the mean temperatures used to enhance the electromechanical modeling are defined as in the equation (25) for the stator, in the equation (26) for the PM-rotor and in the equation (27) for the IM-rotor.

$$T_{stator_{mean}} = \sum_{i \in winding} T_i \Big/ \sum_{i \in winding} i \quad (25)$$

$$T_{PM-rotor_{mean}} = \sum_{i \in magnet} T_i \Big/ \sum_{i \in magnet} i \quad (26)$$

$$T_{IM-rotor_{mean}} = \sum_{i \in \substack{rotor \\ cage}} T_i \Big/ \sum_{i \in \substack{rotor \\ cage}} i \quad (27)$$

These are strong assumptions concerning the thermal behavior of the electric machine. They are however required for the purpose of this work to contain the simulation time during the optimization. The overtaken model used for the thermal modeling of the electric machine is actually able to calculate the temperatures in each sub-parts. However the consideration of the temperatures in all of these sub-parts would increase the size of the interface between the thermal model and the electromechanical model which is not suitable for the purpose of this work. Moreover electric machines in automotive applications have generally only one thermal sensor to evaluate the temperature at the hot-spot in the rotor and therefore the model is already watching over more temperatures as what is really implemented in the vehicle.

3.4 Validation

This section presents the validation of the simulation with measurements performed on the test bench described in Appendix 3. The validation is presented here only for one machine technology since the thermal behavior modelling approach is independent from the machine technology. Since the different losses cannot be isolated during the measurements, the comparison between the simulated and the measured values is done using a coupling between the component modeling and the thermal modeling as presented on Figure 47.

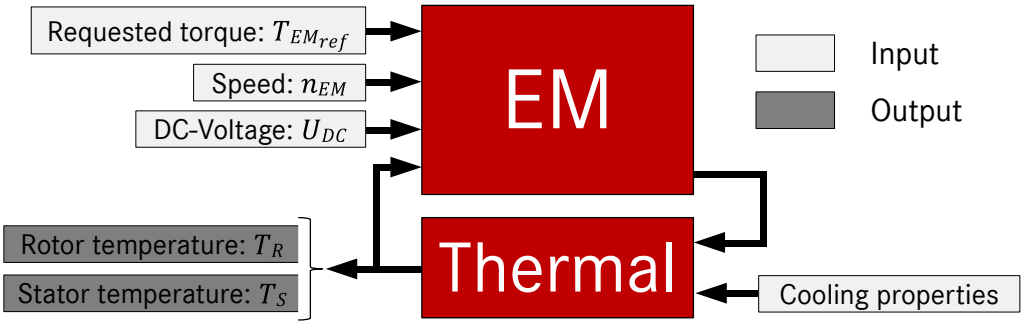

Figure 47: Modeling approach for the validation of the thermal model

The validation is divided in two parts: the first one aims to validate the continuous thermal behavior whereas the second one aims to validate the dynamic behavior. The continuous thermal behavior need to be validated to ensure the reliability of the results during long steady load while the dynamic behavior is required for short-term high load.

3.4.1 Continuous thermal behavior

For the validation of the continuous thermal behavior; driving points are set at the electric machine (torque, speed and DC-voltage) while the temperature and the losses are measured. This approach is performed on a PMSM with an empty rotor structure. The results are presented on Figure 48 and in Table 12.

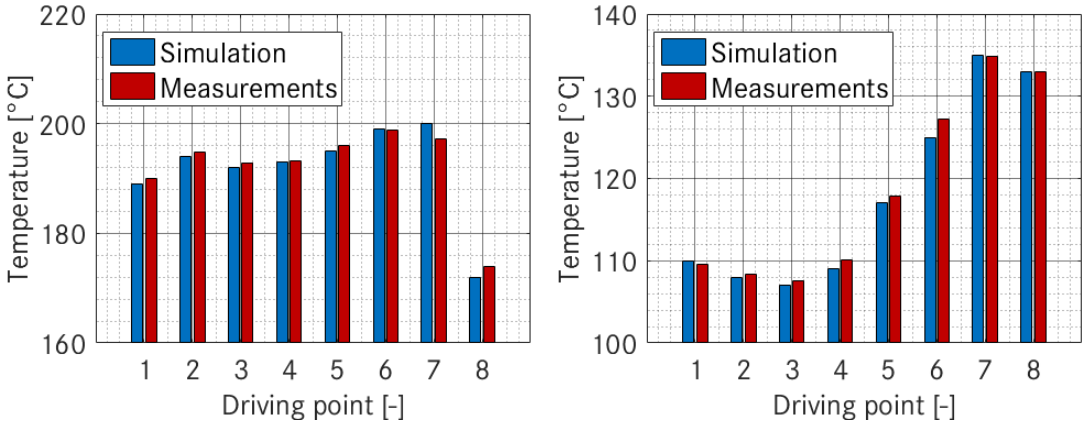

Figure 48: Temperature comparison between simulation and measurements (stator: left and rotor: right)

Max. Deviation [%]	Validation		[73]	
	Stator	Rotor	Improved model	Conventional model
	1.35	1.76	0.9	4.4

Table 12: Validation of the continuous thermal behavior

Despite the coupled simulation, the results show low deviations (up to 1.35 for the stator and 1.76 for the rotor). In Table 12, the results are also compared with the investigations in [73]. The results of the improved model from [73] are slightly better as the model considered in this work but globally the solution chosen shows reliable results for the continuous thermal behavior.

3.4.2 Transient thermal behavior

For the second validation, a torque step is applied on the machine for a given speed. By using this approach, the transient thermal behavior of the electric machine can be observed and thus the modeling can be validated. The dynamic behavior of the machine is particularly important to evaluate the short-term limits of the machine.

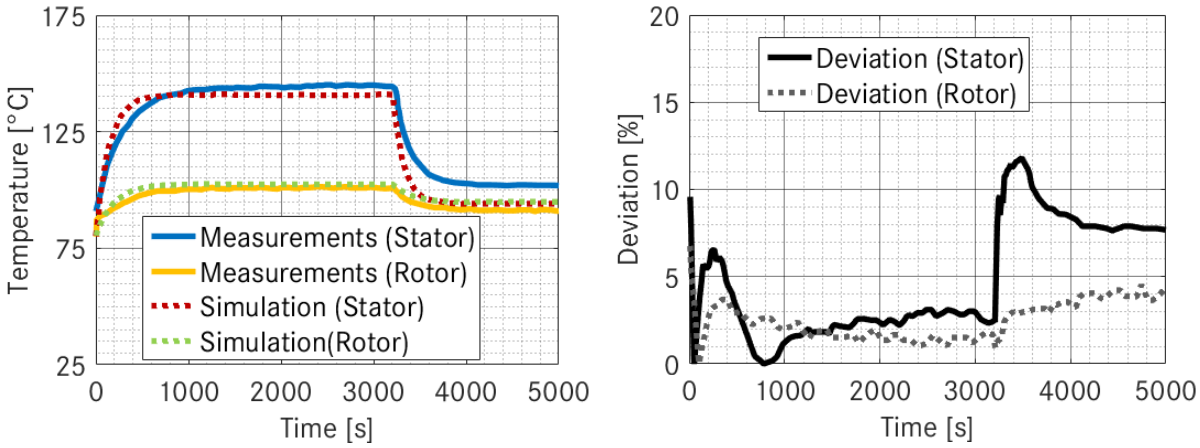

Figure 49: Comparison between simulation and measurements of the transient thermal behavior

	Stator	Rotor
Max. Deviation [%]	11.81	6.78
Correlation [%]	87.88	65.39

Table 13: Comparison of the deviation and the correlation for the transient thermal behavior

The evaluation of the thermal model for the transient behavior shows slightly lower correlation as previously (around 85%) and lightly higher deviation as the continuous one (up to 12%). These deviations are due to the coupled modeling approach used for the validation. Since the losses cannot be isolated during measurements, there is no other possibility to validate the approach. The coupling increases therefore the deviation and reduce the correlation because it actually depicts the combined correlation and deviation of the two models. Considering this hypothesis and the complex structure of the machine, the results presented in this sub-section fulfill the requirements of this work because they represent the best compromise between accuracy, parameter range and simulation effort.

3.5 Contribution for system evaluation

In this sub-section, the contribution of the thermal modeling is shown. For this purpose, the thermal modeling and the electric modeling are coupled and the machine is evaluated on the New European Driving Cycle (NEDC) with and without the thermal modeling for a constant voltage level. The results are then compared by evaluating the losses and the current as previously for the validation. The temperature for the simulation without thermal modeling is constant and assumed to be equal to the coolant temperature.

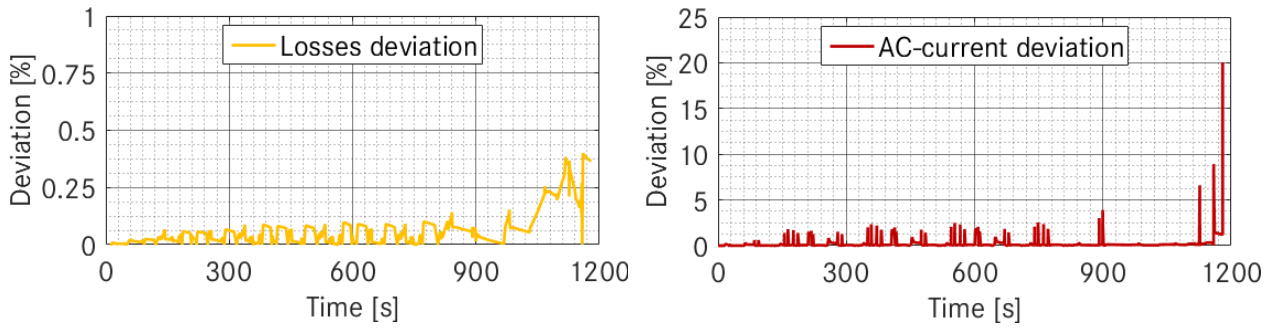

Figure 50: Losses (left) and AC-current (right) deviation for the NEDC

As it can be seen, no particular deviation can be observed for the two considered parameters, they lay both under 5% except at the end of the cycle for the AC-current. The enhancement for the parameters evaluation is thus clearly limited for the considered driving cycle. The thermal modeling is however an important parameter for the design of the vehicle because beside the legislative framework, other requirements such as the continuous power or dynamic driving cycles are considered too. The thermal modeling is therefore an important method for the design even if its relevancy for driving cycle is questionable.

4 Volume and weight evaluation

During the development process, an important aspect for the hybrid electrical drivetrain lies in the integration. Contrary to purely scientific approaches, the focus is not set on the development of components with the best energy- or power-density but to develop components which can be integrated in a drivetrain which already contains a conventional drivetrain. For this purpose, volume and weight evaluation tools need to be developed in order to evaluate the integration of the components in the vehicle. This section is divided in four main parts: the first one defines the aim of the approach, the second one discusses the influence of the investigation level, the third one describes the retained solution and finally the last parts presents the contribution of the method for a concrete example from the automotive industry.

4.1 Evaluation approach

For the evaluation, two types of approaches can be chosen. The first one estimates the component volume and weight while the second only evaluates the integrability. In the case of this work, a Boolean approach is chosen

since the active dimensions of the machine are not a variable because the sub-component design is not considered. The required parameters are therefore depicted on Figure 51: the inputs are described by the available volume, generally described by its diameter and length, the maximal weight for the machine and the machine parameters (integration and winding type) whereas the output is the Boolean answer: integrability or not.

Figure 51: Evaluation approach for the integration of electric machines

The main contribution of this work lies in the considered parameters for the evaluation. A system approach requires evaluating the entire machine and thus not only the active materials (electrical steel dimensions as in [45]). As presented in [44], the winding technology and the rotor excitation play a significant role. Hence this work considers the dimensions of the active materials, the rotor excitation and the winding technology (referred as machine parameters) while other parts such as speed sensor or bearing are not investigated because they are required independently from winding and machine technology.

4.2 Investigation level influence and related approaches

Currently the machine integration is often investigated as both end of the development process: during the early design phase, where the relevancy of the requirements are analyzed (vehicle level) or during the vehicle integration, where the exact dimensions of the components are known (sub-component level). Hence these two investigation levels are presented and discussed in this section.

4.2.1 Computer aided design

Computer aided design software enables a detailed investigation of the integrations and can consider all the sub components. It allows directly testing the integration in the vehicle due to high quality graphic interfaces. Concerning the weight, many CAD programs can estimate weight based on the materials density and the parts dimensions. The investigation requires having information about each sub-component as depicted on Figure 52 and is generally time-consuming approach because of the required information and the integration in the vehicle frame which cannot be automated with the considered simulation environment in this work.

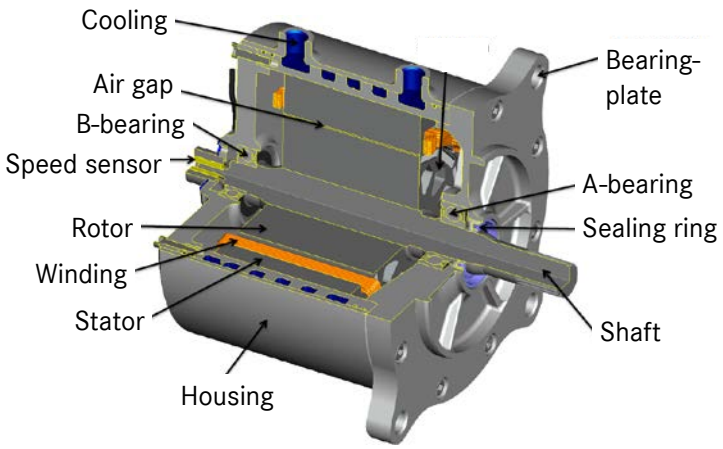

Figure 52: Detailed machine structure and sub-components [8]

4.2.2 Power and torque density

The integration investigation can be performed using torque and power density. The torque and power density can be gravimetric or volumetric. They are expressed in Nm/kg or Nm/m³ for torque density and W/kg or W/m³ for

power density as for example in [44]. These values are estimated based on benchmark and monitoring from components. Among the power and torque density solutions, a well-known one is based on the Esson's Number. It represents the potential of the electric machine based on its bore volume (active rotor materials). In [20], an overview for a defined application (in-wheel electric machine) is presented for the comparison of the different technologies but this method is often constrained to conventional industry applications because the available volume is clearly defined by norms [74]. The use of utilization factor is however more challenging for hybrid vehicles due to the current development status of the technology. Despite being well-known, the new requirements and challenges prevent the use of such approach except for early design approximation or for machine type determination.

4.2.3 Evaluation for electric drive system optimization

Among the previously presented approaches, no one seems to fulfill the requirements. The first one requires too deep investigations and the second is too superficial. The first one is hindered by the lack of consistent interfaces between CAD-software and simulation software as Matlab/Simulink whereas the second one does not answer the main purpose of the investigation: the integration issues. It can evaluate the potential of the available volume and maximal weight or can estimate the required volume and weight but cannot evaluate the integrability of the electric machine. Consequently, the next section presents the specific approach developed for this work.

4.3 Method implementation

Investigations at the system level for electric machines are not present in the current literature. They are either too deep or too superficial investigations but the investigation, as described in [44], has set the premise for a system investigation of electric machine integration. As depicted previously, the aim of the investigation is only to test if the machine is integrable or not. The hypothesis in this work is done that only the active materials, windings and rotor excitation are investigated because they are the varying parts for volume considerations. The volume investigation is then limited to test the integrability through the maximal diameter and length of active materials with consideration of the windings and rotor excitation. The data come from the sub-component design, which define the active materials dimensions (electrical steel and rotor excitation for both rotor and stator) and the winding dimensions. Then, based on the volume values, the weight can be estimated thanks to the density (kg/m^3) of the active materials, the windings and the rotor excitation. The available volume is generally depicted by a cylinder or a ring as it can be seen on Figure 53. The method as presented here does not require any validation because it is only a check of the correspondence between the requirements and the considered machine.

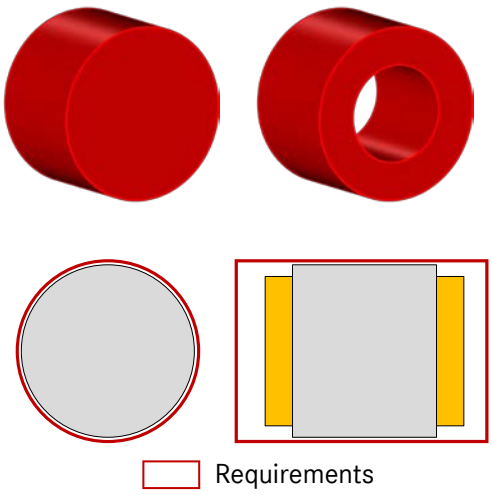

Figure 53: Example of requirements (top) and evaluation of the integration (bottom)

4.4 Contribution for system evaluation

The investigation of the integration plays a preponderant role for system evaluation as shown in this sub-section. An entire system integration needs to compare not only the active materials length but their influence on the global

integration too. In this section, the technology comparison in [12] and [45] are taken as references. In this work, beside the active materials, the windings technology and rotor excitation are considered to evaluate the real integration potential of each technology. Based on the current literature about the technology for automotive applications [44], the comparison is done with three machines: the first one represents the reference (PMSM), the second one is an induction machine (IM) which requires the same integration whereas the third one is a PMSM with the same active materials dimensions as the second machine.

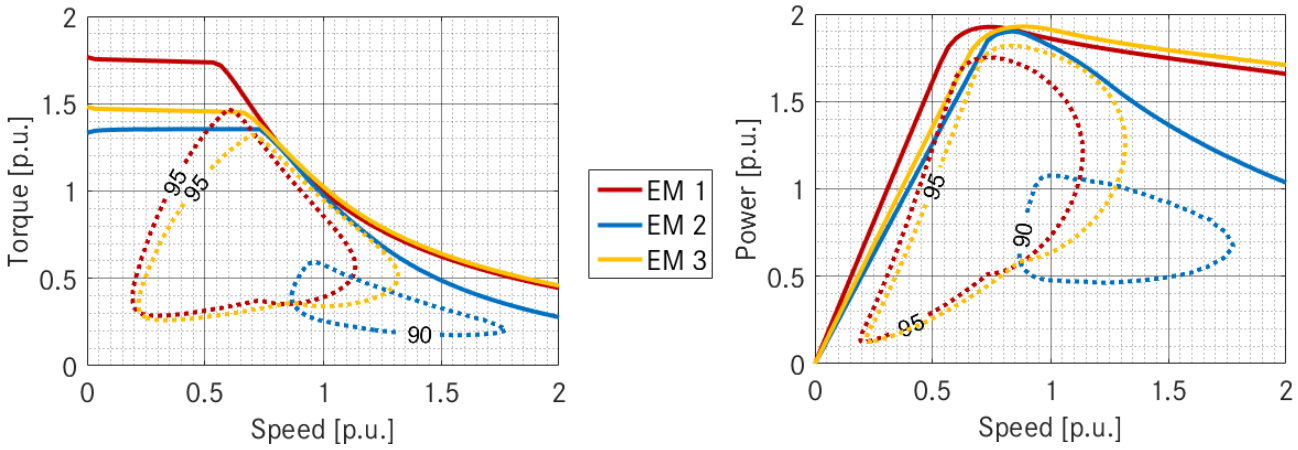

Figure 54: Efficiency, power and torque comparison of different machine technologies under global system hypothesis

The evaluation is done by evaluating the maximal power and torque as well as the efficiency for given voltage and phase-current. Under the assumption of constant active material dimension, machines 2 and 3 need to be compared whereas under global system investigation approach, machines 1 and 2 need to be compared.

Machine	1	2	3
Technology	PMSM	IM	PMSM
Active length [%]	Basis	-25%	
Torque [%]	Basis	-22%	-16%

Table 14: Machine characteristics for technology comparison from a system point of view

The previous figure presents the maximal torque and the maximal efficiency area of the three machines. The investigation presented here considers the case of empty rotor integration. As it can be seen, the results are consistent with the one in [12] and [45], as shown by the comparison of the machine 2 and 3, which confirms that the PMSM has globally a better efficiency as well as a better power and torque density. The comparison of the machine 1 and 2 (global system approach) widens the gap between the two technologies (for the considered integration). It can be explained for several reasons: first the integration considered for the investigation and then the influence of the winding technology. The structure of an empty rotor is extremely challenging for the IM technology and except in [18] and [75], this technology is often considered only for full rotor applications as recommended in [44]. Moreover the compacter winding technology for the PMSM enables to have more available volume for the active materials [44]. This additional space impacts directly the bore volume (rotor dimensions) and thus the resulting torque for the longer machine.

5 Chapter conclusion

The chapter is organized around the topic of modeling electric machine for hybrid system. The different aspects are discussed and analyzed. The chapter begins with an introduction about electric machines, their structures, working principles and losses. This first part is used a basis for the third other parts, where methods and modeling for the electro-mechanical behavior, the thermal behavior and the integration investigation are presented. For each methods, the possible methods from previous works are presented and analyzed before evaluating their potential for the considered investigations. For the electro-mechanical behavior, two solutions are retained and implemented before determining the suitable solution based on the analysis of the accuracy and the simulation effort. In this

chapter, it is shown that using data maps based solutions enables to spare simulation time as well as achieving comparable accuracy as the circuit-based method which despite its high potential, is a time–consuming solution for a system approach. Indeed, the aim is to model the machine as a black-box and thus value such as the magnetic flux or the d- and q-voltage are irrelevant for this work. The data maps based solution also shows a good accuracy, low deviations toward measurements as presented in this chapter and is considered as the most suitable solution for the rest of this work. The same aim is followed to determine a global approach to model the thermal behavior of an electric machine. The thermal modeling is a more challenging topic due to the complexity of the machine structures and the repartition of the loss sources. A real system solution could not be determined but there is however a suitable solution based on a nodal structure. It is an overtaken from an internal modeling approach with some adaptations which are validated using measurements. It is a compromise toward the simulation effort which is required to conserve a sufficient accuracy. Finally, the section about the integration investigation is rather a point-of-view discussion as a real implementation of a modeling approach. The hypothesis of this work and the considered parameters are presented in order to have a suitable method for the rest of the work. Moreover, for each considered method and modeling, the chapter shows the potential and the contribution of a system approach in the case of electric machine investigation. The first contributions of this work is shown and their added-value versus previous works is discussed. Thanks to developed approach a wide range of applications can be covered like in vehicle and drivetrain applications without reducing the range of parameter like in the sub-component and component approaches. These added-values and contributions are an important first step towards the system investigation and can be used as references to evaluate its relevancy versus component oriented design. In order to conclude, the required parameter variation (voltage, current, temperatures) and the integration can be investigated and the approach developed in this chapter enables to investigate the challenges faced current by electric drive system as discussed in the first chapter. Based on a similar structure, the following chapters show how the same goal can be achieved for the power electronics and the battery to build an electric drive system simulation environment.

Chapter 3: Modeling power electronics for hybrid electrical drivetrain

As previously for the electric machine, this chapter presents the determination of a suitable approach for the modeling of power electronics. It begins with detailed explanation about the power electronics structures, working principles and loss types. Then previous works are analyzed and discussed to finally determine the suitable solutions for each considered modeling or method. The retained solutions for components behavior, thermal modeling and integration investigation (volume and weight) are detailed and validated. For each method or modeling, the contributions for system investigation are shown for the power electronics.

1 Power electronics structures, working principle and losses

This section discusses the two structures presented in the first chapter. First the structures and their variants are presented and the semiconductor technologies are detailed. Then their working principle is explained before introducing the losses as considered in this work.

1.1 Power electronics structures

In this work two main structures are used, one for the AC/DC-conversion and one for the DC/DC-conversion. For the realization of these conversions, only the structures discussed in this section are considered.

1.1.1 Inverter (AC to DC conversion)

The inverter realizes the conversion between a direct current voltage source and a multiphase load. The voltage source can be the battery or the second voltage level after the boost-converter (as in Toyota Hybrid System [24]) while the load is the electric machine. The influence of the number of phases on the electric machine is considered only with the following assumption: a three-phase electric machine with a current I is supposed to have the same performance as a double three-phase electric machine with a current $I/2$ for each 3-phase subsystem. From this hypothesis are deduced the two inverter structures on Figure 55 where a three-phase inverter (left) and a double three-phase inverter (right) are considered.

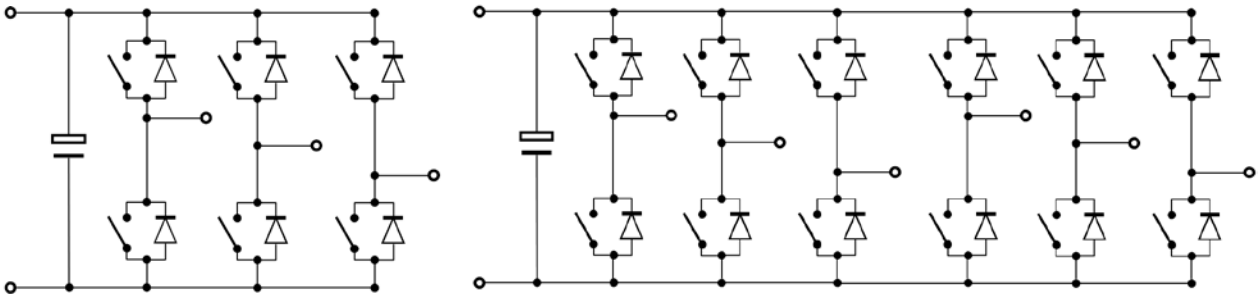

Figure 55: Inverter structures considered in this work

1.1.2 Boost converter (DC to DC conversion)

Several DC/DC-converters are implemented in alternative drivetrain vehicles as the converter between the HV-network and the 12V-network (see Figure 16) or the converter between the battery and the inverter (see Figure 10). The second one is however the only one which is a topic of interest for the investigation of drivetrain electric components and thus only the structure used in the Toyota Hybrid System (HSD [24]) is considered.

1.1.3 Converter structure and assembly

Besides the structure and connection between the semiconductors, the global structure of the converter plays a significant role. Generally the converter is composed of five types of sub-components: the cooling system (heatsink and connectors), the passive elements (DC-link capacitor and other filters), the power semiconductors (power module) and the substrates and interconnections (busbar, control board and connectors) [76]. Finally a non-

negligible part of the component is occupied by air (50%). Automotive converters are generally composed of several sub-converters and the following combinations are possible based on the current electrical architectures: stand-alone inverter, inverter with HV/12V-converter, several inverters, several inverters with HV/12V-converter and several inverters with HV/12V-converter and boost-converter. As already explained, the term power electronics, as considered in this work, refers to the entire converter for traction purposes. The influences of the HV/12V-converter as well as the different structures are discussed later in the related parts. Schematic of the second combination is shown on Figure 56 while other structures are shown Appendix 4.

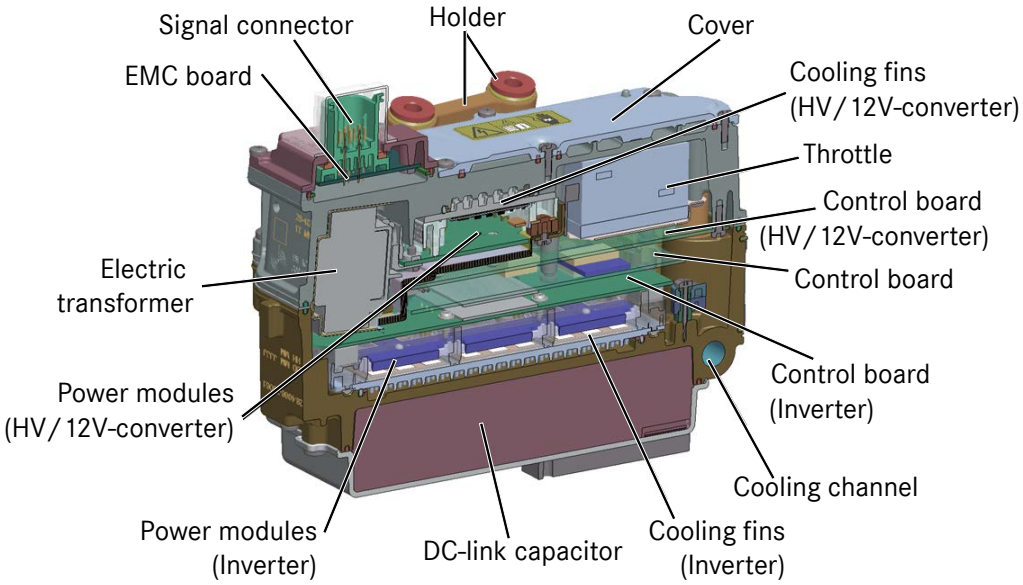

Figure 56: Automotive inverter assembly for an inverter with a HV/12V-converter [23]

1.2 Semiconductor technologies

When analyzing the present current and voltage levels as well as the frequency area in the automotive industry, only two semiconductors technology can fulfill the requirements: the Mosfet and the IGBT [8]. As it can be seen in [8] and [77], the Mosfet is generally more efficient for the low voltage applications whereas the IGBT is used for higher voltage applications. Based on this situation, this section presents the main characteristics of these two technologies. The main difference between them lies in their behavior during conducting phase. While the Mosfet has a continuous behavior over the forward voltage, the IGBT has a discontinuous behavior which implies having a voltage drop before having the possibility to conduct current as shown on Figure 57. This behavior combined with a rising resistance of Mosfet with increasing voltage explains the use of Mosfet for applications up to 200/250V and then IGBT [8], [77] above these values. Beside Mosfets and IGBTs, conventional PN-Diodes are used to ensure the bidirectionality of the system [8]. These switches do not need to be controllable because they conduct automatically in opposing where the other switches are turned off by being placed in parallel of the transistors.

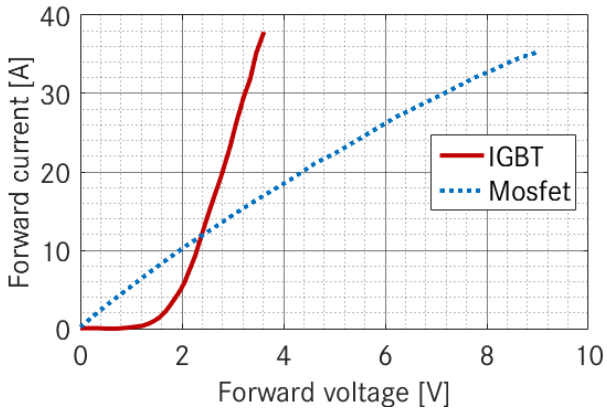

Figure 57: Semiconductor behavior adapted from [8]

1.3 Working principle

In this section, the working principles of the inverter and the boost-converter are presented. For each semiconductor two states are possible: conducting or not conducting but all the combinations are not possible because it could result in invalid states.

1.3.1 Inverter

The aim of the inverter is to convert a DC-power into an AC-power and inversely. By coordinating the conductions of the different transistors and diodes, the inverter realizes this conversion with variable amplitude and quality depending on the control-method. The working principle is first presented generally for the converter structure and then with more details for the PWM (Pulse-Width modulation) control method. Other methods can be used but are not discussed in details in this section.

General working principle:

As previously explained, each semiconductor can have two states. This behavior can be investigated with two states per leg (one leg corresponds to one phase) as depicted on Figure 58 (A) for the case of a Y-coupling of the electric machine. This representation avoids the invalid state where the voltage source is short-circuited. The voltage can thus only take three values: U_{DC}, $-U_{DC}$ and 0. Then depending on the control method, the amplitude and the quality of the phase voltage (U_U, U_V and U_W) can vary. The voltage source is depicted by the DC-voltage (U_{DC}) whereas the legs are represented with a two states switch.

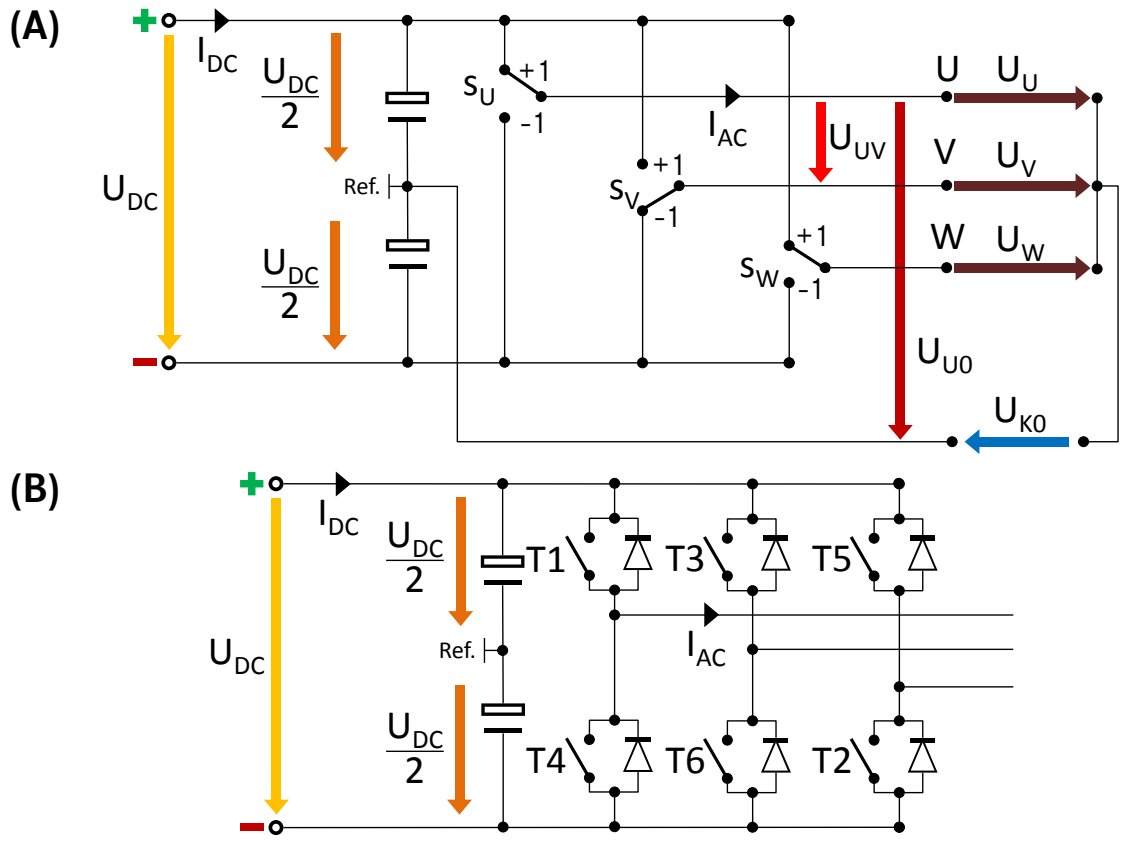

Figure 58: Equivalent circuits of a 2-level 3-phase inverter based on [8] and [78]

PWM control-method:

Besides the global working principle: the control-method influences directly the voltage amplitude and quality. For this purpose, the second representation (see Figure 58 (B)) is used. These variations are based on the occurrence of the switching between the different states. The main methods are the full-wave control or the PWM-method with the possibility to inject a sinusoidal 3rd harmonic signal to increase the amplitude [8]. The control of each transistor for the PWM-method is deduced from the comparison of the reference sinusoidal voltage with a common isosceles triangular carrier. The outputs of the comparison generate the control signals for the three legs of the inverter. When

the sinusoidal reference voltage is greater than the triangular carrier a turn-on signal is sent to the transistor T1, T3 or T5 and turn-off signal to T2, T4 or T6. Thus the three phases of the electric machine have a positive voltage. In the case where the reference signal is smaller than the triangular carrier, turn on signal are sent to T2, T4 orT6 and turn-off signal to T1, T3 or T5 which results in the machine having a negative voltage [78].

1.3.2 Bidirectional boost-converter

The role of the bidirectional boost converter in motor mode is to boost the voltage between the battery and the DC-link and inversely in generator mode by coordinating the conductions of the different transistors and diodes. The term boost refers to the higher voltage at the DC-link. The amplitude can be theoretically variated between 1 and ∞ by variating the duty ratio D. The duty ratio represents the ratio between the conduction time of the transistor T1 (or the transistor T2 in generator mode) and the system period. The conversion is ensured by transistor T1 and diode D1 in motor mode (boost) and by transistor T2 and diode D2 in generator mode (buck).

$$U_{DC}\ /U_{Batt} = 1/(1-D) \quad (28)$$

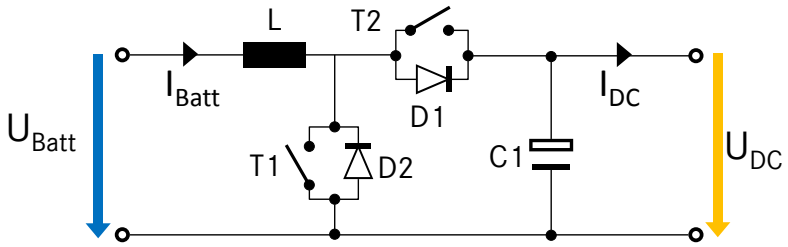

Figure 59: Equivalent circuit of a boost-converter based on [8] and [79]

Boost-mode (motor mode):

In boost-mode, the output voltage U_{DC} is higher than the input voltage U_{Batt}. Thanks to a periodical control of the transistor T1 (T2 is always open) and the energy stored in the input inductance L, the converter enables to increase the voltage by reducing the output current. The output capacitor C1 enables then to reduce the voltage-ripple and to provide a good quality signal to the inverter [8], [79].

Buck-mode (generator mode):

In buck-mode, the input voltage U_{DC} is higher than the output voltage U_{Batt}. When T2 is closed the inverter side provides current to the battery whereas when T2 is opened, the battery side is supplied by the energy stored in the inductance L [8], [79].

1.4 Losses

Considering the scope of this thesis, the losses in the power electronics can be categorized in three main categories: the losses from the power module (diode and transistor), from the passive elements (inductance and capacitor) and from the interconnections (busbar). The global losses balance is presented on Figure 60, where the Sankey diagrams for the inverter (top) and the boost-converter (bottom) are shown.

Semiconductor losses (power module):

There are four main types of losses in the power modules: the conduction losses, the switching losses, the control losses and the blocking losses. The blocking losses are generally neglected [80] due to the higher magnitude of the conduction and switching losses while the losses due to the control of the power electronics are considered within the entire system modeling. These losses are also technology dependent (IGBT and Mosfet).

Passive elements and busbars:

The losses in passive elements are generally magnetic (inductance) or electric (capacitor). Finally the busbar losses are electric losses due to the supplied current. The output capacitor and busbar losses of the boost-converter are not shown on the second diagram because in the case of the architecture with boost-converter the output capacitor and the DC-link capacitor are grouped and designed in such a way that it fulfills the requirements from both the inverter and the boost-converter.

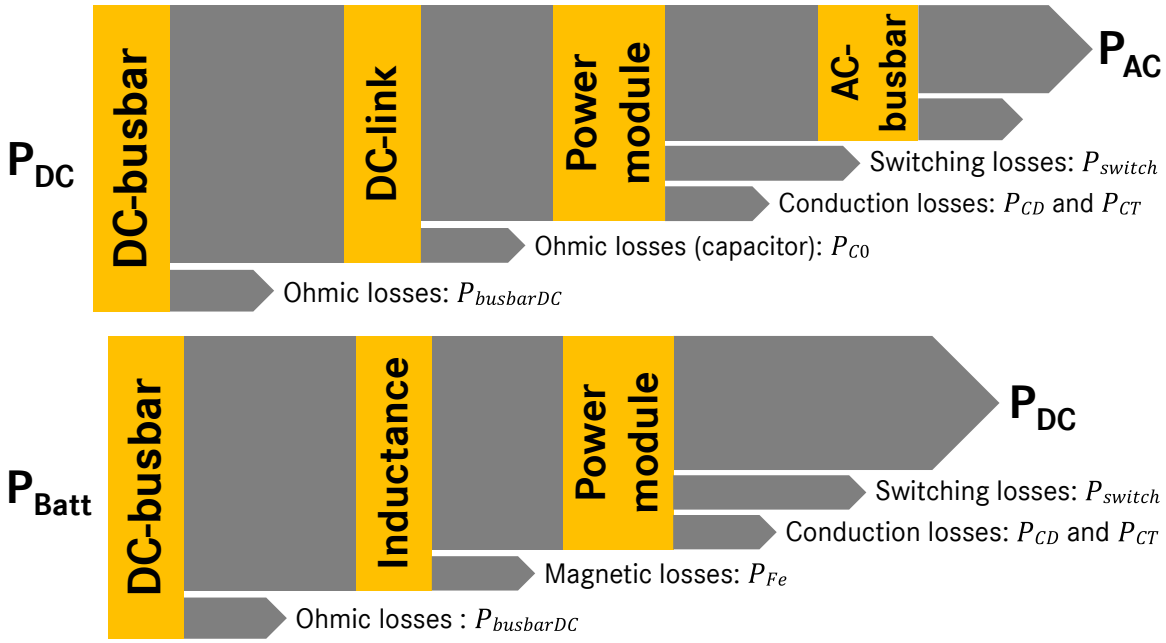

Figure 60: Inverter (top) and boost-converter (bottom) losses based on [8], [79] and [80]

2 Component behavior modeling

Based on the structure, working principle and losses from the previous one, this section discusses the topic of behavior modeling. First the aim of the modeling approach is presented, then it analyzes relevant previous work on the topic. Then based on this evaluation, a suitable solution is chosen and validated based on automotive components measurements. Finally, the contribution of the method is shown by analyzing the losses dependencies.

2.1 Modeling approach

The aim is to model electrical behavior of the inverter and the boost-converter as a “black box”. It means that the intrinsic parameters are not topics of interest. A modeling approach is developed for each converter because the same losses are not considered.

Inverter:

For the modeling of the inverter, the optimal solution should offer the possibility to calculate the following output parameters: DC-power, losses and efficiency. For this purpose two types of input parameters are required: machine parameters (AC-current, AC-voltage, AC-power, power factor) which come from the modeling detailed in the last chapter and external parameters from the control (switching frequency), from the battery/boost-converter (DC-voltage) and from the thermal modeling (IGBT and diode temperatures) as show on Figure 61.

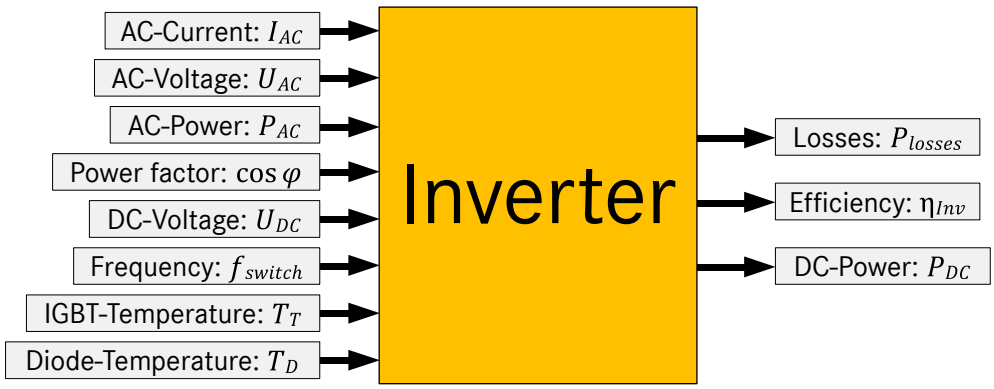

Figure 61: Component behavior modeling approach for and inverter

Boost converter:

In the case of the boost-converter, the input parameters are: Battery voltage, DC-voltage, DC-power, frequency and temperatures (IGBT and diode) while the output parameters are: the battery power, the losses and the efficiency. Contrary to the inverter, the boost-converter has two electrical DC-interfaces and therefore the number of parameters is reduced as it can be seen on Figure 62.

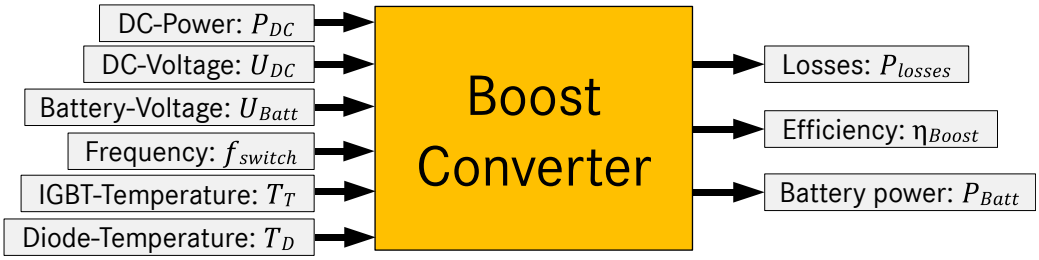

Figure 62: Component behavior modeling approach for a boost-converter

2.2 Previous works and investigation level influence

In order to determinate the suitable modeling approach, the analysis of previous works on the topic for different investigation levels plays a significant role. Therefore, relevant works on the topic is presented and discussed in this sub-section from deep investigations up to more superficial ones.

2.2.1 Investigation of the layer performance in the semiconductors

The analysis of the losses and the components behavior can be directly investigated by considering the different layers in the semiconductors. It offers the possibility to investigate the electrical behavior of the semiconductors for different configurations of these layers. In previous works as [81], the focus is generally set on the evaluation of the parameter for the loss modeling of entire converter using simulations (switching energies or on- and off-state behavior for example). Despite being too detailed for the scope of this work, these evaluations are an important step for the behavior modeling because it is one of the sources of data for modeling at higher level beside direct measurements of the semiconductor parameters.

2.2.2 Circuit based simulation approach

At this level, the modeling considers the voltage and current behavior of the converters and not only the global behavior. Due to the simulation environment chosen for this work, two approaches can be chosen. The first one is based on the Simscape or SimPowerSystem Toolbox from Matlab/Simulink while the second one reproduces the voltage and current behavior by combining different simulation block or mathematical function. The modeling approaches are quite similar and the main difference lies only in the implementation of the modeling. By combining simulation blocks in Simulink, investigations such as in [82] can be performed. As presented in the article, it enables accurate modeling of the behavior of the components and this for both boost-converter and inverter (but also rectifier or buck-converter).

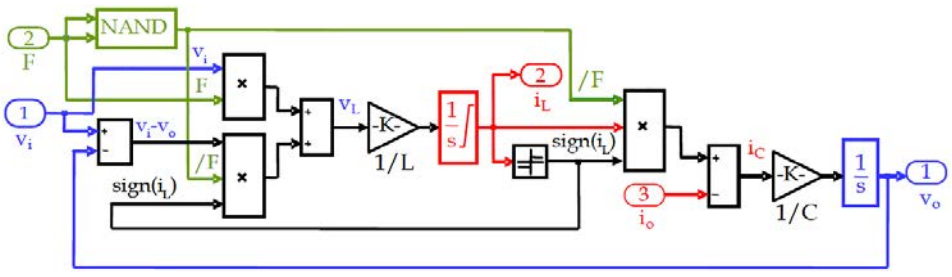

Figure 63: Boost-converter modeling from [82]

Taking as example the case of the boost-converter modeling shown on Figure 63, it requires first analyzing the different operating phases, which enables to determine the behavior of the relevant components such as the input inductance and the output capacitor. Deduced from this analysis, the inductance current (i_L) behavior is modeled using an integrator and a gain depending on the control and the input voltage (v_i), which then allows evaluating the capacitor current (i_c) based on the output current (i_o) and thus calculating the output voltage (v_o). The main change when using Simscape based modeling as in [83] lies in the fact that the sub-components behaviors are not defined by the users through the choice of the simulation blocks but are extracted from a databank. This databank results from several years of investigation and the blocks are built in such a way that they only depict the sub-components behavior. The converter behavior is therefore not deduced from the analysis of the authors but is dependent on the already implemented sub-components from the databank (capacitor, inductance or semiconductors for example) and the architecture implemented by the user. In this case, the users define only the converter architecture, the input values and the sub-component parameters but not the sub-component behavior.

2.2.3 Analytic approaches

Contrary to electric machine modeling, equation based solutions can be considered as a higher level approaches for the modeling of power electronics. This differentiation lies in the periodic behavior of power electronics converters which allows estimating the mean and effective values of the current and the voltage in each sub-component. Based on these values a loss model can be directly calculated between the input parameters and the output parameters considered in this work. The investigation in [84] due to the investigated topologies presents a good overview of the loss models for both the inverter and the boost-converter. Similar approaches can also be found in the applications notes from semiconductor supplier as Infineon [85], which are deduced from renowned papers as [86] and [87]. All the cited examples are based on the same approaches. The work in [85], is taken as example because it also introduces the methodology to extract the diode and transistor parameters from the datasheet. Then, after having defined the hypothesis for the calculation and the considered topologies, the loss calculations methods are presented. These methods link direct the current and the voltage with the losses as desired in this research work. An example of the loss calculation method for the 3-phase inverter topology is shown in the following equations: the transistor conduction losses P_{CT} (29), the diode conduction losses P_{CD} (30) and the switching losses P_{switch} (31) under the assumptions in (32).

$$P_{CT} = U_{ce0} \cdot I_o \cdot \left(\frac{1}{2\pi} + \frac{m_i \cdot \cos\varphi}{3\pi}\right) + r_c \cdot I_o^2 \cdot \left(\frac{1}{8} + \frac{m_i \cdot \cos\varphi}{3\pi}\right) \quad (29)$$

$$P_{CD} = U_{D0} \cdot I_o \cdot \left(\frac{1}{2\pi} - \frac{m_i \cdot \cos\varphi}{3\pi}\right) + r_D \cdot I_o^2 \cdot \left(\frac{1}{8} - \frac{m_i \cdot \cos\varphi}{3\pi}\right) \quad (30)$$

$$P_{switch} = \frac{1}{\pi} \cdot \frac{U_{DC}}{U_{nom}} \cdot \frac{I_{AC}}{I_{nom}} \cdot \left(E_{on} + E_{off} + E_{rec}\right) \cdot f_{switch} \quad (31)$$

$$I_o = \sqrt{2} \cdot I_{ACrms} \quad (32)$$

Where: U_{ce0} and r_c are the transistor parameters, U_{D0} and r_D the diode parameters, m_i the modulation factor, $\cos\varphi$ the power factor, U_{DC} the input voltage, I_{AC} the rms value of the output current, E_{on}, E_{off} and E_{rec} the switching energy for respectively the on-switching of the transistor, the off-switching of the transistor and the recovery of the diode and finally f_{switch} is the switching frequency. The works presented in [84] is also particularly interesting because it considers the efficiency of the global converter. It requires developing methods for both the semiconductors losses as well as the passive elements. This thesis is focused on the comparison of different architectures, among which some are not considered in this work but the presented approach set the basics for this work by considering all the loss sources in the converters.

2.2.4 Higher level and evaluation for electric drive system optimization

The component behavior modeling can be implemented using data maps. The advantages of the efficiency maps are principally linked with the simulation time. Analytic methods for power electronics are faster because the limits

are generally already considered at the electric machine and there are direct relationships between the losses, the voltage and the current. At higher level, the converters are generally considered with a single efficiency or within a combined system efficiency. They are too superficial to offer the possibility to evaluate parameters such as the voltage level and the module strategy even if they enable to compare the different electric architectures. For the purpose of this work and despite doing an energetic analysis, these solutions do not fulfill the requirements set for the modeling. The modeling of power electronics and especially the semiconductors can be really detailed. Considering the requirements described on the Figure 61 and Figure 62. Three main solutions show a good compromise between accuracy, simulation and parameter range: the circuit based approach, the analytic approach and the data maps based solution. The first one offers the wider parameters range because it enables to investigate both the parameters considered in this work as well as other parameters such as the control method. The analytic approach fulfills the requirements set for this work but relies on the following hypothesis: ideal sinusoidal waveforms and an optimal control. The data maps based solution presents the same advantages as the analytic approach with less accuracy due to the interpolation between the maps. The analytic approach presents therefore the best compromise between all the requirements for both inverter and boost-converter.

	Representation	Accuracy	Simulation effort	Parameter range
Circuit-based model	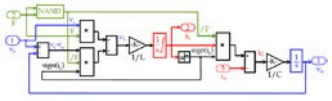	+	-	✓
Analytic approach	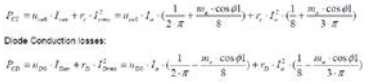	O	+	✓
Maps based	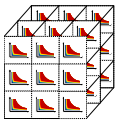	-	+	✓
Single map		-	+ +	X
Single efficiency		- -	+ +	X

Table 15: Comparison of approaches for the behavior modeling of power electronics

2.3 Modeling implementation

This section discusses the topic of the modeling implementation which is based on the analytic approaches depicted in the previous section. It is separated in three parts: first the methods to investigate the losses over a wide range of electrical parameter are discussed. Then the two following parts are discussing respectively for the case of the inverter and the boost-converter.

2.3.1 Investigation of current, voltage and temperature dependency

In the case of the power electronics, the parameters dependencies are discussed before the modeling approach because they are the same for both the inverter and boost-converter. In this sub-section, the solutions to investigate the dependency of the current, the voltage and the temperature in the modeling of semiconductors are introduced. For this purpose, different solutions are discussed, first for the conduction losses and then for the switching losses, finally the case of the passive elements and busbar is discussed.

Conduction losses:

As introduced in [85], the parameters for the conduction losses can be directly extracted from the datasheet (see Appendix 5). These datasheets can be found directly on the website from the suppliers and enable to cover a wide range of voltage and current levels. The influence of the voltage is considered through the variations of the module voltage while the influence of the current is considered through the equations ((29) and (30)). Hence, methods need to be found for the temperature dependency. The values in the datasheet are generally provided for three values (25°C, 125°C and 150°C for example). A polynomial approach cannot be considered due to the properties of polynomial interpolation which ensure a solution with the highest correlation (100%) if only three points are

considered. Hence the following approach is considered: within the range described in the datasheet, the parameters are linearly interpolated between the two nearest values around the considered temperature and outside the range described in the datasheet, the parameters are linearly extrapolated based on the behavior between the two nearest values as shown on Figure 64.

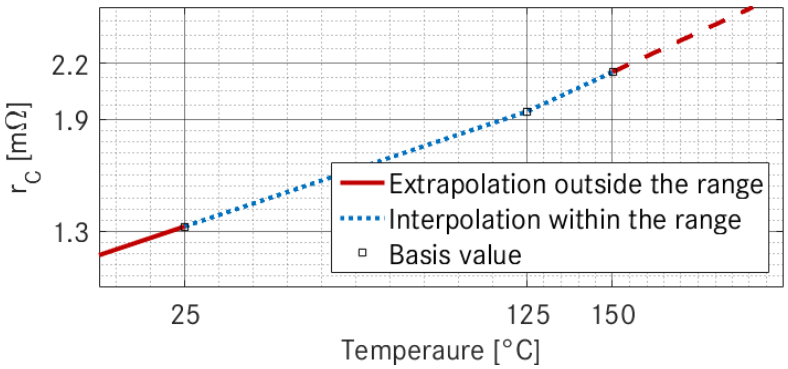

Figure 64: Interpolation approach for the temperature dependency of r_C in an IGBT module

Despite some drawbacks, this approach suits well to the basis values which show a quasi-linear behavior with the temperature variation. More investigations could be performed to evaluate the influence of the temperature but for the scope of this work, this assumption is sufficient because it allows comparing different power modules because the same approximations can be done for each module.

Switching losses:

The switching energy is generally approximated using scaling factors for the current and voltage dependency as shown in (31) which are based on the nominal values. If no better approximation can be found concerning the voltage due to the data generally provided by the semiconductors supplier, the data are given over a wide range of value for the current and thus allow a better approximation. As for the temperature during the conduction losses, a linear approach is used to interpolate the value within the range of the values in the datasheet. The approach is presented on Figure 65 in comparison with the scaling factors based on the nominal values. As it can be seen the interpolation based only on the nominal values lead to high deviations especially in the low load area (underestimation) and in the high load area (overestimation). This solution which is reliable for a system which works around the nominal value cannot be used in the case of this work, where the current variations play a significant role and therefore the solution presented here is chosen.

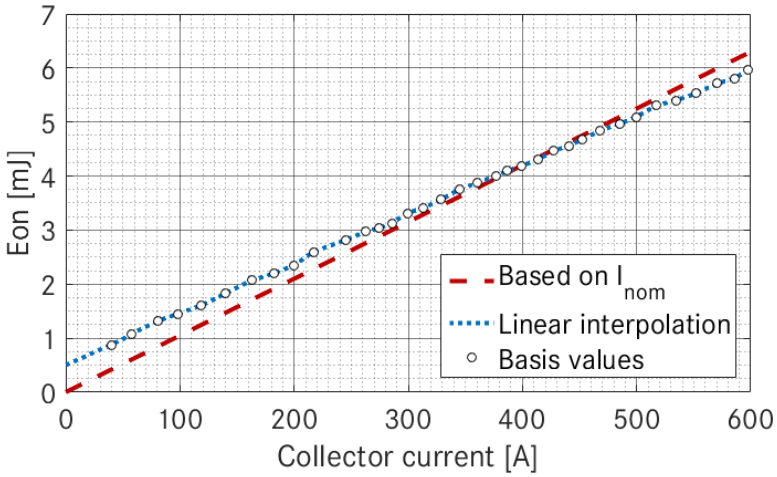

Figure 65: Interpolation approach for the current dependency of Eon

Concerning the temperature dependency, the same approach as for the conduction losses could have been considered but a single value is provided for 25°C. Beside the data from the datasheet: the following hypothesis is done: the switching losses have a linear dependency on the temperature as shown on Figure 66. It shows the

behavior of the switching energies. The values are normalized for a better overview but it shows globally the relevancy of the hypothesis.

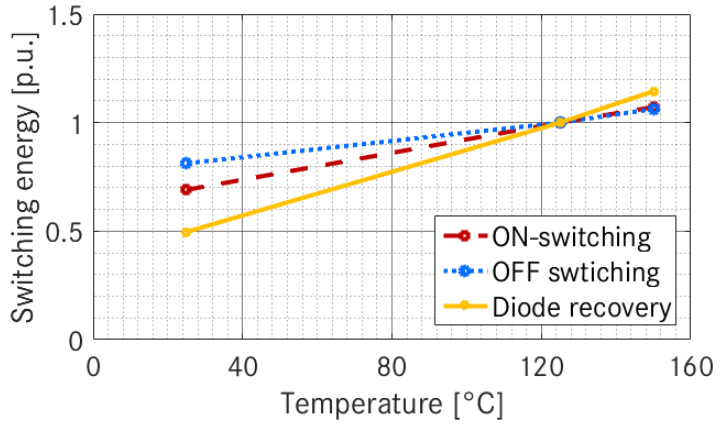

Figure 66: Temperature dependency of the switching energies

Hence, despite the low number of values for the temperature dependency a large area can be covered using a linear extrapolation. The resulting methods for the investigation of the temperature dependency is thus shown on Figure 67, where the grey area show the interpolation area and the orange area the extrapolation area. It is a required compromise to consider a wide parameter range but no strong assumptions are done considering the available data.

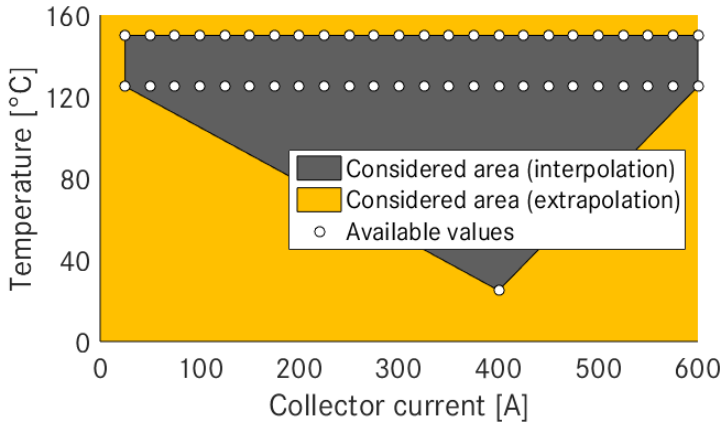

Figure 67: Approach for the current and temperature dependency of switching energies

Passive elements and busbars:

Considering the other elements in the converter, the dependencies have to be considered in two parts: first for the magnetic losses in inductors (only boost converter) and then for the electric losses in the capacitors and the busbars. The temperature dependency in inductance is considered similar to the magnet in electric machine by using the values from datasheet while the voltage and current dependencies are directly considered in the losses modeling as in [84]. For the electric losses in the capacitors and the busbars, the same linear approach as for the electric machine is considered.

2.3.2 Loss model for inverter

After introducing all the dependencies, this section presents the loss modeling for the inverter. As already discussed it only considers multiphase inverter topologies without variations. The number of phases in the system is represented by the values n_{phase} and the converter requires thus $2 \cdot n_{phase}$ transistors and $2 \cdot n_{phase}$ diodes. This section is divided in three parts: one for the conduction losses, one for the switching losses and one for the passive elements and the busbar in the case of an inverter.

Conduction losses:

The conduction losses are considered in this work as in the equations (29) and (30) with some adjustments. First, the parameters of the diode and the transistors are dependent on the temperature and secondly by considering both the motor [85] and generator mode [86]. By combining these two works, the following equations can be deduced and are used in this work. In the transistor losses, the (+) is used in motor mode and the (-) in motor mode while the opposite is used for the diode losses. The temperature dependency as previously discussed is also introduced for the transistor (T_T) and the diode (T_D). Finally the equation (35) condenses the global conduction losses, where the number of phases (n_{phase}) is introduced. The terms (I_o) refers to the equation (32).

$$P_{CT} = U_{ce0}(T_T) \cdot I_o \cdot \left(\frac{1}{2\pi} \pm \frac{m_i \cdot \cos\varphi}{3\pi}\right) + r_c(T_T) \cdot I_o^2 \cdot \left(\frac{1}{8} \pm \frac{m_i \cdot \cos\varphi}{3\pi}\right) \quad (33)$$

$$P_{CD} = U_{D0}(T_D) \cdot I_o \cdot \left(\frac{1}{2\pi} \pm \frac{m_i \cdot \cos\varphi}{3\pi}\right) + r_D(T_D) \cdot I_o^2 \cdot \left(\frac{1}{8} \pm \frac{m_i \cdot \cos\varphi}{3\pi}\right) \quad (34)$$

$$P_{Ctotal} = 2 \cdot n_{phase} \cdot (P_{CT} + P_{CD}) \quad (35)$$

Switching losses:

The main contribution of this work concerning the switching losses lies in the introduction of the temperature and current dependency ($I_{AC_{rms}}$). The dependency on the voltage is done as in previous works since no additional data are provided. The losses as calculated in this work are presented in (36).

$$P_{switch} = 2 \cdot n_{phase} \cdot \frac{1}{\pi} \cdot \frac{U_{DC}}{U_{nom}} \cdot \left(E_{on}(I_{AC_{rms}}, T_T) + E_{off}(I_{AC_{rms}}, T_T) + E_{rec}(I_{AC_{rms}}, T_D)\right) \cdot f_{switch} \quad (36)$$

The previous equation is only valid for the following hypotheses: the switching frequency is high enough to suppose that the fundamental of the phase current is quasi equal to the reference signal used to calculate the PWM. This condition can be translated using the two following conditions (equations (37) and (38)) where f_{output} is the output frequency of the inverter, f_{switch} the switching frequency, m_f the frequency modulation ratio and p_f the pulse number perf half-cycle.

$$m_f = f_{switch}/f_{output} \quad (37)$$

$$p_f = \frac{m_f}{2} - 1 \quad (38)$$

While the condition for m_f is generally defined as a single limit (the value must exceed as described in [79]), the approach based on p_f is defined by two values as described in [88]. The value two is a minimum to reach, to be quasi in the case when it is applicable while the value four defines the minimal value to reach to be sure that the hypothesis is verified. Considering the current status for electric machine in hybrid vehicles, the conditions are in most of the case fulfilled as shown on Figure 68 for several values of the number of poles pair (p).

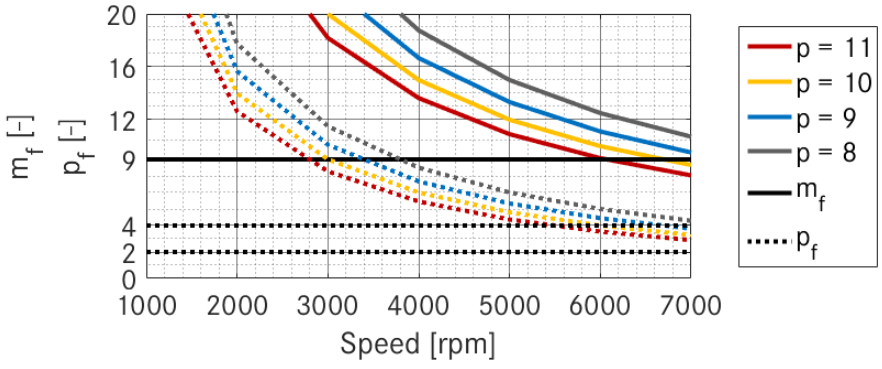

Figure 68: Frequency modulation ratio (m_f) and pulse number per half-cycle (p_f) variations

Losses in passive elements and busbar:

Due to the topology considered in this work, the only losses from passive elements come from the DC-link capacitor (C0). They are considered through the equivalent series resistance of this capacitor (ESR_{C0}) and the stress current applied on this capacitor (I_{Crms}). This current is calculated using the equation (39) based on the works in [89] and enables to deduce the capacitor losses as described in the equation (40).

$$I_{Crms} = I_{ACrms} \cdot \sqrt{\left[\cdot m_i \cdot \left(\frac{\sqrt{3}}{4\pi} + cos^2\varphi \left(\frac{\sqrt{3}}{\pi} - \frac{9}{16} \right) \right) \right]} \quad (39)$$

$$P_{C0} = ESR_{C0} \cdot I_{Crms}^2 \quad (40)$$

Concerning the busbars losses, two types need to be considered: the AC busbar and the DC busbar. The first ones are calculated using the AC current (I_{ACrms}) and the number of phases (n_{phase}) while the second ones are only based on the DC current (I_{DC}). These losses are described by the formulas in equations (41) and (42).

$$P_{busbar\ AC} = n_{phase} \cdot R_{bubsbar\ AC} \cdot I_{ACrms}^2 \quad (41)$$

$$P_{busbar\ DC} = 2 \cdot R_{bubsbar\ DC} \cdot I_{DC}^2 \quad (42)$$

2.3.3 Loss model for boost-converter

As for the inverter, this section introduces the loss modeling for a boost converter. The losses considered in this work are based on the previously presented topology. As already discussed the output capacitor of the boost converter is considered with the inverter which also includes the loss model. The rest of this section presents the solutions for the estimation of the losses in each sub-component (all the proofs for the loss model calculation are presented in Appendix 6). The losses as presented in this work are considering the following assumption: during motoring mode only the transistor T1 is controlled while in generating mode only the transistor T2 is controlled. Under this assumption the calculation of the losses for a bidirectional boost converter can be deduced for a conventional boost-converter in motor mode and a conventional buck-converter in generating mode.

Conduction losses:

The conduction losses are deduced from [85] based on the periodic behavior of the converter and the same temperature and current dependency are considered as for the inverter. As already discussed, both the boost and the buck converter have to be considered to calculate the losses in both generator and motor mode. The equations (43) and (44) can be used in both cases and the differentiation is done through the duty ratio D as shown by the equations (45) and (46) for respectively the motor and generator mode.

$$P_{CT} = U_{ce0}(T_T) \cdot I_{Batt} \cdot D + r_c(T_T) \cdot I_{Batt}^2 \cdot D \quad (43)$$

$$P_{CD} = U_{D0}(T_D) \cdot I_{Batt} \cdot (1 - D) + r_D(T_D) \cdot I_{Batt}^2 \cdot (1 - D) \quad (44)$$

$$D_{motor} = 1 - U_{Batt}/U_{DC} \quad (45)$$

$$D_{generator} = U_{Batt}/U_{DC} \quad (46)$$

The total conduction losses are then the sum of the diode conduction and the transistor power losses with the assumptions discussed previously concerning the conduction of the transistors.

$$P_{Ctotal} = P_{CT} + P_{CD} \quad (47)$$

Switching losses:

Concerning the switching losses, the case of the boost converter is slightly more complicated because despite having a periodic behavior, the current and the voltage are not sinusoidal. Based on the different sequences of the currents during the on-switching and the off-switching can be estimated. They are extracted from [85] and are

presented in the equation (48). Due to the fact that the recovery of the diode corresponds to the on-switching of the transistor, the same current is considered for both the on-switching losses and the recovery losses of the diode. The differentiation between the motor and generator mode is done through the sign, which is presented in the following table for each mode.

$$I_{switch} = |I_L| \pm \Delta I/2 \quad (48)$$

	On-switching $I_{switch_{on}}$	**Off-switching** $I_{switch_{off}}$	**Recovery** $I_{switch_{rec}}$
Motor mode (step-up)	-	+	-
Generator mode (step-down)	+	-	+

Table 16: Sign for the calculation of the switching current

Based on these considerations, the losses are calculated using the same approach as for the inverter and the previously explained switching current as shown in the equation (49).

$$P_{switch} = \frac{U_{DC}}{U_{nom}} \cdot \left(E_{on}(I_{switch_{on}}, T_T) + E_{off}(I_{switch_{off}}, T_T) + E_{rec}(I_{switch_{rec}}, T_D)\right) \cdot f_{switch} \quad (49)$$

Losses in passive elements and busbar:

Due to the topology defined for this work, the following losses in passive elements are considered: the magnetic losses in the inductance. The calculation is based on [90] and [91]. It enables to deduce from the Steinmetz equation (50), a loss model based on the periodic behavior of the currents and voltages in the converter. The steps to find the final form of the loss model (equation (51)) are presented in Appendix 6. In the following equations V_{core} is the volume of the magnetic core of the inductance, D is the ratio of the converter as defined previously, f_{switch} is the switching frequency and k, α and β are the material parameters from the basis Steinmetz equation.

$$\overline{P *_{FE}} = k \cdot f^{\alpha} \cdot \hat{B}^{\beta} \quad (50)$$

$$P_{Fe} = V_{core} \cdot k_i \cdot {f_{switch}}^{\alpha} \cdot \hat{B}^{\beta} \cdot (D^{1-\alpha} + (1-D)^{1-\alpha}) \quad (51)$$

The factor k_i is detailed in the equations (52) whereas the amplitude of $\hat{B}$ is dependent on the mode. The value in motor mode is shown in (53) and in (54) for generator mode, where T_{switch} is the switching period ($T_{switch} = 1/f_{switch}$), N is the number of windings and A is the cross section of the core.

$$k_i = \frac{k}{2^{\beta+1} \cdot \pi^{\alpha-1} \cdot \left(0.2761 + \frac{1.7061}{\alpha + 1.354}\right)} \quad (52)$$

$$\hat{B}_{mot} = \frac{U_{Batt} \cdot D \cdot T_{switch}}{N_w \cdot A} \quad (53)$$

$$\hat{B}_{gen} = \frac{U_{Batt} \cdot (1-D) \cdot T_{switch}}{N_w \cdot A} \quad (54)$$

Concerning the busbars losses, only the losses on the input side are considered. As for the output capacitor, when a boost-converter is used in combination with an inverter, all the losses on the output side are already considered in the inverter losses and the adaptation is done through the design requirements. Thus the same approach as for the DC busbar in inverter can be used by considering the battery current.

$$P_{busbar\ input} = 2 \cdot R_{bubsbar\ input} \cdot I_{Batt}^2 \quad (55)$$

2.3.4 Losses calculation with Mosfet

As explained in the first chapter, most of the current systems are using IGBTs but the current development of 48V-systems has raised the interest for Mosfet. The use of Mosfet only implies changes for the calculation of the conduction losses due to the behavior of the semiconductor as shown in Figure 57. The changes are shown in the following equations; for the inverter (56) and for the boost-converter (57) using the same considerations as previously and based on [92]. The value R_{DSon} represents the resistive behavior of the semiconductor during conducting phase as previously shown and is extracted from the datasheet according to [92]. These two equations replace the equations (33) and (43) for respectively the inverter and the boost-converter.

$$P_{CT} = R_{DSon}(T_T) \cdot I_o^2 \cdot \left(\frac{1}{8} \pm \frac{m_i \cdot \cos\varphi}{3\pi}\right) \quad (56)$$

$$P_{CT} = R_{DSon}(T_T) \cdot I_L^2 \cdot D \quad (57)$$

2.4 Validation

In order to ensure the relevancy of the results, the modeling developed in this work needs to be validated. The validation presented in this section is divided in three parts: one for the inverter, one for the boost-converter and a final one where the analytic approach is compared with a circuit based approach. To validate the modeling approaches as well as the current and voltage dependency, the validations are always presented for different values of the current and the voltage.

2.4.1 Inverter losses validation

The measurements for the validation of the inverter modeling are done on the same test-bench as for the electric machine validation (Appendix 3). As for the electric machine, the losses cannot be directly measured and they result from the subtraction of the AC power to the DC power in motor mode (and inversely in generator mode) and the subtraction of the cable losses. The simulations are performed for with a resistance of respectively 1.7mΩ and 1mΩ for the AC-busbar and the DC-busbar and an equivalent series resistance (ESR) of 55mΩ for the DC-link capacitor. Considering the results in the following figures, three main observations can be done. First, the results of the simulation are showing good correlation (99.73% for both voltages) and low deviations (under 5%) except in the low current area. It is assumed that these deviations are resulting from the linearization done to estimate the IGBT behavior and the approximations done during the measurements as explained previously. An interesting fact is the role of the losses in the passive elements and the busbar. Despite the losses in the in the transistors and the diodes being generally the most important sources of losses in the converter, these results show the importance of the losses in the busbar and the passive elements. It is especially observable for the high load (i.e. high current) due to the resistive aspect of these losses.

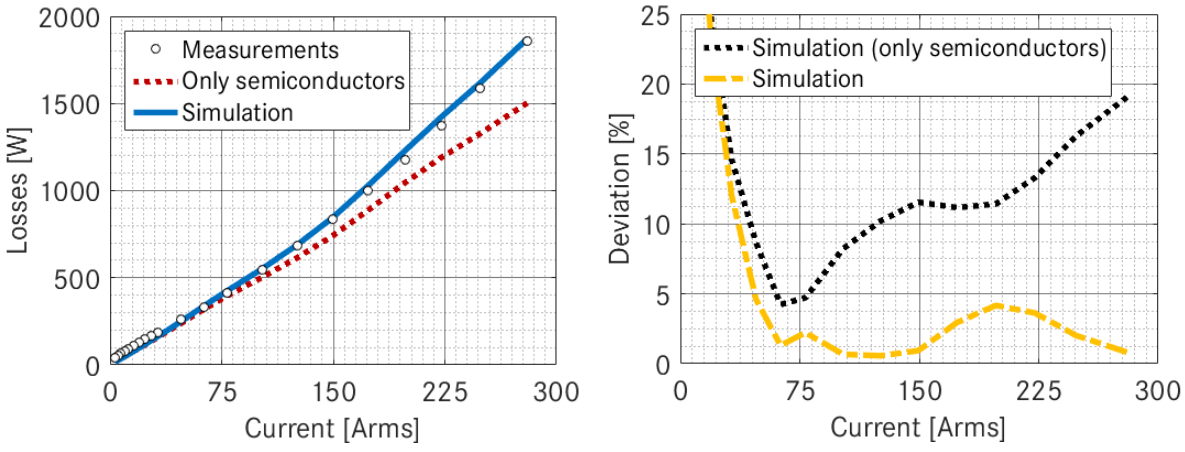

Figure 69: Comparison between simulation and measurements of the inverter losses @300V

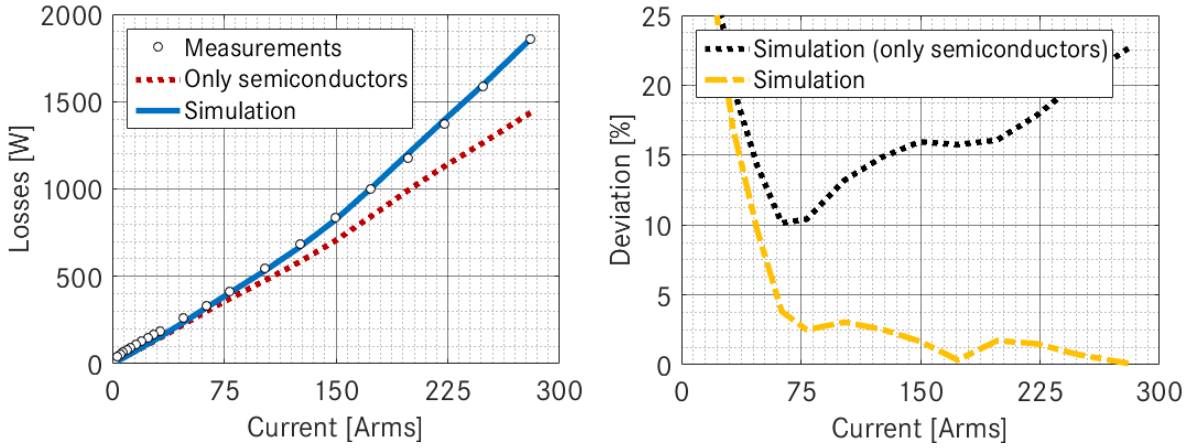

Figure 70: Comparison between simulation and measurements of the inverter losses @ 250V

Inverter with Mosfets:

For the purpose of validating 48V-systems, other measurements are done for the Mosfet technology. Moreover the validation of this second technology offers an additional degree of freedom for future modeling because future technologies such as the SiC-semiconductors [93] are also based on both IGBT and Mosfet. The results are presented on Figure 71 under the following assumption: the development is quite recent and thus no reference values are available for automotive components. The results on Figure 71 are calculated using conventional industrial 100V power module for a frequency of 10 kHz with a resistance of respectively 0.5 mΩ and 0.5 mΩ for the AC-busbar and the DC-busbar and an equivalent series resistance (ESR) of 14 mΩ for the DC-link capacitor.

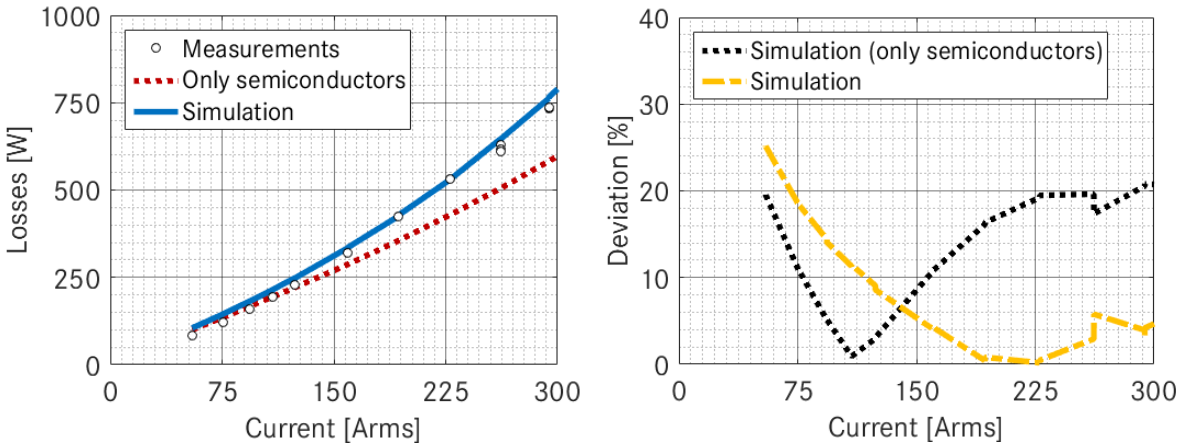

Figure 71: Comparison between simulation and measurements of the inverter losses for Mosfet @44V

The results for the Mosfet show a little lower correlation (95.45%) and a higher deviation (under 10%) except in the low current area. This can be explained as previously due to the approximations done during the measurements but also due to the fact that the module used to calculate the losses is based on values from non-automotive module. Moreover, considering the high correlation of the results, the modeling could be corrected by adjusting the values of the different parameters for the loss calculation.

2.4.2 Boost-converter losses validation

The boost-converter is not a required components for the traction purpose and therefore it is not used in every hybrid electrical vehicles. For this purpose, the availability of the data is quite low. In order to validate the loss modeling of the boost-converter, several approximations are introduced. First concerning the IGBT module for the simulation: the losses are calculated with modules from the Japanese manufacturer Mitsubishi Electric. They are well known to provide Intelligent Power Module (IPM, [94]) as used in the boost-converters from Toyota which are used for this validation [95]. Secondly, the results in [95] only present the efficiency of the boost converter but no details about the test-bench and the measurement approximations. Hence the validation presented in this sub-

section aims to validate the load dependency of the converter and the influence of the voltage level. The results are presented on Figure 72 based on 1200V IGBT power module for a frequency of 5 kHz and an input voltage of 275V.

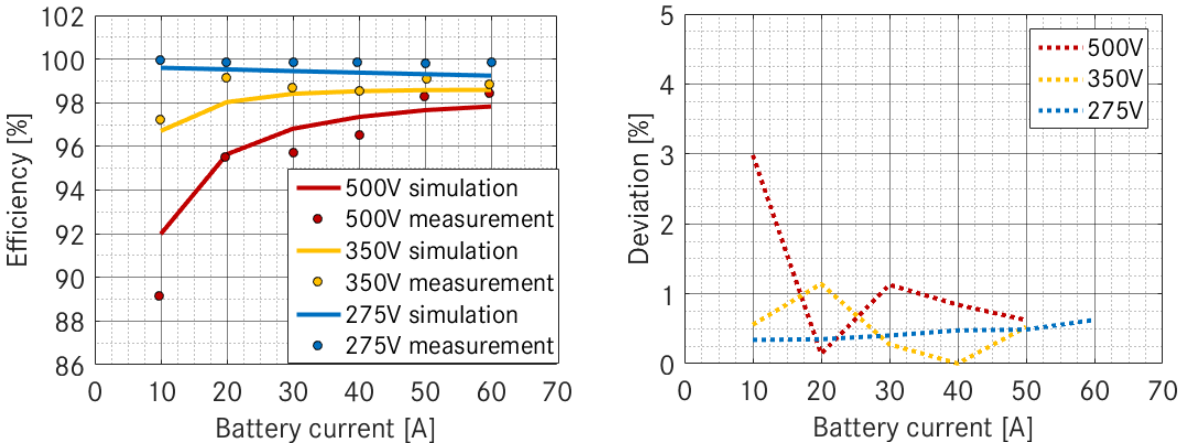

Figure 72: Comparison between simulation and measurements of the boost-converter losses

The results show really low deviations (under 3%) but they need to be considered with caution because the efficiency and not the losses are considered. Globally the simulation has the same behavior as the measurement and show the same dependency. The boost-converter cannot be deeply investigated because it is only used by a low number of automobile manufacturers and thus the converter is not measured. The results presented here also show the typical behavior of a boost-converter as available from Brusa [96].

2.4.3 Circuit based solution

The analytic approaches, as presented in this section have shown a sufficient level of details and a suitable parameter range to fulfill the requirements of the component behavior modeling as depicted in Figure 62. Considering that the aim of this work is to evaluate the different possibilities for the modeling of the components, a circuit-based model is developed using the toolbox Simscape from Matlab/Simulink to ensure that the right compromise is done. The components as well as the circuits are developed to reproduce the same topologies as the ones presented previously. The results compared to the analytic ones are shown too. For the Matlab/Simulink environment, other alternatives such as PLECS [97] and SimPowerElectronics are available but Simscape is chosen for its flexibility. It enables the user to build its own components and also to define the input-parameters. Using these characteristics, the same interpolation for the temperature and the current could have been implemented in order to compare only the modeling approaches.

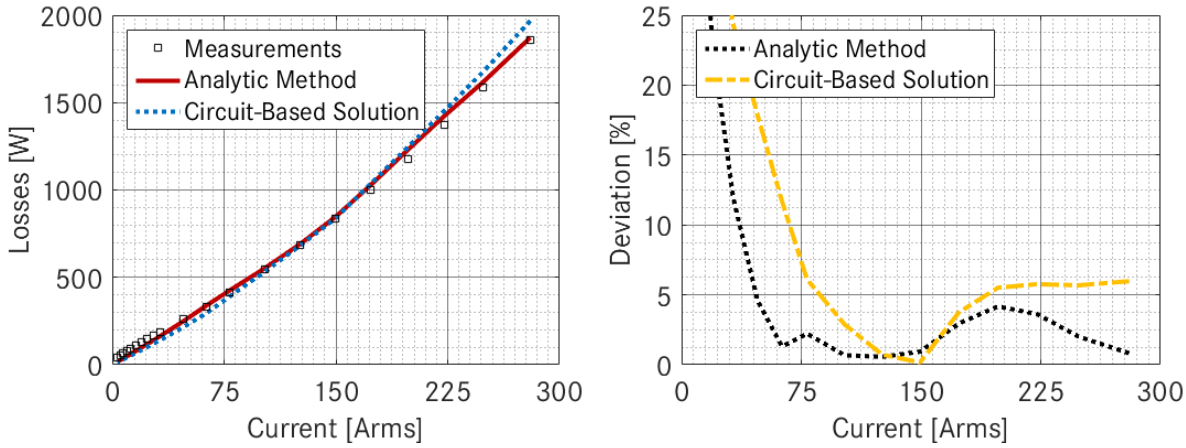

Figure 73: Comparison between measurements, analytic method and circuit-based solutions

As it can be seen, the circuit-based solution presents similar results as the analytic method: high correlation (99.16%) and low deviations (globally under 6%) except in the low load area. Moreover, the circuit based solutions enables to investigate other control methods (full-wave control for example). These advantages are however balanced by the

drawbacks of such a solution. A deepest investigation requires calculating values which are not necessary for the global system analysis such as the current and voltage waveforms. These additional values are requiring more time and thus, considering the scope of this work, the circuit based solutions are not adapted. The circuit based method is more flexible because it is independent from the control method but it does not compensate the high simulation effort.

2.4.4 Summary

In this section, the modeling approaches for power electronics are investigated with the goal to find an adequate solution to fulfill the requirements of this work. The circuit-based solution offers the best compromise between accuracy, parameter range and simulation effort. Some high deviations can be observed in the low current area which could be compensated considering more detailed approach. For the purpose of this work, the retained solution is still sufficient because the focus is not on the accuracy but on the determination of suitable solutions to compare different systems with variable parameters such as the voltage. The assumptions done in this work to develop this solution are fulfilling the requirements and enable this comparison despite the observed deviations.

2.5 Contribution for system evaluation

The loss modeling is developed with the aim to investigate the voltage and current level influence. It is generally assumed that a reduction of the current implies a reduction of the losses. However, as it can be seen in the previous section, the relationship between the losses, the current and the voltage is not trivial and the voltage can also increase the losses through the switching losses. To evaluate this influence and to show the contribution of the chosen method, the losses are calculated for the maximal modulation of the PWM according to [8], using the nominal voltage and the AC-current of the system. The losses are calculated at 25°C with a switching frequency of 10 kHz and a power factor of 0.95. The first main result is the technology dependency: from a maximal voltage of 500V, a technological change is required (600/650V → 1200V IGBT). This technological change as explained previously implies a change of the diode and the transistor parameters and thus the losses.

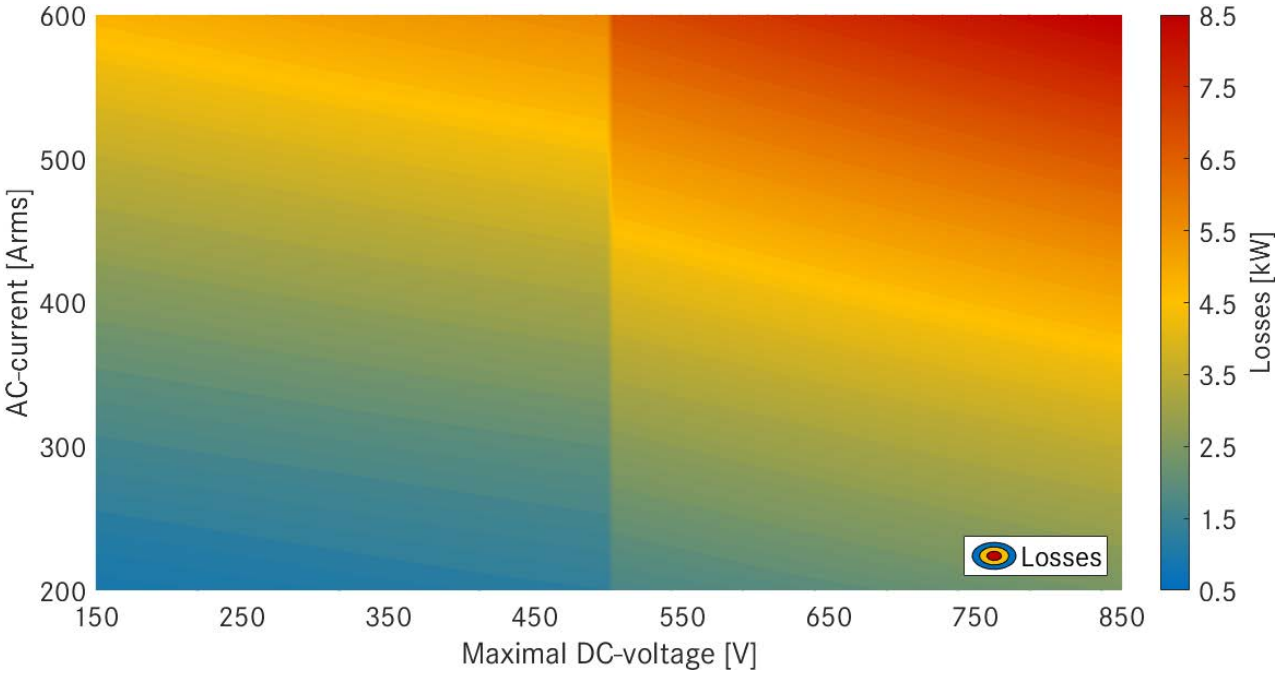

Figure 74: Influence of the voltage and current level on the inverter losses

To have a better overview about this parameter, Figure 75 represents on one side the loss dependency on the voltage for a constant current and on the other side the current dependency for a constant voltage. For the discussion of the results, a system with a maximal voltage of 450V and peak current of 300Arms is taken as reference.

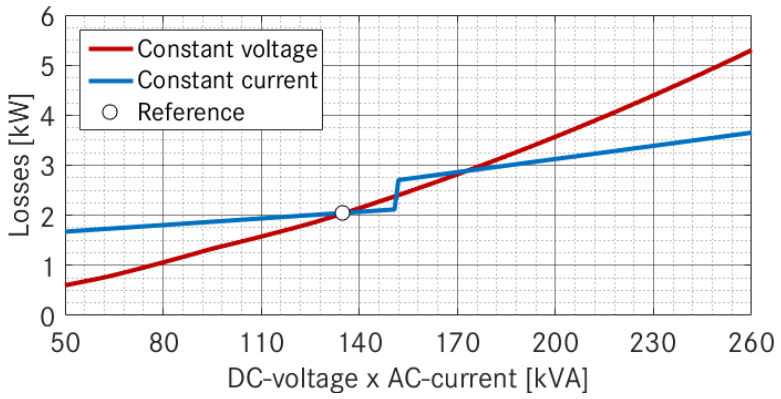

Figure 75: Inverter losses dependency on the current and the voltage

Due to the non-linearity of the voltage dependency, the best solution is clearly depending on the product of the AC-current and the DC-voltage. When a power below the reference is needed, it is more efficient for the system to reduce the current by a constant voltage while when a power above the reference is required: it is more efficient to increase the voltage by a constant current. Around the discontinuities due to the technological change, no real decision can be done because it is fluctuating. The results presented are however only valid for the two considered power modules but give a good overview about the current and voltage dependency.

3 Thermal modeling

This section discusses the topic of thermal behavior modeling. It first begins with the definition of the modeling approach, an analysis of previous works is done and then a suitable solution is chosen, implemented and validated using measurement of automotive components. Finally, the contributions of the modeling approach are shown.

3.1 Modeling approach

By doing a thermal modeling, the aim is to refine the component behavior modeling by adding the possibility to evaluate in real-time the temperature. As it can be seen on Figure 64, it directly impacts the behavior of the system and thus cannot be neglected. For this purpose, the thermal modeling aims to depict the temperature behavior based on the semiconductors losses and the cooling properties (coolant temperature and flow). For this purpose, the approach described on the following figure is retained. The output aims to consider both the diode and transistor temperatures. As for the electric machine, the cooling properties are not investigated in this work and they are defined during the drivetrain design but are considered because the same converter can be used in several drivetrains. Another important aspect concerns the topologies and the technologies: the differences between the two converters (inverter and boost-converter) are done through the loss behavior and the number of semiconductors. However, the thermal path is similar and thus the modeling investigated in this part is independent from the converter.

Figure 76: Thermal modeling approach for the power electronics

3.2 Previous works and investigation level influence

To find the suitable solution to model the thermal behavior of power module, this section analyzes previous works on the topic. They are presented with an increasing level of investigation to show the entire scope of the solutions.

3.2.1 Finite element analysis

Like in many investigations, finite-element analysis is used for detailed and accurate investigation. The modeling approach does not differ for the one used for electric machine and are therefore not discussed in details here. The

finite element can be used to deeply model the components but also to derive reduced model. The investigation in [98] presents different approaches for the thermal simulation of power electronics for hybrid electrical vehicles such as a finite-element simulation of the power modules shown on Figure 77. The aim of this work is however to show the potential to reduce this model. For this purpose, the results of the thermal analysis using finite-element are used to derive reduced model with lower complexity but higher flexibility. The reduced model can then be used in an electrothermal simulation to evaluate the entire converter behavior. This article shows both the potential solutions for the thermal modeling as well as the importance of a system approach. Deep investigations without technical feedback from global system analysis are not relevant. The derived solution is discussed in details in the next section with a more extensive article on this topic.

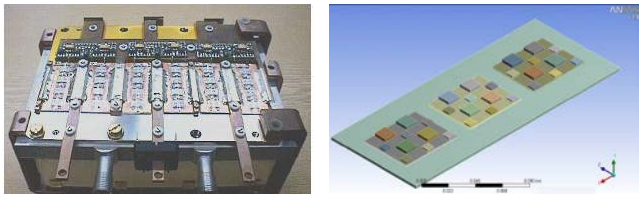

Figure 77: Thermal modeling of power modules using FE with Ansys [98]

3.2.2 Nodal and analytic approaches

The thermal analysis of the power electronics converter is less complicated as the one for the electric machine due to the structure of the power module, as shown on Figure 78. The nodal or analytic approaches which are deduced from this structure are thus less challenging because most of the sub-parts are only connected with two others. It enable thus to do some approximations to find a compromise between the simulation effort, the investigated parameter and the accuracy.

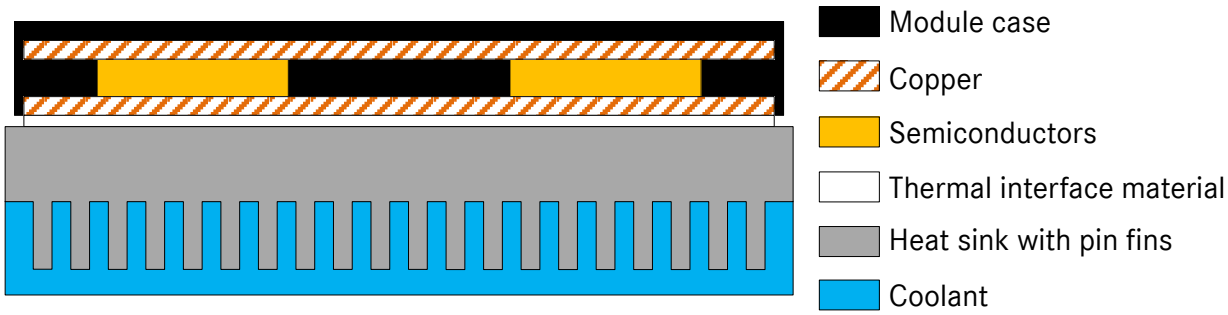

Figure 78: Structure of a power module and its heat sink based on [99]

Considering this structure, nodal and analytic approaches can fulfill both system level and component level approaches. The differentiation is done through the complexity of the structure use for the simulation. At the component level, these approaches can be used to calculate in real time the temperature of the semiconductors for the online thermal monitoring of the power electronics as in [99]. This article presents a solution for the online monitoring of the power semiconductors in converters of electrical and hybrid electrical vehicles. It shows both the nodal representation of the thermal modeling and the corresponding analytic approaches to simulate the thermal behavior. The approach as considered in [99], represented by the following equations, requires having access to the following informations: exact structure of the converter (consideration of the thermal path between the semiconductors), conductance and real-time losses in each semiconductor, to build the matrix A and B as well as the loss vector u (semiconductors losses) which are required to calculate the behavior of the temperature vector x. This detailed structure of the converter enables however to achieve a high accuracy in the results and shows the potential of the nodal approach.

$$\dot{x} = A \cdot x + B \cdot u \quad (58)$$

The nodal model is also often used because the thermal behavior of semiconductors can be modelled using equivalent electrical circuits with low complexity as in [100]. In this article, the thermal behavior of semiconductors is explained before introducing the method to perform a transient thermal simulation of the power module using

these circuits. The nodal approach is used to describe the thermal path between the loss source (T_j) and the cooling system (T_c) as shown on Figure 79. The path between them is depicted by the thermal resistances and capacities (R_{thi} and C_{thi}). These values are calculated using the height of the height of the layer (d), the surface of the layer (A), the specific heat capacity (c), the density (ρ) as well as the thermal conductivity ($\lambda_{th\,i}$). Using this approach, the semiconductor temperatures can be evaluated based only on their losses, on the coolant properties and on the thermal path.

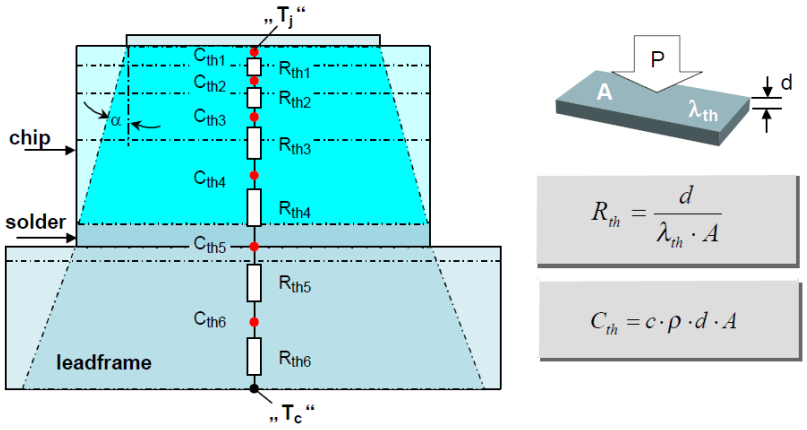

Figure 79: Nodal approach for the thermal modeling of power electronics system [100]

3.2.3 Higher level and evaluation for electric drive system optimization

The only solution at higher level is the use of only the thermal resistance between the losses and the cooling system. It would reduce the complexity of the modeling by giving directly the static temperature increase in the system by neglecting the transient aspects. In the case of automotive applications where the behavior of the system is highly dynamic it is not possible to neglect the typically large thermal time constants of materials due to the low thermal capacity of the semiconductors and high loss density allowed by the designers for transient currents. [101]. The thermal modeling of power electronics is a well-researched topic where both the scientific community and the manufacturers are working to have the possibility to better evaluate the thermal behavior during the design process. Considering the requirements of this work and the position of the investigation during the design process, the use of finite element analysis is excluded. Within the nodal and analytic approaches, different solutions are presented but one is strongly dependent on the converter concept and design and is thus excluded. The second one, presented in [100], is chosen because of its low simulation effort and the possibility to extract the values directly from the datasheet [101], which fulfills the requirements of this work.

	Accuraccy	Simulation effort	Parameter range
Finite element analysis	+ +	- -	✓
Complex nodal model	+	-	✓
General nodal model	o	++	✓

Table 17: Comparison of approaches for the thermal modeling of power electronics

3.3 Modeling implementation

This section presents the implementation of the modeling resulting from the analysis of previous works. The solution discussed in [100] and also used in [102] is retained and implemented. As presented in [101], the values are extracted from the datasheet and implemented in the modeling. This section discusses how the different coolant and thermal properties are considered using these values.

3.3.1 Thermal modeling approach

Resulting from the thermal path shown on Figure 79, the thermal modeling approach presented on the following figure is considered for this work. It enables to depict the thermal behavior as a black box, since the relationships between the parameters from the datasheet (Appendix 5) and the thermal path are not explicit but only synthetically provided (no dependencies on the sub-component parameters such as the layers).

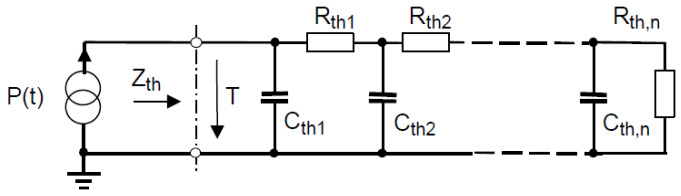

Figure 80: Nodal approach considered in this work [100]

The temperature at the semiconductors (T) is evaluated based on the loss ($P(t)$) and the thermal path which is defined by the different thermal resistance and capacitance (R_{thi} and C_{thi}, $\forall i \in (1, \dots, n)$). Considering this nodal approach, the temperature at both the transistor and the diode can be estimated; temperatures, which enable then to enhance the component behavior modeling and to estimate the limits of the converter.

3.3.2 Coolant flow influence

Based on the nodal approach described previously, this section explains how the coolant flow influence is implemented. The values from the datasheet provide two types of information, first the dynamic behavior which is implemented thanks to the nodal approach and the coolant flow dependency of the thermal resistance. In order to implement the coolant flow dependency the following approach is used: based on the actual current flow the thermal resistance is calculated, this calculated value is then divided by the thermal resistance for the reference coolant flow used for the nodal approach. The resulting factor is then used to scale the value of the thermal resistance and therefore both the amplitude and the dynamic behavior are adapted.

3.4 Validation

Similarly to the previous model validations, the approach chosen to simulate the thermal behavior of power electronics needs to be validated. The measurements used for this validation are done during vehicle tests. Hence only the embedded thermal sensor in the components can be used for the validation. As was the case for the electric machine, the validation is done with a combined simulation and therefore the deviations result from the coupling of both simulations. The results of the measurements and the simulation are shown on Figure 81. During the comparison, the following hypothesis needs to be considered: the temperature sensor is generally placed on the lead frame beside the semiconductors and thus it does not really depict the thermal behavior of the semiconductor temperature. The measurements are thus compared with the semiconductors temperatures and with the first layer temperature which is calculated by considering only the thermal path from the second equivalent RC-circuit.

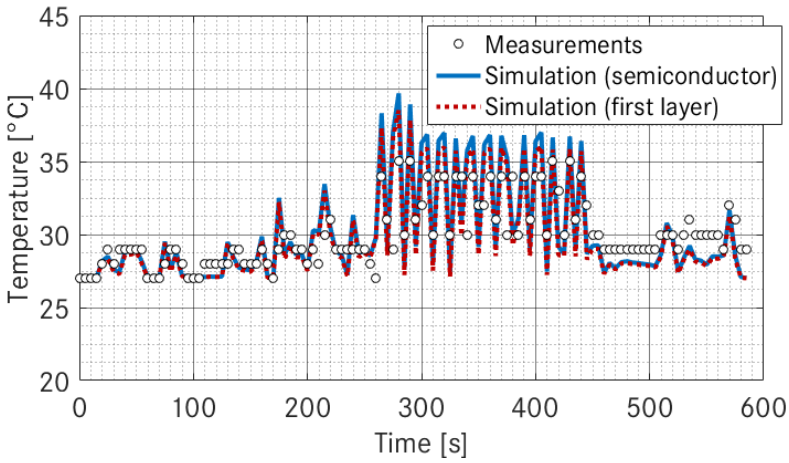

Figure 81: Temperature comparison between simulation and measurement

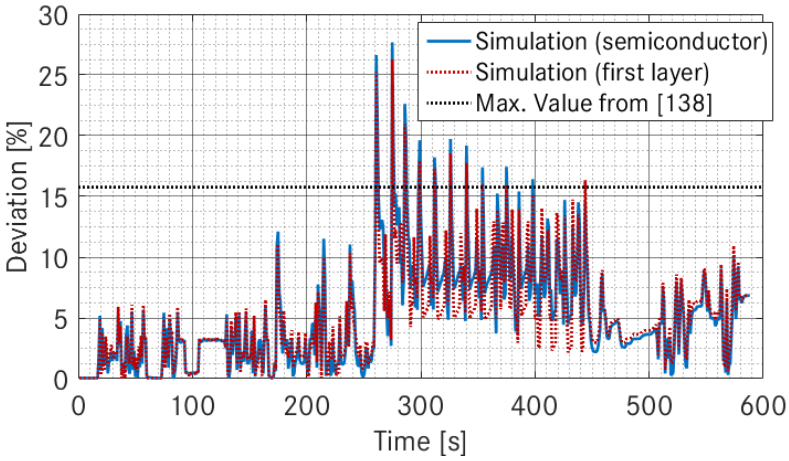

Figure 82: Deviation between the simulation and the measurement of the temperature behavior

Considering the results presented on Figure 81 and Figure 82, two main observations can be done. First it can be observed that the estimated temperatures with simulations are generally higher than the measurement and secondly that the deviations are really high. The hypotheses previously discussed directly influence this comparison because the real temperature measured by the sensor is only approximated in the modeling and also because the vehicle environment greatly influences the results of thermal simulation. The vehicle environment imposes an additional constraint which is not considered during the simulation: during driving phase, there is circulating air in the vehicle which reduces the temperature of the components through convection. More generally, the simulation considers only the thermal path between the semiconductor and the cooling system. Considering the maximal value from [103], where the focus is set on the power module design, the modeling accuracy is acceptable for the research goal of this work where the flexibility for global system modeling is an important aspect.

3.5 Contributions for system evaluation

The role of the thermal modeling during system evaluation is a more sensible topic because as shown in the last chapter, its relevancy is limited on the present driving cycles used for certification purpose. However, it plays a preponderant role during the evaluation of the system limits. To show this contribution, a series of points are simulated to cover the entire range of the considered system. For each points, the simulation is conducted till the temperature in the transistor or the diode exceed the maximal allowed temperature. The results are presented on Figure 83 for an inverter with 650V IGBT modules, a coolant flow of 2l/min and a coolant temperature of 85°C.

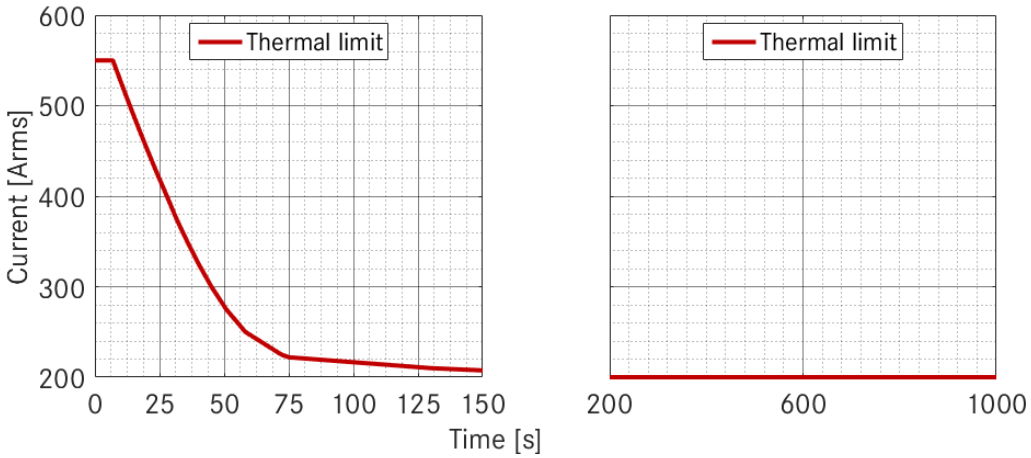

Figure 83: Thermal limits of the power modules @325V

The results presented on the previous figure shows the relevancy of the thermal modeling. Indeed, the implementation of the thermal modeling enables to refine the global simulation because the loss parameters are estimated with the actual temperature but it also allows determining the thermal limits of the inverter as well as the limits of the system depending on the operating conditions.

4 Volume and weight estimation

Contrary to the case of the electric machine, where the volume and weight estimation could be reduced with some hypothesis, the case of power electronics is more complicated: first because the converter box contains generally several converters (see Appendix 4) and secondly due to the converter structures no sub-parts can be neglected. First the evaluation approach is defined before discussing previous investigations on the topic. Then the method implementation and its validation are presented and finally the contributions for system evaluation are shown. The discussions in this chapter do not any differentiation between the boost-converter and the inverter except during the implementation and the validation.

4.1 Evaluation approach

In the case of the power electronics investigation, no Boolean solution can be implemented. The integration of the power electronics is a more modular investigation because it has no direct mechanical connection with the drivetrain. In the case where one dimension is over the requirements, some adaptations can be done by changing the position of adapting the cable path. The required approach is thus defined as follow: based on the available volume and using the electrical requirements of the converter, the approach has to estimate the required dimensions and the weight of the converters as depicted on Figure 84 and Figure 85. The available volume is described by the dimensions while the electric requirements are value of the voltage and the current ripple as well safety requirements. Moreover for the inverter, the modulation factor and the power factor from the machine are required.

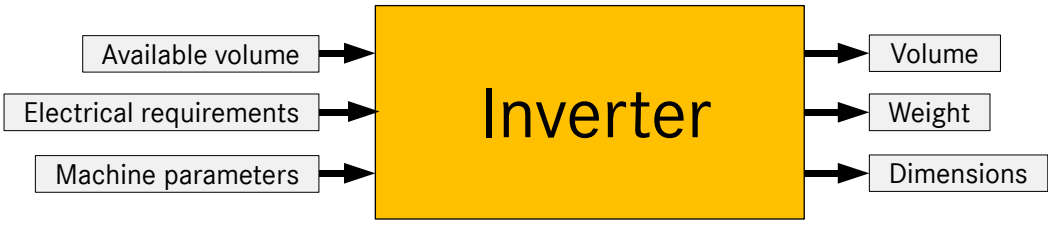

Figure 84: Evaluation approach for the integration of an inverter

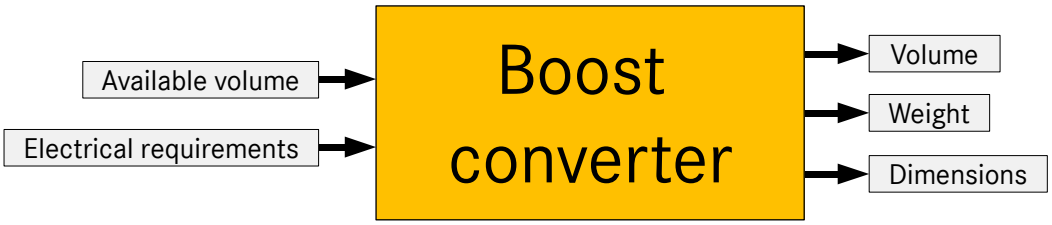

Figure 85: Evaluation approach for the integration of a boost-converter

4.2 Investigation of level influence and related approaches

As for many components, the volume and the weight are generally evaluated during the early design phase to analyze the relevancy of the requirements and during the final development of the vehicle to test the integration with the finally designed component. Most of the investigations are also performed using one of these two approaches even during the other development stage. This section discusses relevant previous works, the drawbacks and advantages of each one and how they only fulfill partially the goals of this work.

4.2.1 Computer aided design

At the end of the development or during the development stages, the computer aided design (CAD) approach enables to test directly the integration of the component. It requires however to have the dimensions of the component or to have the dimensions of each sub-parts (power modules, current sensors or capacitors for example) and the tolerances for the design such as the creepage and clearance distance which defines the distance between two conducting parts. This type of investigations enables to develop high density or highly integrated converters such as in [104], where the converter is directly integrated within the hybrid module, or as in [105], where the power

electronics is directly mounted on the side of the combustion engine (see Figure 86). These two examples are not discussed in details because despite the good and prominent results of these works, they cannot fulfill the requirements of this work concerning the modularity (variable voltage and current) and the topology (variable electric architecture or power electronics topology).

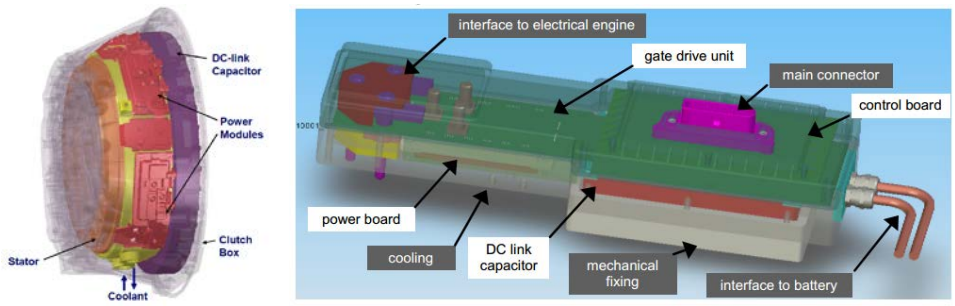

Figure 86: High power density and highly integrated power electronics design using CAD solutions [104] and [105]

4.2.2 Power density

Using power density presents the same drawbacks as for the electric machine. It enables only to evaluate the relevancy of the requirements and not the converter integration. The work presented in [106] shows a good overview of the key factor for the power density of power electronics converters and the limits of the development with the present technology. Moreover the work in [76] shows with accuracy the specific case of power electronics in the automotive industry but stays quite superficial and does not give any real method for the evaluation of the integration. Only some methods are discussed in details for the passive elements and an overview of the volume distribution between all the sub-components is presented. The power density from [106] are shown on Figure 87 and even if they cannot directly fulfill the requirements of this work, they can be used as reference to evaluate the validity of the chosen solutions.

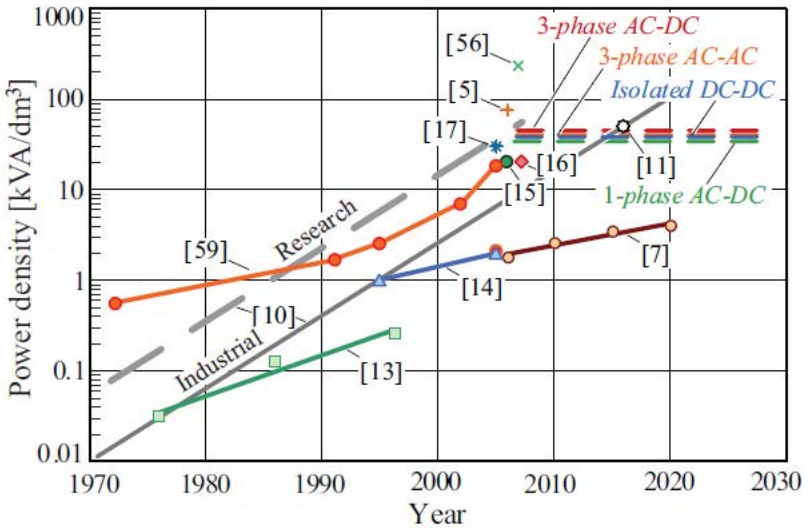

Figure 87: Power density limits from 1970 to 2030 according to [106]

4.2.3 Evaluation for electric drive system optimization

The different methods currently used for the investigation do not fulfill the requirements of this works because they are only based on the power densities and does not allow evaluating the dimensions of the converters. The case of the electric machine is easier because the current methods can be easily enhanced by considering the rotor excitation and the winding technology. For the power electronics however, the investigation of the integration is a more challenging topic which cannot be solved using only the power density. Hence, a new method is presented in the next section but this power density limits are used as reference to evaluate the validity of the results.

4.3 Method implementation

This section is divided into three parts, one for the inverter and one for the boost-converter as well as one for specific cases (48V applications, multiphase system and combined converters). Within these three parts, methods for each sub-component the construction algorithm are discussed before introducing the evaluation approach for the integration evaluation of the converter.

4.3.1 Modular inverter evaluation method

The inverter evaluation consists in two main simulation processes, a first one which evaluates the volume, the dimensions and the weight of each sub-component and a second one, which thanks to the developed algorithm allows evaluating the entire inverter volume. In this section, the method for each sub component is detailed before presenting the algorithm for the construction. Based on the current technologies and the volume distribution presented in [76], the following sub-components, sub-part and requirements of the inverter are considered: current sensors, control-board, cooling connectors, heatsink, housing, busbar, clearance and creepage distance, DC-side and AC-side connectors, X-capacitor (DC-link capacitor), Y-capacitor (common-mode and differential-mode filters), safety resistance and the power modules.

Current sensors:
The dimensions and the weight of the current sensors are extracted from datasheets of the supplier LEM [107] for automotive certified components. It results from the analysis of previous converter for automotive applications. Several sensors are considered in this work, one for each phase to ensure the controllability of the converter.

Control-board:
The dimensions of the control board are estimated based on datasheets from Infineon [108]. Two types of control board are considered: the module board and the converter board. The first one is for the control of each module while the second one supervises the entire converter.

Cooling connectors:
As for the current sensors, the dimensions and the weight are extracted from datasheet [109] and result from the analysis of previous converter. Two connectors are considered, one for the inlet and one for the outlet of the cooling system.

Heatsink:
The heatsink design (coolant path) is not investigated in details in this work but some considerations need to be done for its dimensions and weight. The dimensions are directly related to the converter architecture considered by the algorithm while the weight is estimated with the following assumption: 50% of the heatsink is used by the coolant and 50% by the solid heatsink fins itself. This assumption is done thanks to the analysis of previously designed component. The weight is then calculated using the equation (59), where $W_{heatsink}$ is the heatsink weight, $\rho_{heatsink}$ is the density in kg/dm³ of the heatsink material and $V_{heatsink}$ is the heatsink volume.

$$W_{heatsink} = 1/2 \cdot \rho_{heatsink} \cdot V_{heatsink} \quad (59)$$

Housing:
The housing thickness results from the measurement of previously designed converter. The housing is generally not smooth due to attachment and other requirements for its integration in the vehicle. In this work, the thickness is fixed and the converter is considered as smooth to avoid additional simulation effort.

Busbar:
The busbar dimensions are evaluated based on the current, which is conducted by the converter. Generally, the busbar is designed based on the continuous current and the cross section area of the busbar is directly proportional to it. In this work, the busbar is considered as rectangular and the adaptation is done based on the equation (60), where V_{bubsar} is the busbar volume, I the considered current and $V_{busbar/ref}$ the volume of the busbar for the current I_{ref}. A differentiation is done between the AC- and DC-side, where the following currents are respectively considered: continuous AC-current and continuous DC-current.

$$V_{busbar} = I/I_{ref} \cdot V_{busbar/ref} \quad (60)$$

Clearance and creepage distance:

The clearance and creepage are safety requirements which are calculated based on the corresponding norm [110]. The clearance is defined as shortest distance through the air between two conductive elements whereas the creepage is defined as shortest distance on the surface of an insulating material between two conductive elements. These distances need to be evaluated during the construction algorithm to ensure that the converter satisfies the safety norm for the applications.

DC-side and AC-side connectors:

The dimensions of the connectors are extracted from datasheet from suppliers for automotive certified components [112]. The DC-side connector is a 2-way connector whereas the AC-side connector is generally a 3-way connector.

X-capacitor (DC-link capacitor):

The X-capacitor or DC-link capacitor dimensions and weight are evaluated based on several criterions. First the current stress depicted in the equation (39) is used to calculate the required capacitance C_0, based on the switching frequency f_{switch} and the maximal required ripple voltage ΔU as shown in (61) and based on [113]. Then depending on the voltage level, different capacitor values are used. The volume and weight are then calculated based on the current stress and the required capacitance. For the case of the DC-link capacitor, only the required volume is calculated instead of the dimensions. As it can be seen in [76] and [114], the DC-link capacitor is generally designed specifically for the applications. Hence in this work, the following assumptions are done: the capacitor is implemented in such a way that it aims to optimize the remaining place in the converter to fill the available volume with the smallest dimensions as possible considering the entire converter based on capacitor datasheets [111].

$$C_0 = \frac{I_{Crms}}{2 \cdot f_{switch} \cdot \Delta U} \quad (61)$$

Y-capacitor (common-mode and differential-mode filters):

The topic of the common-mode and differential-mode filters is a challenging topic. More than the other sub-parts, it is outside the scope of the thesis and requires deep knowledge concerning the EMI (Electromagnetic Interference). Since the Y-capacitor cannot be estimated with simple methods based on global requirements, the following assumptions is done: the value of the capacitor is taken as constant and the voltage and current considerations are only done through the variation of the retained sub-components [111].

Safety resistance:

As its name implies, this resistance is designed based on safety requirements. Its function is to discharge the DC-link of the converter in case of failure. Considering the inverter structure in this work, the main energy storage system is the DC-link capacitor (C_0). The resistance aims thus to discharge it during the time t_0 to reach from the voltage U_{max} a voltage less or equal to U_0 (generally 60V) and the value of the resistance can therefore be calculated using the equations (62).

$$R = \frac{t_0}{\ln(U_{max}/U_0) \cdot C_0} \quad (62)$$

Power module:

The last sub-components to be estimated are the power modules. As defined previously, this chapter does not do any sub-component design. Hence the power modules are chosen among the power module form suppliers with automotive certification (Appendix 5). The dimensions and the weight are thus directly extracted from the datasheets of both two-pack and six-pack IGBT and Mosfet-module.

Evaluation approach and construction algorithm:

Based on the estimation of the sub-components and sub-parts, a construction algorithm is developed to fulfill the requirements depicted on Figure 84. The method used to evaluate the entire converter volume is shown on Figure 88. Based on the different requirements discussed in this section, the dimensions, weight and volume of all the sub-parts and sub-components are calculated to be used in the construction algorithm.

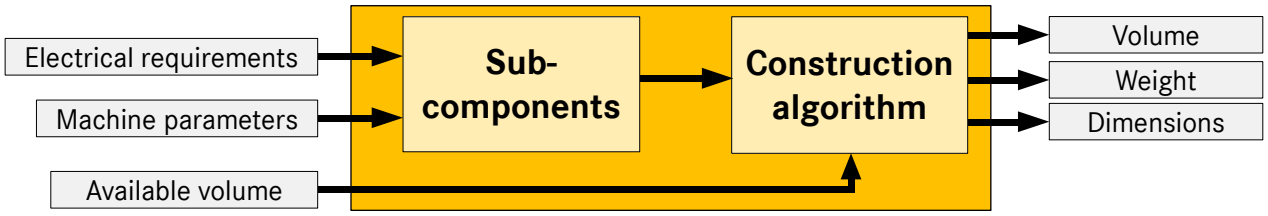

Figure 88: Evaluation approach for the inverter integration

Then using the safety requirements depicted by the clearance and creepage distance, each of them are arranged within the available volume using the following order: heatsink, connectors (DC, AC and cooling), current sensors, power module, control-board, Y-capacitors, discharge resistance and finally the DC-link capacitor.

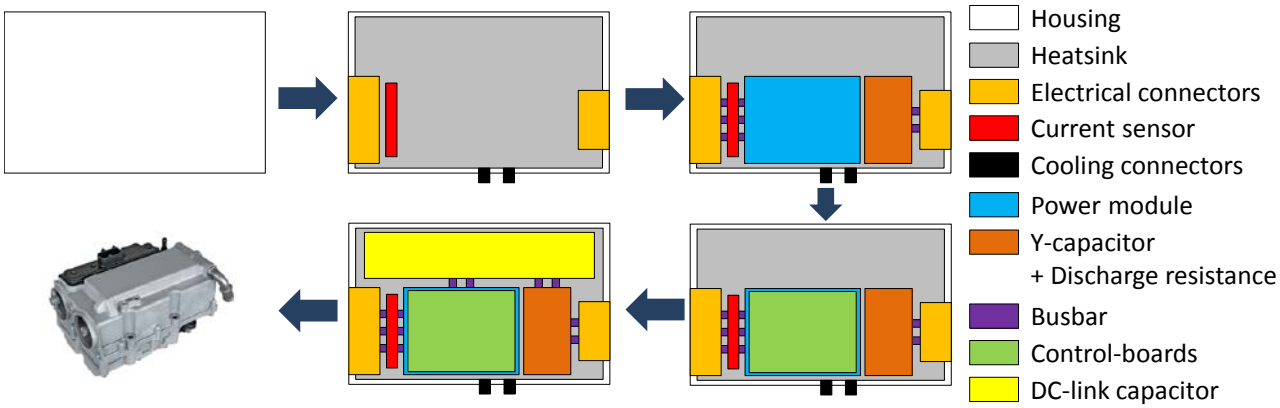

Figure 89: Construction algorithm for the inverter

Beside the construction algorithm, this work considers several assemblies for the inverter (see Figure 90). By considering several architectures, the potential of the results is increased because each assembly has its own potential depending on the application. Moreover, the several assemblies enhance the relevancy of the results because it enables to cover a wider range of different placement in the vehicle. These architectures are deduced from current assemblies of inverter from the automotive industry. After defining the structure of the inverter, the construction algorithm estimates the weight of each sub-component or sub-part. For the ones, where the values are extracted from datasheets, the values are summed while for the housing, the busbar and the heatsink, the weight is calculated using the density in kg/dm^3 of the considered material. Except the specific case of the heatsink, which are previously discussed, the other sub-component weights are estimated using the product of their volume and their density.

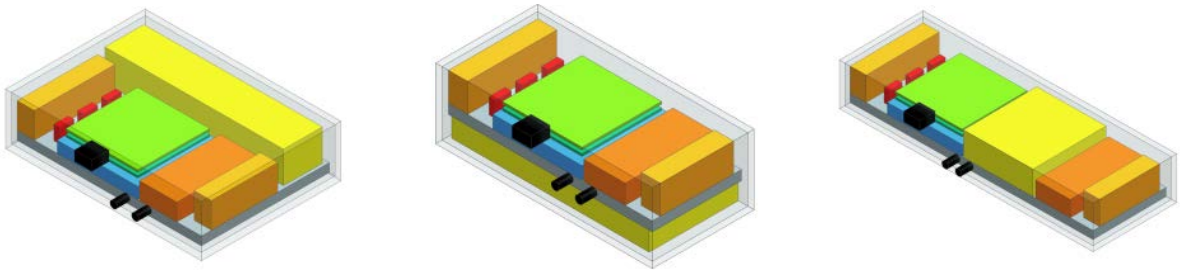

Figure 90: Architectures considered in this work

4.3.2 Modular boost-converter evaluation method

For the case of the boost-converter, the used method does not really differ from the inverter. The dimensions and the weight of each sub-component are estimated and then using a construction algorithm, the entire volume and weight are estimated. Except the input inductance, the other sub-component methods are the same as for the inverter. This portion is hence focused on the design methods for this sub-component and the construction algorithm of the boost-converter.

Input inductance:

The value of the input inductance is estimated based on ripple-current requirements (ΔI). Based on this value and on the maximal value of the duty ratio D_{max} of the boost-converter (63), the value of the inductance is calculated using the equation (64) by adapting the equations used for the ripple-current calculation in [85]. Using the calculated value, the inductance volume and weight are estimated based on parameters extracted from datasheet. The estimation considers two requirements: the inductance and the maximal current of the converter because during operating phases, the inductance is conducting the entire current.

$$D_{max} = 1 - \frac{\min(U_{batt})}{\max(U_{Dc})} \quad (63)$$

$$L = \frac{D_{max} \cdot \max(U_{Batt})}{\Delta I \cdot f_{switch}} \quad (64)$$

Construction algorithm:

As for the inverter, a construction algorithm is developed to estimate the dimensions and weight of boost-converter. The approach is the same as for the inverter and the main differences lie in the algorithm and the architecture. Two architectures are considered: in the first one, the components are lengthwise arranged while in the second one they are stacked. The algorithm is shown on Figure 91 for the lengthwise arrangement.

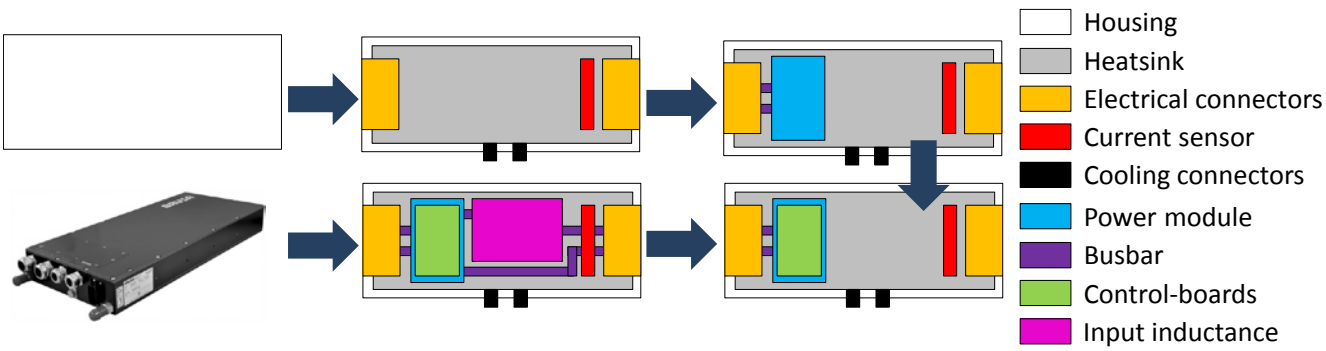

Figure 91: Construction algorithm and architectures for the boost converter

4.3.3 Special cases

Besides the two main methods shown in the previous sections some specific cases are considered here. These specific cases are deduced from components which are still under developments. In this work, three cases are considered: the first one concerns the adaptations of the inverter method for multiphase system, the second one is linked with the 48V-system topic and the third one is linked with the integration.

Multiphase inverter system:

For the purpose of estimating the volume of a multiphase inverter system, no new methods are developed but several hypotheses are considered. They concern the power modules, the connectors and the DC-link capacitor. Concerning the power modules, the semiconductors surface is considered as being the same as for a 3-phase converter. Because of the more complicated connections and due to the increased number of phases, the following hypothesis is done: the power modules are 10% bigger. For the case of the connectors, this work considers two solutions: an inverter which supplies two electric machines or a multiphase electric machine. The first solution considers two connectors while the second one considers the following hypothesis: the frame of the connector for the fixation is using 25% of the width, then when 6 instead of 3 connectors are required, the connector is 75% wider. Finally for the DC-link capacitor, the work in [115] shows that the capacitor size could be reduced by using multiphase solutions. This size is however linked with the control method of the inverter. This topic being outside of the scope of this work, the influence of the DC-link capacitor is neglected.

48V-system:
The case of 48V-system is investigated thanks to the power modules and the DC-link capacitor. The power modules cannot be found using published information. Hence the modules dimensions are based on internally investigated components. Concerning the DC-link capacitor, the adaptation is done through the material used for the estimation of the weight and the volume. The material is adapted to the applications and especially to the voltage level based on [76].

Integration issues:
Depending on the concepts, several integration issues can occur. The first one concerns the integration of multiple converters in a single housing. For this purpose, the available volume is divided in several parts which are allocated to each component. Moreover the wall thickness is subtracted to the available volume and the converter volumes are estimated considering no housing. The second integration issues concerns the converters without connectors (screwed or directly connected solutions). In this case, the external length of the connectors is not considered but only the internal one where the connections (cables or busbar for example) is considered. Finally the final issue concerns the case of inverter with integrated HV/LV-converter. To solve this problem, the require dimensions for this converter are subtracted to the available volume in order to apply the normal method but for a reduced volume.

4.4 Validation

After having defined the method for the weight and volume estimation, this section presents the results of the implementation in Matlab/Simulink. As already discussed in the previous section, some hypotheses are done concerning the architecture and the characteristics of the converters. This section is validated in three parts: first the validation of the inverter is presented with several comparisons, then the validation of the boost-converter and finally the validation of 48V inverter.

4.4.1 Inverter validation

Except the multi-machine drivetrains, all the current hybrid drivetrain solutions are using a single inverter and their requirements are defined in norms and standards. This work considers the following norm and standard: VDA LV123 [116] and ISO6469-3 [117]. The inverter validation presented in this section is done using automotive components.

		Length [mm]	Width [mm]	Height [mm]	Volume [dm³]	Weight [kg]
Component 1	**Ref.**	250	164	157	6.4	8.1
	Sim.	236	158	150	5.6	8.2
Component 2	**Ref.**	230	165	150	5.7	7.6
	Sim.	237	163	150	5.8	8.5
Component 3	**Ref.**	240	154	135	5.0	7.5
	Sim.	236	150	126	4.5	7.6

Table 18: Comparison of simulation results with automotive components from [119] and [120]

All the results presented in this table show deviation under 10% except for the volume of the component 1 (12.5%) and the weight of the component 2 (11.8%). Considering the approximations done for the implementation of the method, these results show that the method can accurately estimate the dimensions and the weight of different inverters.

4.4.2 Boost-converter validation

The validation of the boost-converter method is more critical because except the BDC546 from the firm Brusa [96], no stand-alone converter is available. The example of the Toyota [24] could not be used because it is a highly integrated solution where for example the power module design combines the semiconductors of all three converters in the housing. However, the example from the firm Brusa is using the soft-switching technology and the exact converter topology is not known. As detailed in [8], this control-method requires a commutation-transformer and a third voltage level. These specificities are not considered in this work and the comparison is done under the following hypothesis: no methods are changed and therefore the inputs are used without adaptations in the tool.

		Length [mm]	Width [mm]	Height [mm]	Weight [kg]	Power density [kVA/dm³]
BDC546	Ref.	684	280	80	25.2	12
	Sim.	555.4	171.4	64.3	8.0	29.5

Table 19: Comparison of simulation results with automotive components for the boost-converter

All the results are showing really high deviations, the difference in the converter topology is not negligible. Due to the lack of reference components to evaluate the relevancy, the values in [106] are taken as reference. The power density of all the converter types reaches a limit around 45 kVA/dm³. The BDC546 should theoretically provide a power around 180kW. The simulated converter based on its requirements achieves a power density of 29.5 kVA/dm³ which is under the limit from [106]. Despite the high deviation, the results seem to be consistent because they are clearly under the technological limits and due to the topology difference between the converter considered in this work and the converter developed by the firm Brusa.

4.4.3 48V-inverter validation

As explained previously, the 48V-systems are still under development and no real reference is available to perform a validation, as in [105] where no information about the dimensions is provided. Moreover the 48V-system due to the legislation frame [118] is generally integrated in a single housing with the electric machine [43]. Hence, the same approach is used as for the boost-converter: 48V systems are simulated for the phase-current values presented in Table 20 and then the power density in kVA/dm³ as in [106] is taken as reference for the comparison. The apparent power calculation used for the comparison is expressed in (65). The method is therefore also applied on the components from [121] and [122] by considering a nominal voltage of 325V with a modulation factor of $1/(\sqrt{2}\sqrt{3})$. This modulation factor is a theoretical value considering the following parameters: $1/\sqrt{2}$ for the transformation in rms value, $1/\sqrt{3}$ for the phase-phase to phase-neutral value of the voltage, 0.9 for the duty cycle for the PWM.

$$S_{\mathrm{AC}} = 3 \cdot \frac{1}{\sqrt{2}\sqrt{3}} \cdot 0.9 \cdot U_{\mathrm{DC}} \cdot I_{\mathrm{AC}} \quad (65)$$

	Reference	System 1	System 2	System 3	System 4	[121]	[122]
Peak current [Arms]		600	500	400	300	370	400
Power density [kVA/dm³]	~45	9.81	8.73	7.65	6.21	9.23	14.13

Table 20: Comparison of simulation results with automotive components for 48V-inverter

When analyzing the results, it can be seen that none of the simulated converter exceed the power density limits from [106] and that they are showing similar values as already produced components for high voltage applications. Despite no real reference for the considered converter and its voltage level, the method is showing promising results without any inconsistency.

4.5 Contribution for system evaluation

The integration evaluation method presented in this section is developed in such a way that all the voltage and current level can be evaluated. Considering the currently available power modules for automotive applications, the contribution of the method is shown on Figure 92, which presents the results for a maximal voltage between 150 and 850V. When analyzing the results, it appears that the main dependency of the inverter volume is linked with the voltage. Considering the volume distribution in [76], this observation is validated by the dependency of the creepage and clearance distance on the voltage (air accounts for around 50% of the converter volume) and by the dependency of the DC-link capacitor volume also on the voltage (passive elements account for around 20% of the converter volume). The discontinuities in the inverter volume are due to the capacitor specifications: the suppliers do not develop components for a specific voltage value but for pre-defined ranges. Each discontinuity represents thus a change in the capacitor rated voltage and thus a decrease of its capacitance per volume.

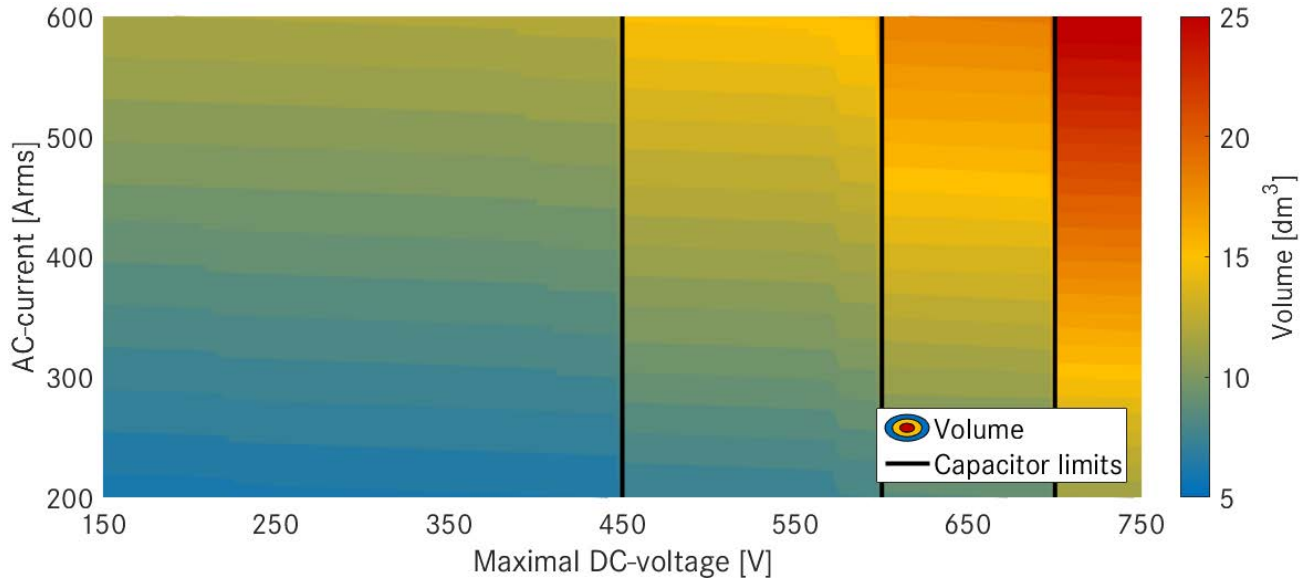

Figure 92: Influence of the voltage and current level on the inverter volume

To do a more detailed comparison, a reference system is considered with a maximal voltage of 450V and a current of 300Arms is taken as reference to analyze the results more deeply.

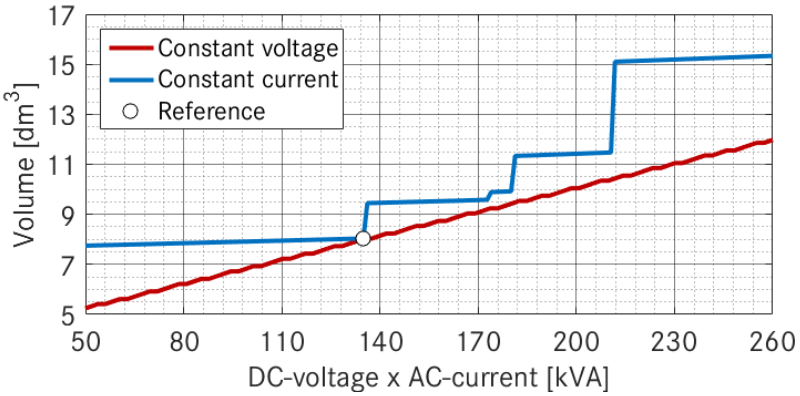

Figure 93: Inverter volume dependency on the current and the voltage

The observations are really deviating from the ones for the losses: a maximal voltage around 450V seems to be the best solution for every power classes considering the capacitor technology investigated here. Considering the previous defined system (450V 300Arms) as reference, the best solution when evaluating the volume is always to variate the current level. The discontinuities are related to the capacitor technology, which also explained the results concerning the voltage level. The 450V systems exploit the full potential of the capacitor technology. Hence either a voltage reduction or voltage increase do not lead to any density improvement.

5 Chapter conclusion

In this chapter, the solutions for the modeling of power electronics are discussed, analyzed and implemented in a simulation environment. Both the inverter and the boost-converter are considered and validated using automotive components. Contrary to the electric machine, for which compromises are required to thermally model the component, solutions are found for each modeling or investigations to work at the system level. Moreover, the contributions of the modeling developed in this work are already shown since a completely new method is developed to estimate the entire volume of the two types of converters and the method for the loss modeling is enhanced with a new interpolation approach. The method presented in this chapter for the loss modeling is based on well-known approaches but widens the parameter range. The loss model developed in this work enables to compare different inverter topologies and boost-converters for different voltage and current levels as well as for different values of the temperatures (diode and transistor) and different semiconductor technologies (IGBT and Mosfet). The thermal model

of the power electronics is depicting the behavior as “black-box” since the temperature can be directly calculated based on the coolant properties and the losses. Using the values extracted from the datasheet, such an approach can be developed and despite some approximations to implement the coolant flow dependency, the validation of the model based on real measurements shows promising results. Concerning the integration, the developed method can consider a wide parameter range thanks to the construction algorithm and the sub-components evaluation methods. The validation for both the inverter and the boost-converter are presented and the method enables to cover a wide range of applications by variating the integration (available volume) and the power (voltage and current). Finally, the contributions of this work are already shown by analyzing the influence of the voltage and current level on the inverter volume and losses. The first investigation shows the relationships between the losses and the voltage level while the second investigation enables to have an overview of how the current and the voltage influence the entire converter volume. Similar to the electric machine, this chapter shows the contribution of a global system approach. For each modeling or investigation, a solution is found to model in a suitable way the components in order to address the challenges described in the first chapter. The differentiation between the suitable modeling and the best modeling is the cornerstone of this work because a global approach needs to find the best compromise between the accuracy, the parameter variations and the possibility to investigate the integration.

Chapter 4: Modeling battery for hybrid electrical drivetrain

The focus of this chapter is on the determination of a suitable modeling approach for the battery. As for the electric machine and the power electronics, this chapter begins with explanations about the structure, the working principle and the losses types. Then previous works on the topics are considered and analyzed for each modeling or method. The suitable solutions are then implemented and validated based on automotive components. Finally, the chapter shows the contribution of the developed methods and modeling.

1 Battery structure, working principle and losses

Before analyzing previous works and implementing the modelings, this section presents the different structures of batteries, their working principle as well as the losses. As previously defined, this work investigates only the lithium-based technology without consideration concerning the cathode and anode technology.

1.1 Battery structure

The main difference concerning the battery structure lies in the configuration of the cells. They can be arranged in series or in parallel. A growing number of cells in series increases the voltage while a growing number of cells in parallel increases the current capability. Both solutions lead to an increase of the energy and the power. The principle of the connection between the cells is shown on Figure 94 for an NpMs configuration where M is the number of cells in series (s) and N is the number of cells in parallel (p) based on the nomenclature from [123]. The initial 48V applications are shown to use the same cells as high voltage applications and therefore does not necessarily require an additional modeling approach or even additional cell parameters.

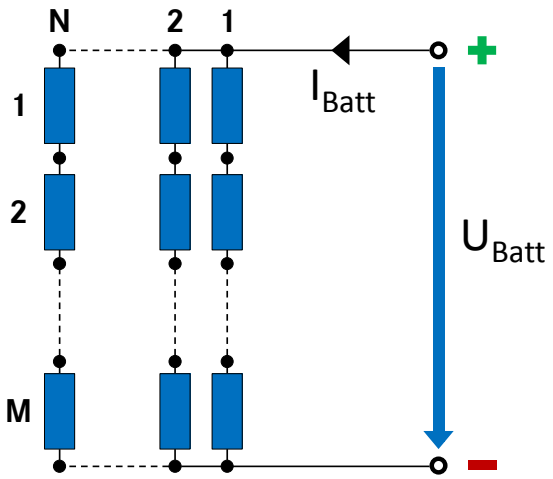

Figure 94: Battery structure for an NpMs configuration

Volume distribution and battery assembly

Beside the cell configuration, the battery assembly needs to be considered too. As presented in [22], the ratio between the cells and the entire components are around 50% for the volume and 65% for the weight. To evaluate the entire component, the assemblies and its influence parameters (cell configuration, cooling system and voltage level) are investigated. As discussed previously for the power electronics, the voltage level influences directly the clearance and creepage distance and thus the resulting assembly. Based on these safety requirements, the cell configuration and the cooling system, the battery assembly could be defined. Currently three types of cooling system are used within the automotive industry: passive air cooling, active air cooling and liquid cooling. Passive air cooling systems are generally used for low power or 12V applications while the active air or liquid cooling can be found respectively in the Toyota Prius [10] and the Mercedes e-Class Hybrid [23]. In this work, only solutions using active liquid cooling are investigated as in [123] and [124]. The assemblies presented on the following figure and in Appendix 7 are showing the challenges and the requirements for this type of cooling and its impact on the structure.

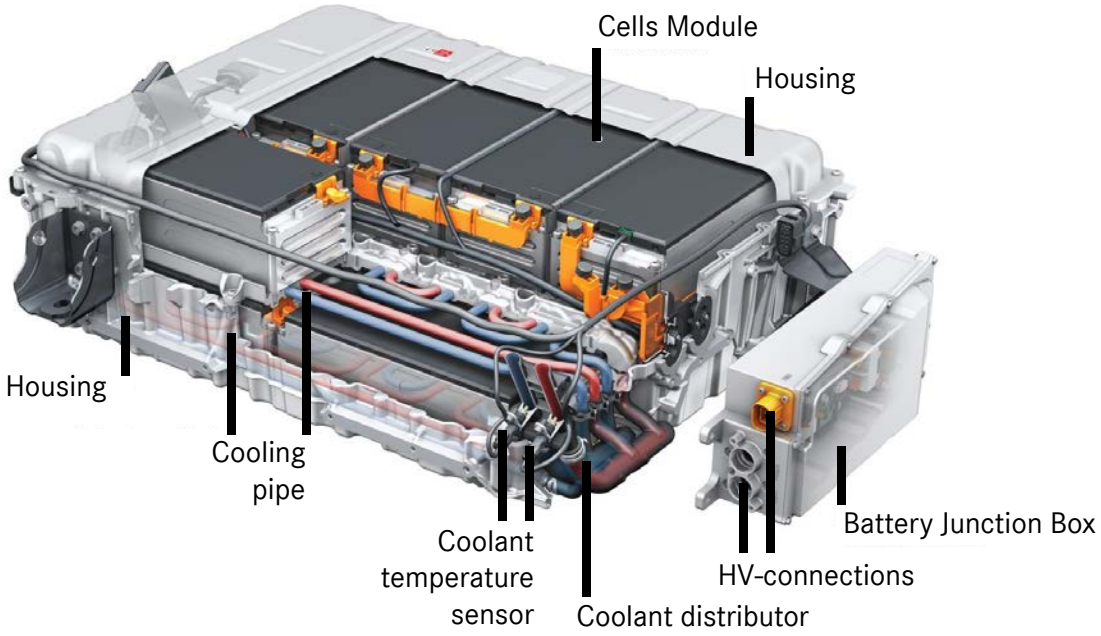

Figure 95: Battery assembly for high voltage applications from [123]

1.2 Working principle and losses

When investigating battery, the following convention is generally considered: a positive/negative current means that the battery is being charged/discharged (respectively generator and motor mode for the inverter and the electric machine) as shown on Figure 94. The working principle of a rechargeable battery is explained generally based on [8], more detailed information can be found in [125]. Assuming a perfect balancing between all the cells in the battery, the principle of the entire component can be represented using the properties of one cell. Each cell is composed of essentially four parts: a positive electrode (cathode), a negative electrode (anode) with an electrolyte and separator between them as shown on Figure 96. The cathode is generally a metal oxide and the anode consists of porous carbon (graphite). During discharging phase, the lithium-ions flow from the anode to the cathode through the electrolyte and the separator while during charging phase the direction is reversed and the ions flow from the cathode to the anode as shown on the following figure.

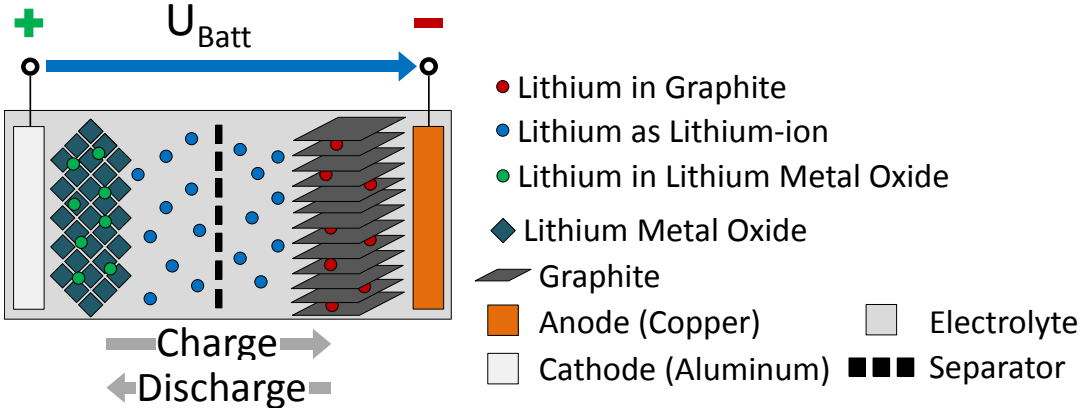

Figure 96: Cell working principle adapted from [8]

The losses are principally due to the internal resistance (ohmic losses) of the cell which produces heat. When no load is applied, the battery has a self-discharge rate which is however neglected in this work due to the scope of the investigation (the components are optimized based on driving requirements). Beside the losses in the cells, the entire components efficiency is influenced by the busbar losses (ohmic losses) between the cells and the connectors. Considering these two sources of losses the energetic behavior of the components is presented on Figure 97.

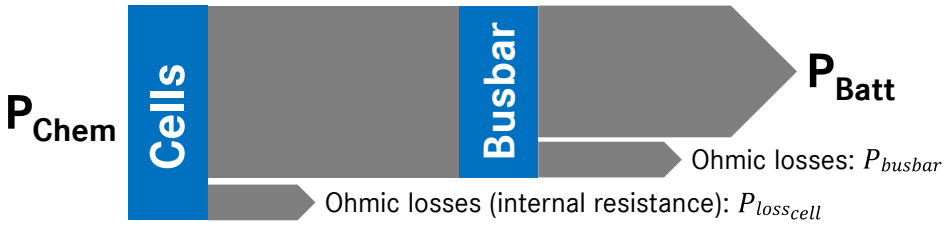

Figure 97: Sankey diagram of the battery as considered in this work

2 Component behavior modeling

The first modeling considers the component behavior. The lithium-ion cells are electrochemical sub-components and their behavior can be really deep modelled when considering the influences from all sub-parts (electrode, lithium-plating, separator, electrolyte or ageing as described in [125]). The aim of this work is however to model the components as "black-box" and therefore to have a reliable model which investigates only the relevant parameters to address the challenges of this work. This section begins by defining the modeling approach, then previous works are analyzed and finally the chosen solution is implemented and validated.

2.1 Modeling approach

The modeling approach of the battery is defined to have a direct relationship between the inputs and the outputs. The modeling approach aims thus to depict the voltage variations, the losses and the efficiency of the battery based on the battery current, the number of cells in both series and parallel as well as the cell temperature. The resulting approach is presented on Figure 98.

Figure 98: Approach for the modeling of the battery behavior

2.2 Previous works and investigation level influence

When determining the suitable approach for a modeling, the analysis of previous on the topics plays a preponderant role. In this section, the current literature on battery modeling is discussed and presented with an increasing level of simplification to identify the challenges and find a relevant solution for a global approach.

2.2.1 Physical models

In [125], an overview of the possible approach to model battery cells is presented by analyzing the different levels of investigation. Deep levels of investigation aim to investigate both the behavior and the physical processes proceeding during cell operation. They enable to depict with a high accuracy the behavior of the cells depending on the state-of-charge (SOC), the state-of-health (SOH) and the applied load. It requires a deep analysis of several phenomena (charge transfer, ion transport, electron transport, cell ageing and porous electrodes for transport) but it is however out of the scope of this thesis and is not discussed in details because they are generally not coupled with a global system approach and are only used to investigate the design or the ageing processes of the cells.

2.2.2 Circuit based and analytic approaches

The circuit based and analytic approaches are solutions which could be considered as component level investigations as well as system level investigation. They extend generally from detailed investigations with investigation of parameters such as the porosity effect, up to superficial model where only the load and state-of-charge dependency are considered. The investigations where the physical effect are considered as in [126] are also

out of the scope of the thesis because it requires to know the exact structure of the cell which is investigated and the influence parameters of this phenomena (equivalent circuit 1). Other alternatives are based on equivalent RC-circuit (resistance/capacitor) which are used to depict the behavior of the cell [127] (equivalent circuits 2 and 3). They require however doing an impedance spectroscopy of the cell to characterize the dynamic behavior of the voltage and the losses in the cell as shown in [125] and [128]. The work in [127] summarizes all the possible external circuit models and shows the advantages of the drawbacks of each of them. The RC-circuit based solutions are the best solutions but is a really time-consuming solution. It is even more time-consuming when considering that the cell needs to be measured and analyzed even if the type of cell is never used in any system. The works introduces also the basis resistive model, where the load-dependency is modelled using only a resistive element (equivalent circuit 4) and where the SOC-dependency can be introduced using SOC-dependent parameters for the open-circuit voltage (OCV) and the resistive element. Finally the differentiation between circuit based and analytic approaches lies in the implementation of the model. The first one is implemented using the equivalent blocks in simulation environment as Simulink or Simscape [129] while the second one can be used in any calculation tools by using the circuit equations (similar to the circuit based model of electric machines).

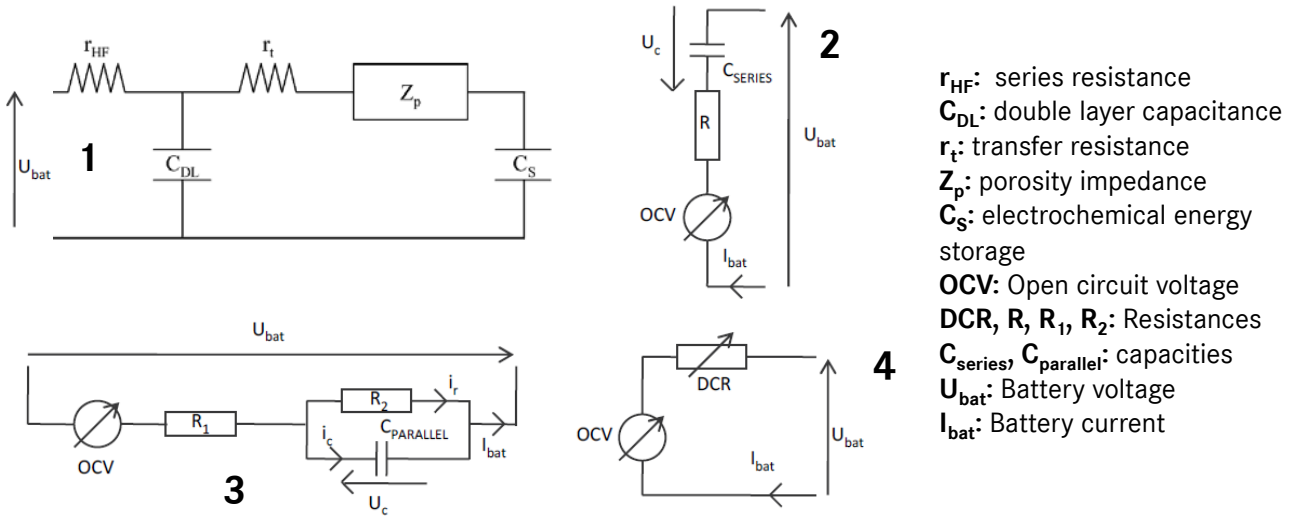

Figure 99: Possible equivalent circuits for the modeling of lithium-ion batteries from [126] and [127]

2.2.3 Higher level and evaluation for electric drive system optimization

One of the main objectives, when modeling the battery is to depict the SOC and load dependent behavior of the voltage in the battery. The loss modeling is not significant for the evaluation of the suitability of the modeling because they are directly linked with the load behavior because the losses are equal to the product of the voltage drop and the current and can also be stored as data maps. The voltage behavior is however an important parameters for the evaluation. The circuit based and analytic approaches are fulfilling the main requirements concerning the simulation effort, the parameter range and the accuracy. In the case of the cells, there is however another important parameter to consider: the highly accurate models require the cell to be measured and analyzed. This complete analysis which is required is incompatible with the considered development stage in this work because the work aims to investigate the current trend and it cannot afford to require all the current available cells to be measured. Hence a simple circuit based approach with only the resistive effect is considered for the modeling of the voltage behavior.

	Extended RC-circuit based model	RC-circuit based model	Resistive model	Data maps based model
Accuraccy	+ +	+	o	-
Simulation effort	- -	-	+	+
Parameter range	✓	✓	✓	X

Table 21: Comparison of approaches for the behavior modeling of battery

2.3 Modeling implementation

This section discusses the topic of the modeling implementation of the lithium-ion batteries. The section is divided in two parts, first the model is presented and then the modeling approach to consider all the parameters is shown.

2.3.1 Circuit based model

In this sub-section the model and the different dependencies are presented. As previously explained, the main aims of the model are to describe the SOC, the load and the temperature dependency of the system as well as the influence of the current direction. For this purpose, a resistive model is chosen. The load dependency is depicted by the resistive element while the parameters variations enable to consider both the temperature and SOC-dependency but also the influence of the current direction. The principle of the model is shown on the next figure.

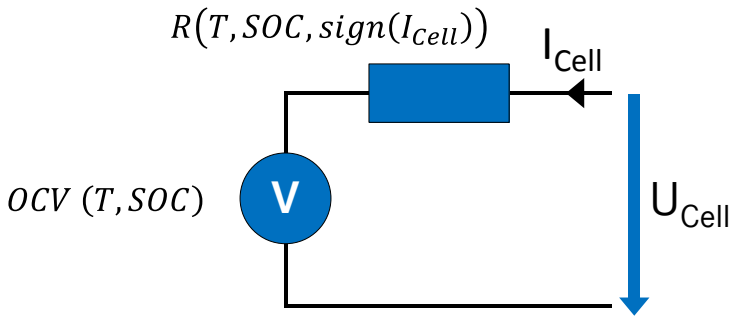

Figure 100: Battery model with SOC and load dependency

This solution, based on [127], is the most modular one because it does not require deep investigations of the cell to provide a first estimation of its behavior. The data are generally coming for the first cell characterization of the cell (done by the supplier) or from the design process (estimated values based on the cell design). The resistance is dependent on the cell temperature, the state-of charge and the current direction while the OCV is only dependent on the temperature and the SOC. The resistance is theoretically also dependent on the duration of the charge of discharge effect, it is however not considered in this modeling approach due to available data during the early development stage, the scope as well as the methods for the investigations. The voltage and loss behaviors in the cells can thus be written as follows.

$$U_{Cell} = OCV\ (T, SOC) + R(T, SOC, sign(I_{Cell})) \cdot I_{Cell} \quad (66)$$

$$P_{loss_{cell}} = R(T, SOC, sign(I_{Cell})) \cdot I_{Cell}^2 \quad (67)$$

Considering the convention used on Figure 100, a discharge (motor load) implies a negative current and a charge (generator mode) implies a positive current which correspond to the voltage-drop and the voltage-rise generally observed. The SOC and temperature dependency is introduced as data matrix while the current sign dependency is introduced using a switch between the two mode.

2.3.2 Modeling approach

The approach consists in several steps. First, the requested current enables to actualize the actual SOC, based on this SOC calculation the parameters for the voltage and loss behavior are interpolated using the maps and finally the battery voltage and the losses are calculated for the current boundary conditions of the battery. The approach described here considers however only one cell, the rest of this sub-section extend this modeling approach for the case of the entire battery system with s cells in series and p cells in parallel. The entire modeling approach is summarized on Figure 101 and then explained in details with the following assumptions: the initial SOC and the battery capacity are not linked with an interface and are not design parameters for the system evaluation. They are therefore considered as internal parameters of the cell and not included in the inputs.

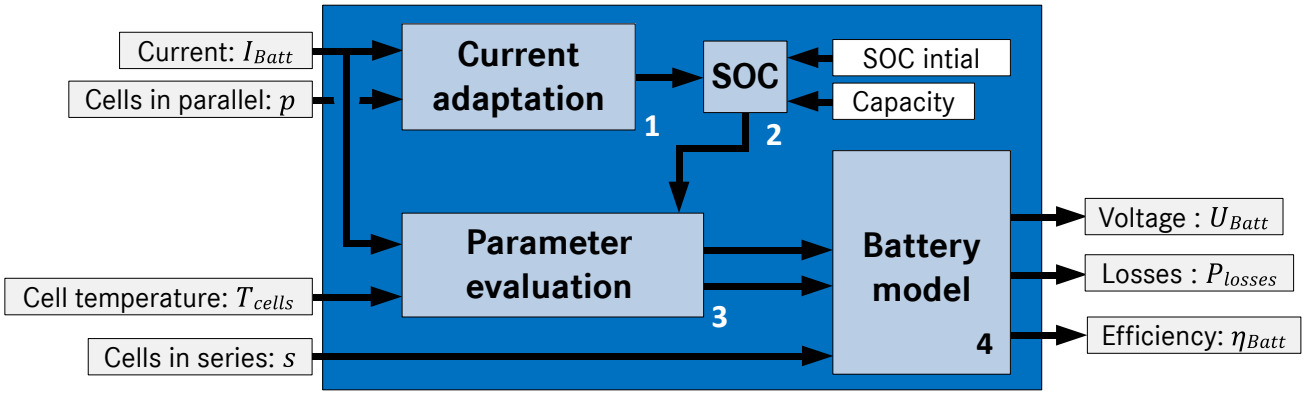

Figure 101: Modeling approach for the entire battery system

Current adaptation (1):

Before calculating the SOC, the current needs to be adapted based on the number of cells in parallel. In the case of the entire battery, the current in each cell and thus the voltage drop varies depending on the number of cells in parallel. For this purpose, the current is adapted considering a perfect balancing in all the cells as described by the following equation.

$$I_{Cell} = \frac{I_{Batt}}{N} \quad (68)$$

SOC calculation (2):

Since the current is adapted, the SOC can be calculated using the following approach: the current is integrated with the time, from which it results in an equivalent capacity (Cap_{equi}). This capacity is normalized with the cell capacity and then added to the initial SOC ($SOC(t_i)$). A negative current (motor mode) results in a decrease of the SOC and a positive current (generator mode) in an increase, which corresponds to the battery behavior. The calculation is summarized then by the following equations when the factor 1/3600 is introduced to convert the calculated equivalent capacity from As in Ah.

$$Cap_{equi}(t) = \int I_{Cell}(t).dt \quad (69)$$

$$SOC_{equi}(t) = \frac{Cap_{equi}(t)}{3600 \cdot Cap_{cell}} \quad (70)$$

$$SOC(t) = SOC(t_i) + SOC_{equi}(t) \quad (71)$$

Parameter evaluation (3):

Based on the calculated SOC, the current sign and the temperature in the cells, the parameters are evaluated. The evaluation is done using data matrix, which are dependent on the SOC and the temperature. The current sign dependency is implemented using a switch. The interpolation of the parameter is linear within and outside of the range as explained previously for the semiconductors parameters.

Voltage and loss behavior (4):

With all the available parameters, the battery voltage is calculated using the previously presented model with one equation for the voltage and one for the losses. The calculated values are for only one cell and therefore the voltage need to be multiplied by the number of cells in series as in (72) and (73). The losses can be considered for only one cell since the assumption of a perfect cell balancing is considered.

$$U_{Cell} = OCV\ (T, SOC) + R(T, SOC, sign(I_{Cell})) \cdot I_{Cell} \quad (72)$$

$$U_{Batt} = s \cdot U_{Cell} \quad (73)$$

$$P_{Loss/Cell} = R\left(T, SOC, sign(I_{Cell})\right) \cdot I_{Cell}^2 \quad (74)$$

Beside the cell behavior, this work considers also the influence of the busbar in the system. More than the losses, the additional voltage-drop need to be considered. The method used is the same as for the power electronics and is not detailed in this section. As explained later for the volume and weight estimation, two types of busbar are considered the one from the module, and the one from the system. Hence the voltage in the battery system can be expressed using (75) and (76).

$$U_{module} = U_{cell} - R_{busbar-module} \cdot I_{cell} \quad (75)$$

$$U_{System} = s \cdot U_{module} - R_{busbar-system} \cdot I_{Batt} \quad (76)$$

2.4 Validation

The validation presented in this part is divided in two parts, first the retained solution is compared with measurements and then the retained solution is compared with other reference model (circuit based models with RC-circuits).

2.4.1 Cell modeling validation

In this case, the measurements are performed on a single cell. The validation is performed by giving the same current and temperature profile and by evaluating the voltage behavior. Since the losses are in the considered modeling approach directly proportional with the voltage drop or rise, the validation of the voltage behavior also validates the losses behavior. For this purpose the approach on Figure 102 is used.

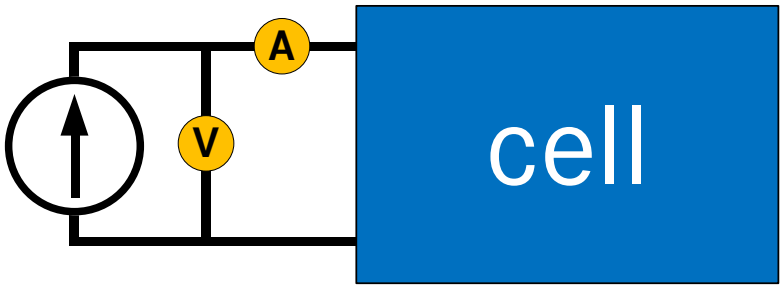

Figure 102: Measurement approach for the cell behavior validation

The results on Figure 103 show a low deviation (under 5%) and a high correlation (97.65%). The highest deviation is reached in the quasi-static area where the only resistive model should show the highest accuracy since it represents the static voltage drop in the cells. However considering the measuring system accuracy and the assumptions done for the model, the simulation results show a high level of accuracy

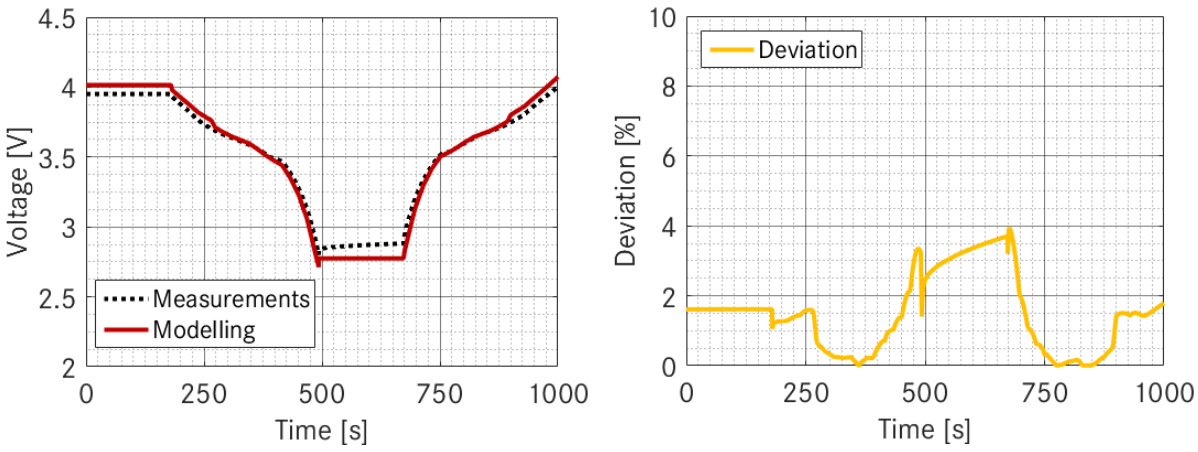

Figure 103: Comparison between simulation and measurements for the cell voltage behavior

2.4.2 Modeling comparison

Beside the absolute validation of the chosen modeling approach, a comparison with the other circuit based approaches is performed to show the suitability of the resistive model for system evaluations. To perform a fair comparison, the required power is given as input and the current is calculated with a voltage feedback loop. As it can be seen in [130], the number of RC-circuit influence the accuracy as well as the simulation and thus it is interesting to compare the resistive model with the RC-circuit based models for different numbers of RC-circuit. The model with two RC-circuits (Figure 104) and a series resistance is taken as reference to evaluate the performance of different modeling approaches.

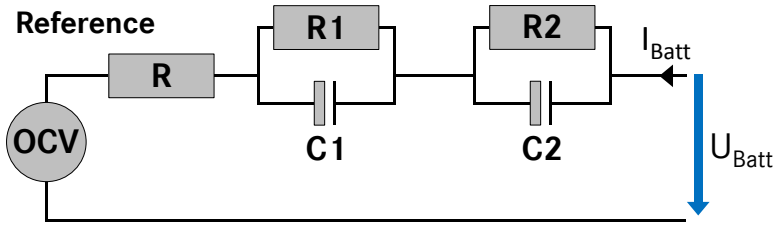

Figure 104: Reference circuit for the battery modeling comparison

The reference is compared with a system without RC-circuit (R), with only the first RC-circuit (R1C1) and with only the second RC-circuit (R2C2), which are shown on Figure 105. All the results presented on Figure 106 are deviations relative to the reference circuit presented on Figure 104 for a given driving cycle.

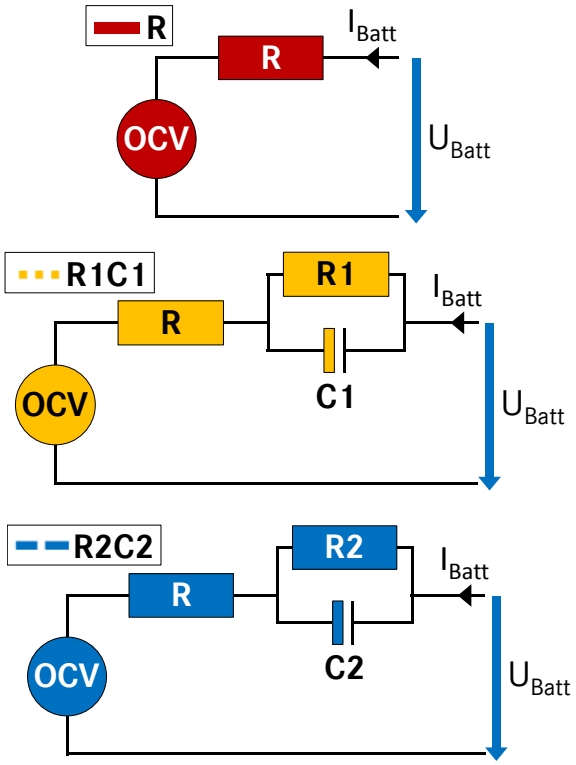

Figure 105: Investigated circuit for the battery modeling comparison

As it could have been expected, the resistive model is showing the highest deviations. The deviations are however most of the time under 10% for the voltage and always under 1.5% for the SOC. The main contribution for the modeling lies in the addition of the R2C2-circuit. As shown in [130], the addition of RC-circuits only refines with a relatively low contribution the modeling but increases the simulation effort. Considering the results presented here, it is considered that the resistive model is suitable for a global system approach because despite its simplicity, it fulfills all the requirements concerning the SOC and load dependency for the voltage and the loss behavior.

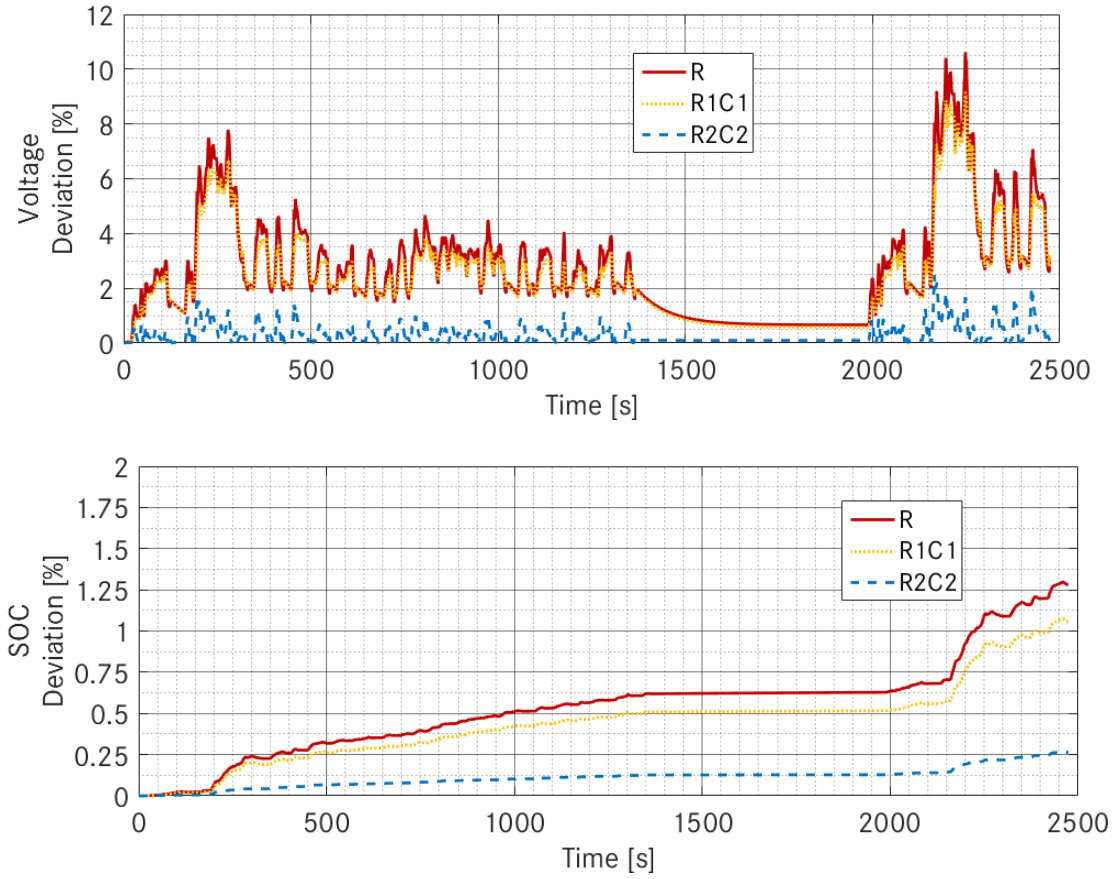

Figure 106: Comparison of the different circuit based models for the voltage (top) and the state-of-charge (bottom)

2.5 Contribution for system evaluation

The contribution of the component behavior modeling cannot be shown directly. Its main influence can only be shown when considering the entire system where the variations of the voltage influence the global behavior of the system (electric machine, power electronics and battery). Indeed contrary to previous works, where the electric machine or the power electronics are optimized individually ([20] and [55]), in this work the components are optimized as an entity and therefore the contribution can only be identified when considering the entire system. A first overview is given on Figure 107 where the voltage variations for a given current profile are shown.

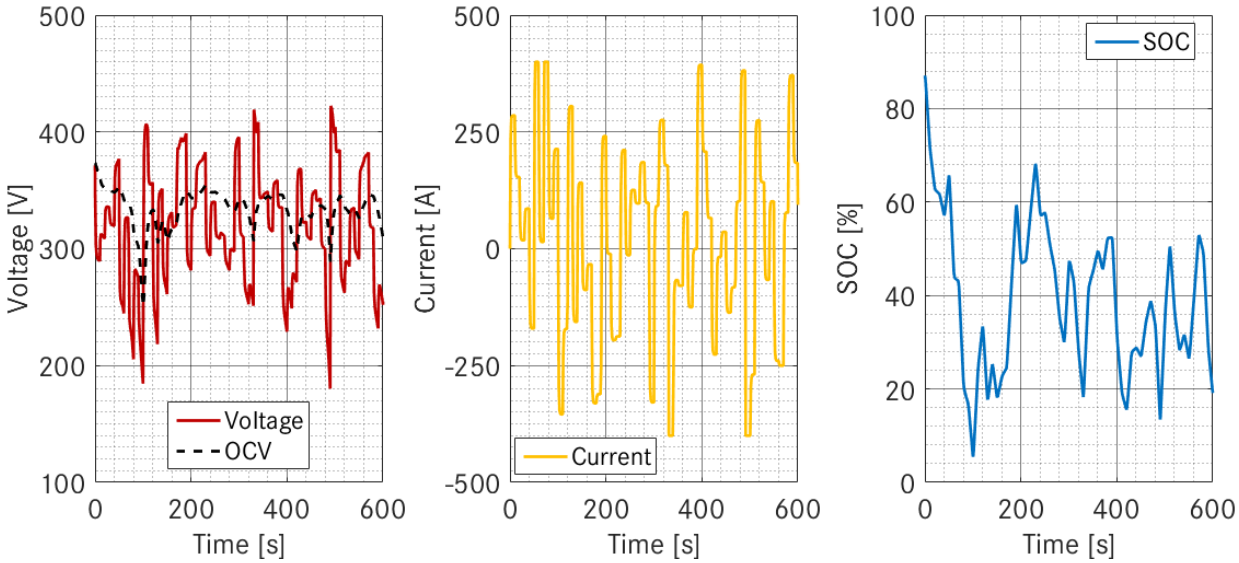

Figure 107: Voltage variations of a battery system using the developed method

As it can be seen the variations of the voltage have a wide amplitude and cannot be neglected when considering the influence of the voltage on the machine performance and on the power electronics losses. It shows that considering a constant voltage for the design is only an initial approximation for component design contrary to system optimization where the variations need to be considered due to the interactions between the components.

3 Thermal modeling

This work considers a thermal modeling of the battery for two reasons: first to enhance the component behavior modeling by adapting the parameters with the temperature and then to estimate the limits of the battery. In this section, the modeling approach is introduced before discussing previous work. Then the modeling implementation is presented and finally the approach is validated based on automotive components measurements.

3.1 Modeling approach

The thermal modeling aims to depict the temperature behavior based on the losses in the battery and the cooling properties. For this purpose, the approach described on Figure 108 is retained where the inputs are the losses and the cooling properties and the output is the cell temperature. As for the electric machine and the power electronics, the cooling properties (coolant flow and temperature) are not investigated in this work and they are defined during the drivetrain design but are considered because the same battery can be used in several drivetrains. The thermal path is dependent on the battery structure but only one modeling approach is considered. Hence the thermal path dependency is investigated by variating the parameters of the model.

Figure 108: Thermal modeling approach for the battery

3.2 Previous works and investigation level influence

The thermal behavior is a challenging topic to model because depending on the considered level of investigation, it can extend from detailed investigations up to really superficial ones. To find the suitable solution to model the thermal behavior of the battery, modeling approach and previous works are discussed.

3.2.1 Finite element analysis

In many areas, the finite-element analysis is used for detailed and accurate investigation and the case of battery is not an exception. The finite element can be used to deeply model the cell as in [131] as well as the entire battery system as in [132]. In both works, the accuracy is really high but the investigations are outside the scope of this work. In [131], only the cell is investigated for a defined structure with the focus on the cell design while in in [132], the entire system/module is investigated but the focus is set on the evaluation of an already designed system. These investigations require having detailed informations about the cell structure and its sub-parts.

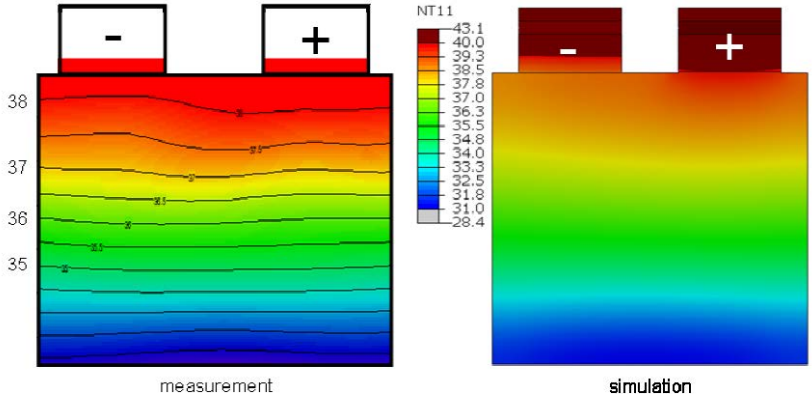

Figure 109: Thermal modeling of cells using FE with Abaqus [132]

3.2.2 Nodal and analytic approaches

The thermal analysis of the battery system is comparable with the one for power electronics because there is only one loss source in the system (the cells) as show on Figure 110. Depending on the assumptions, the cells can be investigated using nodal approach or state space model. They are both based on a network between the cells and the cooling. Beside the modeling approaches (description with block or with equations), the investigations also differ by the considered sub-parts. It can be a thermal investigation where only one cell is considered and thus the thermal balancing is considered as perfect as in [133] or it can consider the variation of the coolant between the cells depending on their position. Both the methods (nodal model or state space model) show a good accuracy and seem suitable for a global system approach.

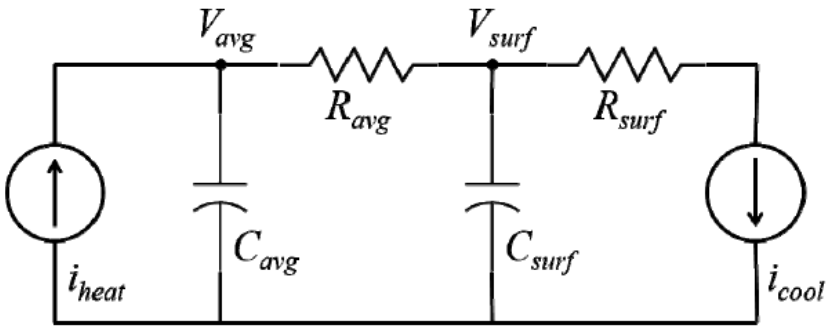

Figure 110: Nodal approach for the thermal modeling of battery system [133]

3.2.3 Higher level and evaluation for electric drive system optimization

Similar to the power electronics, the only solution at higher level is the use of only a thermal resistance and therefore to neglect the dynamic behavior of the temperature. In the case of hybrid electrical vehicles where the behavior of the system is highly dynamic, it is however not possible to neglect these aspects due to the dynamic of the thermal behavior compared to the electrical one. The thermal modeling of battery and cells is a widely researched topic which extends from cell thermal design up to battery system investigation. The suitable solution is therefore strongly dependent on the considered development step. Considering the requirements of this work, the use of finite element analysis is excluded. Hence a general nodal model is thus considered for this work.

	Accuraccy	Simulation effort	Parameter range
Finite element analysis	+ +	- -	✓
Nodal model	+	-	✓

Table 22: Comparison of approaches for the thermal modeling of battery

3.3 Modeling implementation

The modeling implementation does not really differ from the one for the power electronics. However, the temperature in the cell and the temperature distribution of the cooling system are supposed perfect and thus the entire battery can be investigated by considering only the thermal path between one cell and the cooling system. The temperature in the cell is evaluated based on the losses and the thermal path and enables then to enhance the component behavior modeling and to estimate the limits of the battery. The coolant flow dependency is implemented by scaling the thermal resistance (and thus the time constant) of the system as for the power electronics.

3.4 Validation

The validation of the modeling is done with vehicle measurements. When comparing a modeling approach with vehicle measured values, the losses cannot be measured but only the current. For the validation presented in this section, the simulation results from the combination of the electrical modeling and the thermal modeling as presented on Figure 115.

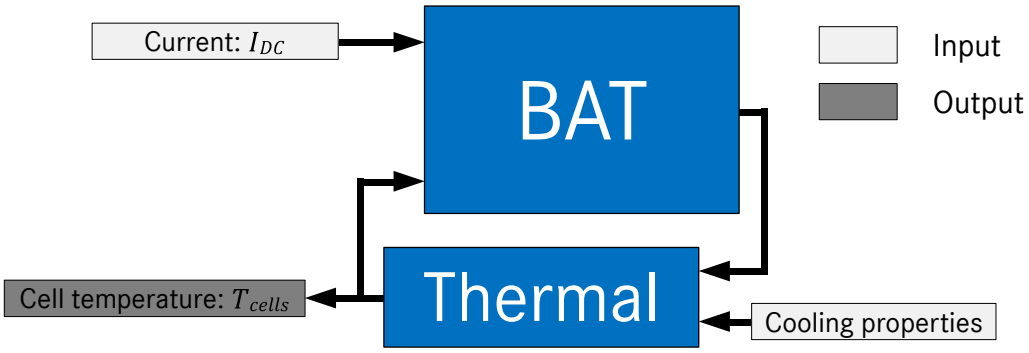

Figure 111: Modeling approach for the validation of the thermal modeling

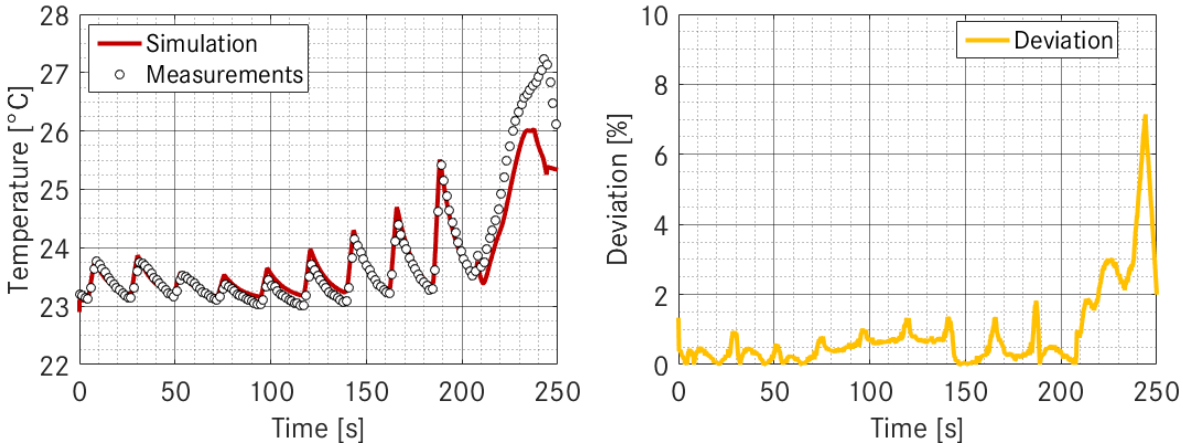

Figure 112: Deviation between the simulation and the measurement of the temperature behavior

The results show low deviation (under 10%) and a relatively high correlation (86.81%). Considering the assumptions done for the simulation which considers the electrical and the thermal model as well as the hypothesis for the modeling, the results as presented on Figure 112 are really promising. They depict with a good accuracy the behavior of the cell temperature and show a consistent order of magnitude considering the fact that the simulation is done with coupled models since the losses cannot be measured directly.

3.5 Contribution for system evaluation

The contribution of thermal behavior does not differ from the ones presented for the electric machine and the power electronics, it enables to determine the component and system limits as well as to refine the components behavior where the loss parameters and the voltage can be estimated using the actual temperature. Therefore no investigations are performed for the battery since the modeling approach is not different from the one presented for the power electronics.

4 Volume and weight estimation

Despite having a less complex structure than the power electronics, the battery also requires a specific method for the estimation of its integration. After defining the evaluation approach, the different possibilities to implement the method are discussed. Then the implementation of the retained method is detailed and a validation with several automotive components is shown. As previously explained, the differentiation between 48V and HV system is only done through the number of cells.

4.1 Evaluation approach

A Boolean solution can only evaluate the power and the energy density of the battery. For the purpose of this work, a similar approach as the one for the power electronics is chosen. Based on the number of cells in series, the number of cells in parallel and the available volume, the volume, the weight and the dimensions are estimated.

Contrary to the power electronics, the electrical requirements are not required as inputs because they can be deduced using the number of cells. The approach is presented on Figure 113 and despite the components limitations done in this work; it could be easily implemented for all kind of electrical energy storage systems.

Figure 113: Evaluation approach for the integration of battery system

4.2 Investigation of level influence and related approaches

The volume and the weight are generally evaluated during the whole development process but they are principally used during the early design phase to analyze the relevancy of the requirements or during the final steps of the development to fit the components in the final frame of the vehicle. This section analyzes previous works on the topics, presents the drawbacks and the advantages of each one before showing how they only fulfill partially the requirements defined previously.

4.2.1 Computer aided design

The computer aided design (CAD) approach enable to test directly the integration of the component. It requires however to know all the dimensions of the entire components or the dimensions of each sub-parts (cells, current sensors or relay for example) and the tolerances for the design such as the one deduces from electrical safety requirements. Considering this, it enables highly integrated solutions, which perfectly suit the vehicle frame as in the Chevrolet volt [18]. The computer aided design approach enables also using the structure to simulate the behavior of the system during crash as in [125].

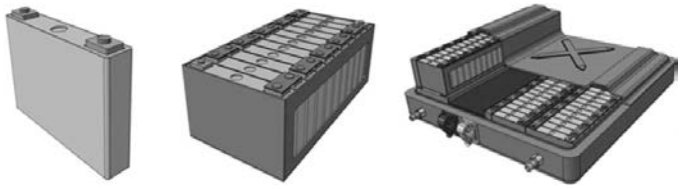

Figure 114: Construction of the battery from cells to battery pack [125]

4.2.2 Power and energy density

Other approaches can be deduced from the power and energy density of the technology. They are generally based on the analysis of the current solutions in order to determine a relationship between the power, the energy, the volume and/or the weight of the battery. It is for example used in [56] where the predicted evolution of the energy density in Wh/dm^3 is shown for lithium-ion system and it assumes that the energy density is independent from the volume and the power. Additional information about the power and energy density can also be found in [49] where the batteries are compared with other storage system technologies.

4.2.3 Evaluation for electric drive system optimization

The aim and goals defined in this work cannot be fulfilled with the previously presented solutions. The CAD based ones are not suitable for an optimization process due to the lack of interfaces with simulation software and their high complexity but they fulfill the evaluation approach. The solutions based only on the energy density are not fulfilling the evaluation approach because the dimensions cannot be evaluated. As it can be seen on Figure 115, the ratio between the entire volume (system) and the cells volume can be used instead of considering the energy density.

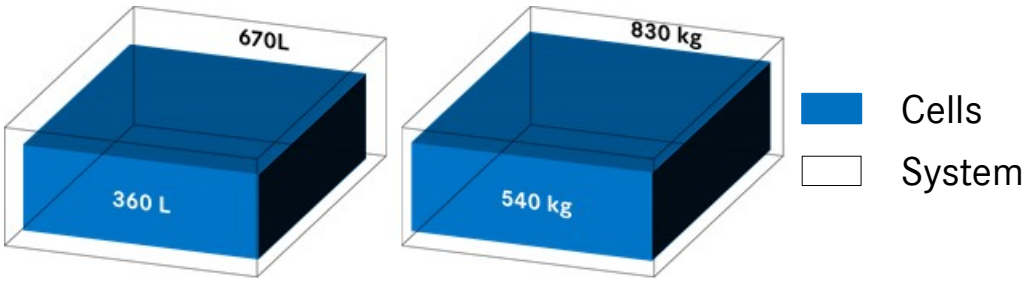

Figure 115: Weight and volume distribution in lithium-ion battery (2010) from [22]

Hence a first approximation based on the ratio between the cells volume and the system volume could allow evaluating the dimensions depending on the implementation. Due to the limitations of the other solutions, this ratio based solution is implemented and analyzed in the next section.

	CAD	Ratio based solution	Energy and power density
Accuracy	+ +	See next section	- -
Simulation effort	- -		+ +
Parameter range	✓		X

Table 23: Comparison of approaches for the volume and weight estimation of battery

4.3 Method implementation

This section is divided in two main parts: a first one about the ratio based solution discussed previously and a second one resulting from the analysis of the ratio based solution. For each one, the model is presented before introducing the modeling approach.

4.3.1 Ratio based solution

The method is based on the results presented in [22] which can also be validated when investigating other automotive components. Deduced from the ratio between the cells volume and the battery volume, an available volume and the corresponding dimensions for the cells can be calculated and therefore the integration can be tested.

Model:

Based on the previously defined ratio between the cells volume and the battery volume (conservative value of 45% based on [22]), the first step consists in defining an available volume for the cells. To develop the model, an initial arbitrary assumption is considered: the utilization in each direction is the same. Hence the dimensions for the cells can be calculated as in (77) and (78) where $Cells_{l/w/h}$ and $Battery_{l/w\ /h}$ can be respectively the length, weight or height of the cells volume and the battery volume, V_{Cells} is the cells volume and $V_{Battery}$ the battery volume.

$$Cells_{l/w/h} = \sqrt[3]{0.45} \cdot Battery_{l/w\ /h} \quad (77)$$

$$V_{Cells} = \sqrt[3]{0.45} \cdot \sqrt[3]{0.45} \cdot \sqrt[3]{0.45} \cdot V_{Battery} = 0.45 \cdot V_{Battery} \quad (78)$$

Modeling approach:

The modeling approach for the evaluation of the battery integration is divided in three parts. First, the available volume for the cells is calculated using the model. Then the maximal number of cells which fits the volume is calculated and finally the battery dimensions are calculated using a reverse factor ($1/\sqrt[3]{0.45}$) and the weight is calculated directly with the ratio between the cells weight and the battery weight. To test the integration, the cells are investigated in all possible directions and the direction which minimizes the volume is chosen. The modeling approach is summarized on Figure 116, where the different steps are shown. The modeling approach as considered in this sub-section requires however an additional assumption.

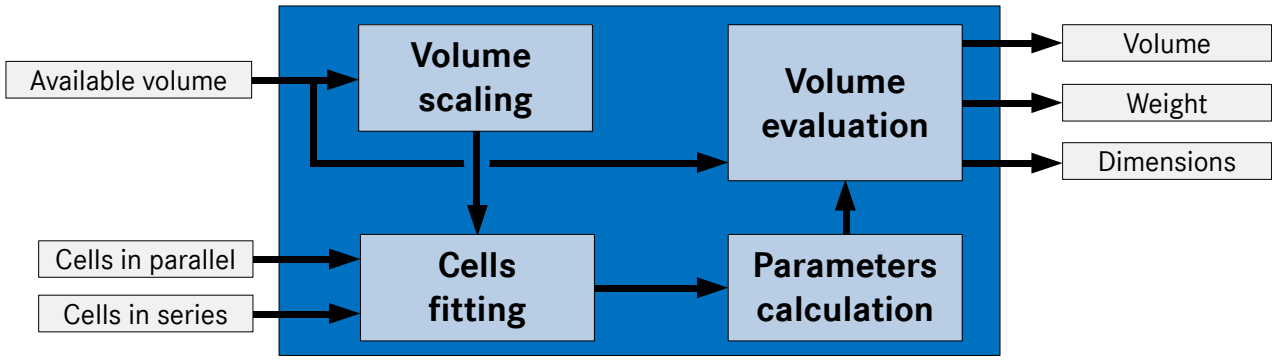

Figure 116: Modeling approach for the evaluation of the battery integration with ratio

Limits of the modeling:

The modeling approach presented here relies on a strong assumption concerning the volume distribution (constant scaling factor in all directions) and shows limits during the model validation. Considering the example of the Mercedes-Benz S500 PHEV [134], the modeling with the considered assumptions cannot fit the automotive component as shown in the following table.

	Number of cells
Reference	120
Simulation	112 (-6.7%)

Table 24: Comparison of the method with a reference automotive component for the battery

The simulation results presented in this table show the maximal possibility of the modeling approaches for the available volume of the reference battery. As it can be seen, only 112 cells can be fitted in this volume with the current method and the method does not fit the requirements. To test the real limits of the methods, the simulation is performed with other scaling factor with the hypothesis that the cells volume is 45% of the battery volume. The results are presented in the following table.

	Length ratio	Width ratio	Height ratio	Cell to battery volume ratio	Number of cells
Reference					120
Simulation	$\sqrt[3]{0.45}$	$\sqrt[3]{0.45}$	$\sqrt[3]{0.45}$	45%	112
Test 1	0.89	0.52	0.97		132
Test 2	0.78	0.62	0.93		84
Test 3	0.93	0.83	0.58		112
Test 4	0.9	0.70	0.71		120

Table 25: Ratio influence for the evaluation of the battery integration

These results show that it is possible with ratio based modeling approach to fit the right number of cells but it also shows that depending on these ratios, the range extends from 84 up to 132 cells (-30% up to +16%). Moreover the ratios presented here are chosen arbitrarily and limits need to be defined in such a way that the other basic sub-component can fit in the battery too. For this purpose, methods need to be done to estimate the dimensions of the other sub-parts. Since all the sub-parts dimensions need to be estimated, an approach similar to the one for the power electronics can be chosen and is detailed in the next sub-section.

4.3.2 Modular battery integration evaluation

This second method is based on the analysis of previous architectures as for the power electronics. The methods presented in this section are deduced from this analysis and based on datasheet from sub-component supplier. For each sub-component, a method is chosen to estimate the volume and the weight and then an algorithm is used to calculate the volume of the entire battery.

Models and methods:

Most of the sub-components dimensions can be extracted from datasheet: cells, case, relay, fuse, sensors, cooling plate, electric connections, cooling connections as well as communication connections. Only the safety requirements (clearance and creepage distance), the battery management unit (BMU), the cells management unit (CMU) and the busbars require a specific method. These methods are explained in this sub-section. Concerning the weight, a ratio based solution is still considered since it does not influence the integration and induces the same deviation with references for all possible technologies.

Clearance and creepage distance:

The clearance and creepage are safety requirements which are calculated based on the corresponding norm [110]. For the calculation, the worst-case maximal voltage in the battery is used to ensure the requirements in all possible working conditions. The voltage for this calculation is expressed in (79) and depicts the worst case which can occur in the battery.

$$U_{max} = s \cdot (OCV_{max} + R_{max} \cdot |I_{max}|) \quad (79)$$

Battery and cell management units:

The battery and cell management units are mainly composed of electronic boards where the structure is often designed for a specific battery. Based on datasheets, the volume and the weight can be extrapolated as presented on Figure 117. As for the DC-link capacitor, the electronic boards are only available for defined number of cells (in this case 12 cells for the entire unit), and thus the volume is a step function of the number of cells. The volume is calculated for the global unit (BMU and CMU). Then based on the datasheet of single electronics boards for these applications and the clearance and creepage distance, minimal dimensions can be calculated to ensure the relevancy of the assumption.

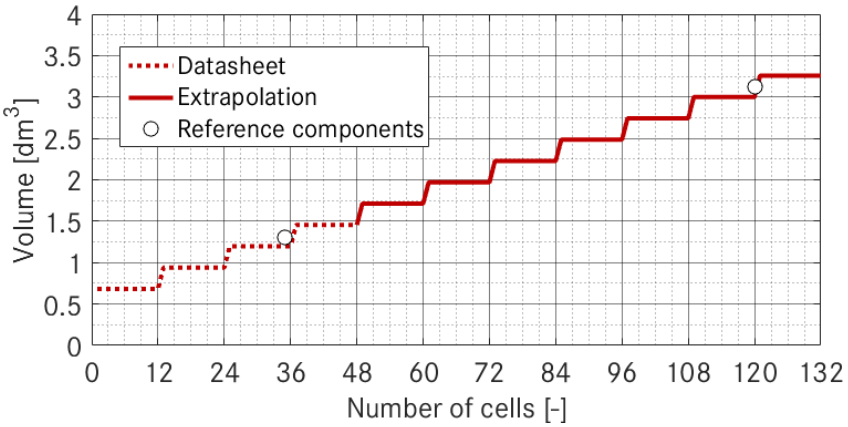

Figure 117: Volume estimation of the CMU and BMU based on data from [32], [123], [134], [135] and [136]

Busbars:

The busbars are calculated using the same method as for the power electronics. The difference lies in the electrical requirements for the estimation of the volume. When the structure is composed of several rows of cells in parallel, there are two requirements: one for the module busbars and one for the battery busbars. The module busbars are estimated with the cell current while the battery busbars are estimated with the entire current. In the case of a single parallel row, the battery current and the module current are equal and no differentiation is done.

Modeling approach:

The modeling approach is based on the same principle as for the power electronics: based on the estimation of each sub-component, an algorithm is developed to estimate the entire battery volume. The method used to evaluate the battery volume is presented on Figure 118. Using the sub-components dimensions, a defined volume for the cells is defined based on the considered architecture. As previously in the ratio based solutions, this volume is used to evaluate the integration by testing the required volume for the defined number of cells in each direction. In this work, two architectures are considered: one for low power applications (<30kW) and one for high power applications

(>30kW). The two architectures are synthetized on Figure 118. These architectures are deduced from current assemblies of battery from the automotive industry but contrary to the power electronics, the cells offer more flexibility and after the calculation of the available volume no specific attention is given to the exact location of each sub-component.

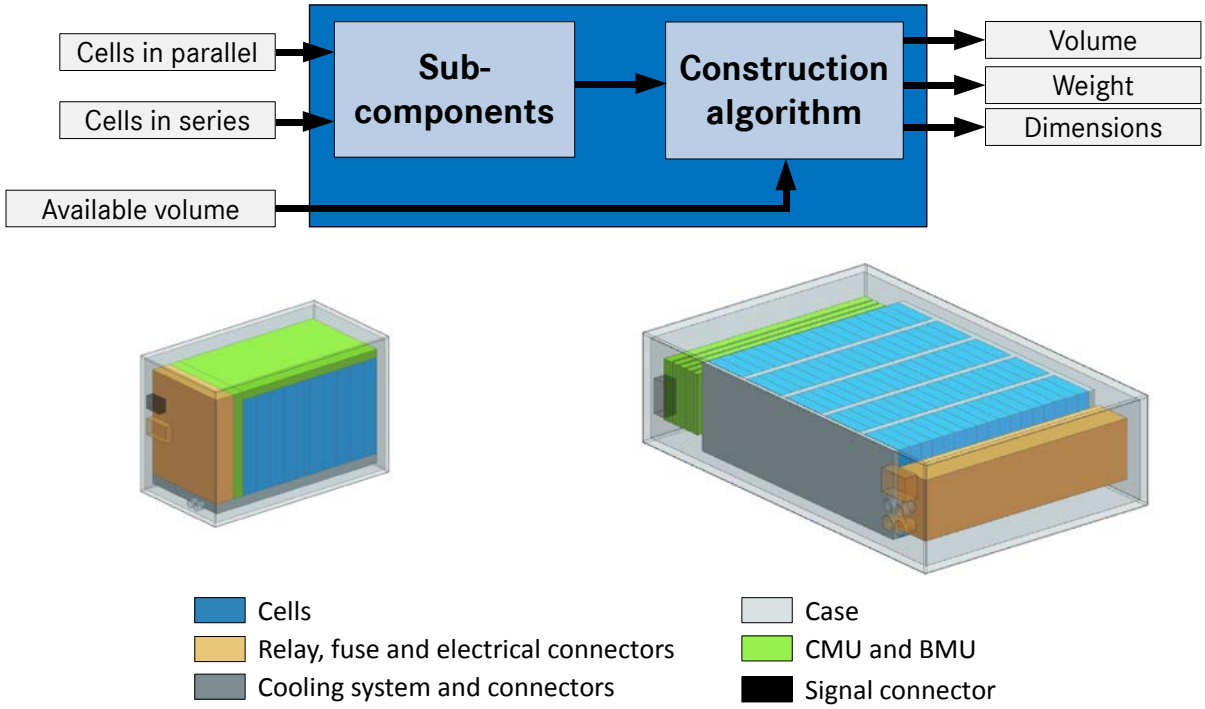

Figure 118: Evaluation approach and architectures for the battery integration

4.4 Validation

The results of the implementation are shown and compared with reference automotive components in this section. The validation is divided into two parts: the first one compares the method with two components and the second one compares the relevancy of the chosen approach (differentiation between low and high power) for different variations of the requirements. The method presented in the previous section is compared with two reference automotive components. The comparison evaluates the dimensions and the cell volume to battery volume ratio. The results are presented in the following table. For each component, the adapted method is chosen: High Power (HP) or Low Power (LP). The results in the following table are showing low deviations (under 5% for all dimensions except the height of the component 1) and consistent cell volume to battery volume ratios. The high power method is based on the component 1 architecture. Despite the approximated sub-components methods and the value being extracted from external datasheets, the deviations are comparably low and acceptable. The same approach is used for component 2, which is used for the low power method and it shows lower deviations. To further validate the methods and ensure the relevancy of the results, the next sub sections shows the results of the cell volume to battery volume ratio for different variations of the requirements.

		Deviation [%]			Cell volume to battery volume ratio
		Length	Width	Height	
Component 1 from [134]	**HP method**	1.4	3.7	9.5	45.4%
Component 2 from [32]	**LP method**	3.2	0.9	1.7	50.5%
Component 3 from [137]	**LP method**	2.5	1.0	1.5	50.1%

Table 26: Comparison of the simulation results with reference automotive components for the battery

4.5 Contribution for system evaluation

One of the main contributions of this work concerning the battery evaluation lies in the volume evaluation because the influence of the voltage (cells in series) and the current level (cells in parallel) can be determined. The results presented in this section investigate the volume and its dependencies on the current and the voltage. For this purpose, a single cell is chosen and the variation of the voltage and the current are explored by varying the structure (number of cells in series or parallel) for a defined total number of cells. Since no half or lower percent of the cells can be considered, the results of the investigations are discrete.

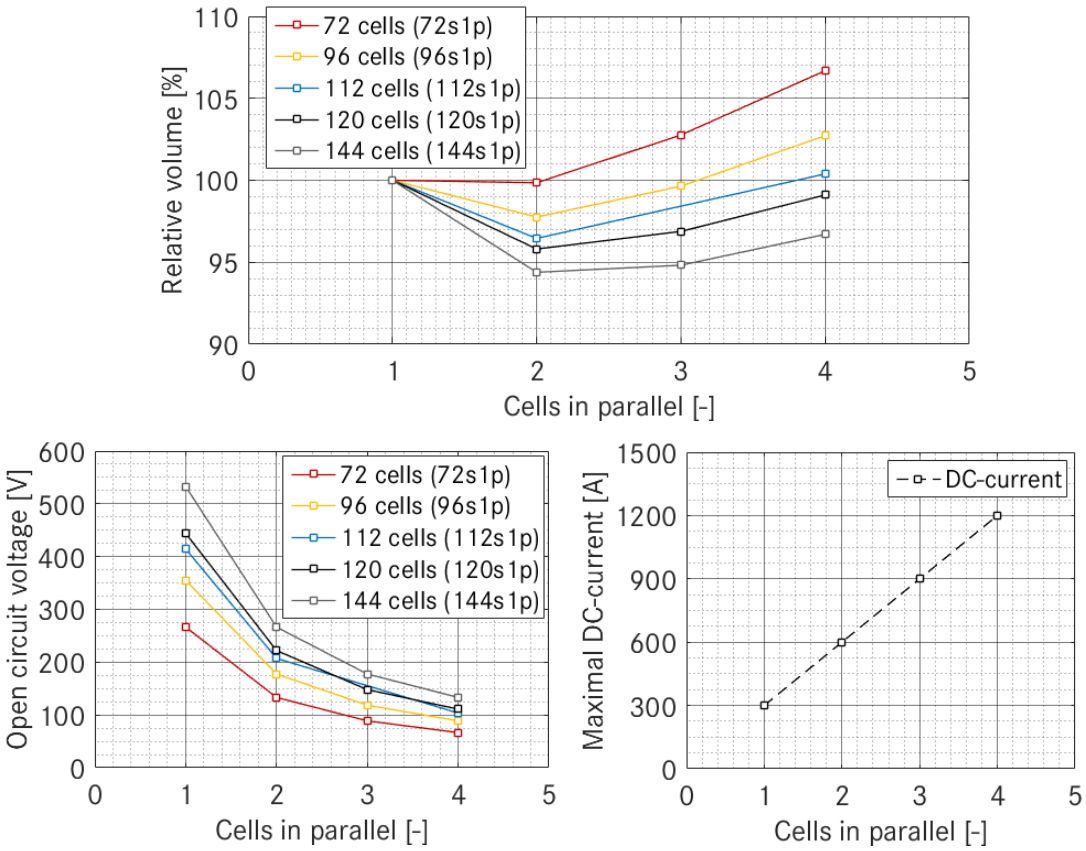

Figure 119: Influence of the voltage and current level on the battery volume (left)

Depending on the basis configuration, a volume reduction is possible by changing the number of cells in parallel. However no clear dependency between the battery configuration and the volume can be inferred. The variation of the number of cells in parallel can be translated as current and voltage level influence due to the considered investigation (constant number of cells in the system). An increase of the current (respectively decrease of the voltage) leads to a reduction of the battery volume up to 2 cells in parallel. From this point and even if the volume stays under the reference values, the relative volume increases with additional number of parallel circuits. This behavior is probably linked with the influence of the voltage and the current on the sub-component methods. An increase of the number of cells in parallel leads in a first step to a decrease of the volume because the voltage and therefore the creepage and clearance distance are reduced. However in a second step, the increasing current and its influence on the busbar design lead to an increase of the battery volume.

5 Chapter conclusion

In this chapter, the solutions for the modeling of battery are discussed, analyzed, implemented in a simulation environment and finally validated based on automotive components measurements. For each method or modeling, a suitable solution can be found to fulfill the requirements of this work. By adapting current modeling to the challenges faced by the components in the automotive industry, the system level methods and modeling approaches are developed. Moreover, the contribution of the methods presented in this work are already shown since a completely new method is developed to estimate the battery volume. The other methods presented in this chapter

are based on well-known approaches but the parameter range is widened. The behavior modeling enables to compare different cells with different properties by considering the thermal, SOC and load-dependency of the voltage and the losses in the cells. The thermal model of the battery depicts as a “black-box” the thermal behavior of the battery system since only the loss sources and the cell temperature are considered. Even if the temperature distribution in the cells and the influence of the environment is neglected, it allows having a first approximation of the battery behavior. The different validations of the modeling show promising results. Concerning the integration, the developed method can consider a wide parameter range thanks to the construction algorithm and the sub-components evaluation methods. The contributions of this work are already shown by analyzing the voltage behavior for a given current profile and the influence of the battery configuration on the battery volume. The first investigation shows the importance of the interactions between the components due to the variating voltage while the second enables to have a first overview of how the voltage and the current influence the battery volume. As for the other components, this chapter has presented solutions to model in a suitable way the components. They allow addressing the challenges described in the first chapter. The determination of the suitable modeling is an important aspect of this work because the aim is not to find the most accurate solution but to identify the suitable approach to model and to compare different systems and therefore to determine the best combination of components instead of the combination of the best components.

Chapter 5: Global system modeling approach for electrical system in hybrid electrical drivetrain

A global system analysis is a key factor for the design and the optimization of the entire electric drive system in hybrid because a component-focused approach could lead to over-dimensioning of the components due to design conflicts and component-specific challenges. This chapter introduces therefore the global system approach for this work and how it allows developing a system which is the best combination of components instead of the combination of the best components. It introduces first global knowledge about the modeling of system and the goal of this work for the global system modeling are set. Then the implementation is discussed and validated using automotive systems and finally the contribution of this work are shown.

1 Modeling system

This chapter presents first the required definitions for the understanding of system modeling, then the current status is analyzed to finally define the goals for this work.

1.1 Definitions and representation

This first sub-section introduces the relevant definitions for system investigation and then the representation of a system is detailed.

1.1.1 Definitions

Some definitions need to be introduced for a clear understanding of system modeling. The term system is defined as a collection of inter-related elements pursuing a common objective. As it is shown previously, in the case of the electric drive system, the entire system is generally characterized by component parameters which are inter-related (see 2.2. Investigation levels for hybrid system optimization). Beside this general definition, the system can be classified as static, quasi-static or dynamic depending of their outputs. In the case of static or quasi-static system, the outputs are generally only dependent on the current inputs while for dynamic system, the time dependency is considered [139].

1.1.2 Representation

A system for modeling purpose is generally defined as a box with one or several inputs (vector u with the sub-values u_1 up to u_m) and one or several outputs (vector y with the sub-values y_1 up to y_n) as shown on Figure 120.

Figure 120: Representation of a multi-input, multi-output system [139]

The system as represented on the previous figure can be modeled as a “black-box” from an external point of view, when the outputs can be written directly with a dependency on the inputs using function or with an internal description of the interactions and the behavior of the components in the system. The modeling approach is generally dependent on the modeled component or system because it is not always possible to describe the behavior with a continuous function.

1.2 Modeling electrical system in hybrid electrical vehicle

This third part discusses the topic of modeling electrical systems in hybrid electrical vehicle. It first introduces the current status for the design of electrical system. Then the goals of this work are defined for the component modeling and the volume and weight estimation.

1.2.1 Present status

Before defining the goals of this work for the entire system modeling, a deeper analysis of the present status is required. In the first chapter, a global overview of the challenges is shown on Figure 25. Focused on the electric component the approach can be detailed as follows:

- First the required battery power (P_{BATT}) is estimated for the mechanical requirements (Torque profiles: T_{EM-ref}) under the boundary conditions of the system (speed profile: n_{rpm} and on-board power: P_{OB}). Generally typical estimated efficiency for the considered technologies of the power electronics and the electric machine are used but without torque, speed, current or temperature dependency.
- Based on the estimated battery power and the current development status of the cells, the battery design and the battery voltage (U_{BATT}) can be estimated.
- Using the estimated battery voltage and the modulation and control method of the power electronics, the available AC-current (I_{AC}) and AC-voltage (U_{AC}) can be estimated.
- Finally the machine performance (T_{EM}) are evaluated under the approximated system characteristics and the global drivetrain performance can be evaluated.

This approach (see Figure 121) leads to over-dimensioned systems due to the approximations and estimations used to design the systems. The aim of this work is therefore to develop based on the previous component modeling a global system approach to address the challenges of this work and to set the basis for further investigation and optimization of hybrid electrical drivetrains.

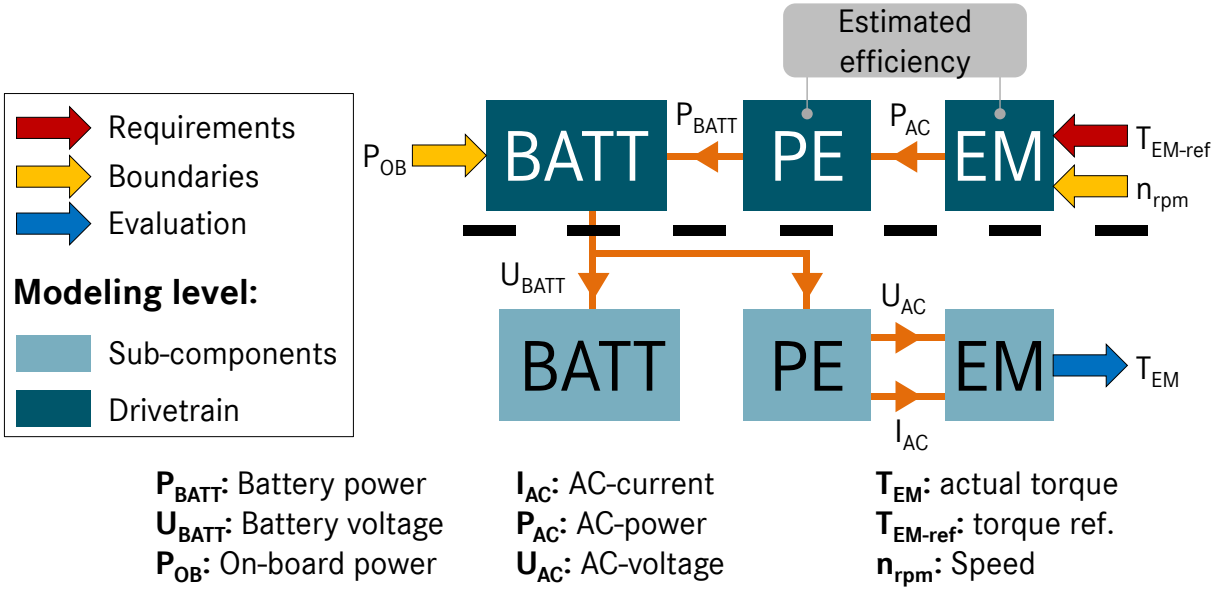

Figure 121: Present approach for the design of electric drive system for hybrid electrical drivetrains

1.2.2 Goals of this work

The approach is based on sub-component databanks (electromagnetic design of the machine, cells and power modules) and aims to identify among them the best combinations of components. This identification is divided in two parts, one for the behavior modeling and one for the integration evaluation. The boundary conditions are defined in the first chapter and therefore the approach does not investigate directly the integration (position of the components in the drivetrain or available volume), the environment (cooling system), the test- and driving cycle (energy management), the sub-components design as well as the costs and the reliability.

Integration evaluation

The system approach is actually the combination of each approach defined in the previous chapters. Contrary to the power electronics and the battery, the integration of the electric machine is considered with a Boolean approach which does not require any change for the system investigation. A system is therefore considered as integrable in the drivetrain, if all the components are integrable. The approach is resumed on Figure 122 where the requirements are component parameters, the boundaries are the available volume and the evaluation is the integrability.

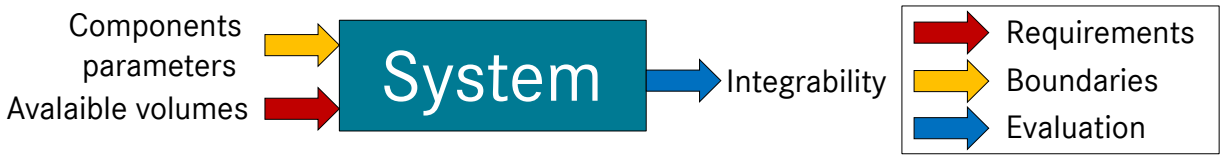

Figure 122: Evaluation approach for the integration of electric drive system

Behavior modeling:

The behavior modeling as considered for the global system investigation is the combination of both the component behavior modeling and the thermal modeling. The approach retained for this work is shown on Figure 123. It does not depict the aim of the work but only the principles and the interfaces required to develop a bidirectional modeling of the entire system. It represents with a direct causality the physical interactions within an electric drive system. Hence the outputs are the results of the effect caused by the inputs as for the thermal modelings where the temperature changes are resulting from losses variations of the electric machine where the required current is the results of the current available voltage, the required torque and the speed. The approach performs simultaneously the requirements analysis and the performance evaluation of the system through the combination of the backward and the forward approaches.

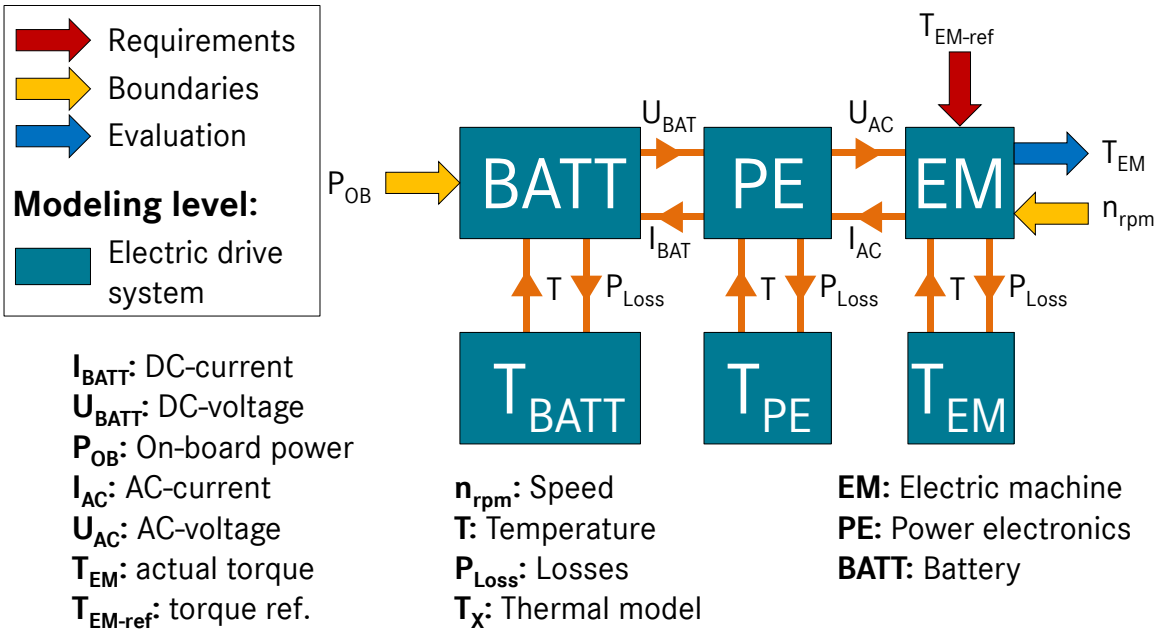

Figure 123: Modeling approach for the investigation of electric drive system

System evaluation:

Beside the modeling approach, the evaluation approach of the global system needs to be defined because it influences the real evaluation parameters which need to be considered for the modeling implementation. The design of a system is in the case of this work based on three requirements: torque and speed profiles and available volumes. The evaluation approach can therefore be reduced to the one presented on Figure 124.

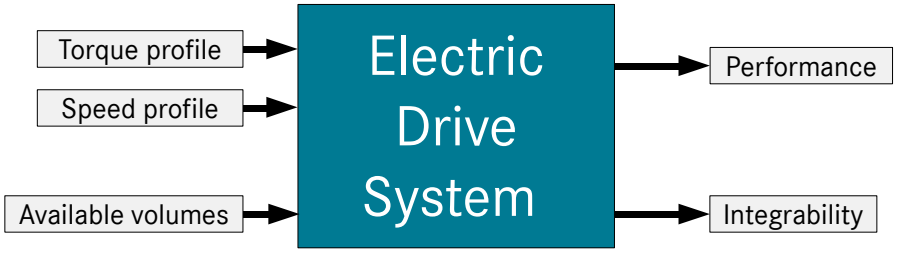

Figure 124: Global evaluation approach for the system evaluation

As for the component modeling approaches, the system can be evaluated as a black-box and the challenges investigated in this work (voltage level, power electronics topology and module strategy) are considered through the boundary conditions of the optimization approach. Hence based on this approach, the next section discusses the modeling implementation.

1.2.3 Modeling environment

The modeling environment is also an important topic when considering a system modeling because it influences the modeling implementation. Due to the industrial environment considered in this work, no review of the different modeling environments is done as in [52] and therefore Matlab/Simulink is used.

2 Modeling implementation of the electric drive system

This section is focused on the implementation of the modeling. It introduces the technical solutions to implement the global system modeling to fulfill the approach depicted on the Figure 124. It discusses first the combination of the component modelings, then the required adaptation for the system evaluation and finally the implementation of the system limits.

2.1 Combined modeling approach

To combine the modeling approaches described in the previous chapters, a serial arrangement is chosen. The components are directly connected using the interfaces previously defined. The resulting diagram is presented on Figure 125 for the behavior modeling and on Figure 126 for the integration investigation, where it can be seen that some adaptations of the interfaces are required to combine the component modeling as well as to define the outputs for system evaluation.

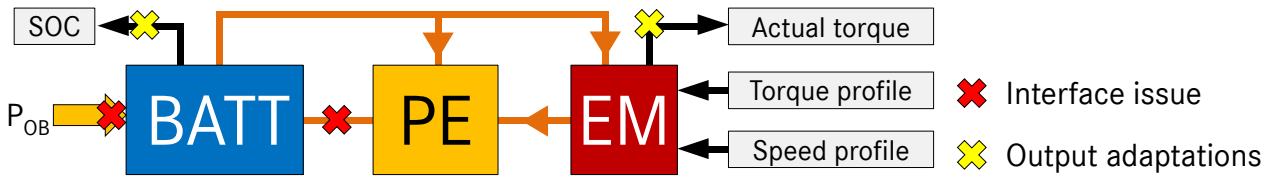

Figure 125: Combinations of the current behavior modelings without adaptations

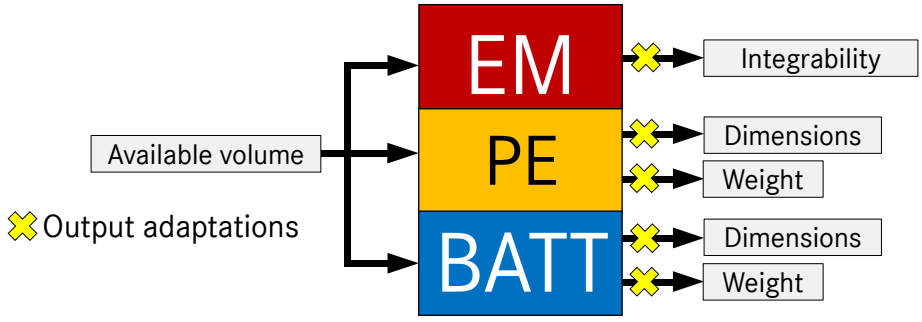

Figure 126: Combinations of the current integration investigation without adaptations

2.1.1 Interface issue

The interfaces as presented on Figure 125 are not coinciding one with another. It is generally due to the fact that the global electrical system is not only the combination of the three components modeled in this work but also of others components as shown on Figure 10. The main adaptations considering the interfaces is between the power electronics (combination or not of an inverter with a boost-converter) and the battery. They are not directly connected but through an additional "component": the Power Distribution Unit. As described by its name, it ensures the distribution of the battery power between the different electric loads. Its modeling approach is shown on the following figure. Depending on the presence or not of a boost-converter the DC-power can be equal to the battery power and the DC-voltage can be equal to the battery voltage.

Figure 127: Modeling approach of the power distribution unit

The model to depict the behavior of the PDU is based on the following process: the power from the traction components (DC-power) is added with the power from the chassis and then the summed power is divided by the voltage on the DC-side. The process can be summarized by the following equation where P_{DC} is the DC-power, P_{OB} is the chassis power, U_{DC} is the DC-voltage and I_{DC} the DC-current.

$$I_{DC} = \frac{P_{DC} + P_{OB}}{U_{DC}} \quad (80)$$

2.1.2 Outputs adaptation

The outputs of the present modelings represent only the physical outputs of the system. For the optimization purpose, these outputs need to be translated as performance and integrability indicators.

Performance indicators:

The performance indicators are defined by the capability of the system to fulfill the requested torque profile or not. This requirements are described by two type of requirements: a mechanical one and an energetic one. Therefore two performance indicators are defined: the torque profile indicator TPI and the SOC indicator $SOCI$ as shown in the following equations.

$$TPI = \frac{1}{t_{cycle}} \cdot \int_0^{t_{cycle}} \frac{T_{EM}(t)}{T_{EM-ref\ (t)}} \cdot dt \quad (81)$$

$$SOCI = SOC\left(t_{cycle}\right) \quad (82)$$

The TPI enables to evaluate the driving cycle requirements as well as the power requirements. The driving cycle requirements are defined by a time dependent time profile while the power requirements are defined by a torque/speed requirement. The SOCI allows in parallel to the TPI to evaluate the system efficiency by considering the remaining energy at the end of the cycle

Integrability indicators:

The integrability indicators are sensible parameters, they are based on a quasi-Boolean approach. The integrability indicator of each components, the CII for Components Integrability indicators, can only take two values: 0 if one dimension or the weight exceed the requirements or the value $eval_i$ as defined in the equations (83) which evaluates the ratio between the reference values and the simulated values. However each CII only depicts the integrability of one components. An additional indicator is therefore introduced, which depicts the integrability of the entire system.

The SII (for System Integrability Indicator) is calculated using the product of the CIIs shown in the equations (84). If one CII is equal to 0, then the SII is also equal to 0. This quasi-Boolean approach would not give any advantage to systems where a component has a really good power density due to these limitations. Hence the indicators enable to evaluate both the power density and to fulfill one of the aims of this work: evaluating the integrability. Hence the methods enable to find the best combination of components instead of a combination of the best components.

$$eval_i = \frac{Length_{ref_i}}{Length_i} \cdot \frac{Width_{ref_i}}{Width_i} \cdot \frac{Height_{ref_i}}{Height_i} \cdot \frac{Weight_{ref_i}}{Weight_i} \quad for\ i = \{EM, PE, ESS\} \quad (83)$$

$$SII = \prod CII \ \ for\ i = \{EM, PE, ESS\} \quad (84)$$

The two adaptations presented in this sub-section enable to have the outputs defined on Figure 124. The global system performance and integration is evaluated and the adaptations can be seen on Figure 131, where the entire modeling is represented.

2.2 Modeling system limits

Beside the adaptations of the modeling for the global system evaluation, the global system investigation as considered in this work requires also to implement modeling approach to consider the limits of the system. There are three main types of limits: energetic, thermal and electrical limits. This sub-section discusses in four parts, one for each type of limits and a final one for their implementation.

2.2.1 Energetic limits

The energetic limits of the system are related to the state-of-charge of the battery. The system cannot provide or regenerate energy if the battery is empty/full. Thus a model is required to limit the power in these cases. However these cases are also related to the electric machine because even if the mechanical power is set to 0 due to the empty battery, it continues to apply a load on the battery due to the no-load losses of the machine. In generator mode, the SOC can limit the regenerative potential and the torque needs to be limited. The limit is set to 0 because it is the point where the load and the losses are minimized for the battery. Therefore two torque limits are defined, $T_{mot_{SOC}}$ which is the torque limit when the battery is empty ($SOC = 0$) and $T_{gen_{SOC}}$ which is the torque limit when the battery is full ($SOC = 100$). The values are defined by the following equations. The ratio to define the torque limit where the battery is empty is chosen arbitrary for simulation purpose.

$$T_{mot_{SOC}} = \frac{1}{100} \cdot \max(T_{EM}) \quad (85)$$

$$T_{gen_{SOC}} = 0 \quad (86)$$

Two solutions are suitable to consider these energetic limits. The first one consists in implementing in the simulation a flag which signals when the system cannot fulfill the torque profile due to energetic and the second one consists in directly implementing the limits in the simulation. The first solution requires having an additional output which does not directly characterize the system while the second one influences directly the actual torque and therefore the TPI. Hence the limits are directly implemented in the model as shown in the related part and no flags are used.

2.2.2 Thermal limits

The thermal limits of the system are related to the temperature in each component. The thermal limits of the system are thus the combination of all the thermal limits from the components. This sub-section is divided in two parts, a first one about the thermal limits and how they are considered and a second one about their translation for an implementation in the system modeling.

Thermal limits:

The thermal limits need to be considered for automotive applications because they define the working areas of the components by defining the maximal available power depending on the actual component temperature. There are

generally three main areas to consider: the unlimited area, the upper limited area (temperature above the unlimited area) where the components provide a limited power and the over-temperature area where the components do not provide any power but are still not being deteriorated. There are therefore three main limits to consider in normal working conditions: the minimal working temperature T_{min}, the temperature T_{cont} which define the limits between the short-term working area and the continuous working area and finally the maximal working temperature T_{max}. Within the short-term area the power is not limited until the components reach the temperature T_{cont}. From this temperature, the component power is limited by its continuous values which are previously evaluated using the coupling of the behavior and thermal modeling under different boundary conditions as shown on Figure 83. When the temperature exceeds T_{max}, the power is limited to 0. When introducing limits without using the implementation with the flags, an additional thermal limit is defined to define the behavior of the components. Generally the continuous power limits are defined in such a way that the component can recover during this period and therefore it reaches a temperature called $T_{recovery}$ in this work, which defines when the components can again provide their full power. The value of the power in which the machine is thermally stable (no changes of the temperature) is referred in this work as $P_{recovery}$. The principles of these limits are shown on the Figure 128.

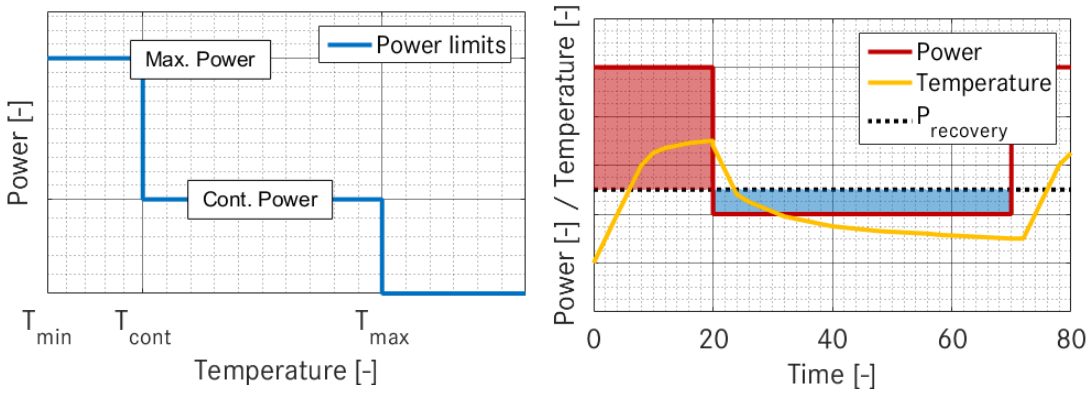

Figure 128: Thermal limits of electric components for automotive applications

Introduction of thermal limits in system modeling:

The thermal limits influence significantly the system behavior and the following approaches are introduced for each component. For the electric machine, the thermal limits can be directly translated as torque limitations using a pre-calculation with a coupling of the behavior and thermal model. For the power electronics and the battery, it results generally in current limitations which are also calculated with the coupling of their behavior and thermal models. The AC-current limitations of the power electronics can be introduced using the phase-current dependency of the torque/speed characteristic from the electric machine. The DC-current limitations are introduced by calculating an equivalent DC-power $P_{DC_{equi}}$ which is then used based on the current efficiency of the other components and the rotational speed. The calculation presented in the following equations enables to investigate the thermal influences of all three components on the system behavior.

$$P_{DC\,equi} = I_{DC\,lim} \cdot U_{DC} \quad (87)$$

$$T_{\mathrm{lim_{DC}}-Mot} = \frac{\eta_{EM} \cdot \eta_{PE} \cdot P_{DC_{equi}}}{n} \quad (88)$$

$$T_{\mathrm{lim_{DC}}-Gen} = \frac{P_{DC_{equi}}}{\eta_{EM} \cdot \eta_{PE} \cdot n} \quad (89)$$

2.2.3 Electrical limits

The voltage limits are defined using several ranges based on the SOC-, temperature- and load-dependency of energy storage system and the semiconductors characteristics to ensure the reliability of electric drive systems. They are described in the following norms and standards: VDA LV123 [116] and ISO6469-3 [117]. Example of these ranges are shown in [140] and [141] for respectively high- and low-voltage applications (HV and LV) on Figure 129.

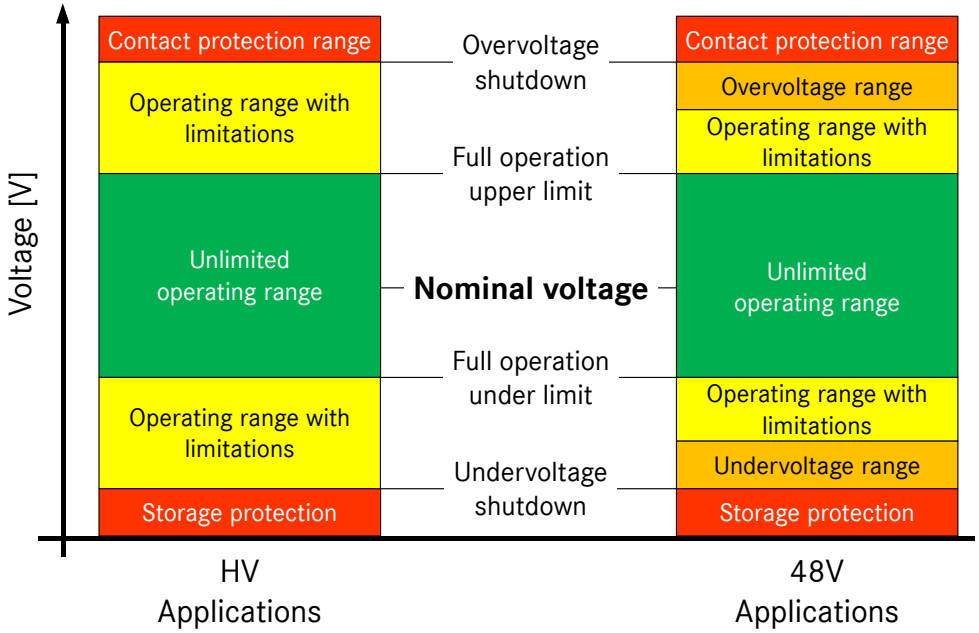

Figure 129: Voltage ranges as defined in the automotive standards and norms, adapted from [140] and [141]

To define the performance outside the unlimited operating range, the power is limited by the current of the power electronics and the battery current. The current is for both components equal to their maximal value until the upper or under limit of the unlimited operating range is reached. From this value, the current is linearly reduced down to 0 when the voltage reaches the undervoltage or overvoltage values. The current limitations are shown on Figure 130 for a HV-system and are introduced in the model as previously for the thermal ones.

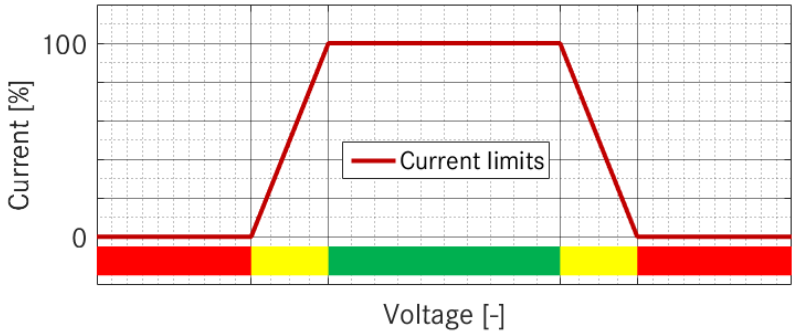

Figure 130: Current limits dependency on the voltage

2.2.4 Limits implementation

The limits discussed in this subsection are implemented using saturation on the torque profile. Each limit is considered with a DC-voltage dependency and they are introduced in the model using an energy management block which is introduced as a filter for the torque profile. The resulting approach for the system modeling is shown on the following figure. This approach enables to fulfill the approach presented on Figure 124 without requiring the implementation of flag to signal an issue in the modeling. This choice is related to the topic of this work, most of the current hybrid electrical systems are compromises due to the sophistication and the complexity of such systems. One goal of this work is thus to also have a solution which does not fulfill one or two requirements but still has a high evaluation to provide feedback for the further development if no valid solution can be found.

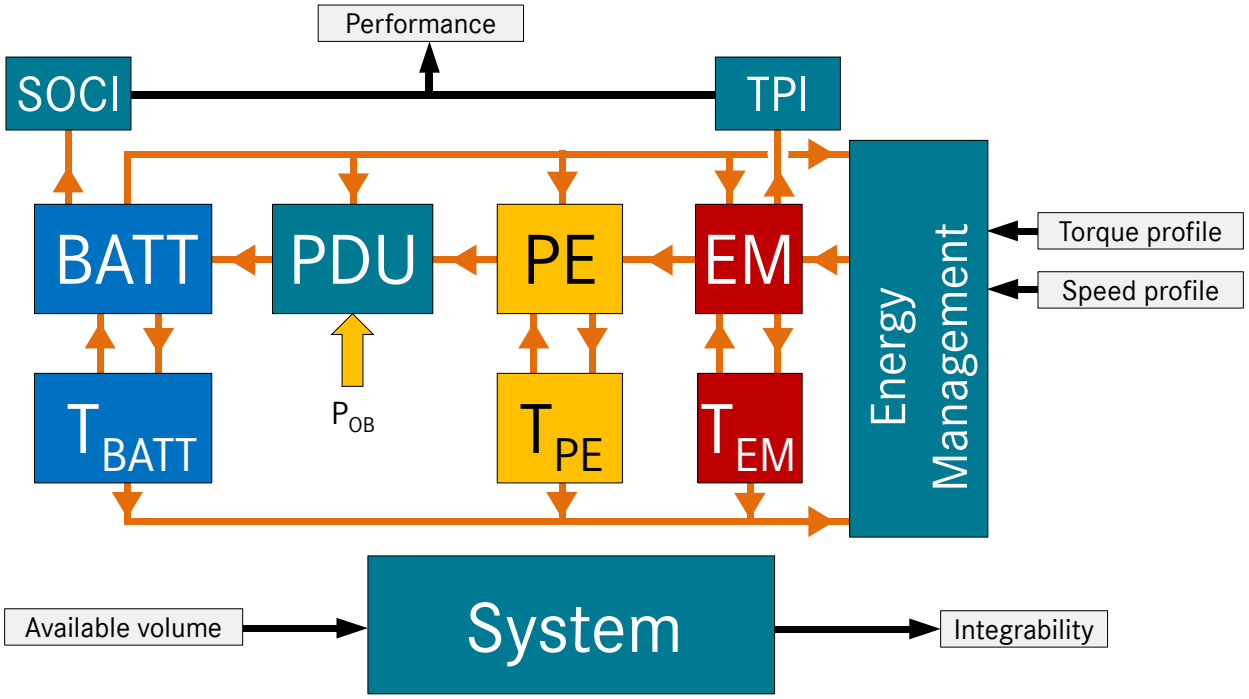

Figure 131: Modeling implementation for the investigation of electrical system in hybrid drivetrains

2.3 Boost-converter integration

The boost-converter is considered separately because it is an optional component. The integration of the boost-converter does not change anything for the interfaces between the components but requires some adaptations in the energy management. Instead of doing a feedback loop with the battery-voltage the energy management provides the output voltage of the boost converter to the electric machine and the inverter while the battery-voltage is provided only to the boost-converter to calculate its losses. The best-voltage for the electric machine and power electronics is calculated during the pre-processing and results in a matrix which provides the best voltage for the components depending on the required torque and speed. The matrix is integrated in the energy management. The case with boost-converter is shown on Figure 132.

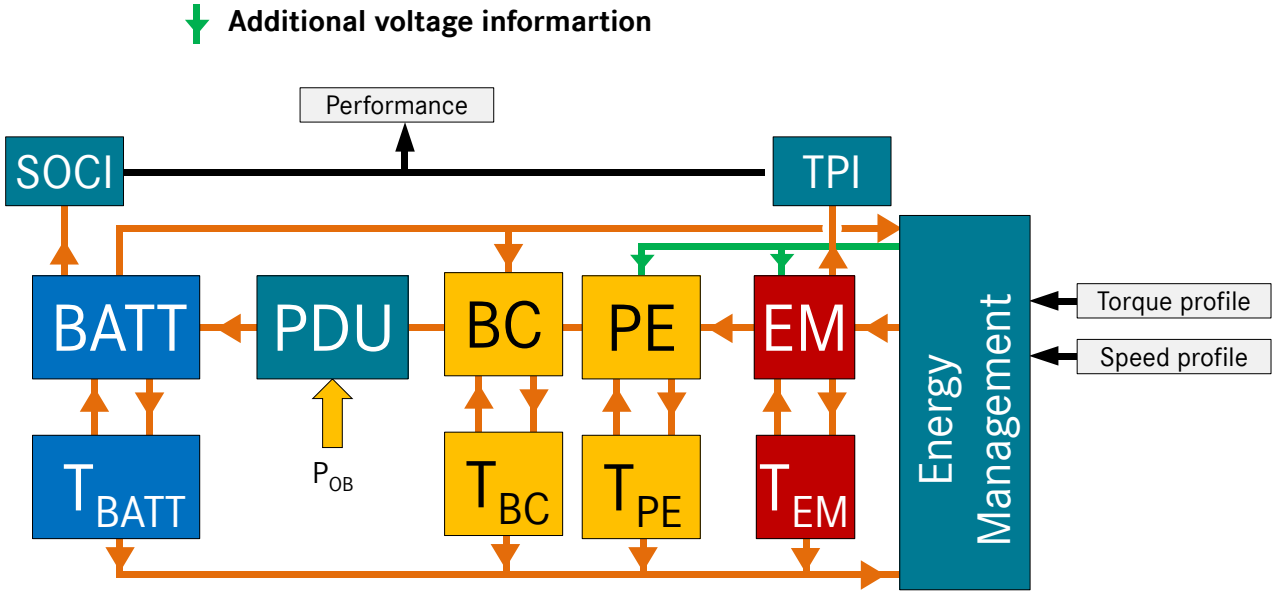

Figure 132: Modeling implementation for the investigation of electrical system in hybrid drivetrains

3 Global system modeling validation

The focus of this section is set on the global system modeling validation. The validation is divided into two parts, a first one with a test-bench validation and a second part with a vehicle validation. Both validations are done with the same system but the test-bench validation only enables to validate the power electronics and the electric machine while a vehicle validation allows evaluating the entire system electrically as well as mechanically and thermally.

3.1 Test-bench validation

The test-bench used for this validation is the same as for the electric machine and the power electronics validation which is used here to validate the entire system behavior. It can only consider the power electronics and the electric machine and thus to depict the behavior of the entire system, a voltage profile is given as input to the test-bench to reproduce the battery behavior.

Considered configuration:

For this first validation, the configuration presented on Figure 133 is used. In the case of this validation the following inputs are considered: the torque and speed profiles, the cooling properties and the voltage profile. The validation is then done using the DC-Power as well as the actual torque and speed as shown on the following figure. Except the validation of the SOC, this validation enables to test most of the parameters of the entire system. The simulation is performed without energy management to spare simulation effort since the torque and speed profiles are estimated considering the torque limits of the machine.

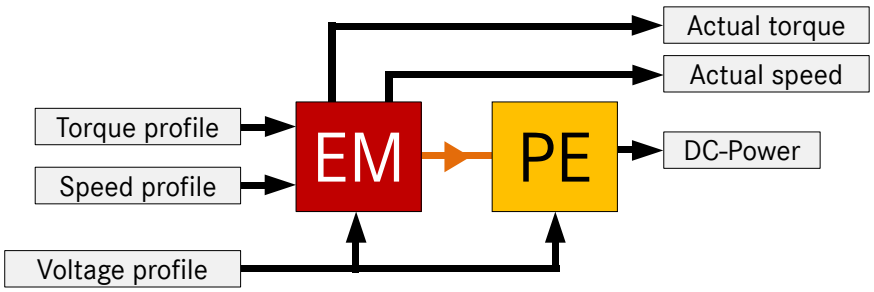

Figure 133: Considered configuration for the test-bench validation

Comparison between simulation and measurements:

The test-bench used for this validation is generally used to measure static point to validate the design of the electric machine or to parametrize the control of the power electronics. Its use for the validation of dynamic simulation of an electric system is possible but imposes some limitations which are discussed when analyzing the results. The results are presented by considering the torque profile (Figure 134), the speed profile (Figure 135) and the DC-power (Figure 136). As it can be seen, both the behavior and the amplitude between the simulation and the measurements are comparable. Moreover, the test-bench is not really adequate for dynamic measurements and when the time scale is reduced a time lag can be seen. This limitation prevents calculating any deviation between the measurements and the simulation. Concerning the amplitude, the DC-power and the speed profile are showing promising results while the torque profile shows higher deviations. These deviations as previously during the component validation could be related to the control of the machine. Different combinations of i_{dq} can be chosen to fulfill the torque requirements but these different variations have a high influence on the entire system. The simulation is done in optimal conditions while the measurements can results in combinations which higher current or lower torque per ampere, which decrease the efficiency. Despite these deviations and the observed time lag, it can be seen that the chosen modeling approach is a suitable solution to depict the behavior of the components in dynamic cases.

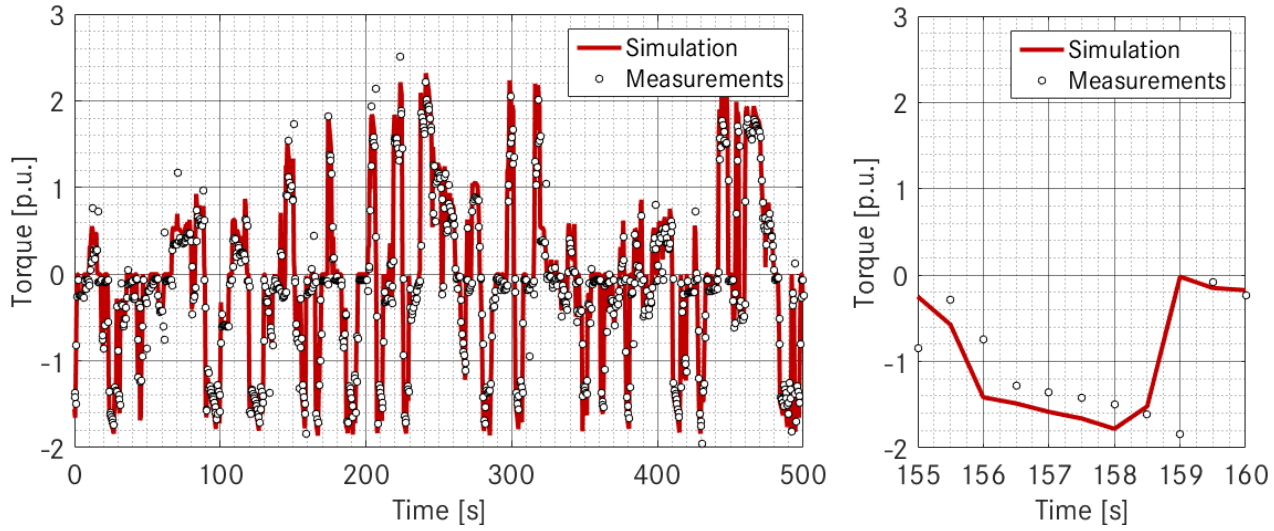

Figure 134: Torque comparison between simulation and measurements

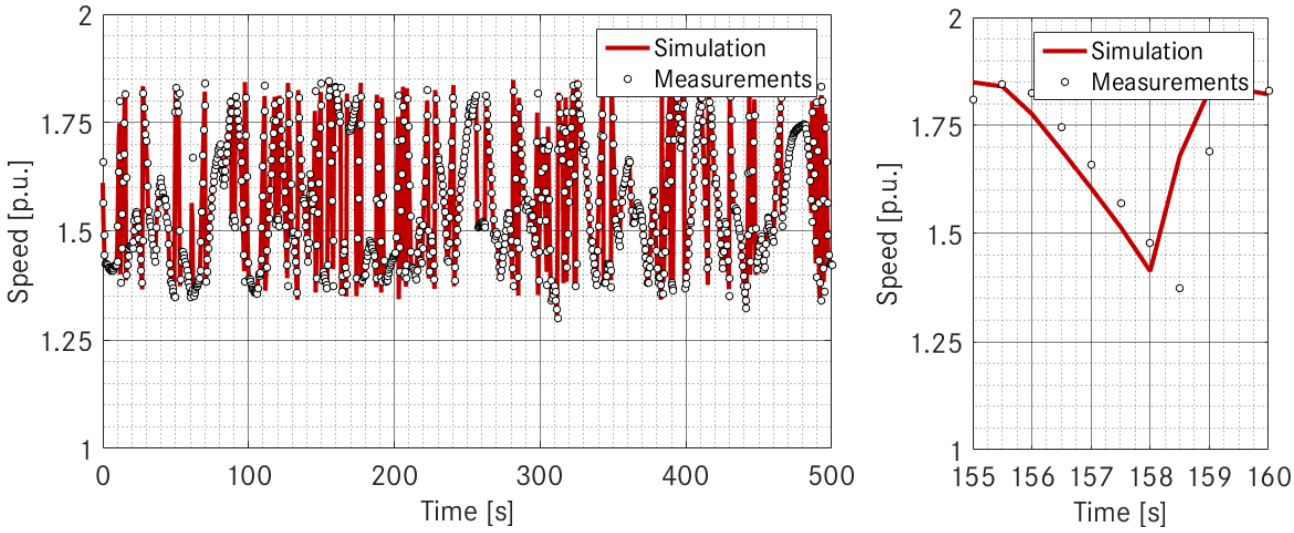

Figure 135: Speed comparison between simulation and measurements

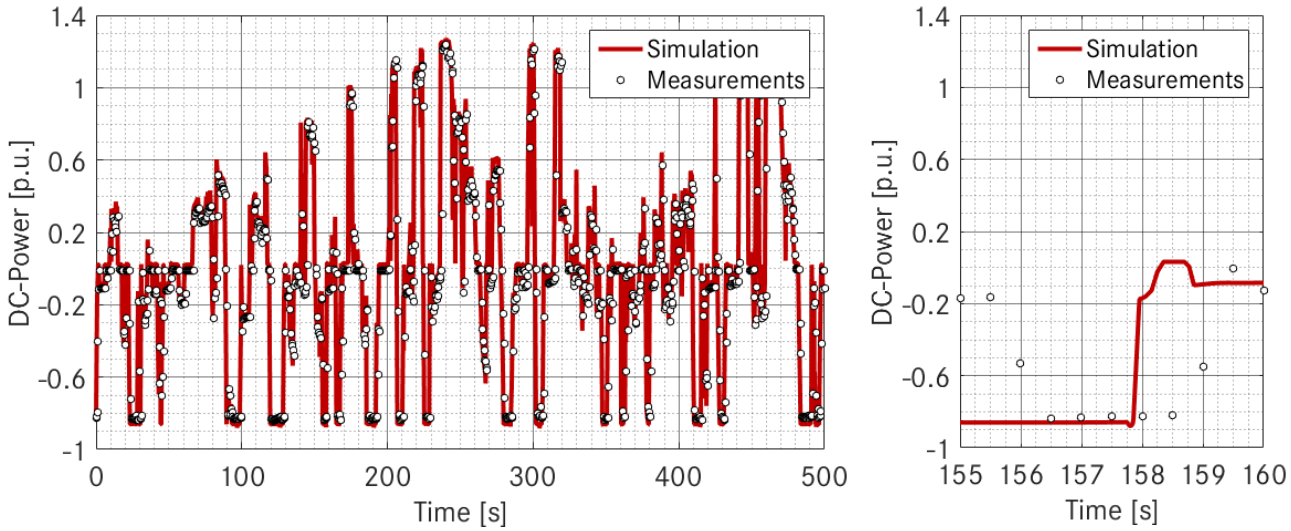

Figure 136: DC-Power comparison between simulation and measurements

3.2 Vehicle validation

To further validate the modeling approach, other measurements are done with the same system as previously in a global vehicle environment, where all the components are measured. Such an environment is quite challenging for the modeling because it has several external parameters which are not considered in this work. For example the influence of the external temperature or the additional cooling power thanks to the air flow around vehicle are outside the scope. In this sub-section, the simulation is performed using the data from the measurements in order to be as near as possible to the real results. For example the coolant temperature is not a constant value anymore but the data from the measurements are used and thus a time dependent coolant temperature is introduced. These adaptations within the simulation require some changes in the implementation without any major influence.

3.2.1 Considered configuration

Contrary to the previous validation, all components are considered. For the three main components, a time dependent coolant temperature profile is implemented and the torque and speed profiles from the measurements are used as inputs. Considering the modeling approach, the models without the energy management are considered because the derating functions are already implemented in the vehicle. Hence the resulting modeling is presented on Figure 137. The validation is done considering the following output parameters: the actual torque, the DC-power, the battery voltage and the SOC which are relevant parameters to evaluate the behavior modeling, the loss models and globally the correlation and the accuracy.

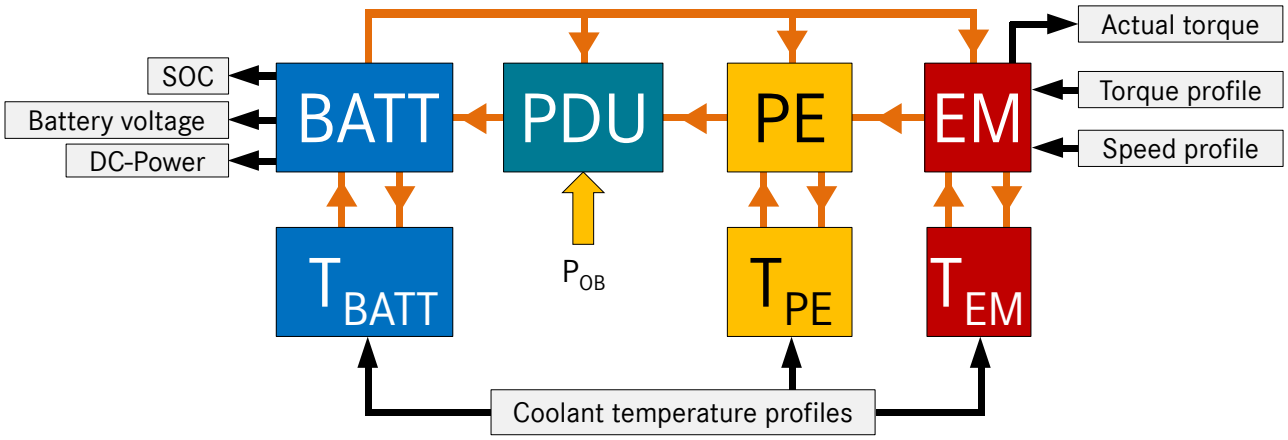

Figure 137: Considered configuration for the vehicle validation

3.2.2 Comparison of the system performance

The focus of this second validation is on the comparison between the simulation and the measurements for the entire system. The results are presented on Figure 138, Figure 139, Figure 140 and Figure 141.

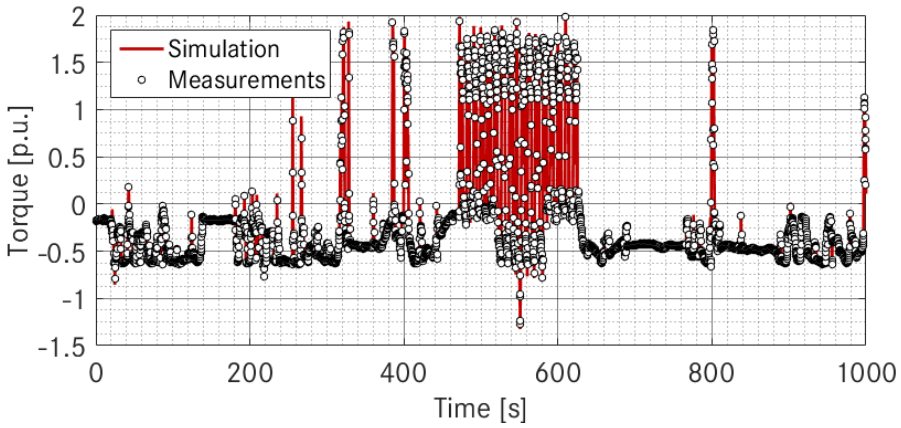

Figure 138: Torque comparison with vehicle measurements

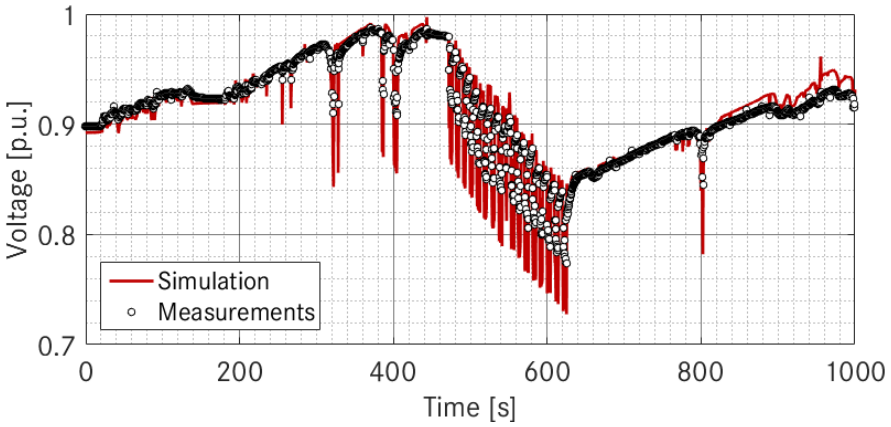

Figure 139: Voltage comparison with vehicle measurements

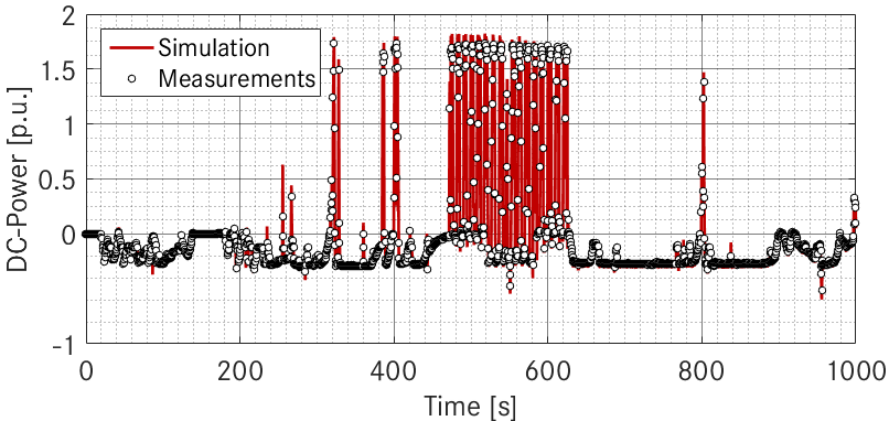

Figure 140: DC-Power comparison with vehicle measurements

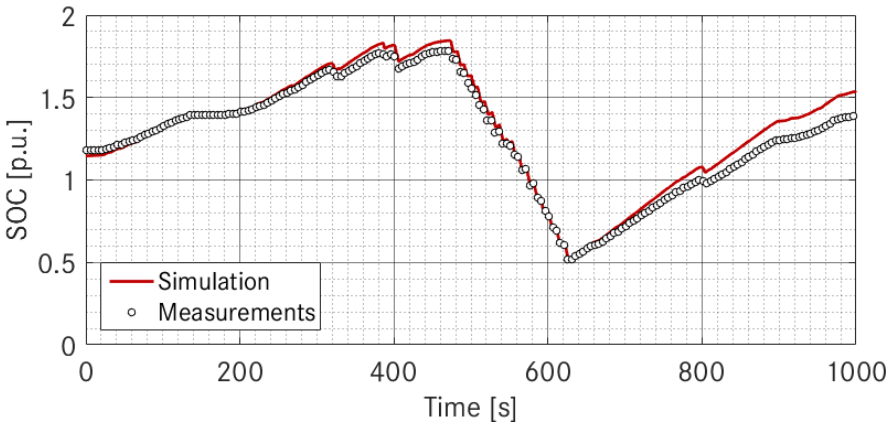

Figure 141: SOC comparison with vehicle measurements

Globally, the previous figures show a good correlation between the simulation and the measurements. Both the behavior and the amplitude between the simulations and the measurements are comparable. Contrary to the test-bench validation, the measurements devices are suitable to measure the dynamic behavior of the components and the deviation as well as the correlation can be calculated as shown in Table 27 and on Figure 142.

	Torque [Nm]	Voltage [V]	DC-Power [kW]	SOC [%]
Highest Deviation [%]	35.0	7.8	16.2	10.2
Correlation [%]	99.9	84.8	99.6	97.7

Table 27: Deviation and correlation for the validation of the global system modeling approach

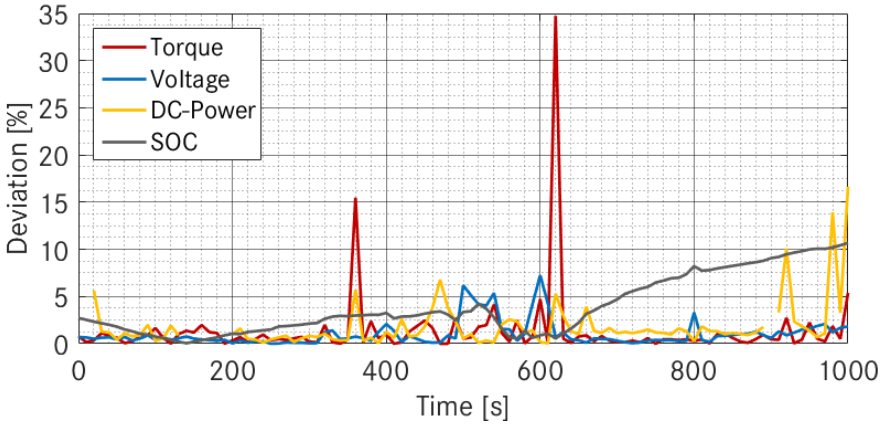

Figure 142: Deviation over the time for the validation of the global system modeling approach

These results confirm the first observations. The torque profile shows good correlations (99.95%) and low deviations except for two points which are probably artefacts from the measurements considering their low frequency of occurrence. The battery voltage shows a lower correlation (84.75%) and peaks are present in the simulations results. These peaks can be explained by the considered approach for the simulation. It aims to depict the energetic behavior of the system and the hypothesis done for the implementation of the modeling results in strong assumptions for highly dynamic behavior. For example, the influence of the DC-link capacitor on the voltage behavior is not considered and thus its damping effect on the voltage is not considered in the simulation. Considering these assumptions and the low deviations, it can be assumed that the simulation approach is suitable for energetic purpose. The DC-power further validates the suitability of the approaches. It shows high correlation and even if the deviations show discontinuities, they never exceed 20%. Finally the SOC shows low deviations and high correlation. The deviations are increasing with time but globally the behavior and the amplitude are highly comparable.

3.2.3 Comparison of thermal behavior

Even if the energy management is not considered because torque and speed profile already consider the thermal limits of the electrical system, the validation needs also to compare the thermal behavior of the system. The influence of the thermal behavior can be neglected on the current driving cycle for certification but remains a topic of interest for high load cycle where the performance are a key aspect.

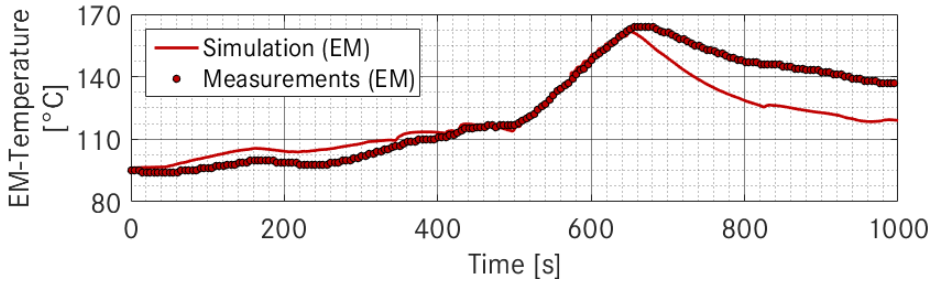

Figure 143: EM-temperature comparison with measurements

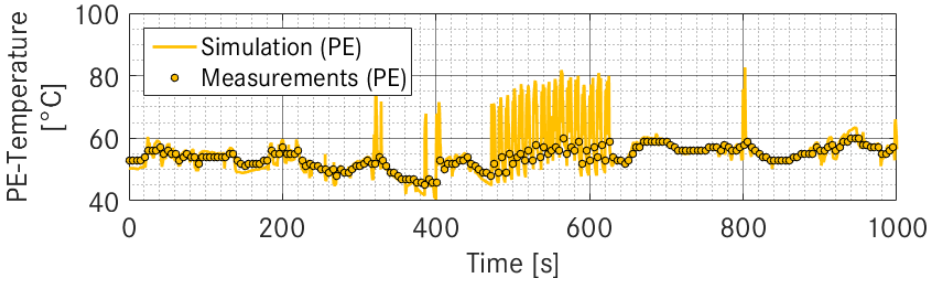

Figure 144: PE-temperature comparison with measurements

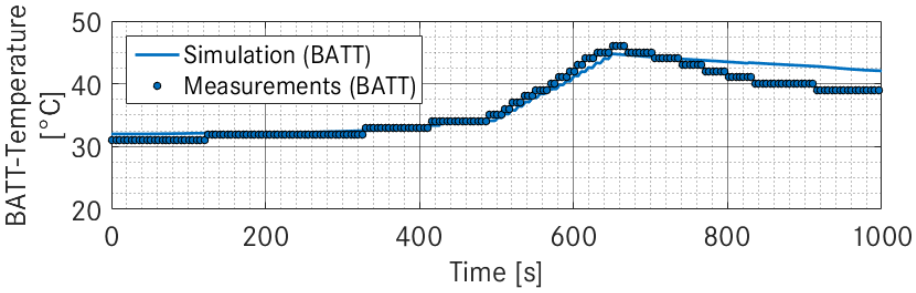

Figure 145: Battery-temperature comparison with measurements

As for the other parameters, the thermal behavior shows promising results for all three components. Considering the electric machine, it can be seen that during the cooldown phase, the temperature is decreasing faster than the measurements. This behavior is linked with the cooling concept of the machine where the coolant flow is depending on the machine torque and speed. Therefore the simulation considers constant coolant flows while in the vehicle, the value of the flows are dependent on the current driving point. For the power electronics, the correlation is quite good except some points where peaks appear. Finally for the battery, the correlation is pretty high and the simulation is actually showing higher temperature during the cooldown phase.

3.3 Summary

Considering the results presented here for both validations (test-bench and vehicle measurements), it can be considered that both the component and the thermal behavior modelings are suitable solutions to address the challenges considered in this work. The first modeling enables to depict with low deviations the behavior of the components under different loads and the second one enables to approximate the thermal behavior with low deviations. Moreover, considering the assumptions for the modeling and the hypotheses of the simulation (no considerations of the external conditions such as the external cooling effect due to the rolling car or dynamic behavior of the voltages and the currents), the global system modeling approach shows promising results.

4 Contributions of global system modeling

In this section the contributions of the chosen approach are discussed. They are shown by considering first the influence on the system torque, then the influence on the system properties (efficiency, voltage and current) and finally the influence on the energetic behavior as well as the integrability and efficiency.

4.1 System limits

To evaluate the influence on the system limits, the modeling approach introduced in this chapter is used. The investigations are divided in two sub-sections. In the first one, the contribution of the approach is show by considering the maximal system torque and in the second one the continuous torque is considered.

4.1.1 Maximal system torque

To show the influence of the method on the maximal torque, the system is modeled without energy management. Only the electric machine, the power electronics and the battery are considered. The considered modeling approaches are shown on Figure 146, where the top one show the global system approach (GSA) and the bottom one shows the modeling approach with a constant voltage as currently used. The comparison is done by evaluating the machine torque in different situations. In the first situation, the global system is considered and therefore the machine modeling is coupled with the modeling of the power electronics and the battery. It depicts the results of the modeling approach developed in this work. All other situations need only to consider the electric machine modeling because the voltage is supposed to be constant and thus the system torque is only related to the voltage level. The voltage is for all other situations considered as constant and taken equal to the open-circuit voltage (OCV) for the second situation and to the worst case voltage (U_{WoC}) for the third situation which is expressed in the following equations. After having analyzing the behavior of the machine, the voltage can be adapted to depict more accurately the behavior of the system by considering not the maximal current but the maximal battery current

observed during the first investigations. This voltage is generally called the design voltage (U_{Design}) and is expressed as follows.

$$U_{WoC} = OCV(SOC) - R(OCV) \cdot I_{max} \quad (90)$$

$$U_{Design} = OCV(SOC) - R(OCV) \cdot I_{design} \quad (91)$$

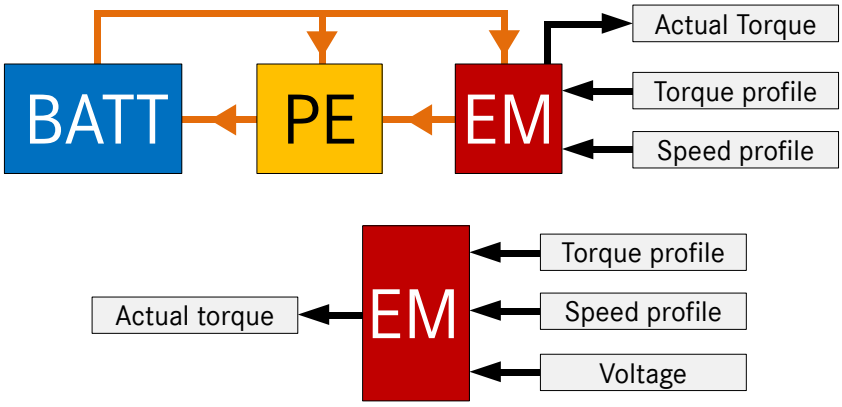

Figure 146: Considered modeling approaches to show the contribution of the global system modeling approach

The different voltage levels as well as the modeling approaches are compared on Figure 147, where the torque and the voltage over the speed are shown. For all the comparisons, the global system approach (GSA) is taken as reference to evaluate the other methods. The method based on the design voltage (U_{Design}) is really near the reference and the deviations are always under 2.5% while the two other cases are showing higher deviations up to 12% for the torque and up to 15% for the voltage. These comparisons show the first contribution of the method developed in this work. The global system approach can depict accurately the system behavior without knowing the behavior of the system or the required current while the other approaches have either high deviations or require pre-analysis of the system to determine the design current (I_{design}). To extend this analysis, the same approach is applied on the continuous torque.

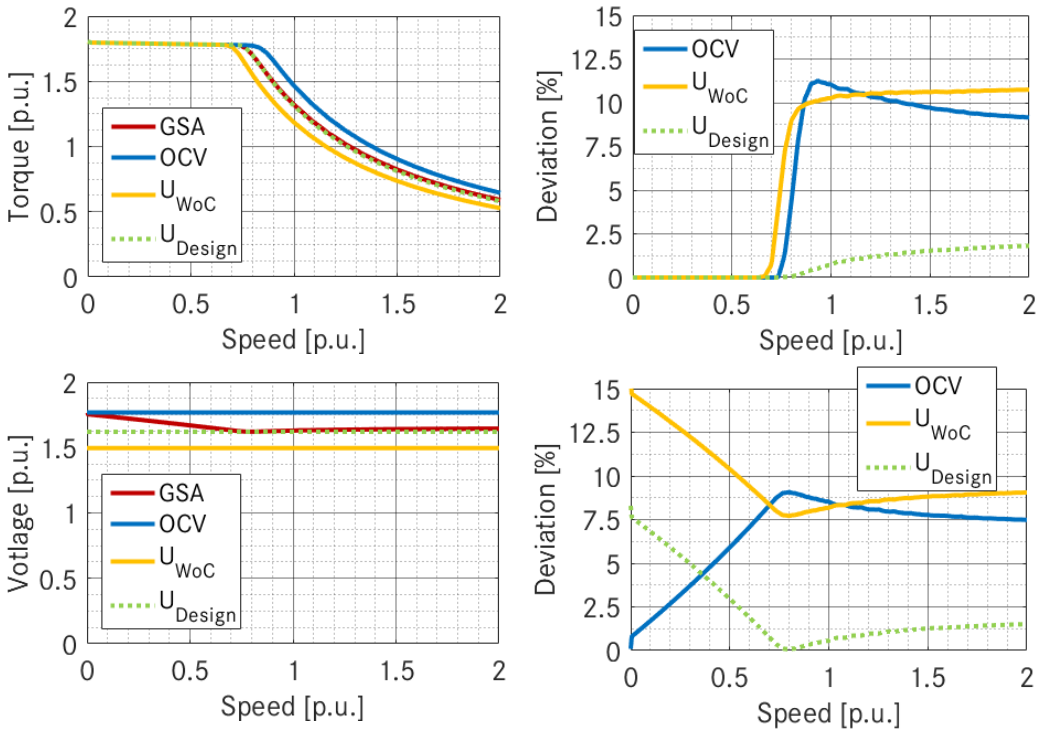

Figure 147: Results of the torque and voltage comparison between the different approaches and voltages

4.1.2 Continuous system torque

The continuous torque is defined as the torque which can be provided with a thermal load which results in an equilibrium in the system. It is an important parameter to consider because it depicts the machine performance in a partial load area where the behavior of the power electronics and the battery are different. To investigate the influence of the global system modeling, the same approaches as before are applied and the torque limitations due to thermal derating are introduced. In the case of the analysis presented here, the stator temperature limitation is activated to impose a limit on the torque. For each of the previous situations, the thermal limits are considered and the results are presented on Figure 148 and Figure 149 for respectively the torque and the voltage. On each figure the comparison is shown between the absolute values on the left and the relative evaluation is shown on the right using the deviation with the GSA as reference.

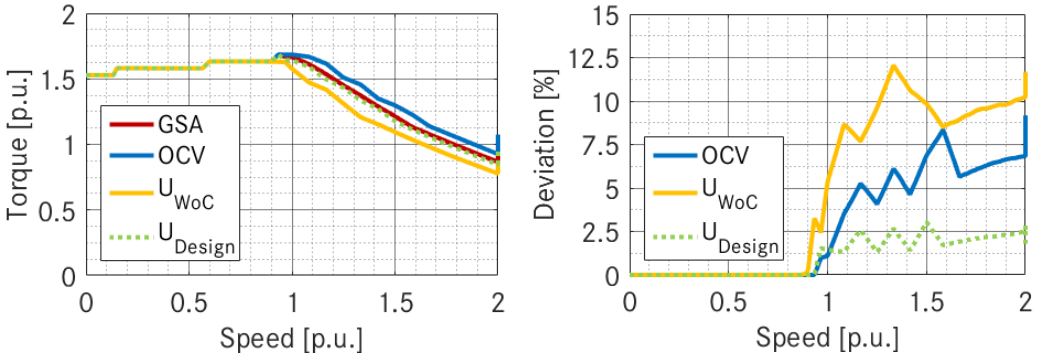

Figure 148: Results of the continuous torque comparison between the different approaches and voltages

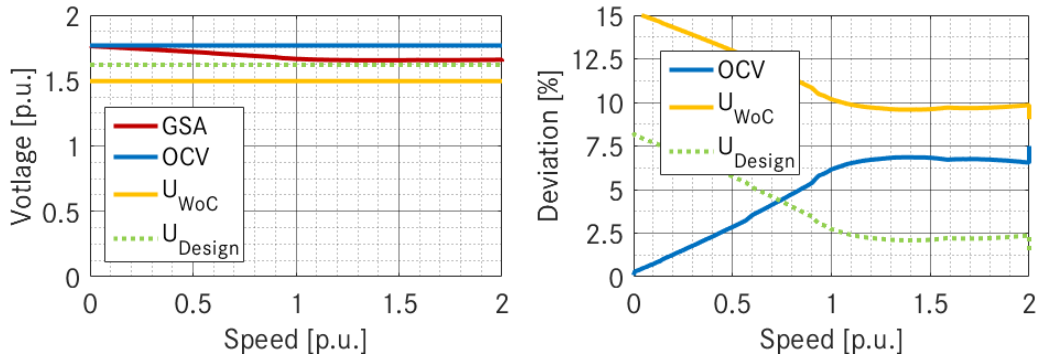

Figure 149: Results of the voltage comparison between the approaches and voltages for the continuous torque

Similar observations as for the maximal system torque can be done: the global system approach is the only method which enables to calculate directly the system performance without any pre-analysis (Design voltage) or without high deviations (Worst-case). The figure shows that the OCV overestimates the performance of the system while the worst-case method and the voltage design method are too conservative. However among the three methods, they are the most suitable because they underestimate the performance of the system and therefore ensure the fulfillment of the requirement while the OCV based method can lead to under-dimensioning because the performance is overestimated.

4.2 System properties

Beside the system torque which is an important criterion of evaluation for the system, this sub-section investigates the influence of the retained modeling approach on the global system properties. Indeed not only the system limits are investigated but also the efficiency, the current and the voltage of the system.

4.2.1 System efficiency

In this first part, the system efficiencies for the different approaches are compared. For this purpose the isolines for different values of the efficiency are shown and the deviations between the curves are considered. The results of

the investigation are shown on Figure 150. As for the system torque, the design voltage approach shows promising results but requires pre-analysis of the system. The other two approaches both show higher deviations but do not require any pre-analysis of the system. The worst-case approach shows really diverging behavior compared with the global system approach while the OCV are showing comparable results in the maximal torque area and higher deviations in the field-weakening where the behavior is directly linked with the maximal available voltage as depicted by the equations (6) and (7). The deviations are also really dependent on the considered efficiency and on the load, in the low speed and low torque areas (contour eta 90% for example), the deviations between the systems can be only hardly recognized because the voltage have less influence while in the higher load area (contour eta 94% for example), the deviations are explicite. As previously for the system torque evaluation, the design voltage approach shows the best results but requires pre-investigation while the worst case approach is too conservative and the OCV approach too optimistic.

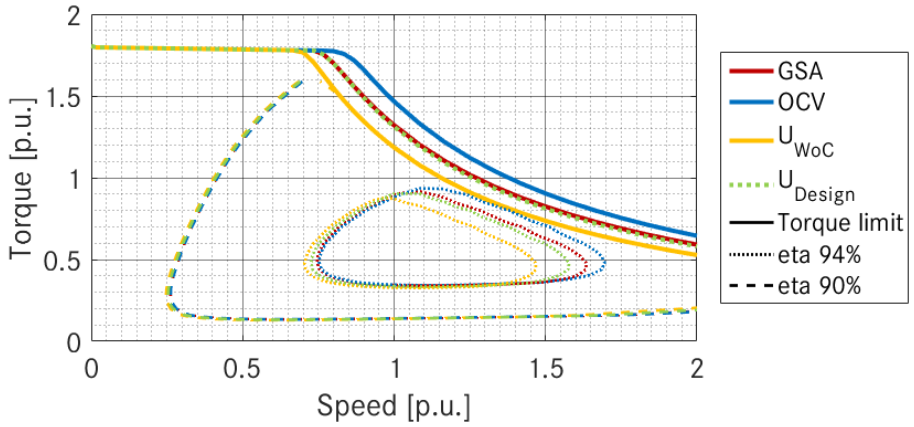

Figure 150: Comparison of the calculated efficiency for different modeling approaches

4.2.2 System voltage

In this second part, the system voltages for the different approaches are compared. For this purpose the deviations between the different solutions are shown and analyzed and the results are presented on Figure 151.

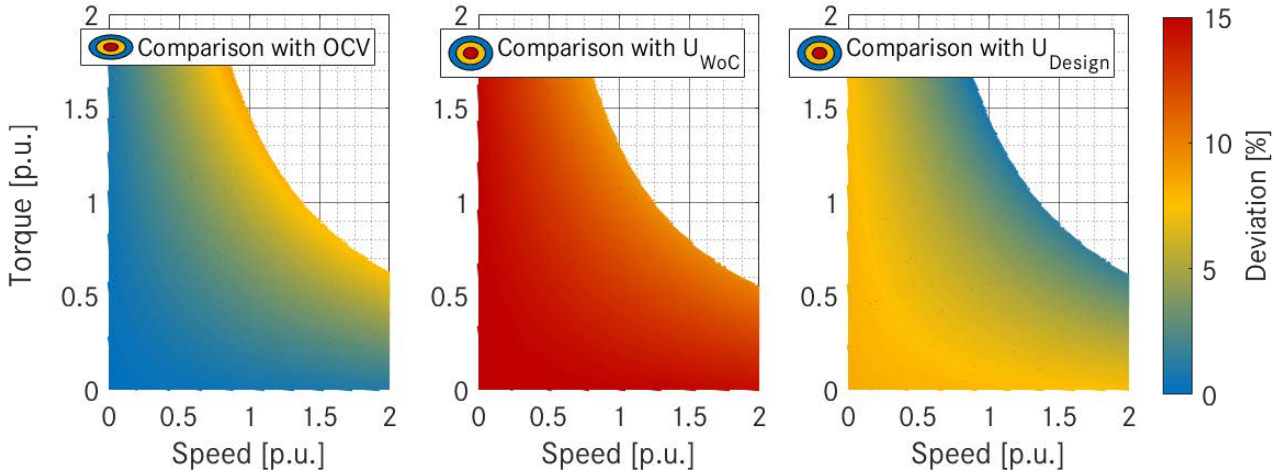

Figure 151: Comparison of the calculated system voltage for different approaches

All solutions are showing deviation because the global system approach is the only solution with a load-dependent voltage. The OCV and the design voltage approaches are showing opposite behavior because one represents an approximation of the voltage behavior near the torque limits while the other one is the voltage when no load is applied. The worst case voltage is as previously for the system torque showing really high deviations (up to 15%) and is not adapted for the design process. From these results, it can be deduced that the OCV approach would be the "most suitable" solution in the partial load area and the design voltage approach in the high load area. These results show the importance of the voltage variations during the investigation of the electric machine and electric drive

system and how the global system approach enables to design system which fit the requirements without requiring pre-analysis.

4.2.3 System current

Finally the AC-current is also compared to show the influence on the global system which. As for the system voltage, the deviations between the different approaches are calculated and presented on Figure 152, where the global system approach is taken as reference for the calculations.

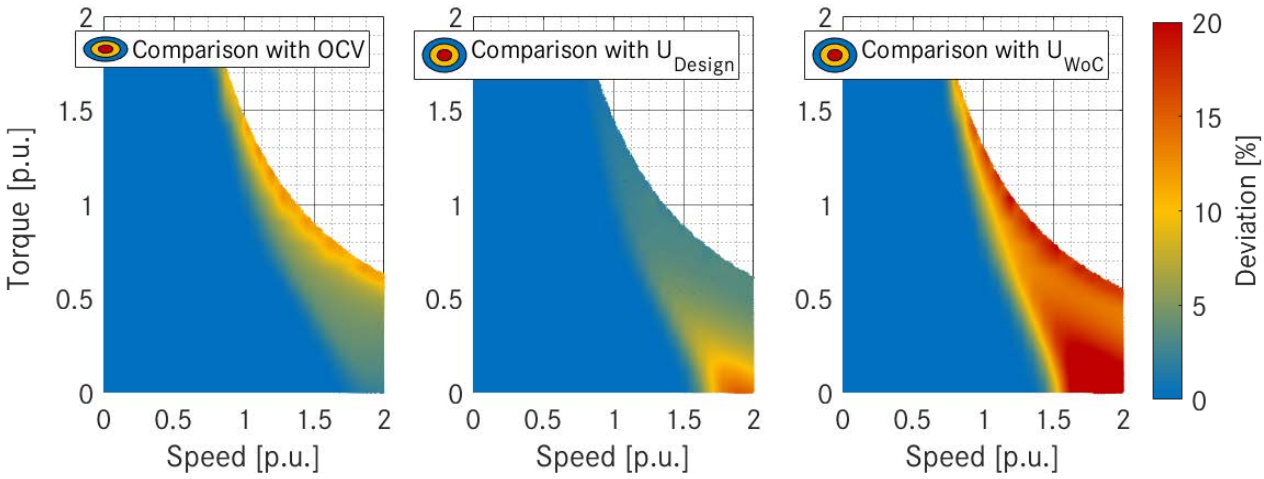

Figure 152: Comparison of the calculated system current for different approaches

Considering the behavior of the electric machine, the deviations of the AC-current can be principally observed in the field-weakening area where the maximal available voltage plays a preponderant role. Indeed, before reaching this area, the voltage gap between the different approaches can be compensated by the modulation and no effects are observed. However in the field-weakening area, near the limits of the machine, the influence of the voltage gap can be observed and lead to deviations up to 30% for the worst case approach. As for the system torque, the design voltage approach is the solution which shows the most reliable behavior considering the global system approach as reference.

4.3. Energetic behavior

In sub-section, the global modeling approach as presented on the Figure 131 is used. The energetic behavior of the system is simulated and analyzed. First the topic of the time dependency is discussed, then the driving cycle is evaluated first with the time-dependent method developed in this work and finally with a time-independent solution.

4.3.1 Time dependency

For the purpose of this work, a time-dependent modeling approach is considered. However, other solutions can be considered such as driving points based solutions as in [142]. These solutions investigate the components by analyzing their performance for defined points but neglect their chronological order. The representations of these methods are shown on Figure 153. The same driving cycle is considered but on the left, only the speed and the torque are considered (time-independent) while on the right, the time-dependency of the torque and the speed is investigated. To show the contribution of this work, the comparison is divided in two parts, first the influence of the voltage approach is considered and then the influence of the time dependency in the two next sub-sections.

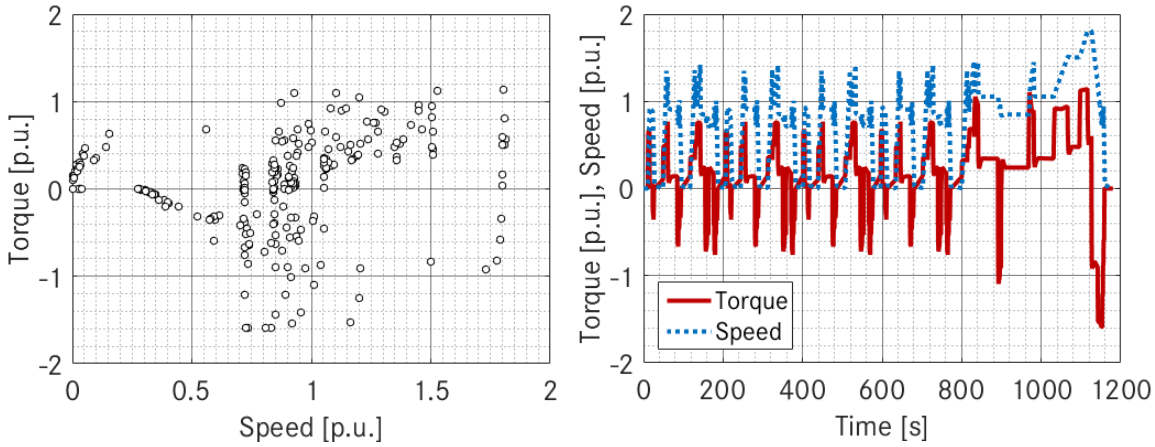

Figure 153: Representation of the driving cycle for the different analysis method for hybrid electrical vehicles

4.3.2 Contribution of the global system approach

The time dependent approach developed in this work is applied on the four design solutions (GSA, worst-case, OCV and design voltage) used previously to compare the system torque and performance. To analysis them, two parameter are considered: the TPI and the SOCI, which results are presented in Table 28 and on Figure 154.

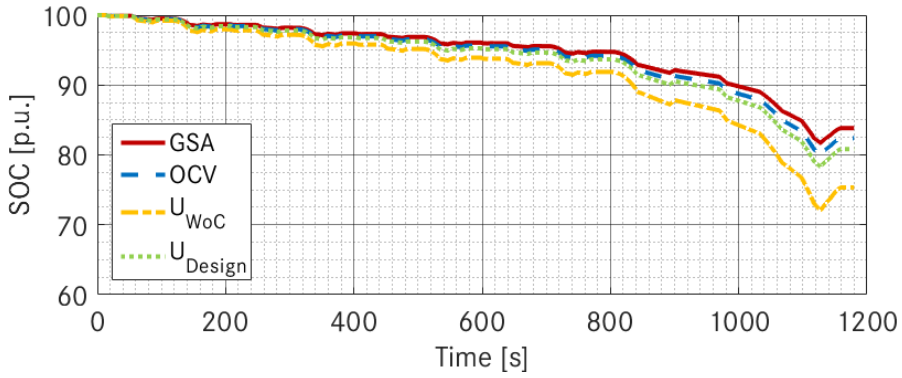

Figure 154: State of charge over time for the different methods

	GSA	OCV	U_{WoC}	U_{Design}
TPI	100%			
SOCI	100%	98.3%	89.9%	96.4%

Table 28: TPI and SOCI for different values of the voltage for design purpose

All the systems can achieve the torque requirements and thus no difference can be seen considering this factor. However when analyzing the SOCI, higher deviations are reached depending on the assumptions concerning the voltage. These differences show how the GSA method leads to a system which fit the requirements while the other can lead to over dimensioning of the system. For the calculation of the SOCI, the GSA is taken as reference and therefore a value over 100% could have been expected for the OCV method. However, beside the voltage-dependency, the GSA method considers also the SOC dependency. Under this assumption, it happens that the voltage is over the OCV at 50% SOC during driving cycle analysis which explains why the GSA has a higher SOCI.

4.3.3 Comparison with time-independent solutions

To compare the time-independent solution an equivalent to the SOCI need to be found (the TPI is not considered since all the solutions achieve the torque requirements). For this purpose, the mean system efficiency is considered because it is the one of the most representative parameter for the energetic behavior in time-independent solutions. The results are presented in Table 29 and show opposite results to the time-dependent solution. These results can be explained by the fact that the other methods (OCV, worst case and design voltage) are based on assumptions which neglect the load and SOC-dependency and could lead to higher efficiency. Moreover the system mean

efficiency is an arithmetic value while the SOCI is load and SOC dependent. Consequently it shows that beside the design aspects, the GSA also enables to evaluate the real behavior of the system and the time-dependency is required to fulfill the goals set for this work.

	GSA	OCV	U_{WoC}	U_{Design}
Mean system efficiency [%]	88.8%	89.1%	89.7%	89.3%
SOCI	100%	98.3%	89.9%	96.4%

Table 29: Comparison between time dependent and time independent solutions

4.4 Integrability and efficiency

In this part, the contribution of methods for the integration investigation are shown. The methods are analyzed by comparing them with the results of a component focused investigation as the one presented in the chapter 2 where the influence of the voltage on the electric machine is investigated. For this purpose, the same system is considered and some assumptions are done: only one electric machine, two power modules (650V and 1200V) and one cell type are considered because the focus is on the voltage dependency and not on the sub-components properties. The SOC and load dependency of the voltage as well as the thermal behavior are also neglected to set the focus on the voltage dependency, the efficiency and the system integrability. The considered machine is a permanent magnet synchronous machine and no adaptations of the design are made and therefore the voltage and the current influence the performance as defined by the equations (6) and (7). The SOCI requirements are defined by the following conditions: a SOC higher than 60% is expected at the end of the driving cycle. Finally the integrability is evaluated considering only the power electronics and the battery with the following assumption: since only one cell type is used, non-integer values are considered to show the voltage dependency and not the dependency on the cell properties. The references presented in Table 30 are used to evaluate the integrability. The aim of this investigation is not to determine any optimum but only to show the contribution of the global system modeling approach considering the integrability.

	Length [mm]	Width [mm]	Height [mm]	Weight [kg]
Power electronics (reference)	300	250	200	9
Battery (reference)	1000	500	300	60

Table 30: Reference for the integrability evaluation

The results are presented on Figure 155 for a 50V step and the assumptions previously discussed. In the case of this investigation the CIIs are not considered with the quasi-Boolean approach but only by considering the ratio between the reference values and the simulated values. The results compared the efficiency for the maximal power and the utilization of the machine as in the chapter 2 for the components focused design with the SOCI and the CIIs for the global system approach.

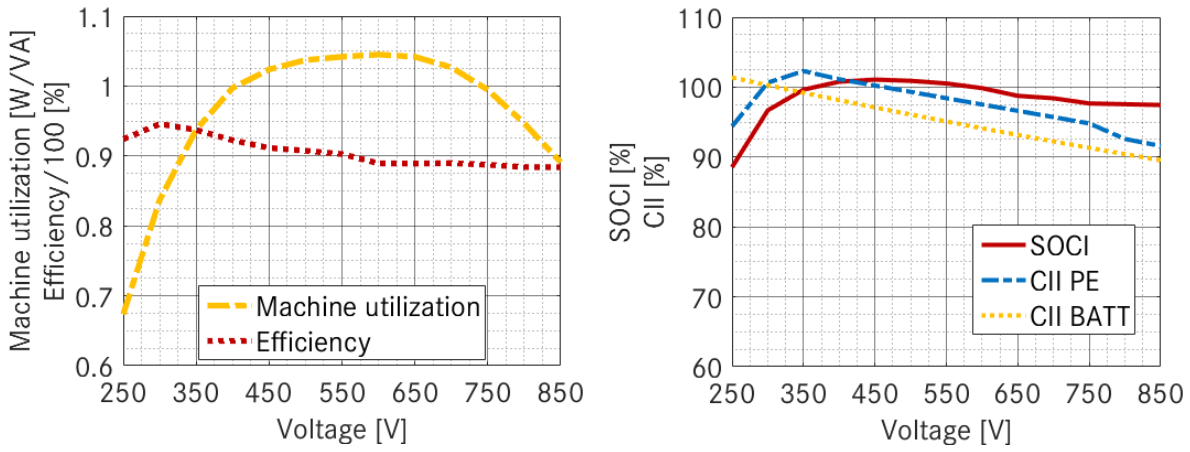

Figure 155: Influence of the voltage on the electric machine for a constant mechanical power

The necessity of the global system approach is first validated by the voltage dependency of the results. For the considered components and hypothesis, the SOCI reaches a maximal value for 450V, the CII of the PE for 350V and

250V for the battery. Even if the results are linked with the hypotheses of the investigation (single machine, only two power modules and non-integer number of cells), they enhance the previous results for single component investigations and confirm the diverging voltage dependency of the components. The necessity of the global system approach is also confirmed by the divergence between the machine investigation results (left on the figure) which shows optimum around 350V (efficiency) and 600V (utilization) and the global system results (right on the figure) which shows optimum around 250V (battery integration), 350V (power electronics integration) and 450V (SOCI).

5 Chapter conclusion

This chapter is focused on the global system modeling and organized around the following topics: the review of the present methods, the implementation of the components modeling to develop a system method, the validation of the methods with measurements and finally the contributions of the global system approach. In the first section, the required definition and representation for a good understanding of the challenges are introduced. Then the current methods are reviewed and their suitability for the considered problem is analyzed. Based on the results of this analysis, a time-dependent bidirectional approach is set as focus for the component behavior modeling and the interfaces for the evaluation are defined. The inputs are characterized by the torque profile, the speed profile and the available volume while the outputs are defined by the performance and the integrability of the system. In the third section, the implementation is discussed and the required adaptations are introduced. The methods for the calculation of the outputs based on the components characteristics are explained and the implementation of the different limits (thermal, electrical and energetic) is detailed. After this, the modeling approach is validated based on two measurements series: one on a test-bench where only the electric machine and the power electronics are measured and a second one where the entire electrical system is measured during vehicle tests. For both measurements, the simulations are showing promising results with low deviations which are generally due to external parameters which cannot be considered (passive cooling in the vehicle for example). Finally the contributions of the global system approach are shown for several parameters: system limits, system properties, energetic behavior and system integrability and efficiency. The most significant contribution is the influence of the voltage level. Present design methods are based on a single voltage value and even if the evaluation are performed for variable voltage, this section has shown that it also plays an important role for design purpose. The method enables to increase the accuracy of the design during the early development phase by estimating the global system performance without requiring any pre-analysis or conservative methods. The variations of the battery voltage influence all the other components and lead to a design which fits the requirements while the other methods (OCV, worst-case and design voltage) leads to over- or under-dimensioning of the system. The analysis of the energetic behavior shows the importance of the time-dependency through the voltage variations with the load and the SOC. It also shows from an integration point of view the influence of the voltage and how the integration investigation methods enable to enhance the investigation since the volume can be estimated for different values of the voltage instead of optimizing the design of the components for an estimated value of the voltage under load. Hence, this chapter has further shown how the combination of the suitable components modeling with the suitable approach enable to enhance the design despite the assumptions done during their development and it sets the basis for the optimizations presented in the next chapter.

Chapter 6: Optimization of eDrive systems for hybrid electrical drivetrain

After having defined the right modeling approaches for the components and the global system method, this chapter discusses the topic of the optimization. It introduces first basic knowledge for the understanding of the topic, then discusses the relevancy of the different methods and algorithms, the determination and the implementation of the chosen method with the DIRECT algorithm. Then the method is coupled with the global system model presented in the previous chapter and the combined method is applied on several examples for three drivetrains to address the challenges considered in this work.

1 Optimization, evaluation methods and algorithms

The electro-thermal modeling of the components and the investigation of their integration is the first step toward the optimization of the electric drive system but beside the determination of the right modeling approach, another challenge is to find the suitable optimization approach. In this section, some definitions are introduced to avoid any confusion in the rest of the chapter and then the evaluation methods for optimization purpose are detailed.

1.1 Definition

In this first sub-section, the differentiation between the terms constraints and criterions are defined and explained to avoid any confusion. The following definitions are extracted from a reference English (US) dictionary [143]:

- **Constraint:** something that limits or restricts someone or something.
- **Criterion:** something that is used as a reason for making a judgment or decision.

Taking into account these definitions and the automotive industry environment of this work, the requirements which are used for the optimization in the rest can be split in two categories. First there are the criteria which need to be fulfilled to consider a solution as suitable for the application. Then other criteria are used to differentiate a suitable solution which fulfils the constraints from an optimal solution which fulfils them in the best manner. Considering the SOCI defined in the previous section, the criterion is to have a SOCI greater than 100% while a SOCI greater than this value is only required to compare the solution which fulfils the requirements.

1.2 Evaluation methods

Optimization problems are defined by a function based on the criteria which needs to be minimized or maximized considered the constraints. An example of a mathematical description is shown in the following equations where the function(s) f_i need to be maximized considering the constraint(s) g_j which must be lower than the constant(s) a_j for the input vector X.

$$\begin{cases} \max(f_i\,(X) \;\; i \in \{1, \dots, n\} \\ g_j\,(X) \leq a_j \;\; \forall j \in \{1, \dots, m\} \end{cases} \quad (92)$$

The optimization problems can be multi-criteria (n>1) with one or several constraints. Multi-criteria problems are recurrent for system optimization since the aim is to find an optimal system and not the combination of optimal components. This type of problem can be solved using several methods as shown in [144] and [145]. The rest of this section is focused on the different methods for multi-criteria problems due to the considered investigations.

1.2.1 The weighted sum method

The principle of the weight sum method is to transform the multi-criteria problem into a single-criterion problem using a weighted sum. To each criterion is affected a weight to express its importance in the system evaluation, then instead of minimizing (or maximizing) each criterion, the sum of the product of each criterion with its weight is considered. The approach is resumed in the following equation where f_i are the criterions and ω_i the corresponding weights (example for a minimization problem). The methods to solve a single criterion problem are well-known and the problem can then solved by choosing the adapted coefficient ω_i and by using conventional algorithm for single-

criterion optimization such as: deterministic methods (local or global), metaheuristic methods, genetic algorithm or the particle swarm algorithm as described in [144] and [145].

$$\min \sum_{i=1}^{n} \omega_i \cdot f_i(X) \quad (93)$$

1.2.2 The optimum in the mean of Pareto

This method does not search a single optimum but all the solutions that satisfy the requirements equally well as depicted on Figure 156. Each of these solutions satisfies the constraints of the investigation but does not equally minimize or maximize the criterions. All of the points depict compromises between the criteria.

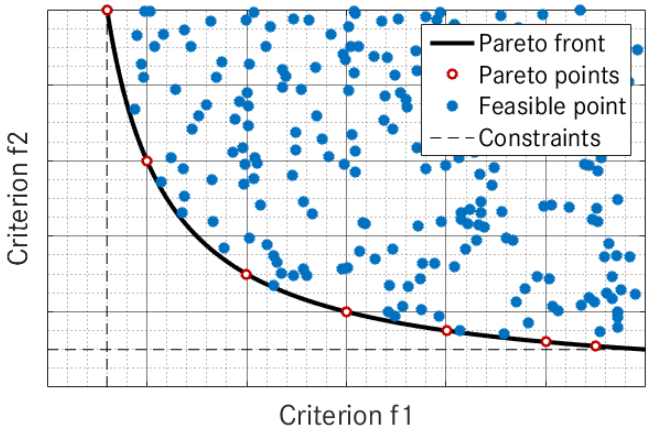

Figure 156: Example of a Pareto front for two criteria f1 and f2 to minimize

This approach can determine a range of equally good solutions for the solution space: one criterion cannot be improved without worsening the others. For this method, the solution space generally evolves through the generation of solutions until the front identification. This approach is generally combined with Genetic Algorithms (GA) or with Particle Swarm Optimization (PSO) which create new generations for each iteration as described in [144] and [145].

1.2.3 Other methods

The two previous methods represent two types of multi-criteria optimization methods, one where the problem is transformed into a single-criterion problem and the second one which determines compromises and does not search for the global optimum. Beside these methods, variants can be deduced or hybrid methods can be used. The variants are based on the same principle as one of the previous methods but differ in their evaluation. For example, based on the weighted sum method, the same approach can be used to transform the multi-criteria problem into a single-criterion problem by considering the product or the ratio of the function which are being maximized or minimized. On the other side, the hybrid methods can be divided into two categories: the first one is the conversion of multi-criteria problems into several single-criterions while the second one is the combination of local optimal methods with exploration methods. The first approach tends to concentrate its research on the extreme limits of the Pareto front because it considers the criteria separately and can be solved using the Vector Evaluated Genetic Algorithm (VEGA) which is an adaptation of the genetic algorithm for multi-criteria problems [144]. The second approach has shown potential to solve global optimization of multi-criteria problems by combining exploration methods with conventional algorithm (such as the gradient method) as it can be seen in [146].

1.3 Optimization algorithms

After having defined the environment of the optimization and the different methods, this sub-section reviews the different algorithms for optimization purpose. The review is divided into two parts, the first one discusses the case of the evolutionary algorithm and the second one deals with the case of the exploration algorithm. In each case the type of algorithm is explained from a general point of view and then its relevancy for the considered problem is discussed considering a simple example.

1.3.1 Evolutionary algorithm for system investigation

The evolutionary algorithms as considered in this work, regroup in one category the algorithms which are using crossing and mutation based on an initial generation to determine the optimal solution. This algorithm are based on the following approach:

- A first generation is randomly given
- The generation is evaluated
- From the selected solutions, crossing and mutation are done to create a new generation
- While the stopping criteria of the algorithm is not reached, steps 2 and 3 are repeated

This type of algorithms is generally used for early development stage of the development process, where different power and energy combinations are investigated as it was shown in the first chapter. Most of the investigation are based on the genetic algorithm which is a recurrent and reliable solution for design purposes. This approach is detailed on Figure 157 for the generation N and the generation N+1. During the process, the solutions (c), (d) and (e) are selected among the generation N while the solution (f) and (g) are resulting respectively from the crossing of (c) and (d) and the crossing of (d) and (e).

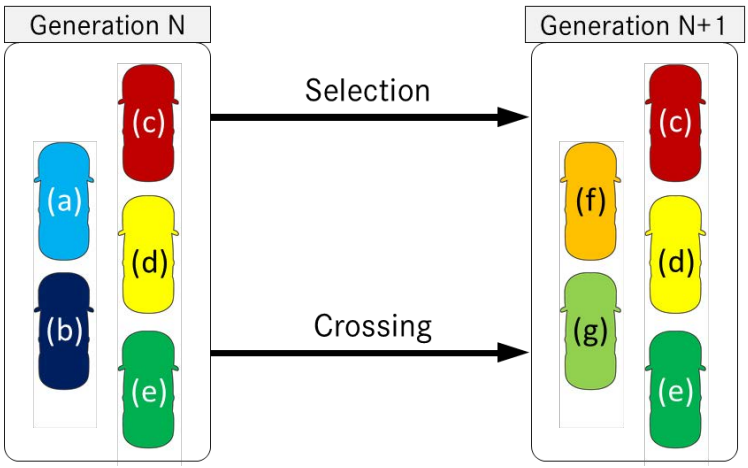

Figure 157: Evolution between the generations in genetic algorithm based on [144] and [145]

Evolutionary algorithms are suitable solutions for design process where geometrical (for example combination of stator and rotor geometries) or for drivetrain concepts investigation (combination of different power and energy classes) but the crossing process which is the core of these algorithms is also the main issue for the considered problem in this work due to the investigated parameters (especially the voltage and the current level). To explain this issue, the situation in the Figure 157 is taken as example. The following arbitrary hypotheses are considered (which are chosen on purpose to identify the issue of the evolutionary algorithms):

- (c) has the best electric machine, (d) has the best power electronics and (e) has the best battery
- (c) has a voltage level of $450V_{DC}$, (d) of $300V_{DC}$ and (e) of $600V_{DC}$
- (f) is the crossing of (c) and (d) taking (c) as basis and replacing the power electronics in (c) with the one from (d)
- (g) is the crossing of (d) and (e) taking (e) as basis and replacing the power electronics in (e) with the one from (d)

When considering the different combinations we have theoretically improved (c) with the power electronics from (d) and (e) with the power electronics from (d). However considering the voltage levels (second hypothesis) none of these solutions can be considered as valid due to non-corresponding voltage. These solutions could be filtered by the selection steps by defining a penalty or a constraint for these cases.

1.3.2 Exploration algorithm for system evaluation

In [47], the authors compare different algorithms for a hybrid vehicle design optimization (optimal power, energy and weight). Among them, another type of algorithm can be identified: the exploration algorithm as the PSO (Particle

Swarm Optimization) or the DIRECT algorithm. These algorithms do not calculate successive generations by doing crossing and or mutation but define an efficient way to explore and find the optimal solutions as shown on Figure 155 for the DIRECT algorithm.

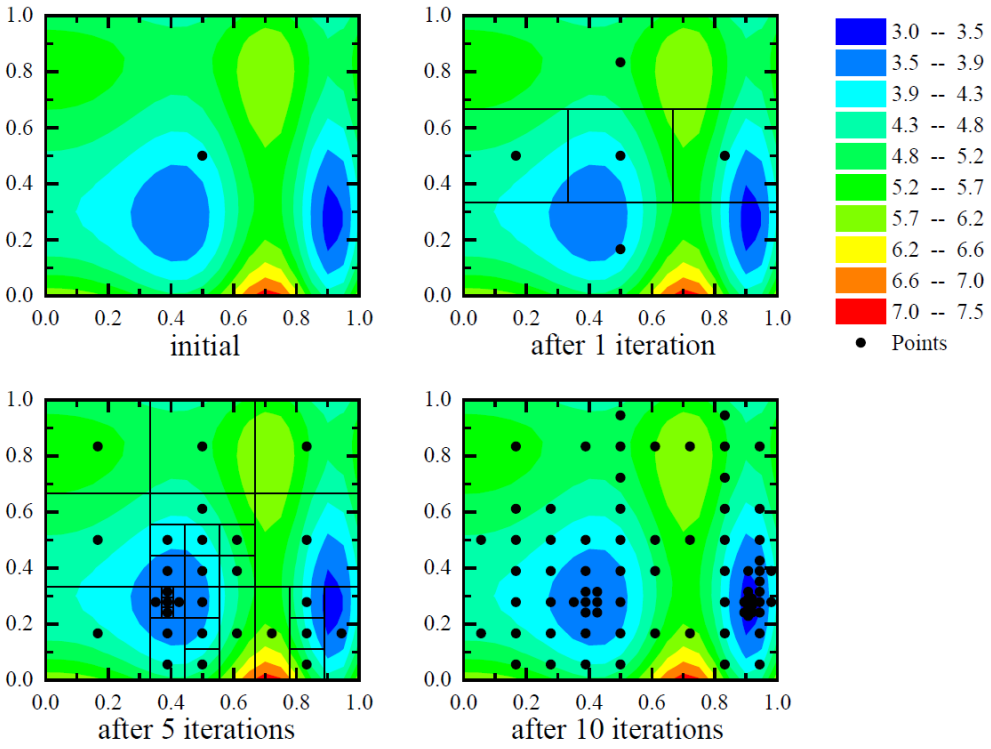

Figure 158: Example of use for the DIRECT algorithm for a minimization problem from [47]

The exploration algorithms are not based on the crossing of the previous generation but define the next generation based on the search of an optimized way to cover the entire range. It requires that the combinations are already defined and that the algorithm only defines the optimal way to explore the investigated area using the divided rectangles from the DIRECT algorithm or the particle swarm effect (based on the observation of bird or ants behavior). This type of algorithm is suitable for the considered problem since it can filter the invalid solutions in the pre-processing instead of eliminating them (which include evaluating them) during the optimization process.

2 Determination and implementation of the optimization approach

Based on the analysis of the optimization algorithms and the evaluations methods, this section is focused on the determination and the implementation of the right optimization approach by considering in more details the environment of the problem. It describes first the evaluation approach considered in this work, then the chosen optimization algorithm and finally the implementation in the simulation environment are shown. For each part, the contribution versus conventional solutions are shown.

2.1 Evaluation approach determination

This first sub-section discusses the determination of a suitable evaluation approach for the considered problem. It describes first the environment of the considered problems: the automotive industry and then the chosen approach based on the review performed in the previous section. Finally, the contribution of the chosen evaluation approach is shown on an example.

2.1.1 Optimization environment: the automotive industry

One of the main aspects of this work is the consideration of an industrial environment and the implementation of its boundary conditions directly in the methods and evaluations of this work. The case of the automotive industry is already addressed in the previous chapter to define the evaluation of the components integrability. Indeed, the

industry does not primarily focus on extending the technical boundaries of the components power or energy density. It requires having a Boolean approach: the components fulfill the constraints or not, but also the possibility to determine valid systems. A system is considered as valid if all the components are integrable (SII) and if the entire system fulfills the performance constraints (TPI and SOCI). Moreover the term compromise needs to be discussed in detail. In the case of a Pareto-Front or a weighted sum approach, compromises can be the best combinations of the components as aimed in this work but also a combination of a really good component with worse components whose performance are compensated through the weighted sum. Since the multi-criteria problem is reduced to a single-criterion evaluation, it is difficult to identify these non-valid solutions. Hence another approach needs to be defined to identify the best combinations of components instead of the combinations of the best components.

2.1.2 Evaluation approach

To fulfill the requirements of this work, the weighted sum is replaced with a product of the different criteria. The criteria included both the evaluations (performance) and the constraints (integrability) and are based on a Boolean approach. The evaluated value is therefore the product of the SPI (System Performance Indicator) and the SII (System Integrability Indicator). While the SII is already defined as the interface to evaluate the system integrability and already considered the Boolean aspect of the problem, the SPI still need to be defined. The SPI is the product of the SOCI and the TPI if and only if both indicators are greater or equal 1 (or 100%) as depicted in the following equation.

$$SPI = TPI\ (if\ TPI \geq 1) \cdot SOCI(if\ SOCI \geq 1) \quad (94)$$

2.1.3 Contribution versus conventional approaches

The contribution of the chosen evaluation approach relies on the Boolean aspect and the choice of a product instead of a weighted sum. To show the contribution of these two aspects, a drivetrain concept is chosen, constraints and criteria are set and components are defined. The evaluation is based on combination from three electric machines, three inverters and three batteries. The details of the components as well as the methodology is presented in the Appendix 8. The comparison is done using the three following methods: the weighted sum method (WSM), the product approach (PA) and the product approach combined with a Boolean approach (PAB). The evaluation criterion of each methods is depicted in the three following equations. The chosen example is exaggerated on purpose to show the differences between the considered methods and the weighted sum method. The aim is thus not to evaluate the performance of the considered components but to compare the method. The results on Figure 159 shows the difference between the method and the contribution of the chosen is directly observable. Considering the weighted sum method, the “best” system is System 5 because the higher torque and power compensate the worse integrability due to the considered approach. When applying the product approach, the “best” system is the third one. In the product, there is less compensation and therefore the system 5 which does not fulfill most of the integration requirements lost its first place. Moreover considering the Boolean approach, only systems 2 and 3 are valid and the third system is confirmed as the “optimal” one. This short example shows the added-values of this evaluation, it directly considers the integrability issues and thus only the valid systems. It also does not allow any kind of compensation by considering a product instead of a weighted sum and show how the PAB fulfills the requirements of the optimization done in this work.

$$WSM = \frac{1}{n}\sum_{i=1}^{n} f_i(x) \quad (95)$$

$$PA = \prod_{i=1}^{n} f_i(x) \quad (96)$$

$$PAB = \prod_{i=1}^{n} f_i(x)\ (if\ f_i(x) \geq 1) \quad (97)$$

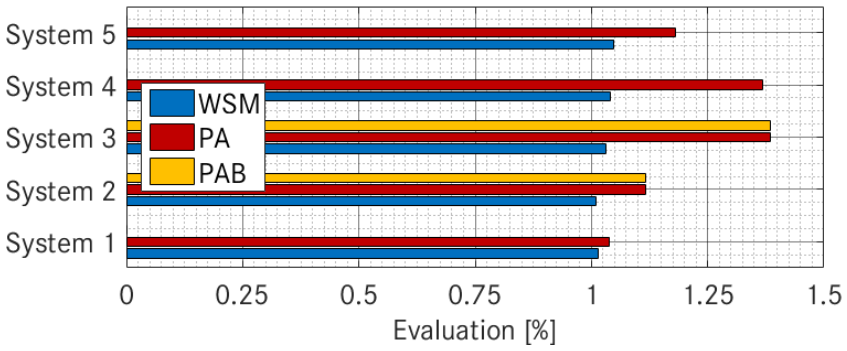

Figure 159: Comparison between the different evaluation approaches

2.2 Algorithm determination

This second sub-section addresses the challenge of the algorithm determination for the problem addressed in this work. In this case, the determination is not influenced by the environment but by the considered components and systems. Hence this section discusses first the case of the sub-components databank based optimization in this work and then the algorithm is determined, its implementation is discussed and the contribution is shown.

2.2.1 Sub-components databank based optimization

The main aspect of this work to determine the right algorithm for the considered problem is the fact that the optimization is based on already designed sub-components. These aspects required several constraints due to the databank but also the nature of the sub-components. The investigation is based on a databank which is built using a pre-processing. It calculates all the possible combinations of components for the considered system and its boundary conditions. Moreover the components in this databank are not continuous, i.e. there are no power modules for each voltage and current level or no non-integer number of cells can be considered. Hence a suitable algorithm need to be chosen to address these challenges.

2.2.2 Optimization algorithm

Considering the analysis done in the previous section, the exploration algorithms are more suitable than the evolutionary ones because they avoid using the crossing process which is unnecessary for a databank based optimization. The PSO is based on the estimated gradient in each direction of the considered area while the DIRECT algorithm simply defines an efficient way to cover the area. Nevertheless, the algorithm needs to be applicable on a discrete problem. For this purpose, two approaches are possible: the first one is to solve the problem with a continuous algorithm such as the PSO, then constraints are defined to neglect the non-integer solutions or the results are rounded to obtain only integers while the second solution is to adapt the DIRECT algorithm to consider only integer solutions by defining the initial values correctly and the possible steps for the algorithm. The second solution is retained because it avoids an additional approximation due to the rounding. This fact is proved in the fourth part of this sub-section, where the contribution of the chosen algorithm is shown.

2.2.3 Implementation

The implementation of the DIRECT algorithm is based on the code from the North Carolina State University [147] and [148]. The ground principle is not changed but some adaptations are done to solve only discrete problems. The results of the implementation are shown on Figure 160 for the function described in (98). This function is chosen to show the good convergence of the algorithm because it is only a slight decrease with X but still shows several local optima which could be sensitive for optimization algorithm. The functions is calculated only for strictly positive values (greater than 0) within [0 400] for X and [0 10] for Y.

$$Function\ (X,Y) = \cos\left(\frac{(X+Y)}{10}\right) - \frac{X}{500} \quad (98)$$

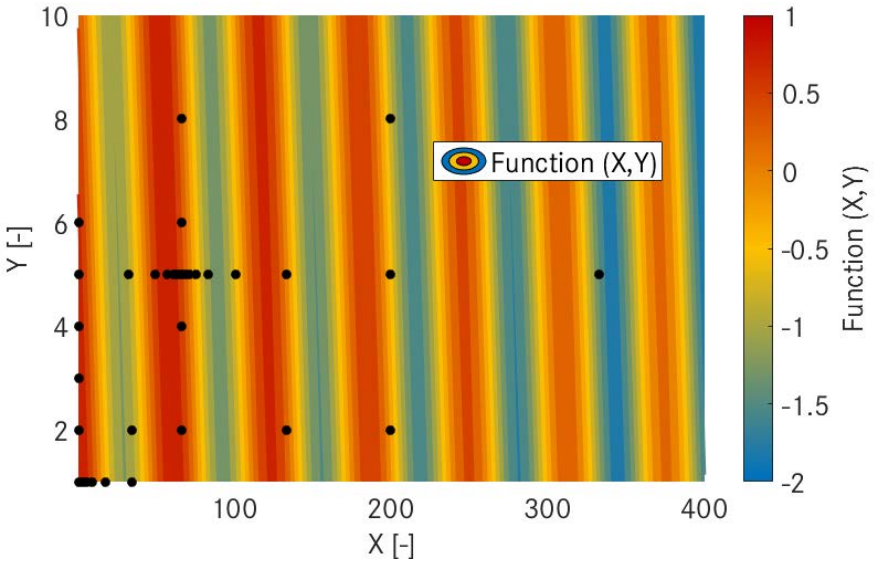

Figure 160: Results of the DIRECT algorithm with discrete values

The DIRECT algorithm suits the requirement for this work and it converges with a restrained number of iterations to the maximal value for strictly positive integer values of X and Y. Even if the gradient of the function is increased (with a ratio of 1/5000 instead of 1/500), the algorithm converges fast to the maximal value which is also the global optimum of the function for integer values.

2.2.4 Contribution of the discrete algorithm

Beside the good performance of the DIRECT algorithm, an important aspect of the considered problem is the discretization of the investigated area. This discretization can be investigated using a non-discrete algorithm but it could lead to high deviations. To have a clear overview, an example is chosen to show the relevancy of an implementation adaptation. The following arbitrary function (see equation (99)) is used and some boundary conditions of the automotive industry are introduced to show the relevancy of a discrete algorithm.

$$Function\ (X) = e^{-\frac{18}{X}} - \frac{X}{500} + 1 \quad (99)$$

This function is chosen because it has all the drawbacks which can be found considering the automotive industry environment. The global optimum considering only one decimal place is 85.4, value which would have been found using a non-integer global algorithm. To show the relevancy of the discrete algorithm, the two following cases are studied considering X as the number of cells in series and a maximization:

- Only integer values are considered and therefore a rounding to nearest higher value
- Only integer values which are multiple of 12 are considered and nearest higher multiple of 12

Considering these hypotheses, the results of the optimization with a global algorithm and the rounding as well as the discrete optimization algorithm are shown in the following table. The second hypothesis is due to a present typical automotive module strategy assumption to use cell modules comprised of 12 NMC Graphite cells as the base unit of high voltage batteries as described in [123]. Considering the global algorithm, the hypothesis 1 leads to a wrong estimation of the value X which maximizes the function. Hypothesis 2 leads to an even higher wrong estimation of the value X. Instead of a value of 84, the global algorithm combined with the rounding estimates that a value of 96 is required to maximize the function. Hence this short example has shown why an adaptation of the algorithm is relevant because the automotive industry imposes boundary conditions which cannot be investigated using a global algorithm and a rounding.

	Hypothesis 1	**Hypothesis 2**
Global algorithm + rounding	86	96
Discrete algorithm	85	84

Table 31: Contribution of the discrete algorithm

2.3 Implementation of the investigation approach

After having determined the suitable evaluation approach and optimization algorithm as well as their implementation, the coupling with the modeling approach defined in the previous chapter needs to be detailed. This section presents thus shortly the coupling between the optimization approach and the system modeling.

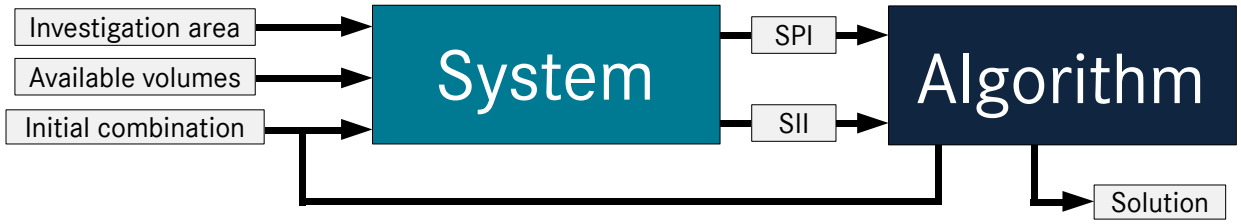

Figure 161: Coupling of the system modeling and the optimization approach

The coupling as presented on Figure 161 is deduced from all the modeling approaches, interface adaptations, evaluation approaches and optimization algorithm discussion in this thesis. Based on the boundary fixed by the investigation area and the available volumes, an initial combination is analyzed. It results then from the system modeling two indicators discussed previously: the System Performance Indicator (SPI) and the System Integrability Indicators (SII) which consider a Boolean approach. Based on these values, the algorithm is able to define other combinations which need to be evaluated in order to determine the optimal solutions.

3 Optimization of eDrive systems for hybrid electrical drivetrains

This section is focused on the boundary conditions and the optimization process. The first sub-section introduces the boundary conditions for the optimization process, the second sub-section discusses the determination of suitable systems for the different investigation (drivetrain architectures and power classes), and finally the third sub-section discusses the global optimization process and how it enables to consider in an efficient way the boundary conditions, the global optimization as well as the special cases (technology comparison, module strategy and power electronics topologies).

3.1 Boundary conditions

The boundary conditions are detailed in the first chapter where the following topics where considered: the voltage level, the system architecture, the power electronics topology, the machine technology and the module strategy. Based on this status, this part aims to define relevant cases to investigate these different aspects of the design of eDrive systems for hybrid electrical vehicle based on the modeling developed in this work. For each parameter, a short analysis is performed and recommendations for the optimization are defined.

Voltage level:

As shown on Figure 15 and considering only the hybrid electrical drivetrains, a slight correlation can be inferred between the voltage level and the power. To consider this behavior, systems with different power classes need to be considered and one special case is defined. Three classes are chosen within the present solutions (power between 15kW and 150kW) while a special case considers the investigation of a power increased outside this range. Beside the influence on the voltage, the case of 48V systems is also considered. For this purpose, a special case is defined for the lower power class and the comparison is done between the solution determined with the optimization algorithm and the same system based on the 48V technology.

System architecture:

As discussed in the first chapter, three main architectures can be identified. If the case of the boost-converter is discussed within the topic of the power electronics topology, the number of machines remains a topic of high interest. Most of these systems (as the power-split systems from Toyota and Chevrolet or the range-extender solutions as in the Fisker Karma) use two machines. One is generally used as generator and the second one as motor. Therefore the topic of the system architecture is considered by defining a special case. For the purpose of

these investigations, a comparison is done between the results when considering only the motoring driving points and the results when considering only the generating driving points. Hence the influence of the generator mode, the motor mode on the eDrive system design can be evaluated and the relevancy of a dual machine system can be analyzed.

Power electronics topology:
The investigation of the power electronics topology is divided in two parts: the number of phases and the implementation of a boost-converter. The first one is considered within the global optimization while the second one is considered within special cases.

Machine technology:
Considering the intrinsic parameters and under the assumptions that the costs are not investigated in this work, the PMSM solution is the best solution for hybrid electrical drivetrains. Therefore, the machine technology comparison is done within a special case to show the modularity of the developed method and also the influence of the machine technology on the global system design.

Module strategy:
In the first chapter, the example of a module strategy is shown. Module strategy can be applied on several levels, the ones which directly influence the eDrive design are the following ones: use of the same inverter for different power classes, use of the same machine for different applications, use of the same cells for different systems and finally a module based design of the battery using a fixed number of cell per module. If the last one can be directly implemented within the global optimization, the first three are considering within special cases to better identify the synergies between the systems based on the results of their design optimization.

3.2 System determination

Considering the boundary conditions and the current development status, this sub-section aims to determine three relevant systems for the optimization purpose. It discusses first the case of the drivetrain architecture and then the cases of the power classes for the global optimization.

3.2.1 Drivetrain architecture and vehicle characteristics

Since the focus is set on the electric drive components, a drivetrain architecture with a low complexity and a high modularity is chosen. The P2-architecture (integration between the combustion engine and the gearbox) seems to fit this purpose. It can be used for different power classes, for different voltage levels and by considering only one architecture, the focus is concentrated around the electric components. The P3 or P4 architecture are relevant alternatives because they enable to fit perfectly the mechanical requirements to the electric machine by varying the ratio between the machine shaft and the wheels. However, there is a lack of reference systems for this architecture and therefore an integration of the electric machine between the combustion engine and the gearbox is chosen. The drivetrain architecture is shown on Figure 162.

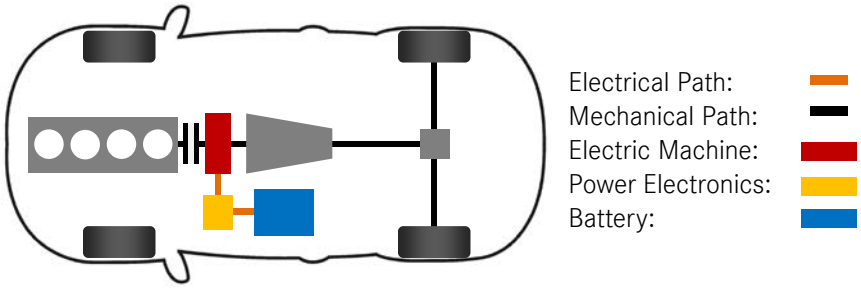

Figure 162: Considered drivetrain architecture for the optimization of the eDrive system

3.2.2 Power classes

Concerning the power, three classes are chosen: 15kW, 60 kW and 85kW. They enable to cover a wide range but also to investigate the 48V systems. The present status of development of the 48V systems shows a power around

15kW. Hence the chosen systems are based on three power classes. It enables to perform both the global optimization but also to analyze the special cases defined previously.

3.3 Optimization process

After having determined the system to perform the global optimization, this sub-section discusses the optimization process. It is divided into two parts: First the range for the investigation is defined and then the process is described.

3.3.1 Investigation area

After having defined which boundary conditions are considered and which system enables to address the challenges of this work, this part details the investigation area. To cover the entire range of applications of hybrid electrical drivetrain and especially the current and voltage levels, the following assumptions are done for the components:

- **Cell in series:** A range between 1 and 300 cells in series
- **Cell in parallel:** A range between 1 and 5 cells in parallel
- **Cells type:** 119 different cells
- **Power module:** 14 power modules
- **Number of phases:** Three-phases and six-phases system
- **Maximal AC-current:** 11 values of the AC-current within the range of a power module
- **Electric machine:** Several variations of the number of winding turns

Except the maximal AC-current, all these hypotheses validate the use of a discrete algorithm. However, the focus of this work is on the evaluation of the influence parameters. This evaluation can be performed even if the AC-current is considered with a discrete approach too. The variation of the AC-current is considered to compensate the discretization of the power modules. Indeed the semiconductor supplier (as previously for the capacitors) does not produce any possible current level, therefore an application which requires a current level between two values of the power module could be oversized when considering a higher current or undersized when considering a lower current. Hence this additional discretization enables to address all the challenges considered in this work without excessively increasing the size of the investigation area.

3.3.2 Optimization process

After having defined the range of the optimizations, the process can be defined, it is divided in three main steps: first using the integration, the torque and the power requirements, a first set of invalid solutions can be removed, then the global optimization is performed to consider the range defined previously (cell in series, cell in parallel, cells type, power module, number of phase, maximal AC-current and electric machine) and finally the special cases are considered. The process is based on the coupling of the modeling and the algorithm presented previously on the Figure 161. Within the filter, several specific requirements from the automotive industry such as the voltage level (see Figure 129) or some design parameters such as the number of cells in a standard module are also implemented. The results of the global optimization are thus automotive “qualified” system which show not only the technical boundary conditions discussed previously but also how the automotive environment influence the results of the design. The next section is focused on the presentation and the discussion of the results for the global optimization and the special cases.

4 Optimization results

This section presents and discusses the results of the optimization process defined in the previous section throughout three sub-sections. The first one discusses the case of the filters and how they enable to reduce the number of variants, to consider the automotive environment and therefore to provide in an efficient way automotive “qualified” systems for the optimization algorithm. The second one presents and discusses the results of the global optimization and bring an answer to several of the challenges addressed by this work and finally the last one presents the special cases and how they are easily introduced within the optimization process and the modeling approach developed in this work.

4.1 Pre-processing filter

This first sub-section discusses the filtering of the solutions. Different filters are considered: a first one for the integrability, then one for the automotive specific requirements and finally a last one for the design requirements. These filter are required to avoid neglecting any influence parameters, this work considers a large investigation area as shown in Table 32 for each considered parameter. The following sub-sections show how the filter enables to reduce the number of valid conditions with the different filters without evaluating the entire system.

Parameter:	Cell in series	Cells in parallel	Cells type	Power module	Number of phase	Max. AC-Current	Electric machine
Number of combinations:	300	5	119	14	2	11	6
					Total:	329868000	

Table 32: Investigation area considered in this work

4.1.1 Integrability

An important parameter for the design of hybrid electric drivetrain is the integrability because the eDrive system needs to be integrated in a drivetrain which contains already the conventional components. Therefore this first filter is based on the components integrability. This filter can be integrated independently from the optimization algorithm because the methods presented in the previous chapter can be quickly simulated. The electric machine is considered independently because the only parameter considered is the number of winding turns. To evaluate the velocity of the simulations, a test is performed. For each component 20000 simulations with variable parameters are done and the mean simulation time is calculated, the results are presented on Figure 163.

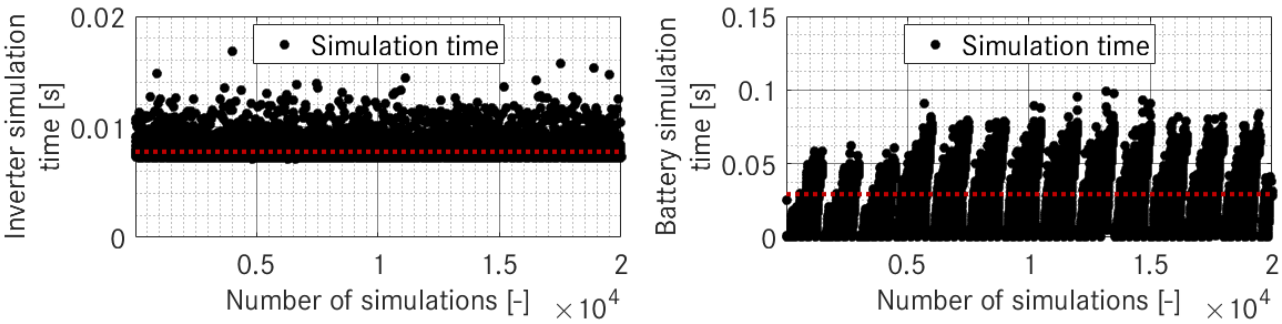

Figure 163: Simulation time for the battery and inverter integrability

Both simulation methods are quick and despite the large number of combinations, it can filter efficiently the investigation area. Moreover, the same inverter or battery are used in several combinations within the investigation area. Thus it can filter the entire area without simulating the total number of combinations.

4.1.2 Specific automotive requirements

The aim of this work is to address the technical challenges faced by the electric components by considering the specific automotive requirements. These requirements can also be implemented within the filter to reduce the number of combinations. These specific requirements are depicted especially by the voltage area as shown on Figure 129. They are implemented within the filter through two methods: the first one limits the maximal number of cells due to the maximal permissible voltage depicted in the VDA LV123 norm [116] and the second one limits the number of calculated power electronics because a power module can only be used with the corresponding voltage level as defined in [116].

4.1.3 Design requirements

Beside the integrability and the specific automotive requirements, the investigation area can be filtered using design requirements. These design requirements are depicted by three main requirements: the number of cells in battery modules, the maximal torque and the maximal power. If the influence of the number of cells in battery modules is

manifest, the two other parameters require at first sight to simulate the entire system. They can however be restricted by defining redundant requirements. For example if the maximal possible power of the battery cannot fulfill the power requirement without even considering the power electronics and electric machine efficiency, the entire system can neither fulfill this requirement. For this purpose, (100) and (101) are used to calculate the maximal voltage in the battery and to deduce the maximal power using the maximal current. Thus it enables thus to filter solutions with a redundant requirements.

$$U_{max} = OCV_{max} + R_{max} \cdot I_{max} \quad (100)$$

$$P_{max} = U_{max} \cdot I_{max} \quad (101)$$

Concerning the maximal torque requirement, it can be evaluated by using the data used for the energy management which is used to limit the current when the power electronics reaches its thermal limits. The torque limits for different value of the current are shown on Figure 164.

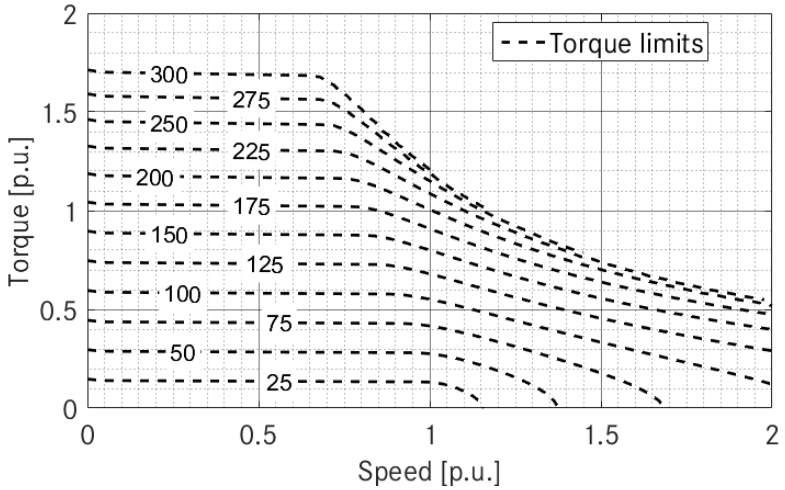

Figure 164: Current-dependency of the maximal torque

Using these limits the solution where the power electronics cannot fulfill the torque requirements due to a limited AC-current can be filtered and the investigation area can be reduced. This filtering considers however only the maximal torque in the low speed area which is independent from the voltage and therefore enable to filter the systems independently from the battery configurations.

4.1.4 Influence of the filter of the combination

In this last part, the influence of the filter previously discussed is shown. The results presented in Table 33 are calculated for the three considered systems (P2-15, P2-60 and P2-80). The requirements from the integrability, the torque and the power are deduced from system estimated with the design voltage method described in the previous chapter. These system are also considered as references for the optimization results presents in the next sub-sections. The results consider a strategy using 12 cells per module.

Case:	Total	P2-15	P2-60	P2-85
Number of combinations:	329868000	3330	2424	5516

Table 33: Results of the filter implementation

These combinations are then used in the algorithm to evaluate the optimal solution which are presented in the next sub-sections first for the global optimization and then for the special cases.

4.2 Global optimization

After having shown the influence of the automotive industry requirements and the importance of the integrability on the results through the reduction of the number of combination, this second subsection is focused on the global

optimization. For the analysis of the results, the following parameters are considered: the maximal power, the continuous power, the evaluation on a driving cycle and the integration. In order to discuss in detail the optimization results, the section is divided in two parts. First the results for the P2-85 system are presented and analyzed and then a summary for the three considered systems is done before considering the correlation between the voltage, the current and the power. For each system, the New European Driving Cycle (NEDC) is considered as shown on Figure 11 and the detailed results are presented in Appendix 9 for the P2-15 and the P2-60 systems.

4.2.1 Results for the P2-85 system

In this first part, the results for the P2-85 system are presented in three steps. First the variations of the investigation area considering the automotive requirements, the integrability and the design requirements are discussed, then the global system performance for the three best systems are presented and compared to the reference system calculated with components focused design and a detailed comparison between the optimal system and the reference is presented.

Variation of the investigation area:

One of the focus in this work is to develop scientific methods which allows evaluating from a technical point of view, the challenges faced by the electric components in the automotive industry. In Table 34, the influence of the automotive requirements, the integrability and the design requirements through the filter is shown.

Parameter:		Cells in series	Cells in parallel	Max. AC-Current
Filter	Automotive requirements	1 → 190	1 → 5	100 → 600
	Integrability	29 → 118	1 → 3	100 → 400
	Battery module	36 → 108		
	Torque and power requirements			200 → 400
Solution		96	1	350

Table 34: Variation of the investigation area considering the filter and the solution for the P2-85 system

These results show the importance of the filter, it enables to remove several solutions before doing any evaluation of the entire system. The automotive requirements and especially the maximum voltage allowed in a road vehicle limits the number of cells in series. The integrability reduces the investigation area by reducing the range for both the number of cells and the maximal AC-current. The number of cells in series and parallel are limited by the available volume for the battery while the maximal AC-current is limited by the allocated location for the power electronics. The battery module further constrains the area by considering only the solutions where the number of cells is a multiple of 12. Finally the torque and power requirements reduce the range of the maximal AC-current principally due to the torque requirements.

Global system performance:

Within the solutions in the investigation area determined using the filters, the optimization process allows identifying the best solution. Among the results, the three best system are considered as presented in Table 35, where the DC-voltage, the maximal AC-current, the number of winding turns, the number of phase, the SOCI, the dimensions of the power electronics as well as the battery characteristics are analyzed. These solutions are compared with the reference solution calculated using the design voltage based method. The aim of this work is to find the relationships between the design of the eDrive system and the parameters presents in the following table (voltage, current and integration). Therefore the different results are analyzed and discussed independently before doing a global summary about the system.

Parameter:	Reference	1st solution	2nd solution	3rd solution
DC-Voltage	350	311 (approximated using design voltage)		
Max. AC-Current	300	350		
Number of winding turns	=			
Number of phases	3		6	3
SOCI [%]	100%	111.9%	111.6%	112.1%
PE length [%]		-5.4%	-4.6%	-5.4%
PE width [%]		-6.2%	-2.3%	-6.0%
PE height [%]		-5.8%	-6.1%	-5.8%
PE weight [%]		-10.3%	-9.5%	-4.0%
Semiconductor module	1	10		9
Battery length [%]		-2.7%		
Battery width [%]		-12.1%		
Battery height [%]		-1.2%		
Battery weight [%]		-6.7%		
Cell type	13	1		
Configuration	108s1p	96s1p		

Table 35: Optimization results for the P2-85 system

→ DC-voltage and AC-current: the DC-voltage and the AC-current cannot be analyzed independently because a reduction of one of them implies an increase of the other to conserve comparable performace. All three best solutions show the same results, a more optimal system for the considered power class under the hypothesis of this work requires a lower DC-voltage and a higher AC-current than the reference. This results can be explained based on two parameters: the system maximal power and the considered driving cycle. The system has a maximal power of 85 kW and as it can be seen on Figure 165, the driving points from the considered cycle are mainly in the base speed range where the limits of the DC-voltage are not reached. Hence a reduction of the voltage does not influence greatly the machine efficiency since the driving points are the same and thus the inverter efficiency is the relevant parameters to consider. As shown on Figure 165, it can be seen that for lower DC-voltage the inverter losses in the base speed range are lower (isolines for the same value are higher for 350V as for 311V). Considering the evaluated driving points (for example here in motoring area), a reduction of the DC-voltage is therefore advantageous for the global system and the increase of the current is here to compensate the DC-voltage reduction.

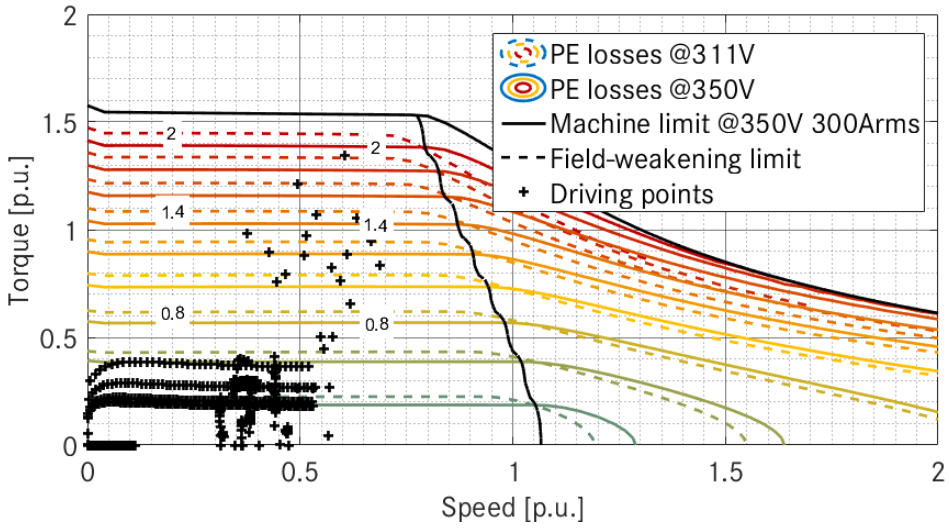

Figure 165: Influence of the voltage level on the inverter losses (311V and 350V)

→ Number of winding turns: the results show that the number of winding turns is not changed between the reference solution and the three best solutions from the optimization. The number of winding turns influence the flux linkage and thus the efficiency and the torque per ampere of the machine. According to the results, the

adaptation of the current and the voltage is more advantageous than an adaptation of the number of winding turns.

→ Number of phases: the results for the number of phases are quite interesting since the two best solutions are using the same semiconductor module but with different number of phases. As explained previously, the influence of the number of phases is neglected for the electric machine and therefore the influence of the number of phases is only observable on the power electronics. These results show a little lower efficiency with a six phase system (reduction of the SOCI). These results can be explained by the enhancement of the methods presented in this work. The switching losses are generally calculated using the formula of the equation (31) which considered a proportional scaling while the method in this work considers the real variations of the switching energies. Therefore the behavior between the current and the losses is strongly dependent on the power module and thus based on the hypothesis of this work, six phase system are advantageously in high speed area as shown on Figure 166 and it presents no benefit for the driving cycle efficiency.

→ Power electronics: the topic of the power electronics is more sensible. If the difference between the three systems are cleared based on the semiconductors modules and number of phases, the information concerning the volume reduction need to be considered with caution because the volume reduction are in the same range as the deviations between real automotive components and the simulated dimensions presented in Table 18. The main observations is about the semiconductors module. All three system used the same battery and machine configurations and thus, the main difference in efficiency lies in the module chosen for the power electronics. If the module 9 shows a higher efficiency (highest SOCI of all three systems), it also shows a lower integration and particularly concerning the weight.

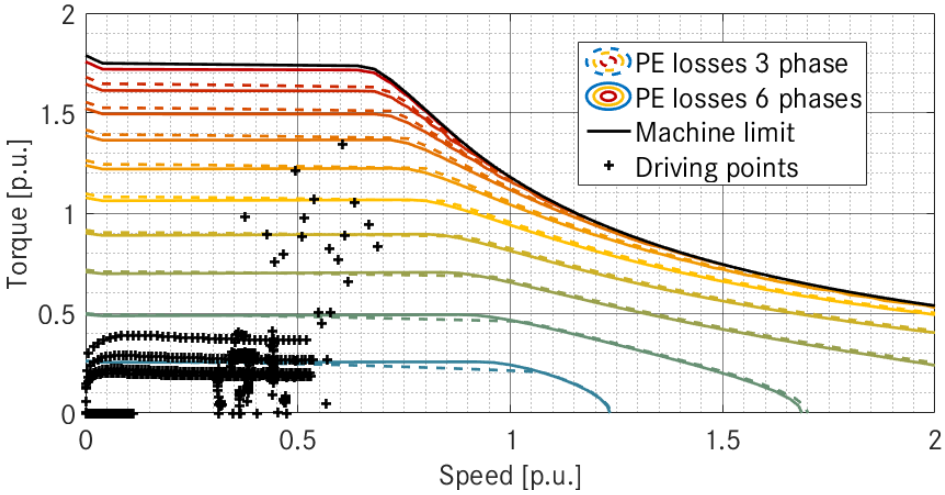

Figure 166: Influence of the number of phases on the inverter losses

→ Battery: all the systems use the same battery configuration with the same cell type. Hence it can be assumed that the cell type is the best compromise between, efficiency, integrability and performance for the considered application. Moreover a reduction of the voltage can lead to a reduction of the volume as shown on Figure 119. Even if the number of cells is only slightly reduced, it shows another reason why the DC-voltage is reduced by the optimization process. The DC-voltage influences directly the battery volume and therefore is a meaningful factor for the eDrive system design since it can increase the efficiency and reduce the battery volume.

→ Combination: beside the system parameters, the analysis of the combination is an important aspect. The chosen evaluation approach aims to be neutral and not to benefit one or another parameters in order to find the best combinations of components. In the previous table, the best solution for each parameter is marked in green while the worst is marked in red. Considering the results presented here, it can be assumed that the chosen approach really search for the best compromise because the solution with the best SOCI is not considered as the global best solution, the second best solution optimizes only one of the parameters and the global best solutions has no clearly advantages over the other for any parameters.

Detailed analysis:

To analyze more deeply the performances of the system, the comparison is done on Figure 167 where the maximal (solid line) and continuous (dotted line) power for a SOC of 50% as well as the driving points are shown. For the

reference machine, the limit curves are calculated using the design voltage while for the optimal solution the limit curves are calculated using the developed method.

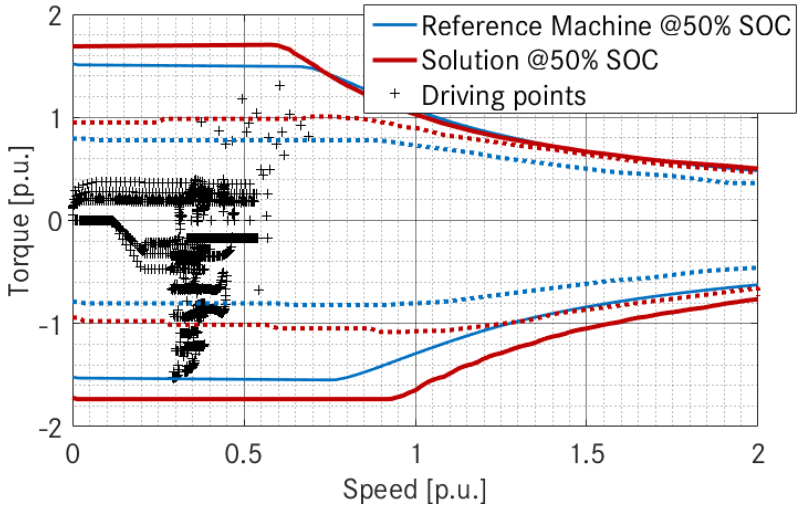

Figure 167: Comparison between the solution and the reference curves for the P2-85 system @50% SOC

As shown on Figure 167, the solution from the optimization presents a higher torque in base speed range and a similar torque profile in the field-weakening area in motoring mode and globally a higher torque in generating mode for the maximal power. The differences in motoring mode are only dependent on the DC-voltage and AC-current combination since it is shown that the design voltage method allows estimating with a good accuracy the maximal limit curves of the machine. The higher torque in generating mode is due to both the DC-voltage, the AC-current and the method developed in this work. Instead of using a constant voltage for the machine design, the method developed in this work considered the load dependency of the battery voltage. This consideration is particularly interesting in generating mode where the behavior of the battery is advantageous for the evaluation of the entire system because during the charge of the battery the voltage level is above the open circuit voltage. Concerning the continuous power, the method developed in this work influences greatly the results because the design voltage is approximated using the maximal DC-current in the system. To extend this comparison, the efficiency of the two systems is shown on Figure 168 using isolines.

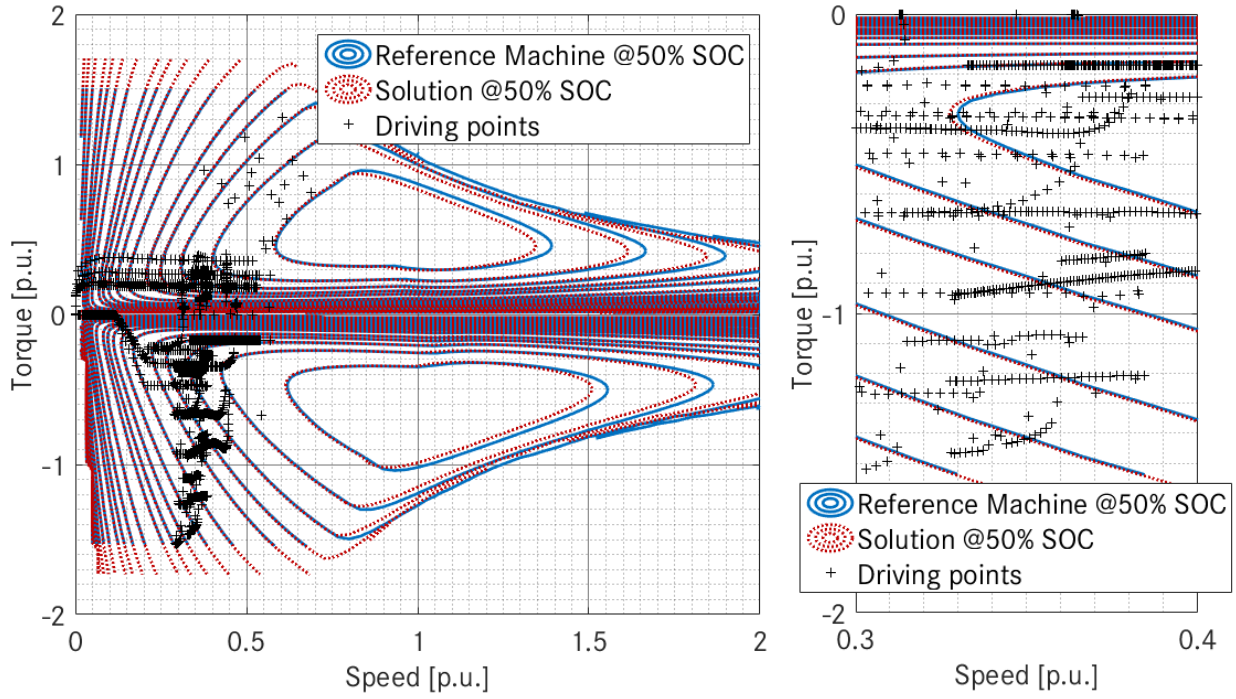

Figure 168: Efficiency comparison between the reference system and the solution @50% SOC

As it can be seen on Figure 168, the efficiency of the determined solution is slightly shifted to the left. Hence the area where most of the driving points are located have a better efficiency with the optimized system as with the reference system for this value of the SOC. It shows that considering this driving cycle, the base speed range is more important to investigate as the maximal power area.

4.2.2 General results of the global optimization

Considering the results of the P2-85 system discussed in the previous part and the results of the P2-60 and P2-15 systems in Appendix 9, this part presents a summary of the general results about the system. Globally, all the system shows the same trend: a reduction of the voltage and an increase of the current. To understand the technical aspect under these results, a global analysis is performed. Its aim is to identify the global relationships between the voltage, the current and the power for the design of eDrive system but before discussing the results, two parameters need to be defined: the equivalent power and the equivalent energy. The first one aims to evaluate the utilization of the system and is calculated using the equation (102) while the second one is here to evaluate the influence of the current for different number of winding turns by considering an equivalent energy as shown in the equation (103). It represents the energy provide to the machine and is dependent on the inductance and the square of the current. Since the number of winding turns (TC) is the only variable parameters, the energy can be approximated using the equations in (103). It is more relevant to analyze this energy the P2-60 results show a reduction of the number of winding turn. For the purpose of the comparison, the voltage used in the equation is the design voltage as in (91). Using these two additional parameters, the relationships between the voltage, the current and the power can be analyzed by using the results presented on Figure 169.

$$P_{equi} = (U_{DC} \cdot I_{AC}) \,/\, 1000 \quad (102)$$

$$Energy_{equi} = TC \cdot {I_{AC}}^2 \quad (103)$$

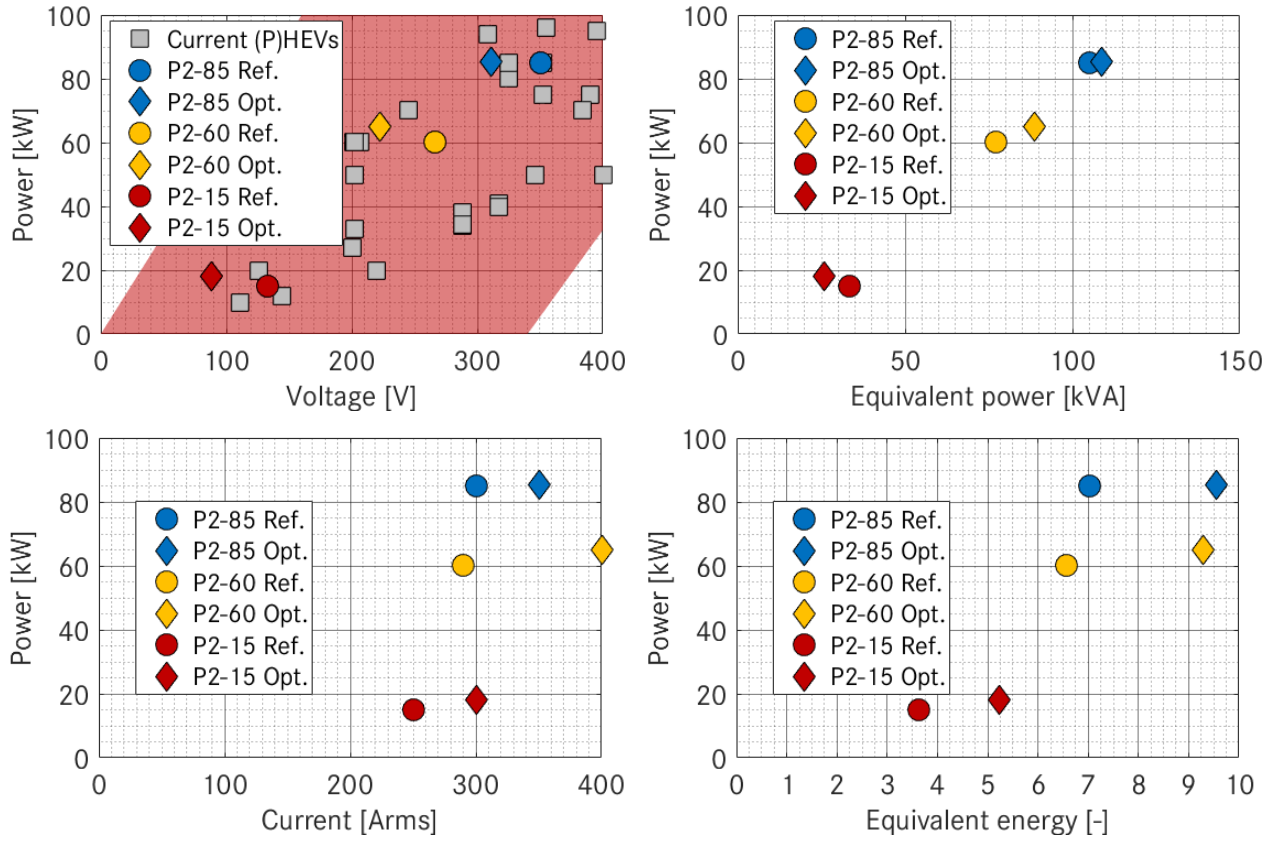

Figure 169: Global relationships between the power, the voltage and the current for the considered systems

As it was already observed, all three systems present after the optimization a reduction of the DC-voltage and an increase of the AC-current or more generally the equivalent energy. This behavior can be explained by considering

the influence of the DC-voltage on the system efficiency. To enhance the results presented on Figure 165, the optimal voltage for the minimization of the losses is shown Figure 170 versus the torque and the speed for the reference machine of the P2-85 system. As the optimization tends to show it for the considered driving points a reduction of the voltage can be advantageous. Thus the current needs to be increased, to compensate the voltage reduction but still have the required power.

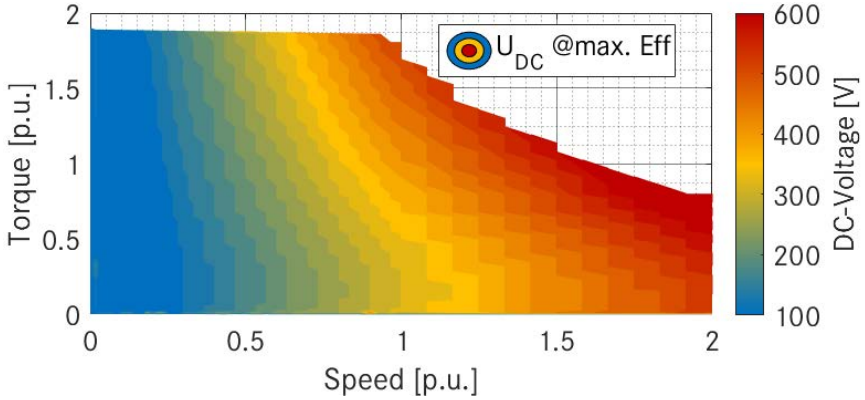

Figure 170: Torque and speed dependency of the DC-voltage for a given machine

Considering the system utilization (power pro equivalent power), it can be seen that the reference system, based on assumption on the power electronics and the battery to evaluate the system performance at the electric machine, are showing a higher utilization and show similar results as the ones presented in the chapter on electric machine, where higher voltages show better utilization. It can be explained that this approach is component focused and therefore the aim is to use its fully potential while the rest of the system is only superficially investigated using two reference values: the design DC-voltage and the maximal AC-current. Hence the results of the global optimization have addressed the challenges set at the beginning of this work and show the influence of the voltage and the current on the design and eDrive system. Moreover, it shows the contribution of the method developed in this work which finds the system optimum instead of a components focused optimum, how the model enables to identify the best combinations of components instead of the best components combination and the importance of a global system optimization.

4.3 Special cases

Beside the global optimization, one aim of this work is to build a modular simulation environment to investigate the influence of several challenges of the automotive industry using scientific methods. For this purpose, several special cases previously defined are investigated in this sub-section. It includes: 48V-system, high power applications, the implementation of a boost-converter, the machine technology and the module strategies, which are discussed each one in a related part.

4.3.1 48V-System

In this first part, the case of the 48V-systems is discussed. The same optimization process as previously is performed as for the P2-15 system which is taken as reference. The results are presented on Figure 171 and in Table 36. The 48V-system show promising results especially concerning the power electronics integration. The rest of the results are validating further the relationships between the current, the number of winding turns and the voltage. The differences concerning the power electronics integration are linked to the technology: the 48V-systems are outside the high-voltage applications (as considered in the automotive industry). Hence other technologies are used and especially for the power electronics, where Mosfet instead of IGBT are used and alternative technologies are used for the DC-link capacitor. The detailed investigation of such parameter lies outside the focus of this work and thus no further investigation are done but it shows the modularity of the model and method developed in this work. They enable without complex adaptations to cover the entire range of automotive applications and especially the entire range for the voltage level.

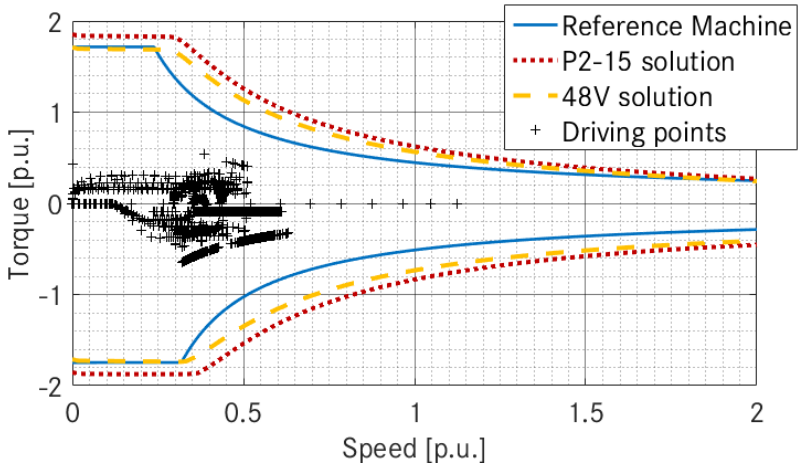

Figure 171: Comparison between the P2-15 solution and the 48V-system

Parameter:	Reference P2-15	Solution P2-15	48V-system
DC-Voltage	111	88	44
Max. AC-Current	250	300	410
Number of winding turns	=	=	↘
Number of phase	=	=	↗
SOCI [%]	100%	116.0%	105.0%
PE length [%]		-3.8%	-18%
PE width [%]		-5.8%	-25%
PE height [%]		-9.1%	-10%
PE weight [%]		-2.4%	-2.1%
Battery length [%]		-3.2%	-3.2%
Battery width [%]		-5.3%	-2.9%
Battery height [%]		-6.7%	-6.6%
Battery weight [%]		-6.7%	-6.7%
Cell	13	2	
Configuration	30s1p	24s1p	12s2p

Table 36: Comparison of the P2-15 solution and of the 48V-system with the reference machine

4.3.2 High power system

The second case is the increase of the system power. The same drivetrain architecture is considered and the optimization process is applied to the same reference as the P2-85 system except that the power requirements are doubled. The results are presented on Figure 172 and in Table 37.

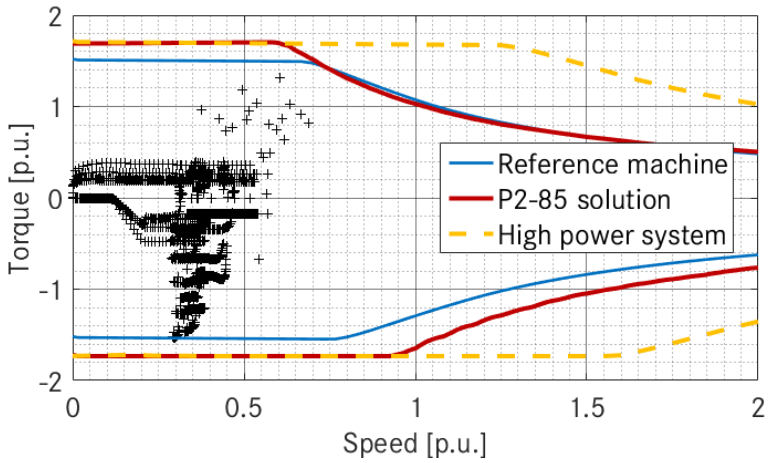

Figure 172: Comparison between the P2-85 reference, the P2-85 solution and the high power system

Parameter:	Reference P2-85	Solution P2-85	High power system
DC-Voltage	350	311	622
Max. AC-Current	300	350	
Number of winding turns	=		
SOCI [%]	100%	11.9%	96.1%
PE length [%]		-5.4%	+5.8%
PE width [%]		-6.2%	+4.3%
PE height [%]		-5.8%	=
PE weight [%]		-10.3%	+1.5%
Battery length [%]		-2.7%	+5.6%
Battery width [%]		-12.1%	+88.4%
Battery height [%]		-1.2%	+1.1%
Battery weight [%]		-6.7%	+100%
Cell	13	1	
Configuration	108s1p	96s1p	192s1p

Table 37: Comparison of the P2-85 system with the results of the high power system

The relationships between the voltage, the current and the power are not trivial and especially for high power system. It is a complex relational system between the different components where their behavior (saturation in the machine), and their technologies (600V, 650V and 1200V IGBT) influences the results. From an energetic point of view, it implies a reduction of the SOCI and thus of the efficiency due to the increase of the voltage. It is however the best solution found thanks to the optimization which means that an increase of the current with an adaptation of the number of windings turns has no advantages. From an integration point of view, the battery volume is more than doubled due to the increase of the voltage. The power electronics volume is less impaired which is probably due to a module strategy from the manufacturer of the semiconductor module. Globally the increase of the power influence mainly the battery. By increasing only the voltage versus the reference, the machine presents no saturation and the power requirements are fulfilled.

4.3.3 Boost-converter

The topic of the boost-converter is directly linked with the results of the previous part which show the load dependency of the voltage but also the voltage dependency of the battery integration as it is shown in the fourth chapter. Hence this part investigates the topic of the boost-converter. For this purpose, it compares the following systems: the solution of the P2-85 system optimization and the same system where the number of cells in series and in parallel are respectively divided and multiplied by 2. To compensate the voltage drop, a boost converter is implemented between the battery and the inverter. To evaluate the performance of this new system, the following parameters are evaluated: the SOCI, the battery integration, the boost converter volume and the limit curves of the new system. The results are presented on the following figure and in the table below where the relative evaluation versus the P2-85 solution without boost-converter is shown.

	System with boost-converter
SOCI [%]	-1.0
Battery integration [%/dm³]	-1.0 /-0.4
Boost-converter integration [dm³]	5.2
Additional power [%]	up to 15

Table 38: Influence of the boost-convert on the P2-85 system

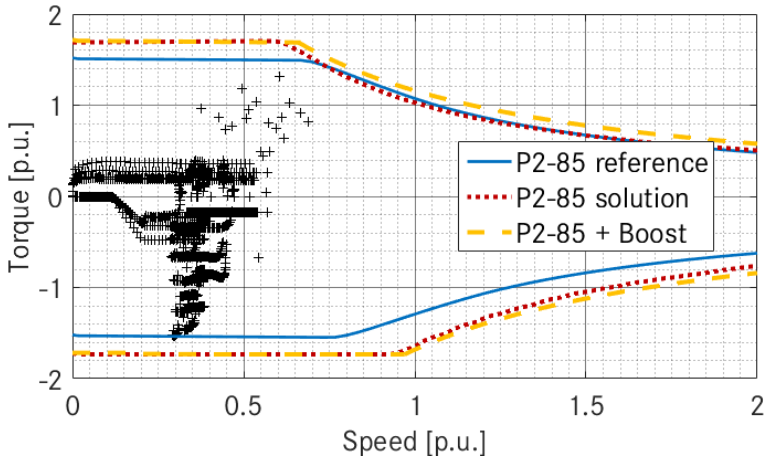

Figure 173: Comparison of the limit curves for the P2-85 system with and without boost-converter

Despite a reduction of the SOCI and the additional volume required for the integration of the boost-converter, its implementation shows potential. The volume reduction of the battery is lower that it could have been expected considering the results from the chapter 4 due to the consideration of the automotive requirements (pre-defined voltage level) but the addition of a boost-convert enables to better utilize the machine since the voltage limit is higher. The maximal power is thus only limited by the DC-power and as it can be seen, the global system power is increasing. Moreover, the system with a boost-converter is SOC-independent and can deliver the full power even if the voltage would have limited the possible AC-voltage at the electric machine. The boost-converter requires however 5.2dm³ which corresponds approximately to a doubling of the power electronics volume while the battery volume reduction is only 0.4dm³. However despite its integration issues, the boost-converter should be considered in the case of SOC-sensitive solution and in applications where the power by high speed is a key factor because the system with boost-converter can bring around 15% more power in this area without excessively deteriorating the efficiency and for only a slight reduction of the integration considering the entire system.

4.3.4 Machine technology

The machine technology is a sensible case to discuss because the potential of the technology is strongly related to the considered integration. As it was shown on Figure 54, the induction motors are not suitable for applications where the torque and power density are key factor and therefore the influence of the technology is analyzed by considering the P2-15 system. For this purpose, only the limit curves and the SOCI are compared by considering the design of the power electronics and the battery as fixed. The results are presented on Figure 174.

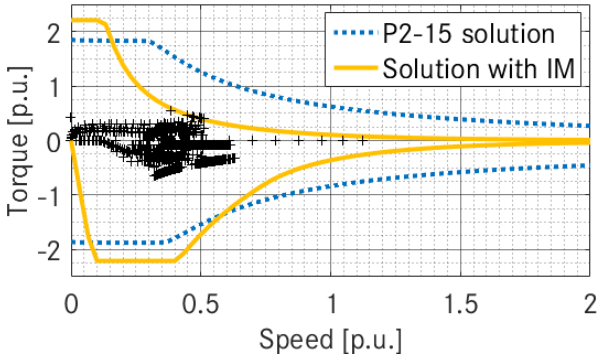

Figure 174: Influence of the machine technology on the limit curves for the P2-15 system

The IM technology is highly sensitive to the voltage due to its working principle. As shown on Figure 174, the solution is barely able to be evaluated on the driving cycle. When analyzing the SOCI, the drawbacks of the IM technology are even higher, the IM has a 20% worse SOCI that the P2-15 solution for the considered integration and application. This is not a general conclusion about the technology but considering the integration and application considered in this work, the induction machine is not a suitable solution. It is particularly interesting considering the results from

[12] and [149], which tend to show from a global point of view that the induction machine is the most suitable solution for HEV applications. The results are strongly dependent on the considered integration, battery, power electronics as well as the system architecture as shown here.

4.3.5 Module strategy

This last part discusses the topic of the module strategy. One is already investigated within the global optimization with the number of cells per module (strategy of battery configuration based on 12 cells module). The global optimization also answers to most of the solution to implement a module strategy for the eDrive system components:

- Use of the same inverter for different applications
- Use of the same cell for different applications
- Use of the same machine for different applications

Concerning the use of the same inverter for different applications, the same module is used for the P2-85 and the P2-60 solutions. Thus the following solutions could be deployed: the inverter is designed to fit the highest requirements and can be then used for both applications. The voltage level is the same for both applications but the P2-60 system requires a higher current. This higher current lead then to a worse integration of the power electronics for the P2-85 system but could lead to global savings because the number of ordered components is higher. The same reason motivates to use the same cell or machine for different applications. It is the case for the P2-85 and the P2-60 solutions where the same cells are used in different configuration or for the P2-60 and the P2-15 solutions where the machine is used with different number of winding turns.

5 Chapter conclusion

The focus on this chapter is on the optimization of the eDrive system and organized in four sections: one concerning basic knowledge about optimization methods and algorithm, one about the determination of the right approach for the considered problem, one about the specificities of the eDrive system optimization and a final one about the results. In the first section, definition about optimization and the related method and algorithms are introduced to define the basis used in the rest of the chapter. The different evaluation methods and algorithms are presented and analyzed in order to define a basis for the second section. The second section is thus focused on the determination of the right approach. It begun with the evaluation approach and the influence of the considered problem. For the purpose of this work, a multiplication and ratio based solutions are used. The ratio is defined in such a way that the evaluation approach can directly identify the invalid solutions but also reward the good solutions. The final evaluation is then performed by calculating the product of the ratios by aiming to determine the best combinations of components instead of the combination of the best components. After it a suitable algorithm is defined considering the following aspect: the variables are discrete. Hence the DIRECT algorithm is chosen to fit this requirement and the contributions of a discrete adaptation are shown on an example. The third section is focused on the optimization and its boundary conditions. The aim of this work is to consider both the technological range (voltage and current levels, topologies, technologies…) but also to analyze these parameters in an automotive context. This section presents therefore the different boundary conditions and how they are investigated in this work. It also defines a suitable system and different power classes for it to address the challenges considered in this work and an adapted optimization process is defined by introducing several combinations and pre-processing filters. Finally the last section discuss the optimization results. First the influence of the pre-processing filter is presented and it shows the influence of the automotive requirements on the considered problem. The pre-processing filter enables to reduce the investigation area by defining integration and design constraints as well as defining redundant requirements. Then the global optimization results are discussed by analyzing the results of three power classes. For each system, the three best solutions are presented. The P2-85 system is analyzed in details to understand the phenomenon under the results of the algorithm. The relationships between efficiency, power, voltage and current are discussed and analyzed before doing a global comparison between all the systems to answer the challenges of this work. An important aspect of these results lies in the fact that the solutions show really an identification of the best combination of components instead of the combination of the best components. It also shows the contribution of the method versus the current one which is highly focused on the machine optimization. Finally the last part of the section analyzes the different special cases: 48V-System, high power system, implementation of a boost converter,

the influence of the machine technology and of a module strategy. These different cases complete the previous results and show the modularity of the developed methods. Based on all the results presented in this work a global analysis about the influence of the voltage and current level can be performed and the results are presented on Figure 175.

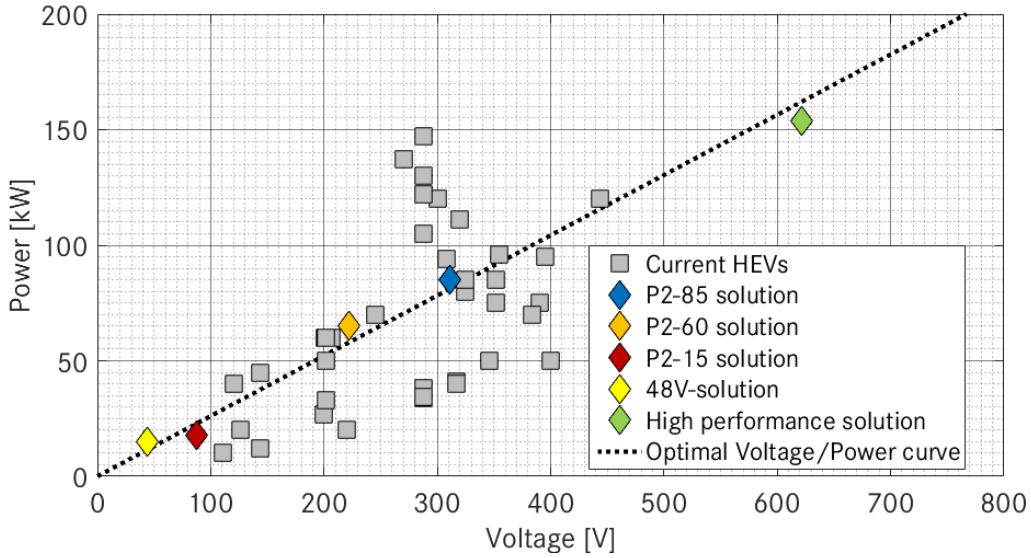

Figure 175: Relationship between the power and the voltage level

A clear trend between the voltage and the power can be identified. It shows the relationships between the power and the voltage and can be used as basis for further investigations, it is however only valid for the considered systems under the hypothesis of this work. The consistency of the method and the simulations developed in this work is also validated since all the results show the same trend depicted by the dotted line. In order to conclude, this chapter shows the contribution of the developed method, it allows optimizing several applications but also investigating a wide range of parameters: power, machine technology, power electronics topology, semiconductor types, cells technologies as well as the voltage and current level and the module strategy. Using the method in this work, other architectures could be analyzed and a more global analysis of the voltage and current influence can be determined for the entire range of more electrified vehicles.

Global conclusion

The investigations presented in this work are focused on the challenges faced by the electric components in hybrid electrical vehicles. The system in interest, the eDrive system considers the behavior and the interactions between the following components: the electric machine, the power electronics and the energy storage system. These components are investigated as an entity for hybrid electrical vehicle development in order to shift the challenges to a restrained scope and to refine the analysis as well as to identify optimized systems instead of combining optimized components. The investigations in this work are organized around the following guideline:

Determine the sufficient level of details in modeling electric components at the system level and develop models and tools to perform dynamic simulations of these components and their interactions in a global system analysis to identify ideal designs of various drivetrain electric components during the design process.

It aims to address the following topics: voltage and current level, power classes, module strategy and electrical architecture. These different research topics are the guidelines for the development of the methods and the various model in this work. Thanks to it, propositions and feedback for the further development of eDrive systems can be determined.

The first chapter sets the basis for the investigations in this work. It presents the current status of hybrid electrical drivetrains and their components in the global automotive context. It discusses first the drivetrains architectures, before shifting the focus on the electric components. The different technologies, architectures and the specificities of the components for automotive applications and the challenges they are currently facing are presented. The second focus of this chapter is on the modeling of electric drive system. It analyzes the current simulation methods and the previous works on the topic. Finally, at the end of the chapter, the aim and scope are defined as a guideline for the rest of the work.

The electric drive system is composed of three main components: the electric machine, the power electronics and the battery. The second chapter is focused on the development of methods and models for the evaluation of the electric machine. It determines for each considered modeling the suitable solutions for the considered problem. The main aspect is to find solutions which represent a good compromise between the automotive challenges, the optimization purpose and the results accuracy. It is shown that a maps based solution is a suitable method to analyze the influence of the voltage, the current and the thermal behavior of the machine. It is compared with other methods and with measurements and the results validate the chosen method. The same approach is used to determine the best solutions for the thermal behavior and the integration. As for the component behavior, the integration investigation can be easily determined contrary to the thermal behavior where a compromise toward the simulation effort is done due to the complex structure for thermal investigation.

The third chapter is focused on the determination of suitable methods and modeling for the power electronics. For each modeling, there are two parts, one for each type of converters (voltage source inverter and boost-converter). For the component behavior, an analytical method is chosen and suitable interpolation methods are determined to consider the influence of the voltage, the current and the semiconductor temperatures. Contrary to the electric machine, the thermal behavior can be modelled using a compromise between accuracy and parameter range by using a thermal equivalent circuit based on the thermal resistances and capacities which are available in the specification sheets. Finally a new solution for the estimation of the dimensions and the weight for power electronics is shown. Results from sub-components investigations are analyzed and built in a more global algorithm to evaluate the integration of both converter depending on the system requirements (voltage, current, frequency or voltage ripple for example).

In the fourth chapter, the topic of modeling the electric components is closed by determining the right approaches for the battery. Concerning the component behavior, a simple model is chosen based on the open-circuit voltage and the internal resistance. It shows some deviations versus the model based on RC-circuits but it does not require a time-consuming impedance spectroscopy. Considering the stage of the development where this research is focused on, it is a suitable compromise between modularity, parameter range and simulation effort to address the challenges considered in this work. Concerning the thermal behavior and the integration evaluation, similar solutions

as for the power electronics are chosen. They both show reliable results versus present automotive components and enable to consider a wide parameter range as required for this work.

In each chapter about the component modeling, investigations are performed to show the contributions of the method but also to bring a first answer to the challenges addressed by this work. In this fifth chapter, the entire system is considered. First some definitions and knowledge about systems are introduced and analyzed in order to determine the best solution to combine the models presented in the previous chapter. Based on this analysis, the different adaptations for the combinations of the components models are presented: interface adaptations, outputs adaptations and the implementation of the system limits (energetic, thermal and electrical). Using the global system model, the results can then be validated using measurements. The validation is performed in two steps. One with an electric machine and power electronics test bench and a second one with vehicle measurements. Both show good results with low deviations and a suitable level of accuracy to compare systems in the context of the early development stage of hybrid electrical drivetrains. The chosen method to model the entire system is finally compared to show the contribution of the method and to show the importance of a global system approach.

In the last chapter, the optimization of eDrive systems is discussed. It begins with global knowledge about optimization and show progressively the determination of the right optimization process and evaluation for the problem considered in this work. The automotive requirements, the technological limits and the design requirements are analyzed and implemented within a pre-processing filter. Then a drivetrain architecture, power classes and special cases are defined to address the challenges of this work and the results are finally presented. The results aim first to determine the global relationship between the voltage, the current and the power while special cases are there to investigate supplementary challenges such as a module strategy, the machine technology or the 48V-systems. At the end a global analysis of the challenges of this work is done and a global overview of the relationships between power and voltage level is presented. Moreover, the results in this chapter also show that the best combinations of components are not always a combination of the best components and that system focused components design lead to better performance as well as a better integration.

This work has set the basis for the optimization of the electrical component in hybrid drivetrains as an entity. It enables to shift system requirements to a deeper level but also to consider relevant components behaviors. The relationships between the power and the voltage level as presented in this work are an overview of the global context of the hybrid electrical drivetrains and with always higher electrical range requirements, this topic remains of high interest and the following points still need to be addressed:

- The method is applied for a defined drivetrain architecture with one electric machine. The results of the voltage level and power class investigations can therefore greatly vary depending on the considered architecture and the number of electric machines.
- This work considers selected technologies which are already used in current automotive applications. It is however built in a modular way and since both the Mosfet and the IGBT technologies are considered, future technologies could also be investigated. The introduction of other machine technologies such as the separately excited synchronous machine or the switched reluctance machine would require some adaptations but this work has already set the basis to determine time efficient and accurate solutions.
- The simulations are validated for one or two components and for one entire system, it could be interesting to show the validity of the modeling approaches for other systems and or technologies.
- Concerning the investigation of the machine, the analytic model based solution is limited by its simulation time due to the determination of the limit for each simulated points. It could be interesting to see the performance of such an approach when the limit curves are calculated in a pre-processing and can filter the driving points before calling the analytic model.
- Finally, analytic approaches for other power electronics structure could be integrated by replacing the current ones in the developed model.

BIBLIOGRAPHY

[1] International Energy Agency; CO2 Emissions from fuel combustion, highlights, International Energy Agency, 2013 Edition

[2] European Automobile Manufacturers Association; Link: http://www.acea.be/

[3] B. Hense; Energy Balance. Future mobility and its energy sources, Energy Efficient Vehicle Conference (EEVC) 2011, 30.06.2011

[4] M. Freyssenet; La production automobile mondiale, des quatre continents et des principaux pays constructeurs, 1898-2014, Michel Freyssenet, Vers une théorisation des rapports sociaux, CNRS. ISSN 17760941, Link: http://freyssenet.com/?q=node/367

[5] The International Council on Clean Transportation; European Vehicle Market Statistics, Pocketbook 2013, Link: http://eupocketbook.theicct.org/

[6] ECE R-101; Uniform provisions concerning the approval of passenger cars powered by an internal combustion engine only, or powered by a hybrid electric power train with regard to the measurement of the emission of carbon dioxide and fuel consumption and/or the measurement of electric energy consumption and electric range, and of categories M1 and N1 vehicles powered by an electric power train only with regard to the measurement of electric energy consumption and electric range

[7] PSA Peugeot-Citroën; Hybrid Air, an innovative full hybrid gasoline system, official website from PSA Peugeot-Citroën, consulted on 02.07.2015, Link: http://www.psa-peugeot-citroen.com/en/automotive-innovation/innovation-by-psa/hybrid-air-engine-full-hybrid-gasoline

[8] M. Doppelbauer; Lecture slides, Hybrid and electric vehicles, Winter semester 2012/2013, Karlsruhe Institute of Technology

[9] K. Reif, K. Noreikat and K. Borgeest; Kraftfahrzeug-Hybridantriebe. Grundlagen, Komponenten, Systeme, Anwendungen. Wiesbaden, Springer Vieweg ATZ/MTZ-Fachbuch), 2012, ISBN 978-3-8348-2050-1 (eBook)

[10] P. Hofmann; Hybridfahrzeuge, 2010 Springer-Verlag/Wien, ISBN 978-3-211-89190-2

[11] B. Kaehler, M. Brouwer and T. Christ; Design criteria, methods of analysis, and evaluation of power split transmissions explained through a Two-Mode Hybrid Application, Aachener Kolloquium 2007

[12] T. Finken, M. Felden and K.Hameyer; Comparison and design of different electrical machine types regarding their applicability in hybrid electrical vehicles, Institute of Electrical Machines, RWTH Aachen University, Proceedings of the 2008 International Conference on Electrical Machines

[13] Z. Q. Zhu and D. Howe; Electrical Machines and Drives for Electric, Hybrid, and Fuel Cell Vehicles, in Proceedings of the IEEE, vol. 95, no. 4, 2007

[14] H. Hannoun, M. Hilairet and C. Marchand; Analytical modeling of switched reluctance machines including saturation, 2007 IEEE International Electric Machines & Drives Conference, Antalya, 2007

[15] Tesla Motors; Roadster Technology – Motor, consulted on 06.07.2015, Link: http://my.teslamotors.com/roadster/technology/motor

[16] A. Vignaud and H. Fennel; Efficient Electric Powertrain with Externally Excited Synchronous Machine without Rare Earth Magnets using the Example of the Renault System Solution, Vienna Motor Symposium, April 27, 2012

[17] Robert Bosch GmbH; Official website consulted on 08.04.2015,Link: http://bosch.com/en/com/home/index.php

[18] General Motors Company; Official media website, consulted on 08.04.2015, Link: http://media.gm.com/

[19] Daimler AG; Official Media Website, consulted on 13.05.2015, Link: http://media.daimler.com/

[20] R. Doolittle; Design and Optimization of a Direct-Drive-In-Wheel Electric Motor for Automotive applications, PhD Thesis, Universität des Bundeswehr München, 2015, ISBN: 978-3-8440-4351-8

[21] R. Gehm; 2013 Honda Fit EV applies 'lessons learned' from fuel-cell Clarity, SAE articles, consulted on 15.11.2015, Link: http://articles.sae.org/11591/

[22] R. Forst; Elektromobilität bei Opel – Die Zukunft des Verkehrs, 19. Aachener Kolloquium Fahrzeug- und Motorentechnik, 2010

[23] M. Weiss, T. Ruhl, C. Enderle, U. Keller, F. Nietfeld and C. Mohrdieck; The E-Class Diesel Hybrid by Mercedes-Benz, 21st Aachen Colloquium Automobile and Engine Technology 2012

[24] M. Olszewski; Evaluation of the 2010 Toyota Prius Hybrid Synergy Drive System, March 2011, U.S., Department of Energy, Vehicle Technologies

[25] The National Petroleum Council; Advancing Technology for America's Transportation, Report, Link: http://www.npc.org/reports/trans.html

[26] E. Brée, F. Metzner and D. Neumann; Integration eines PHEV Antriebsstranges in den modularen Querbaukasten MQB von Volkswagen, 13th International CTI Symposium Berlin, December 2014

[27] M. Rashid; Power Electronics Handbook, Devices, Circuits and Applications, Third Edition, Buttwerworth-Heinemann, ELSEVIER, ISBN 978-0-12-382036-5

[28] ECE R-100; Uniform provisions concerning the approval of vehicles with regard to specific requirements for the electric powertrain

[29] R. Helldörfer; VPID–Hochkompakte Leistungselektronik durch Einsatz von bond- und lötfreien Leistungshalbleitermodulen, 1. VDI-Fachkonferenz, Leistungselektronik im Elektro- und Hybridfahrzeug, 13, - 14. March2012

[30] T. Burress; Benchmarking EV and HEV Technologies, Oak Ridge National Laboratory, U.S. DOE Vehicle Technologies Office, June 9, 2015

[31] Toyota Motor Corporation; Toyota Global Site, consulted on 15.03.2016, Link: http://www.toyota-global.com/

[32] F. Blome; Current status and future challenges for automotive energy storage production, 12. Symposium: Hybrid- und Elektrofahrzeuge, 24. February 2015, Braunschweig

[33] Dr. Ing. H.c. F. Porsche AG; Official website, consulted on 20.03.2015, Link: http://www.porsche.com/

[34] M. Weiss, N. Armstrong, J. Schenk, F. Nietfeld and R. Inderka; Hybridantrieb mit höchster elektrischen Leistungsdichte für den ML450 Hybrid, 30. Internationales Wiener Motorensymposium 2009

[35] UNECE R83; Agreement concerning the adoption of uniform technical prescriptions for wheeled vehicles, equipment and parts which can be fitted and/or be used on wheeled vehicles and the conditions for reciprocal recognition of approvals granted on the basis of these prescriptions; Uniform provisions concerning the approval of vehicles with regard to the emission of pollutant according to engine fuel requirements;

[36] H. Palm, J. Holzmann, S. Schneider and H. Koegeler; Die Zukunft im Fahrzeugentwurf - Systems-Engineering-basierte Optimierung, Automobiltechnische Zeitschrift 115

[37] F. Walliser; 918 Spyder – Concept of a super sports car for the future, Dr. Ing. H. c. F. Porsche AG, 14. Internationales Stuttgarter Symposium, 18-19.03.2014

[38] M. Zillmer, H. Neußer, H. Jelden, P. Lück and G. Kruse; The electric drive of the Volkswagen e-up! – A step towards modular electrification of the powertrain, 34. Internationales Wiener Motorensymposium 2013

[39] G. Renda; Method of balancing batteries, US-Patent 7602145 B2, Publication date: 13 Oct. 2009, Tesla Motors, Inc.

[40] Daimler AG; Mercedes AMG SLS e-cell microsite, consulted on 30.09.2015, Link: http://www.mercedes-amg.com/webspecial/sls_e-drive/deu.php

Bibliography

[41] Dr. Ing. H.c. F. Porsche AG; Porsche mission e microsite, consulted on 29.09.2015, Link: http://www.porsche.com/microsite/mission-e/germany.aspx

[42] A. Engstle, M. Deiml, M. Schlecker and A. Angermaier; Entwicklung eines Heckgetrieben 800-V-Elektrofahrzeugs, ATZ – Automobiltechnische Zeitschrift, 2012, Springer Automotive Media

[43] M. Sattler, A. Kufner and E. Kirchner; 48V Electric Axle for Electric Maneuvering, Recuperation and Torque Vectoring, 13th International CTI Symposium, December 2014, Berlin

[44] R. Inderka; Optimal E-Motor Systems for Propulsion, Advanced E-Motor Technology 2013, February 18th

[45] D. Dorrell, A. Knight, M. Popescu, L. Evans and D. Staton; Comparison of Different Motor Design for Hybrid Electrical vehicles, in Energy Conversion Congress and Exposition (ECCE), 2010 IEEE, 12-16 Sept. 2010

[46] C. Betram, D. Buecherl, A. Thanheiser and H.-G. Herzog; Multi-Objective Optimization of a Parallel-Hybrid Electric Drive Train, in Vehicle Power and Propulsion Conference (VPPC), 2011 IEEE, 6-9 Sept. 2011

[47] W. Gao and C. Mi; Hybrid vehicle design using global optimisation algorithm, Int. J. Electric and Hybrid Vehicles, Vol. 1, No. 1, 2007

[48] P. Dumouchel; An optimization approach for hybrid powertrain design, 13th International CTI Symposium, December 2014, Berlin

[49] R. Isermann; Elektronische Management motorische Fahrzeugantriebe, Elektronik, Modelbildung, Regelung und Diagnose für Verbrennungsmotoren, Getriebe und Elektroantriebe, ATZ/MTZ Fachbuch, Vieweg+Teubner, 1. Auflage 2010, ISBN 978-3-8348-0855-4

[50] Xin Li and S. S. Williamson; Efficiency and suitability analyses of varied drive train architectures for plug-in hybrid electric vehicle (PHEV) applications, 2008 IEEE Vehicle Power and Propulsion Conference, Harbin, 2008

[51] F. Sangtarashm V. Esfahanian, H. Nehzahti S. Haddadi, M. A. Bavanpour and B. Haghpanah; Effect of Different Regenerative Braking Strategies on Braking Performance and Fuel Economy in a Hybrid Electric Bus Employing CRUISE Vehicle Simulation, SAE, International Journal, Fuels and Lubricants Congress, June 2008, Vol.1, Issue1

[52] W. Lhomme; Gestion d'énergie de véhicules hybrides basée sur la représentation énergétique macroscopique, PhD. Thesis, Université des Sciences et Technologies de Lille

[53] Y. Kano; Design optimization of brushless synchronous machines with wound-field excitation for hybrid electric vehicles, in Energy Conversion Congress and Exposition (ECCE), 2015 IEEE, 20-24 Sept. 2015

[54] T. Hofman, D. Hoekstra, R.M. van Druten and M. Steinbuch; Optimal design of energy storage systems for hybrid vehicle drivetrains, in Vehicle Power and Propulsion, 2005 IEEE Conference, 2005

[55] U. Schwalbe and M. Schilling; Topology comparison and system optimization for a modular 25 kW motor-inverter drive train system, PCIM Europe 2015, 19 – 21 May 2015, Nuremberg, Germany

[56] M. Ried; Lösungsraumanalyse für Plug-In-Hybridfahrzeuge hinsichtlich Wirtschaftlichkteit und Bauraumkonzept, PhD. Thesis, Universität Duisburg-Essen

[57] T. Schoenen, M. Kunter, M. Hennen, R. De Doncker; Advantages of a variable DC-link voltage by using a DC-DC converter in hybrid-electric vehicles in Vehicle Power and Propulsion Conference (VPPC), 2010 IEEE, Sept. 2010

[58] W. Pflieger; Eine methodischer Ansatz zur modularen Auslegung von Antriebsstrangkomponenten im Rahmen der Entwicklung von Hybridfahrzeugen, PhD. Thesis, Forschungsberichte / IPEK, Band 84

[59] R. Sadoun, R. Nassim, P. Bartholomeus, B. Barbedette and P. Lemoigne; Optimal sizing of hybrid supply for electric vehicle using Li-ion batteries and supercapacitors, IEEE, VPPC'11, Chicago, 2011.

[60] L. Guzella and A. Sciaretta; Vehicle Propulsion Systems, Introduction to Modeling and Optimization, Third Edition, Springer Verlag, 2005, ISBN 978-3-642-35912-5

[61] L. Jishun, L. Jun, W. Qingnian, W. Jiaxue and S. Jinhu; Study on mechanism of energy saving for double motor configuration hybrid electric vehicle, Mechatronic Science, Electric Engineering and Computer (MEC), 2011 International Conference on, Jilin, 2011

[62] J. Wang, Q. Wang, J. Liu, and X. Zen; Forward simulation model precision study for hybrid electric vehicle" in Proc. of the Conf. on Mechatronics and Automation, Changchun, China, 2009

[63] M. Ade and A. Binder; Modeling the drive train for two parallel Hybrid Electric Vehicles in MATLAB/Simulink in Proc. of the Vehicle Power and Propulsion Conference (IEEE-VPPC), Lille, France, 2009

[64] J. Lee, W. Kim, J. Yu, S. Yun S. Kim, J. Lee and J. Lee; Comparison between concentrated and distributed winding in IPMSM for traction application, Electrical Machines and Systems (ICEMS), 2010 International Conference on, Incheon, 2010

[65] D. Gomez, A. Rodriguez, I. Villar. A Lopez-de-heredia, I. Exteberria-Otadui and Z. Zhu; Improved permeance network model for embedded magnet synchronous machines, Electrical Machines (ICEM), 2014 International Conference on, Berlin, 2014

[66] A. Fonseca, C. Chillet, E. Atienza, A. Bui-Van and J. Bigeon; New modeling methodology for different PM motors for electric and hybrid vehicles, Electric Machines and Drives Conference, 2001. IEMDC 2001. IEEE International, Cambridge, MA, 2001

[67] T. Miller; SPEED's Electric Motors: An Outline of some of the Theory in the SPEED Software for Electric Machine Design, University of Glasgow, 2002-2007

[68] C. Chen, M. Mohr, and F. Diwoky; Modeling of the System Level Electric Drive using Efficiency Maps Obtained by Simulation Methods, SAE Technical Paper 2014-01-1875, 2014

[69] G. Mohan, F. Assadian and S. Longo; An Optimization Framework for Comparative Analysis of Multiple Vehicle Powertrains, Energies, Link: http://www.mdpi.com/journal/energies

[70] S. Lukic and A. Emadi; Modeling of electric machine for automotive applications using efficiency maps, Electrical Insulation Conference and Electrical Manufacturing & Coil Winding Technology Conference, 2003. Proceedings, 2003

[71] K. Zhou, J. Pries and H. Hofmann; Computationally-efficient 3D finite-element-based dynamic thermal models of electric machines, Electric Machines & Drives Conference (IEMDC), 2013 IEEE International, Chicago, IL, 2013

[72] V. Matosevic and Z. Stih; 2D Magneto-thermal analysis of synchronous generator, University of Zagreb, PRZEGLĄD ELEKTROTECHNICZNY, ISSN 0033-2097, R. 90 NR 12/2014

[73] G. Dajaku and D. Gerling; An Improved Lumped Parameter Thermal Model for Electrical Machines, Institute for Electrical Drives, University of Federal Defense Munich

[74] DIN EN 50347; General purpose three-phase induction motors having standards dimensions and outputs – Frame number 56 to 315 and flange numbers 65 to 740, German version EN50347:2001

[75] M. Burwell, J. Goss and M. Popescu; Performance/cost comparison of induction-motor and permanent-magnet-motor in a hybrid electric car, International Copper Association, 2013 – Tokyo

[76] M. März, A. Schletz, B. Eckardt, S Egelkraut and H. Rauh; Power Electronics System Integration for Electric and Hybrid Vehicles, Fraunhofer Institute of Integrated Systems and Device Technology, Erlangen, Germany

[77] H. Schäfer; Neue elektrische Antriebskonzepte für Hybridfahrzeuge, Renningen: Expert-Verlag, 2007

[78] M. Ehsani, Y. Gao, S. Gay and A. Emadi; Modern Electric, Hybrid Electric and Fuel Cell Vehicles, Fundamentals, Theory, and Design, CRC Press, Power Electronics and Applications Series, ISBN: 0-8493-3154-4

[79] J. Specovius; Grundkurs Leistungslektronik, Bauelement, Schaltung und Systeme, 7th Edition, Springer Vieweg, ISBN 978-3-658-03309-5 (E-Books)

[80] J. Lutz; Halbleiter-Leistungsbauelemente, Springer-Verlag Berlin, 2012, ISBN: 978-3-642-29796-0

[81] H. Iwamoto, H. Haruguchi, Y. Tomomatsu, J. F. Donlon and E. R. Motto; A new punch through IGBT having a new N-buffer layer, Industry Applications Conference, 1999. Thirty-Fourth IAS Annual Meeting. Conference Record of the 1999 IEEE, Phoenix, AZ, 1999

[82] C. Batard, F. Poitiers, C. Millet and N. Ginot ; Simulation of Power Converters Using Matlab-Simulink, Lunam University - University of Nantes, UMR CNRS 6164,Institut d'Electronique et de Télécommunications de Rennes (IETR), France

[83] G. Varshney, D. Chauhan and M. Dave; Simscape Based Modeling & Simulation of MPPT Controller for PV Systems, IOSR Journal of Electrical and Electronics Engineering (IOSR-JEEE) Volume 9, Issue 6 Ver. I (Nov – Dec. 2014)

[84] A. Battiston; Modélisation, commande, stabilité et mise en œuvre des onduleurs à source impédante. Application aux systèmes embarqués, Phd. Thesis, Université de Lorraine, 2014

[85] D. Graovac and M. Pürschel; IGBT Power Losses Calculation Using the Data-Sheet Parameters, Application Note, V 1.1 January 2009, Infineon

[86] J. W. Kolar, H. Ertl and F. C. Zach; Influence of the Modulation Method on the Conduction and Switching Losses of A PWM Converter System, in IEEE transaction on industry applications, Vol. 27, No. 6, 1991.

[87] F. Casanellas; Losses in PWM inverters using IGBTs, in IEE Proceedings - Electric Power Applications, vol. 141, no. 5, Sep 1994

[88] F. Labrique; Power Electronics Converters, Electric Energy Systems and Engineering Series (EESES), Springer Verlag, ISBN: 978-3-642-50324-5

[89] M. H. Bierhoff and F. W. Fuchs; DC-Link Harmonics of Three-Phase Voltage-Source Converters Influenced by the Pulsewidth-Modulation Strategy–An Analysis, in IEEE Transactions on Industrial Electronics, vol. 55, no. 5, 2008

[90] J. Mühlethaler, J. Biela, J. W. Kolar and E. Andreas; Core Losses under DC Bias Condition based on Steinmetz Parameters. IEEE Transactions on Power Electronics, Vol. 27, No. 2, 2012

[91] K. Venkatachalam, C. R. Sullivan, T. Abdallah and H. Tacca; Accurate prediction of ferrite core loss with nonsinusoidal waveforms using only Steinmetz parameters, Computers in Power Electronics, 2002. Proceedings. 2002 IEEE Workshop on, 2002

[92] D. Graovac and M. Pürschel; MOSFET Power Losses Calculation Using the Data-Sheet Parameters, Application Note, V 1.1 July 2006, Infineon

[93] D. Kinzer; Welcome to the Post-Silicon World: Wide Band Gap Powers Ahead, Key Notes 10.05.2016, PCIM Europe 2016, Nuremberg, Germany

[94] T. Nakajima, S. Yoshida, A. Uenishi, T. Shirasawa, S. Ukita and Y. Kimura; New intelligent power module for electric vehicles, Industry Applications Conference, 1995. Thirtieth IAS Annual Meeting, IAS '95., Conference Record of the 1995 IEEE, Orlando, FL, 1995

[95] M. Olszewski; Evaluation of the 2007 Toyota Camry Hybrid Synergy Drive System, Oak Ridge National Laboratory for the U.S. Department of Energy, April 2008

[96] Brusa Elektronik AG; Official website, consulted on 08.04.2015, Link: http://www.brusa.biz/

[97] Plexim official website; PLECS, Simulation Software for Power Electronics, consulted on 19.11.2015, Link: https://www.plexim.com/

[98] A. Dehbi, W. Wondrak, E. Rudnyi, U. Killat and P. van Duijsen; Efficient electrothermal simulation of power electronics for hybrid electric vehicle, Thermal, Mechanical and Multi-Physics Simulation and Experiments in Microelectronics and Micro-Systems, 2008. EuroSimE 2008. International Conference on, Freiburg, 2008

[99] M. Warwel, G. Wittler, M. Hirsch and H-C. Reuss; Online thermal monitoring for power semiconductors in power electronics of electric and hybrid electric vehicles, 14TH Stuttgart International Symposium, Automotive and Engine Technology, 2014

Bibliography

[100] M. März and P Nance; Thermal Modeling of Power-electronic Systems, consulted on 18.10.2015, Link: http://www.infineon.com/dgdl/Thermal+Modeling.pdf?fileId=db3a30431441fb5d011472fd33c70aa3

[101] Infineon AG; Automotive IGBT Module, Application Note, Explanation of Technical Information, AN2010-09, Revision 1.0, Electric Drive Train

[102] Z. Jakopovic, V. Sunde and Z. Bencic; Electro-Thermal Modeling and Simulation of a Power-MOSFET, ISSN 0005-1144, ATKAAF 42(1-2), 71-77 (2001).

[103] J. Ortiz-Rodriguez; Electro-Thermal Modeling of a Power Electronic Module, Master Thesis, University of Puerto Rico

[104] M. Maerz, M. Poech, E. Schimanek and A. Schletz; Mechatronic Integration into the Hybrid Powertrain – The Thermal Challenge, Results of the ECPE Research Program "System Integrated Drive for Hybrid Traction in Automotive"

[105] A. Rekofsky, R. Brey, M. Thoben, C. Mertens, G. Löcher et al.; Modularity bridging future Power Electronics in automotive volume applications – speeding up HEV applications, Integrated Power Systems (CIPS), 2008 5th International Conference on, Nuremberg, Germany, 2008

[106] J. Kolar, U. Drofenik, J. Biela, M. Heldwein, H. Ertl, T. Friedli and S. Round; PWM Converter Power Density Barriers, IEEJ, Transaction on Industrial Applications, Vol. 128, No. 4, 2008

[107] LEM; Automotive Current Sensor HC6H500-S, Datasheet, 070420/1, consulted on 20.12.2014, Link: http://www.lem.com

[108] Infineon; Application Note, Hybrid Kit for HybridPACK™ 2, V2.4, 2014-08-11, consulted on 16.12.2014, Link: http://www.infineon.com/

[109] Methode Electronics, Inc.; Liquid Cooled Systems, Liquid-Cooled Chill Blocks Data Sheet, consulted on 18.12.2014, Link: http://www.methode.com/power/thermal-management/liquid-cooled.html#.WFi-fmVviCo

[110] Norm DIN EN 60664-1; DIN EN 60664-1:2008-01, VDE 0110-1:2008-01, Insulation coordination for equipment within low-voltage systems - Part 1: Principles, requirements and tests (IEC 60664-1:2007), German version EN 60664-1:2007

[111] Kemet, Electronics Components, Capacitor datasheets for various applications, consulted on 20.11.2014, Link: http://www.kemet.com/

[112] Kostal; Connectors for HV-applications, consulted on 14.12.2014, Link: http://www.kostal.com/kks/en/produktfelder_hochstrom.php

[113] R. Robutel; Etude des composants passifs pour l'électronique de puissance à "haute température" : application au filtre CEM d'entrée, PhD. Thesis, INSA de Lyon, 2011.

[114] TDK COMPONENTS; TDK Components, the Customer Magazine of RDK-EPC Corporation, Applications &Cases, Space-saving DC link solution, EPCOS AG · A Member of TDK-EPC Corporation · Edition 2011

[115] N. Rouhana, E. Semail and J. F. Duguey; Impact of PWM Strategies on RMS Current of the DC-Link Voltage Capacitor of a Dual-Three Phase Drive, 2014 IEEE Vehicle Power and Propulsion Conference (VPPC), Coimbra, 2014.

[116] German Association of the Automotive Industry; VDA LV123 (norm), Electrical characteristics and electrical safety of high voltage components in road vehicles, Requirements and tests

[117] International Organization for Standardization; ISO6469-3 (international standard), Electrically propelled road vehicles - Safety specifications - Part 3: Protection of persons against electric shock

[118] German Association of the Automotive Industry; VDA Recommendation 320 Electric and Electronic Components in Motor Vehicles 48 V On-Board Power Supply, Requirements and Tests, Based on the german version VDA 320 (August 2014)

[119] B. Klein; Hybridization Tailored to Fit, Continental Automotive, Plug-in-Hybride und Range Extender, Haus der Technik, 2016, Darmstadt

[120] Hitachi Automotive Systems; Hitachi Automotive Systems Delivers Compact, High-Output Inverters and DC/DC Converters for the first Plug-in Hybrid from Mercedes Benz, consulted on 23.06.2015, Link: http://www.hitachi-automotive.co.jp/en/

[121] D. Hoheisel; E-Mobilität - Chancen und Herausforderungen für Automobilzulieferer, 05.02.2013, TU Braunschweig

[122] Bosch GmbH; Bosch product portfolio for hybrid vehicles synergies between PC and CV, 2014, 11. Symposium für Hybrid- und Elektrofahrzeuge – Braunschweig

[123] S. Knirsch, R. Straßer, G. Schiele, S. Möhn, W. Binder and M. Enzinger; The powertrain of the new Audi Q7 e-tron 3.0 TDI Quattro, 36th International Vienna Engine Symposium, 7th - 8th May 2015, Vienna

[124] U. Keller, S. Schmiedler, J. Strenker, N. Ruzicka and F. Nietfeld; PLUG-IN Hybrid from Mercedes-Benz – The next generation PLUG-IN Hybrid with 4-cylinder gasoline engine, Daimler AG, 15. Internationales Stuttgarter Symposium, Proceedings, Springer Fachmedien Wiesbaden 2015

[125] A. Thaler and D. Watzenig; Automotive Battery Technology, SpringerBriefs in Applied Sciences and Technology, Automotive Engineering: Simulation and Validation Methods, Springer Verlag, ISBN: 978-3-319-02523-0

[126] M. Urbain, M. Hinaje, S. Raël, B. Davat and P. Desprez; Energetical Modeling of Lithium-Ion Batteries Including Electrode Porosity Effects, in IEEE Transactions on Energy Conversion, vol. 25, no. 3, 2010

[127] M. Debert, G. Colin, M. Mensler, Y. Chamaillard and L. Guzella; Li-ion battery models for HEV simulator, Advances in Hybrid Powertrain, 2008, Institut Prisme, Renault SAS

[128] P. Keil and A. Jossen; Aufbau und Parametrierung von Batteriemodellen, TU München, Institut für Electrical Energy Storage (Lehrstuhl für Elektrische Energiespeichertechnik)

[129] F. A. Rusu and G. Livint; Study of hybrid power sources for electrical vehicles,2016 International Conference on Development and Application Systems (DAS), Suceava, Romania, 2016

[130] Hanlei Zhang and Mo-Yuen Chow; Comprehensive dynamic battery modeling for PHEV applications, IEEE PES General Meeting, Minneapolis, MN, 2010

[131] W. Renhart, C. Magele and B. Schweighofer; FEM-Based Thermal Analysis of NiMH Batteries for Hybrid Vehicles, in IEEE Transactions on Magnetics, vol. 44, no. 6, 2008

[132] K. Yeow, H. Teng, M. Thelliez and E. Tan; 3D Thermal Analysis of Li-ion Battery Cells with Various Geometries and Cooling Conditions Using Abaqus, AVL Powertrain Engineering

[133] H. Kim, S. Kim, T. Kim, C. Hu and B. D. Youn; Online thermal state estimation of high power lithium-ion battery, Prognostics and Health Management (PHM), 2015 IEEE Conference on, Austin, TX, 2015

[134] U. Keller, M. Back, F. Nietfeld, M. Mürwald and A. Docter; PLUG-IN Hybrid von Mercedes-Benz – Der Antriebsstrang des S500 Plug-In Hybrid, 35. Internationales Wiener Motorensymposium 2014

[135] Lion Smart GmbH; Allgemeine Beschreibung des modularen Batterie-Management System, Li-BMS V3, Datenblatt V1.0t, consulted on 14.02.2014, Link: http://www.lionsmart.de

[136] Lithium Balance; LiTHIUM BALANCE Scalable Battery Management System (s-BMS v6), Housed and loose board battery management solutions and accessories, SYSTEM INFORMATION, Litt. no. 6100-0010, consulted on 16.02.2014, Link: http://www.lithiumbalance.com

[137] U. Wagner, M. Rauch, T. Eckl, A. Schamel, C. Weber, M. Sptringer, O. Maiwald, T. Knorr and S. Lauer; 48 V P2 hybrid vehicle with an optimized combustion engine – Fuel economy and costs at their best combined with enhanced driving behavior, 37. Internationales Wiener Motorensymposium 2016

[138] V. Weisberger and J. Duhr; Power Electronics for Electric and Hybrid Vehicles, Traction Inverter, DC/DC convert and On-board Charger: Components and Technical Challenges for Power Electronics, VDI Conference Frankfurt/Main, March 13-14, 2012

[139] J. Fernandez de Canete, C. Galindo and I. Garcia Moral; System Engineering and Automation, An Interactive Educational Approach, Springer Verlag, 2011, ISBN 978-3-642-20229-2

[140] R. Foley, R. Nagappala, G. Ressler, P. Andres and B. Maretel; Application of Insulation Standards to High Voltage Automotive Applications, in SAE International, 2013

[141] ZVEI - Zentralverband Elektrotechnik und Elektronikindustrie e.V.; 48-Volt-Bordnetz – Schlüsseltechnologie auf dem Weg zur Elektromobilität, 2015

[142] M. Ade, A. Binder and H. Neudorfer; Modellierung der parallelen Antriebsstränge für ein Hybrid-Elektrofahrzeug vom Typ „Hybrid Through The Road“, e&i elektrotechnik und informationstechnik, heft 4, 2004

[143] Webster; English dictionary, an Encyclopedia Britannica Company, consulted on 09.09.2015, Link: http://www.merriam-webster.com/dictionary/

[144] R. Andreux; Modélisation et optimisation des démarreurs à inducteur bobiné pour l'application “Stop-Start” ou micro-hybride, Phd. thesis, Université de Lorraine, 19.02.2013.

[145] M. Ehrgott; Multicriteria Optimization, second edition, Springer Verlag, ISBN 3-540-21398-8

[146] R. Desai and R. Patil; SALO: combining simulated annealing and local optimization for efficient global optimization, in Proceedings of the 9th Florida AI Research Symposium, Key West, June 1996

[147] D. Finkel; DIRECT Optimization Algorithm User Guide, Center For Research in Scientific Computation, North Carolina State University, 2003

[148] D. Finkel; DIRECT Research and Code, North Carolina State University, consulted on 25.06.2016. Link: http://www4.ncsu.edu/~ctk/Finkel_Direct/

[149] M. Zeraoulia, M. Benbouzid and D. Diallo; Electric Motor Drive Selection Issues for HEV Propulsion Systems: A Comparative Study, in IEEE Transactions on Vehicular Technology, vol. 55, no. 6, 2006.

[150] S. Matsumoto; Advancement of hybrid vehicle technology, in Power Electronics and Applications, 2005 European Conference on, 2005

[151] K. Toyoshima; Prius, Toyota Media Tour 2015, Tokyo Motor Show, Toyota Motor Corporation

[152] J. Li, T. Abdallah and C. R. Sullivan; Improved Calculation of core Loss with Nonsinusoidal Waveforms, IEEE, 2001

[153] P. Desai, M. Anwar, S. Gleason and S. Hawkins; Power Electronics for GM 2-Mode Hybrid Electric Vehicles, SAE Technical Paper, 2010

[154] K. Arai, K. Higashi, T. Iiyama, H. Murai et al.; High Power Density Motor and Inverter for RWD Hybrid Vehicles, SAE Technical paper, 2011

[155] Volkswagen AG; Official Volkswagen Media Website, consulted on 16.10.2015, Link: https://www.volkswagen-media-services.com/

APPENDIX

Appendix 1: CO_2 restrictions in the automotive industry
Appendix 2: Hybrid functionalities
Appendix 3: Measurements and validation of electric machine and inverter modeling
Appendix 4: Power electronics structures
Appendix 5: Datasheets and parameters extraction for power electronics modeling
Appendix 6: Loss models for power electronics
Appendix 7: Battery structures
Appendix 8: Contribution of the evaluation approach
Appendix 9: Results of the P2-60 and P2-15 systems

Appendix 1: CO_2 restrictions in the automotive industry

In this first appendix, the legislative framework of the CO_2 restrictions is deeper explained to have an overview of what it really involves for the development of new vehicles. The first diagram shows the future CO_2 restrictions for different countries and how they evolved over the last years.

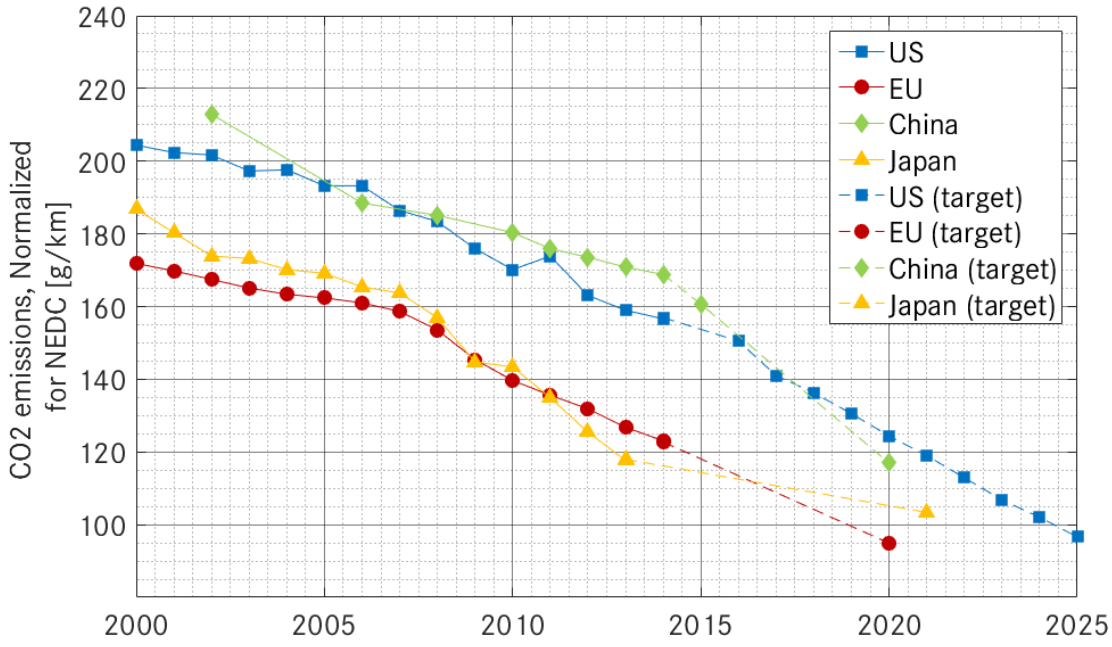

Figure: CO_2 emissions legislative framework for the automotive industry [2]

The CO_2 restrictions are not only evolving with the years but are also based on the vehicle weight to enable a fair comparison between the different manufacturers.

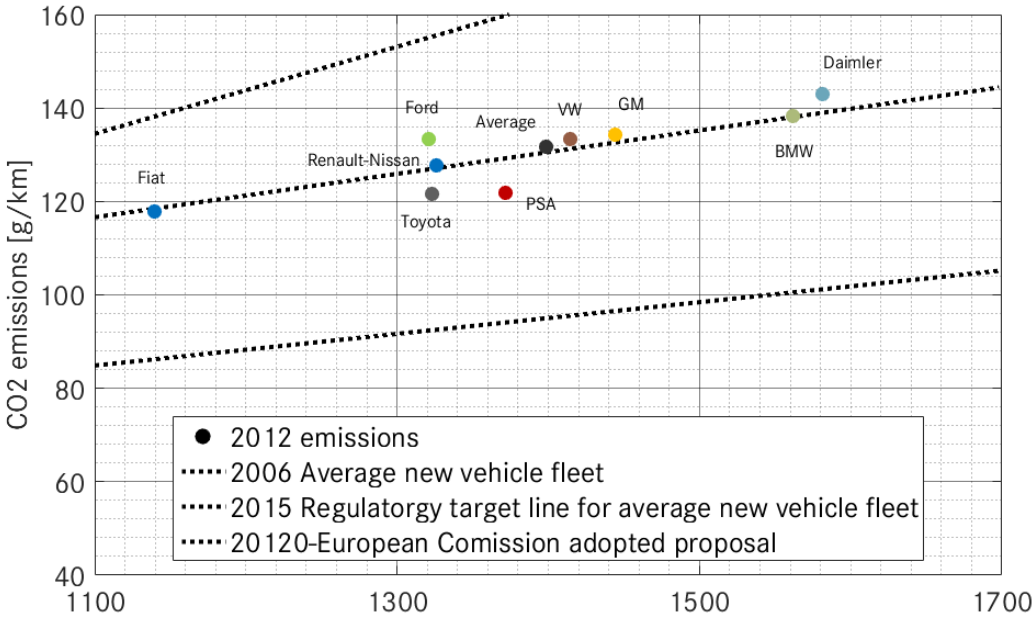

Figure: EU new passenger vehicles CO2 emissions (2012) [5]

Appendix 2: Hybrid functionalities

This appendix presents the additional vehicle functionalities which can be achieved thanks to the electric components in hybrid drivetrain.

Start/Stop:
It depicts the possibility to shut down and restart quickly the internal combustion engine when the car stops to reduce the time spent idling. This functionality requires a direct connection between the engine and the electric machine to be achieved by the hybrid drivetrains components (it is for example not possible for P4-architectures) and the required torque for the restart needs to be achievable by the electric machine.

E-Drive:
This functionality describes the ability of the vehicle to be only driven by the electric machine. It is no mandatory requirement for a hybrid vehicle because it is linked with its architecture. Differentiation is sometimes made between E-Drive and the ability to leave a parking lot or to park a car. It is not differentiated in this research work because it does not influence the design or the simulation of the components.

Load point shifting:
The load point shifting can be both a motor and generator mode functionality. With the combination of an electric machine ans a combustion engine, operating points can be optimized. The electric machine can compensate the torque when the best consumption point for the current speed is above (case of driving point 1) or under (case of driving point 2) the required torque for driving. Moreover this functionality depends on the system state-of-charge because when the energy storage system is full, it cannot regenerate the additional power or when it is empty, it cannot deliver additional torque.

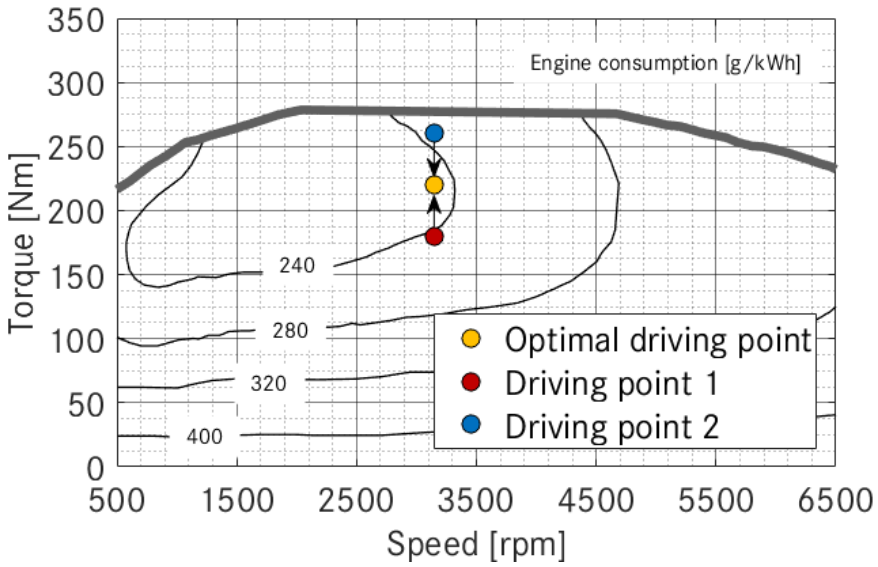

Figure: Principle of load-point shifting based on [9] and [10]

Boost:
Boost depicts the possibility for the electric machine(s) to assist the combustion engine in order to provide more power. Contrary to load-point shifting, it only aims to bring more performance and though the combustion engine already brings the maximal power. Similar to the previous functionality, it is only meaningful when the state of charge allows it.

Regenerative braking:
The generator mode offers the possibility for the drivetrain to store the generated energy during braking. The electric machine applies a negative torque on the wheels and the mechanical energy is converted into electrical energy.

Appendix 2: Hybrid functionalities

Sailing:

When the vehicle is off throttle or going down an incline, the electric machine can be used to lightly brake or maintain a constant speed. In this case the machine can regenerate energy or simply work in no-load area.

Charging:

The plug-in variants of hybrid vehicles have the possibility to be connected to a charging station. By charging the vehicle, the electrical range can be increased and thus the use of the combustion engine can be reduced.

Engine charging:

Beside the possibility to charge the vehicle at a station, electrical energy can be generated by the combustion engine. When the car stands, the combustion is used at an optimal working point and drive the electric machine to store energy. It is less efficient for the consumption reduction than the conventional charging mode but still more efficient than driving with the combustion engine because the working point can be optimized.

Appendix 3: Measurements and validation of electric machine and inverter modeling

Measurement set-up:

The following measurement setup is used for the validation of electric machine and inverter modeling. The battery is represented by a simulator and only the inverter and the electric machine are measured. Beside the mechanical and electrical measurements, thermal measurements can be done. They are however independent from the measurement set-up and are related to the installed thermal sensors in each component.

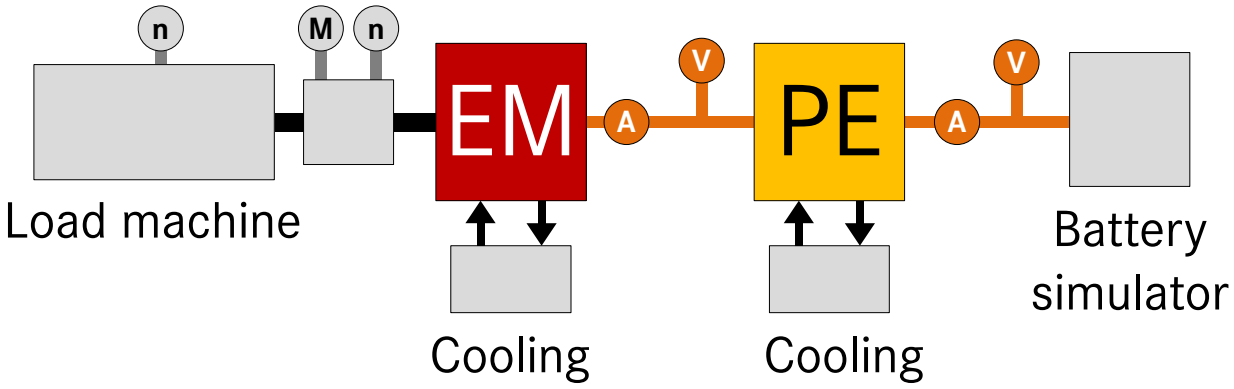

Figure: Measurement set-up for the validation of electric machine and inverter modeling

Figure: Electric machine and inverter in the measurement set-up

Appendix 4: Power electronics structures

In this appendix, the different structures for power electronics are presented. The converters box considered in this appendix are based on current automotive converters for hybrid electrical vehicles applications. Additional structures can be implemented for electric or fuel-cell vehicle but are not investigated in this work.

Stand-alone inverter:

The stand-alone inverter consists in housing with only the sub-component for the bidirectional AC/DC-conversion. The HV/12V-converter is therefore integrated in another housing. This solution offers high flexibility due to the separation of the converters but low integration potential since two housing and additional connectors/screw are required.

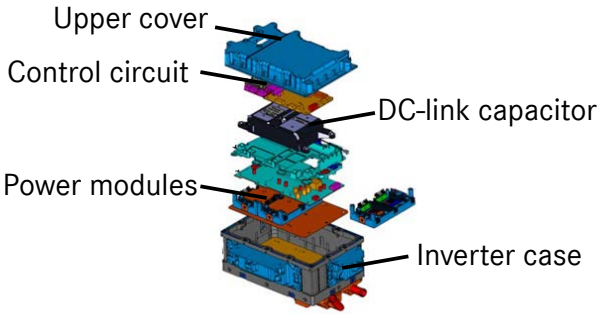

Figure: Stand-alone inverter structure [154]

Structure with inverter and HV/12V-converter:

This structure is presented in chapter 3. It is used in most of the hybrid vehicles with only one electric machine to restrain the number of converters and thus the number of connectors. Contrary to the previous structures with at least four connectors (2 per converter), this structure needs at least 3 connectors: a DC-connector (HV), an AC-connector (HV) and a 12V-connector.

Several inverters structure:

This structure contains two converters, one for each electric machine. They are integrated together to reduce the number of connectors and to enable synergies and better communication between the two inverters. As for the stand-alone inverter, a variant with HV/12V-converter is possible depending on the drivetrain structure.

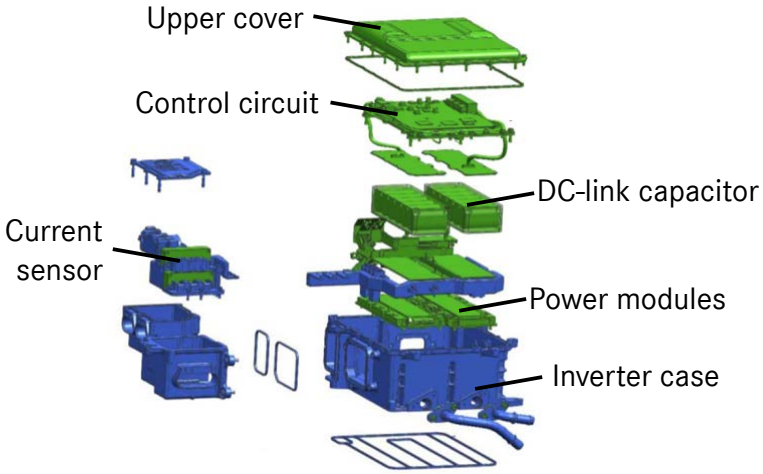

Figure: Structure with several inverters [153]

Structures with several inverters, HV/12V-converter and boost-converter:

Within the structures with several inverters, HV/12V-converter and boost-converter, the number of machines can vary. Here two structures are presented: one with two inverters and one with three inverters. These two structures as previously explained aim to reduce the number of connectors. By integrating all converters in the same housing

the number of DC-connectors for the inverter can be reduced. It enhanced also the power density since the housing is used for all the converters.

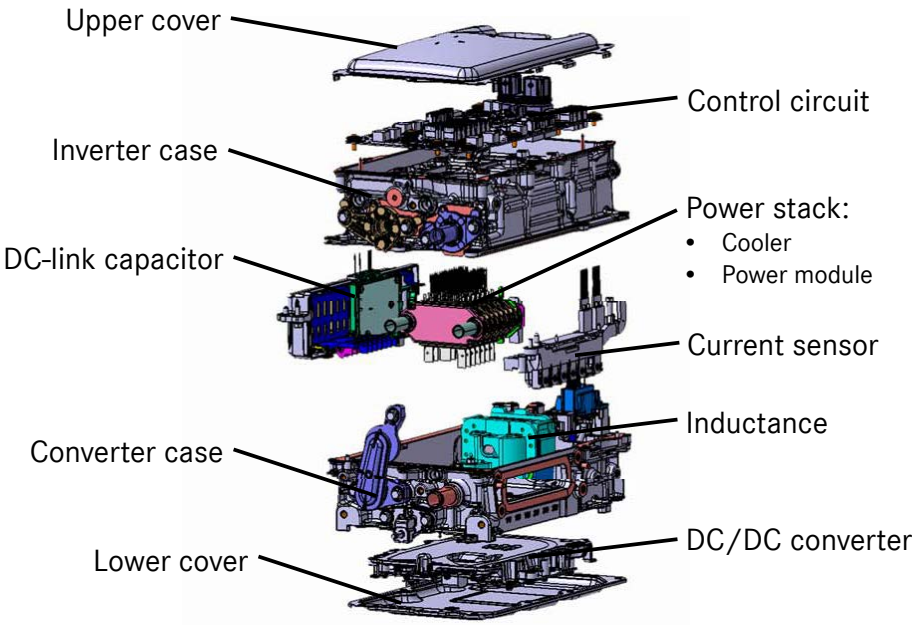

Figure: Structure with two inverters, HV/12V-converter and boost-converter [151]

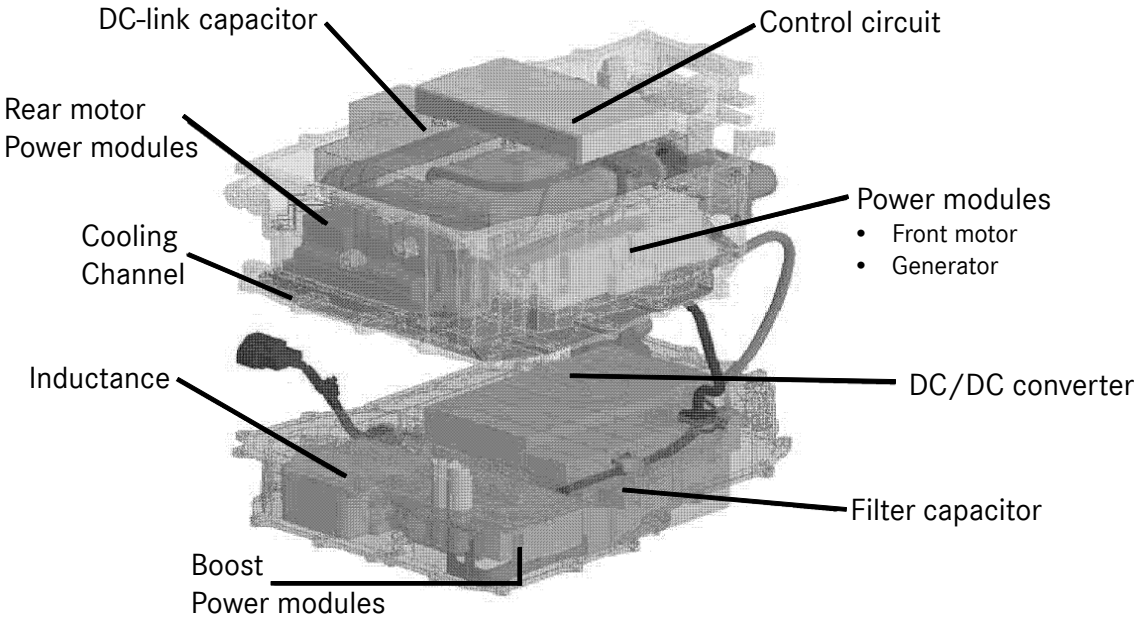

Figure: Structure with three inverters, HV/12V-converter and boost-converter [150]

Appendix 5: Datasheets and parameters extraction for power electronics modeling

This appendix presents the different types of datasheets used for power electronics modeling (electrical, thermal as well as volume and weight estimation). It presents the power modules datasheets (IGBT and Mosfet) and the extraction of the parameters for the electrical and thermal modeling

1. IGBT power module

This section presents the typical datasheets of IGBT power module as well as the extraction of the parameters. The extraction method is based of [85] while the datasheets can be found directly on the website of typical automotive suppliers:

- Infineon: https://www.infineon.com/
- Mitsubishi electric: http://emea.mitsubishielectric.com/en/index.page
- Fuji Electric: http://www.fujielectric.com/

The datasheets are generally composed of several tables and figures which summarized the performance and the characteristics of the power module. In this appendix, only the diagram used for the modeling are presented.

Conductions losses:

For the calculation of the conduction losses, the methods presented in [85] are used. The same method is applied three times for each of the temperature. The influence of the gate-voltage is not considered in this work. The extraction is presented on the next figure for a temperature of 25°C. The value U_{ce0} und U_{D0} can be directly during the extraction while the values of the resistances are calculated using the following equations:

$$r_c = \Delta U_{ce} / \Delta I_c$$
$$r_D = \Delta U_D / \Delta I_D$$

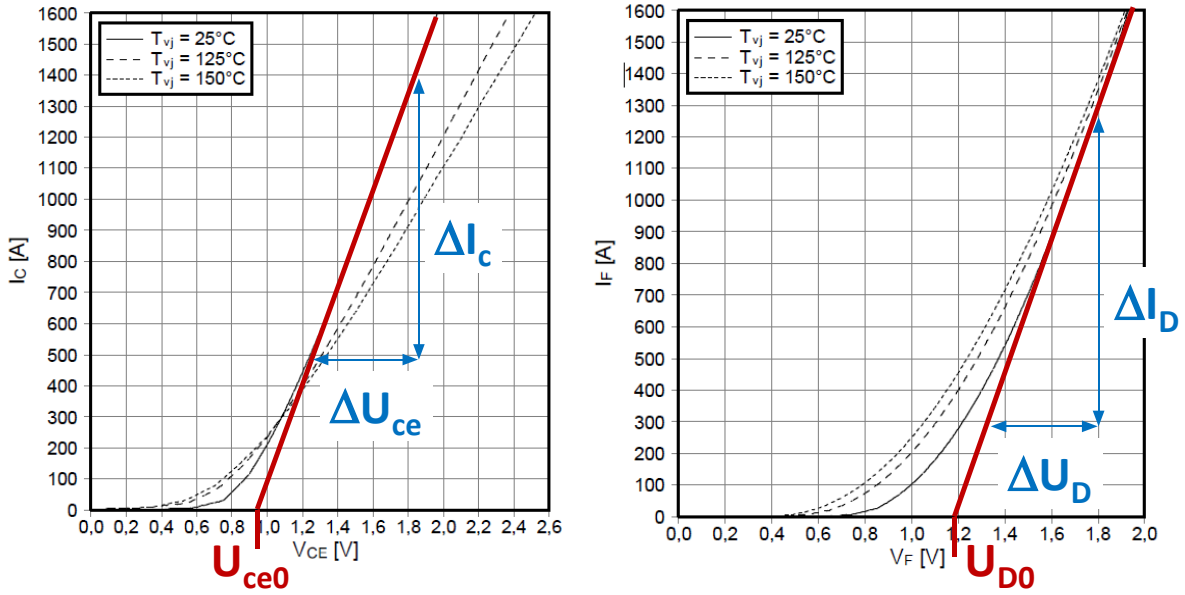

Figure: Conduction losses parameters extraction for the IGBT (left) and for the diode (right)

Switching losses:

For the calculation of the switching losses, two sources of data are used. First the temperature dependency is extracted using the data stored in the IGBT- and diode-parameter as the ones presented on the following figure and then the current dependency is extracted from the performance diagram as the ones presented below. The extraction of the parameters for the current dependency is done using a tool which provides the data by calibrating the x- and y-axis.

Einschaltverlustenergie pro Puls Turn-on energy loss per pulse	I_C = 550 A, V_{CE} = 300 V, L_S = 20 nH V_{GE} = ±15 V, di/dt = 5500 A/µs (T_{vj}=150°C) R_{Gon} = 1,8 Ω	T_{vj} = 25°C T_{vj} = 125°C T_{vj} = 150°C	E_{on}	10,5 12,0 12,5	mJ mJ mJ
Abschaltverlustenergie pro Puls Turn-off energy loss per pulse	I_C = 550 A, V_{CE} = 300 V, L_S = 20 nH V_{GE} = ±15 V, du/dt = 2700 V/µs (T_{vj}=150°C) R_{Goff} = 0,75 Ω	T_{vj} = 25°C T_{vj} = 125°C T_{vj} = 150°C	E_{off}	21,0 25,0 26,0	mJ mJ mJ
Abschaltenergie pro Puls Reverse recovery energy	I_F = 550 A, - di_F/dt = 5500 A/µs (T_{vj}=150°C) V_R = 300 V V_{GE} = -15 V	T_{vj} = 25°C T_{vj} = 125°C T_{vj} = 150°C	E_{rec}	4,00 9,50 11,5	mJ mJ mJ

Figure: Switching losses parameters for the IGBT (top) and for the diode (bottom) for the temperature dependency

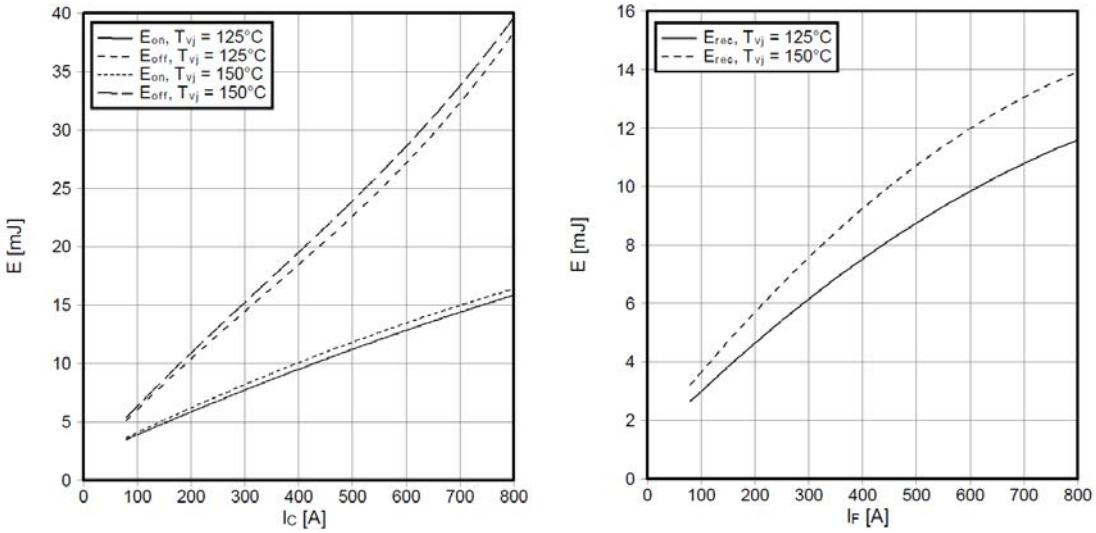

Figure: Switching losses parameters for the IGBT (left) and for the diode (right) for the current dependency

Thermal modeling:

For the thermal modeling, two series of data for each semiconductor are extracted: the thermal equivalent resistance and capacitance which can be directly extracted and the coolant flow dependency which is extracted using the same tool as for the switching losses. Examples are presented on the following figure.

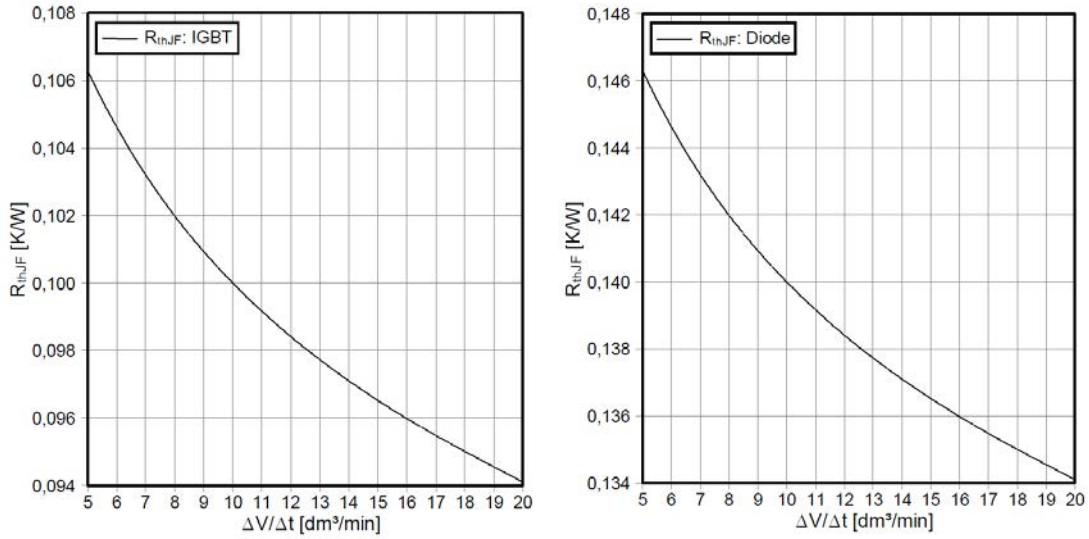

i:	1	2	3	4	5
r_i[K/W]:	0,0062	0,022	0,0238	0,038	0,01
τ_i[s]:	0,0005	0,02	0,058	0,45	2,19

i:	1	2	3	4	5
r_i[K/W]:	0,0126	0,0391	0,0417	0,0331	0,0135
τ_i[s]:	0,0006	0,017	0,053	0,39	3,2

Figure: Thermal modeling parameters for the IGBT (left) and for the diode (right)

2. Mosfet power module

In the case of the Mosfet power modules, the datasheet are very similar. The main difference is due to the semiconductor technology for the extraction of the parameters for the conduction losses. Hence, this section details only the method for the extraction of the Mosfet parameters for these losses based on the method presented in [92]. As it can be seen on the following figure, the current has quite no influence on the value of R_{DSon} and therefore only the temperature dependency is considered in this work. In the case of the Mosfet, the temperature dependency of R_{DSon} is directly provided as diagram and can be directly extracted using the same tool as previously.

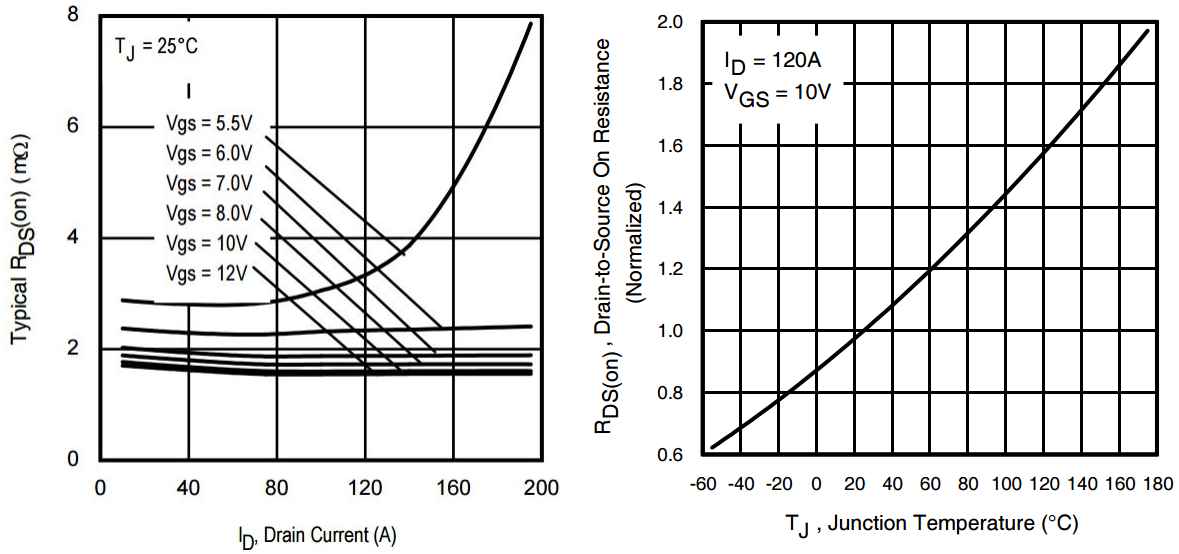

Figure: Switching losses parameters for the IGBT (left) and for the diode (right) for the current dependency

Appendix 6: Loss models for power electronics

This appendix presents the calculation for the different loss models used in this work. If some of them are trivial because they are only depicting the resistive behavior of the components, the others are based on some assumptions. In this appendix, the calculation for the inverter conduction losses, the calculation of the boost-converter conduction and switching losses as well as the input inductance loss calculation are presented. The case of the DC-link capacitor is not discussed but a deep analysis of the calculation is presented in [86].

Inverter conduction losses:

For this calculation, the output current of the inverter is supposed to be perfectly sinusoidal. As discussed in chapter 3, these assumptions can be made due to the ratio between the electric machine frequency and the inverter frequency. The output current is therefore represented by the following equation:

$$I_{out}(t) = I \cdot sin(\omega t)$$

Depending on the semiconductor technology, the voltage of the transistor can be expressed in two different ways. The IGBT behavior is composed of two parts while the Mosfet behavior is purely resistive. The two expressions are presented in the following equations respectively for the IGBT and the Mosfet.

$$U_{ce_{IGBT}} = U_{ce0} + r_c \cdot i_{IGBT}(t)$$

$$U_{ce_{Mosfet}} = R_{DSon} \cdot i_{Mosfet}(t)$$

None of these parameters are depending on the current and thus the same calculation approach can be used for both of them. The conduction losses are therefore expressed by the following equations.

$$P_{CT} = \frac{1}{T_{switch}} \int_0^{T_{switch}} U_{CE} \cdot i(t) \cdot \alpha(t) \cdot dt$$

where α is the ratio between the conduction time of the transistor and the switching period. This factor can be expressed by considering the motor displacement factor φ and the ratio m_a between the input voltage and the output voltage (modulation factor) as in the following equation.

$$\alpha(t) = \frac{1}{2}\,(\,1 + m \cdot \sin(\omega t + \varphi))$$

Considering a PWM based control method and the previously discussed parameters, the following equations can be solved for respectively the IGBT and the Mosfet.

$$P_{CT} = \frac{1}{T_{switch}} \int_0^{T_{switch}} (U_{ce0} + r_C \cdot I \cdot sin(\omega t)) \cdot I \cdot sin(\omega t) \cdot \frac{1}{2}\,(\,1 + m \cdot \sin(\omega t + \varphi)) \cdot dt$$

$$P_{CT} = \frac{1}{T_{switch}} \int_0^{T_{switch}} R_{DSon} \cdot I \cdot sin(\omega t) \cdot I \cdot sin(\omega t) \cdot \frac{1}{2}\,(\,1 + m \cdot \sin(\omega t + \varphi)) \cdot dt$$

When integrating these equations, the conduction losses as presented in chapter 3 can be found and are expressed as follows:

$$P_{CT} = U_{ce0} \cdot I_o \cdot \left(\frac{1}{2\pi} + \frac{m_a \cdot \cos\varphi}{3\pi}\right) + r_c \cdot I_o^2 \cdot \left(\frac{1}{8} + \frac{m_a \cdot \cos\varphi}{3\pi}\right)$$

$$P_{CT} = R_{DSon} \cdot I_o^2 \cdot \left(\frac{1}{8} + \frac{m_a \cdot \cos\varphi}{3\pi}\right)$$

The same approach can be used to calculate the diode losses and also the generator mode loss calculation as presented in chapter 3 which enables to build the energetic model of the three-phase inverter.

Boost-converter conduction losses:

For the case of the boost-converter, the following assumptions are done: only the transistor T1 and the diode D1 are conducting during motor mode, only the transistor T2 and the diode D2 are conducting during generator mode and the converter is working in continuous conduction mode.

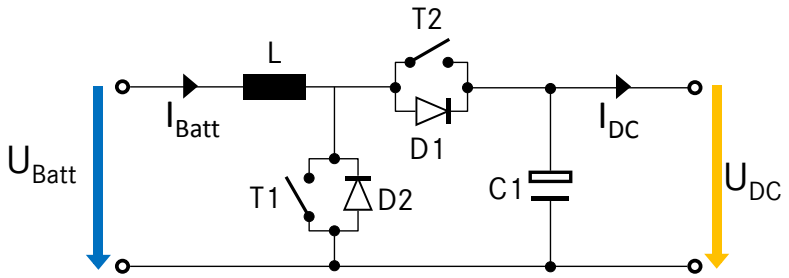

Figure: Equivalent circuit of a boost-converter based on [8] and [79]

Using the nomenclature on the previous figure and based on the waveforms and control described in [8] and [79], it results that the transistor is conducting current during the duration $D.T_{switch}$ and the diode is conducting during the rest of the period which is equal to $(1-D)\cdot T_{switch}$, where D is the duty ration which is depicted in the following equations for respectively the motor mode and the generator mode.

$$D_{motor} = 1 - U_{Batt}/U_{DC}$$

$$D_{generator} = U_{Batt}/U_{DC}$$

The two different phases of the converter can be resumed using the following equivalent circuit, where the first one represents the conduction of the transistor and the second one the conduction of the diode.

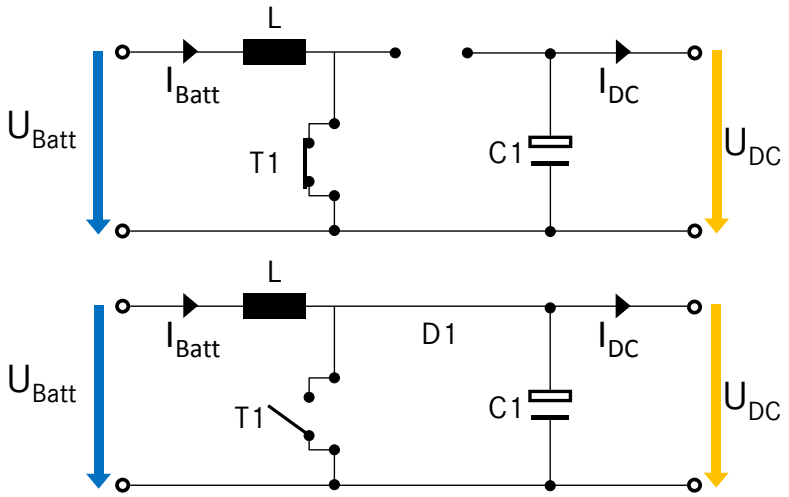

Figure: Equivalent circuit of a boost-converter during the conducting phase of the transistor (top) and the diode (bottom)

During their respecting phase, the transistor and the diode are conducting the input current (battery current) and thus the conduction losses of both can be calculated as follows.

$$P_{CT} = \frac{1}{T_{switch}} \int_0^{T_{switch}} \left(U_{ce0} + r_C \cdot I_{Batt}(t)\right) \cdot dt = \frac{1}{T_{switch}} \int_0^{D.T_{switch}} \left(U_{ce0} + r_C \cdot I_{Batt}(t)\right) \cdot dt$$

$$P_{CT} = \frac{1}{T_{switch}} \int_0^{T_{switch}} \left(U_{D0} + r_D \cdot I_{Batt}(t)\right) \cdot dt = \frac{1}{T_{switch}} \int_0^{(1-D)\cdot T_{switch}} \left(U_{ce0} + r_C \cdot I_{Batt}(t)\right) \cdot dt$$

The resolution of the previous equations results in the loss calculation presented in chapter 3. Moreover the same method can be applied to the generator mode, where only the duty ratio changes.

Boost-converter switching losses:

The calculation of the switching losses is based on the ripple current values in the input inductance. Even if the mean value of the input current can be supposed constant, the current has slight variations which can be expressed by the following equation.

$$\Delta I = \frac{D \cdot U_{Batt}}{L \cdot f_{switch}}$$

Based on the previously defined behavior of the different phases, it results the following waveforms:

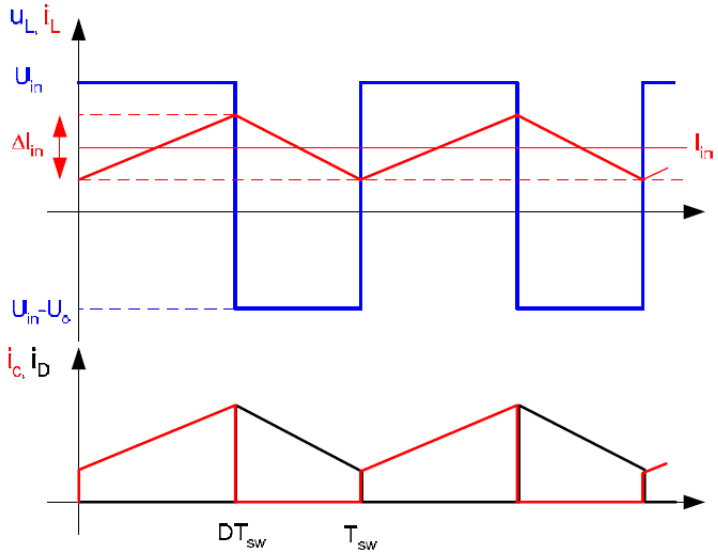

Figure: Boost-converter waveforms

Based on these waveforms the switching current can be estimated. During the on-switching of the transistor, the maximal value of the input current is reached, which also corresponds to the recovery of the diode, while during the off-switching the minimal value of the input current is reached. This behavior can be summarized by the following equation and the following table.

$$I_{switch} = |I_L| \pm \Delta I/2$$

	On-switching $I_{switch_{on}}$	**Off-switching** $I_{switch_{off}}$	**Recovery** $I_{switch_{rec}}$
Motor mode (step-up)	-	+	-
Generator mode (step-down)	+	-	+

Table: Sign for the calculation of the switching current

Based on the same approach, the switching losses in generator mode can be calculated and hence the energetic model of the boost-converter as presented in the chapter 3 can be built.

Boost-converter input inductance losses:

When using an inductance to filter the current at the converter input, the core used to build this inductance results in magnetic losses. These losses can generally be described for alternating current applications by using the Steinmetz equation:

$$\overline{P^*_{Fe}} = k\, f^{\alpha}\, \hat{B}^{\beta}$$

where $\hat{B}$ is the magnetic flux density, f is the frequency of the signal, k is a material parameter, α and β are the Steinmetz parameters of the material. This equation is however only valid for sinusoidal signal and thus adaptations are required. For this purpose, this work considers a Modified Steinmetz Equation (MSE) as described in [90] and [91]. To calculate this MSE, the Steinmetz equation needs first to be generalized as described in [152]. The Steinmetz parameters need therefore to be adapted and the completed generalization of the Steinmetz equations results in the two following equations.

$$\overline{P^*_{Fe}} = \frac{1}{T}\int_0^T k_i \left|\frac{dB}{dt}\right|^{\alpha} \left(\hat{B}\right)^{\beta-\alpha} dt$$

$$k_i = \frac{k}{2^{\beta+1}\pi^{\alpha-1}\left(0{,}2761 + \frac{1{,}7061}{\alpha + 1{,}354}\right)}$$

The resolution of the previous loss equation can be simplified due to the triangle behavior of the current in the input inductance. The integration can be therefore divided in two, one when the IGBT is open and one when the IGBT is conducting. The equation is then reduced as follows where n represent the two phases of the conversion.

$$\overline{P^*_{Fe}} = \frac{1}{T}\sum_{n=1}^{2} k_i \left|\frac{dB_n}{dt}\right|^{\alpha} \left(\hat{B}\right)^{\beta-\alpha} \Delta t_n$$

The flux density can be summarized by the two states, the value of dB_n/dt can be discretized as follows.

$$\hat{B} = \frac{dB_1}{dt}\Delta t_1 = \frac{dB_2}{dt}\Delta t_2$$

Using the previous equations and assumptions, the losses can be calculated as presented in the following equations. Moreover the flux density needs to be calculated. For this purpose, the induction law is used to express its amplitude based on the electric parameter which results in the following expressions.

$$\overline{P^*_{Fe}} = k_i\, f^{\alpha}\, \hat{B}^{\beta}(D^{1-\alpha} + (1-D)^{1-\alpha})$$

$$\hat{B} = \frac{dB_n}{dt}\Delta t_n = \frac{d\Phi_n}{dt\, A}\Delta t_n = \frac{d\Psi_n}{N\, A\, dt}\Delta t_n = \frac{U_{L,n}}{N\, A}\Delta t_n$$

$$\hat{B}_{mot} = \frac{U_{Bat}\, D\, T}{N\, A}$$

$$\hat{B}_{gen} = \frac{U_{Bat}\, (1-D)\, T}{N\, A}$$

These equations depict however only the losses power density in the magnetic core and thus need to be multiplied by the core volume to have the inductance losses. When the converter is not boosting the voltage between the battery and the inverter (U_{Batt}=U_{DC}). The variation of the flux density is equal to zero and therefore no losses are resulting.

Appendix 7: Battery structures

In this appendix, the different structures for battery are presented. The structures in this appendix are current automotive structures for different applications. Additional structures can be implemented for supercaps solutions or for hybrid energy storage system but they are not considered in this work.

Motor area battery:
In several concepts of hybrid vehicle, the battery is implemented directly in the motor area. It reduces the required length of the connections between the components because all the components are integrated in the same area of the vehicle. This solution is for example retained for the Mercedes-Benz S400Hybrid.

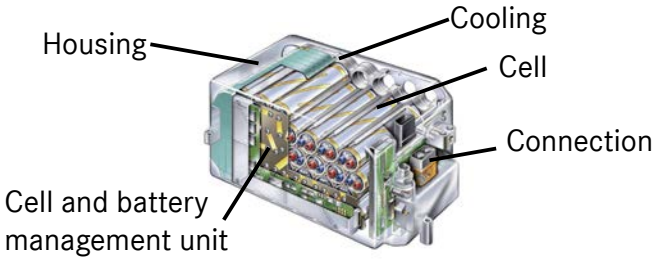

Figure: S400 Battery integrated in the motor area [32]

Tank/trunk area battery:
In the hybrid vehicle concepts with higher energy and power, the battery is generally integrated in the tank or trunk area. It requires longer cable to supply the electric drive but there is more available volume. Some implementations reduce the trunk volume or limit the modularity of the rear seats in the vehicle. This solution is chosen for the Volkswagen Golf GTE as presented on the following figure or for the Audi Plug-In System as shown in chapter 4.

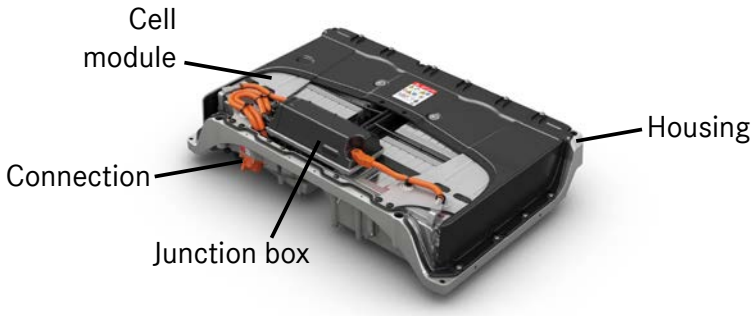

Figure: Golf GTE battery integrated in the tank area [155]

Purpose design battery:
Beside the previous structures, there are also structures which are designed purposely for the vehicle concept. Some of them are also light adaptation as in the AVL coup-e 800 [42] but most of the time the battery and the vehicle concept are commonly developed to achieve high integration as in the Chevrolet Bolt or in the Chevrolet Volt [18] which are directly integrated in the vehicle frame. These structures are not linked with the concept and are used for both electrical and hybrid vehicle.

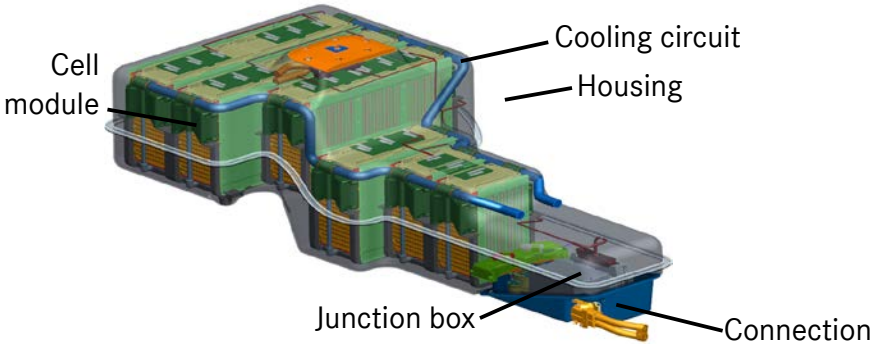

Figure: AVL coup-e 800 battery concept

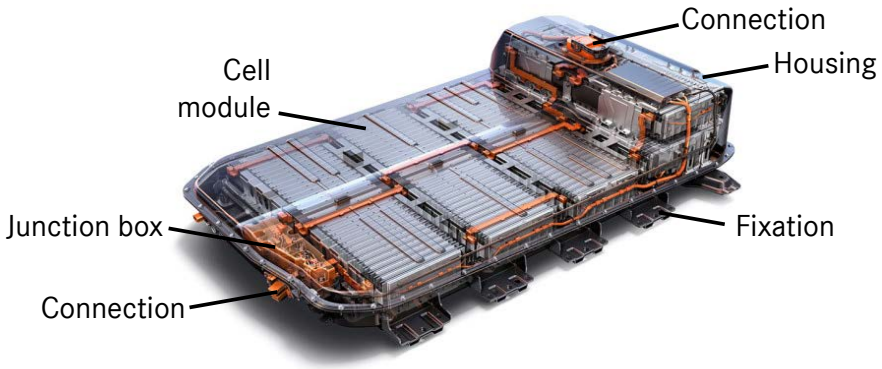

Figure: Chevrolet Bolt battery

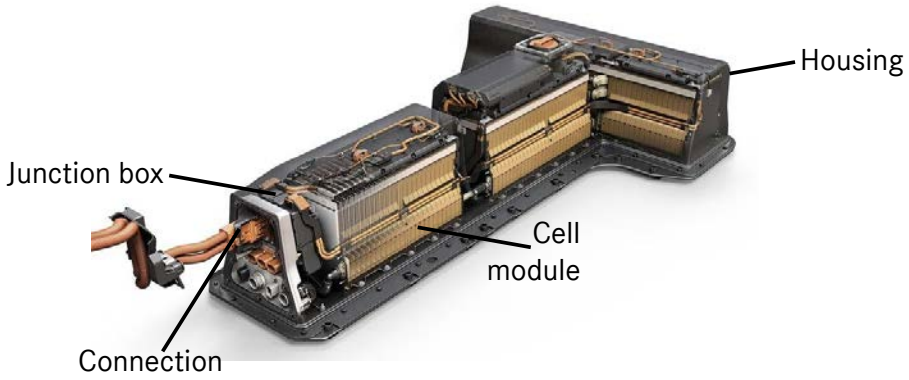

Figure: Chevrolet Volt battery

Appendix 8: Contribution of the evaluation approach

This appendix presents in details the contribution of the considered evaluation approach in this work, the components used for the example in chapter 6 are from the firm Brusa: the data can be found online (http://www.brusa.biz/). The data are summarized in the following tables and the method to calculate the evaluation values are detailed.

	Electric machine	Inverter	Battery
System 1	HSM1-6-17-12	DMC524	EVB1-350-40
System 2		DMC534	
System 3	HSM1-10-18-13		EVB1-350-40-HP
System 4		DMC544	
System 5	HSM1-10-18-22		EVB1-400-40-HP

Table: Investigated system based on the components from the firm Brusa

These three systems are evaluated using the TPI and the CII as defined in chapter 5 with the requirements defined in the first table. The Boolean approach is added in the next step when discussing the evaluation approach.

	Electric machine	Inverter	Battery
Available volume [mm]	292x250 (DxL)	500x240x88 (LxWxH)	800x516x300 (LxWxH)
Weight [kg]		12.5	130
Torque [Nm]	300		
Power [kW]	120		

Table: System requirements

The system can then be evaluated using these requirements and by calculated the ratios defined by the TPI and the CII. In this case the CII is divided in three parts, one for each dimension (L: length, W: width or H: height) and the TPI is evaluated for both the torque and the maximal power.

	System 1	System 2	System3	System 4	System 5
Power [kW]/Torque [Nm]	96/220	120/320	156/305	185/385	220/460
TPI [-]	0.8/0.7	1.0/1.1	1.3/1.0	1.5/1.3	1.8/1.5
EM: Diameter/Length [mm]	292/250	292/250	292/250	292/250	292/340
CII [-]	1/1	1/1	1/1	1/1	1/0.7
PE: Length [mm]	386	496	496	606	606
PE: Width[mm]	240	240	240	240	240
PE: Height [mm]	88	88	88	88	88
PE: Weight [kg]	9.5	12.5	12.5	15.5	15.5
CIIs [-]	1.3/1/1/1.3	1/1/1/1	1/1/1/1	0.8/1/1/0.8	0.8/1/1/0.8
ESS: Length [mm]	770	770	770	770	844
ESS: Width [mm]	516	516	516	516	511
ESS: Height [mm]	300	300	300	300	300
ESS: Weight [mm]	130	130	130	130	145
CIIs [-]	1/1/1/1	1/1/1/1	1/1/1/1	1/1/1/1	0.95/1/1/0.9

Table: System performance and evaluation

The systems are then evaluated using the weighted sum method (WSM), the product approach (PA) and the product approach with Boolean approach (PAB) as shown in chapter 6.

Appendix 9: Results of the P2-60 and the P2-15 systems

This appendix presents in details the results of the optimization of the P2-60 and the P2-15 systems using the same representations and the same parameters as for the P2-85 systems. The results are not discussed but presented as reference for the comparison and discussion in the chapter 6.

Results for the P2-60 system:

Parameter:	Reference	1st solution	2nd solution	3rd solution
DC-Voltage	266	222 (approximated using design voltage)		
Max. AC-Current	300	400		
Number of winding turns		↘		
Number of phases	3		6	3
SOCI [%]	100%	112.9%	112.8%	112.1%
PE length [%]		-1.5%	-0.6%	-5.4%
PE width [%]		-6.2%	-2.3%	-6.0%
PE height [%]		-14.1%	-14.4%	-5.8%
PE weight [%]		-10.4%	-10.3%	-4.0%
Semiconductor module	1	10		9
Battery length [%]		-3.9%		
Battery width [%]		-10.1%		
Battery height [%]		-8.1%		
Battery weight [%]		-10.3%		
Cell type	13	1		
Configuration	72s1p	60s1p		

Table: Optimization results for the P2-60 system

Results for the P2-15 system:

Parameter:	Reference	1st solution	2nd solution	3rd solution
DC-Voltage	133	89 (approximated using design voltage)		
Max. AC-Current	250	300	350	300
Number of winding turns	=			
Number of phases	3			
SOCI [%]	100%	116.0%	116.0%	115.0%
PE length [%]		-3.8%	-3.6%	-3.8%
PE width [%]		-5.8%	-5.6%	-5.8%
PE height [%]		-9.1%	-8.9%	-9.1%
PE weight [%]		-2.4%	-2.2%	-2.4%
Semiconductor module	1	4		7
Battery length [%]		-3.2%		
Battery width [%]		-5.3%		
Battery height [%]		-6.7%		
Battery weight [%]		-6.7%		
Cell type	11	2		
Configuration	36s1p	24s1p		

Table: Optimization results for the P2-15 system

LIST OF PUBLICATIONS

- High performance drives for hybrid electric vehicles through voltage stabilization
  Quentin Werner, Norbert Neidig, Serge Pierfederici, Noureddine Takorabet, 2016 18th European Conference on Power Electronics and Applications, (EPE'16 ECCE Europe)

- Voltage levels comparison and system optimization for electric drives in hybrid vehicles
  Quentin Werner, Serge Pierfederici, Noureddine Takorabet, PCIM Europe 2016, International Exhibition and Conference for Power Electronics, Intelligent Motion, Renewable Energy and Energy Management

- Influence of a variable reluctance resolver on an E-motor-system
  Norbert Neidig, Andreas Wanke, Quentin Werner, Martin Doppelbauer, 2016 18th European Conference on Power Electronics and Applications (EPE'16 ECCE Europe)

- Optimization of hybrid electrical vehicles with coupled thermal and electrical simulation
  Quentin Werner, Serge Pierfederici, Noureddine Takorabet, Babak Nahidmobarakeh, 2016 IEEE Transportation Electrification Conference and Expo (ITEC)

- The influence of geometrical deviations of electrical machine systems on the signal quality of the variable reluctance resolver
  Norbert Neidig, Quentin Werner, Markus Balluff, Hristian Naumoski, Martin Doppelbauer, Electric Drives Production Conference (EDPC), 2016 6th International

- Thermal modelling of electric machine during the early development phase
  Robert Lehmann, Quentin Werner, Norbert Neidig, Frank Gauterin, 17. Internationales Stuttgarter Symposium

- Influence of rotor position sensor on the design of electric drive system
  Norbert Neidig, Quentin Werner, Robert Lehmann, Martin Doppelbauer, 17. Internationales Stuttgarter Symposium